In vivo studies of stem cell-like divisions in *C. elegans*

Suzanne E.M. van der Horst

ISBN:

Printed by:
Layout and design:
Cover image

In vivo studies of stem cell-like divisions in *C. elegans*

In vivo studie naar stamcel-achtige delingen in *C. elegans*

(met een samenvatting in het Nederlands)

Proefschrift

ter verkrijging van de graad van doctor aan de
Universiteit Utrecht
op gezag van de
rector magnificus, prof.dr. H.R.B.M. Kummeling,
ingevolge het besluit van het college voor promoties
in het openbaar te verdedigen op

vrijdag 12 juli 2019 des ochtends te 10.30 uur

door

Suzanne Elisabeth Maria van der Horst

geboren op 2 december 1985
te Roermond

Promotor: Prof. dr. S.J.L. van den Heuvel

Table of contents

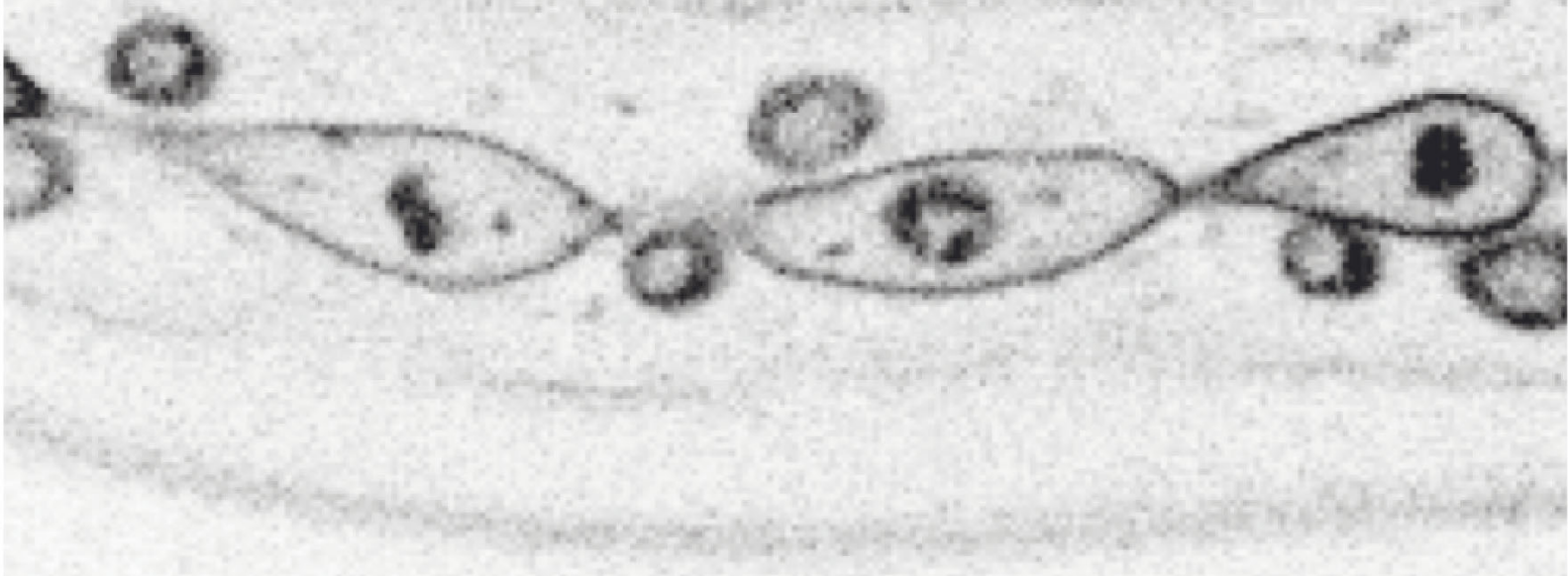

1

Control of symmetric and asymmetric epithelial stem-cell divisions in *C. elegans*

Suzanne van der Horst, Adri Thomas and Sander van den Heuvel

Developmental Biology, Department of Biology, Faculty of Science, Utrecht University,
Padualaan 8, 3584 CH Utrecht, The Netherlands

Introduction

Stem cells are key to the development of organisms and maintenance of specialized cell types and tissues. Hence, central in biomedical research is the question which factors control stem cell proliferation and differentiation. Tissue-specific stem cells need to combine long-term maintenance with the generation of differentiating daughter cells. This can be achieved by asymmetric cell divisions that simultaneously generate uncommitted stem cells (self-renewal) and daughter cells that enter a differentiation program. Alternatively, the uncommitted stem cell state may be instructed by the microenvironment that constitutes a niche, with cells exiting the niche initiating differentiation (Figure 1). In addition to fate, external factors determine whether stem cells proliferate or remain quiescent. The proper combination of external signals and cell-intrinsic factors creates a balance between proliferation and differentiation that underlies tissue homeostasis and prevents tumorous overproliferation or premature differentiation. Deep insight in the molecular mechanisms that control this balance will be needed for our understanding of animal development, stem cells maintenance, cancer formation and tissue regeneration.

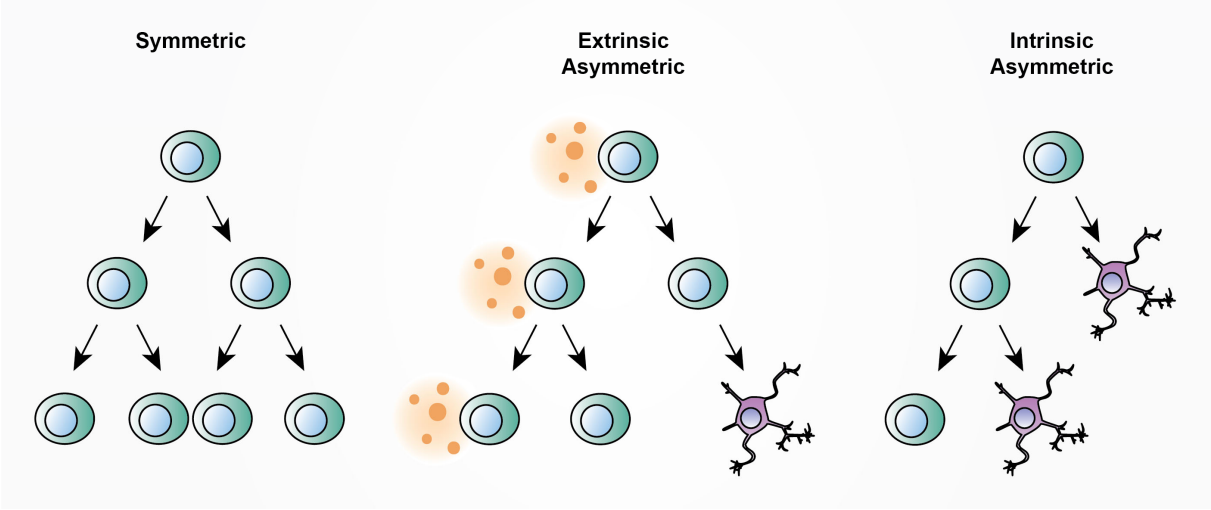

Figure 1. Illustration of tissue-specific stem cell division modes. Tissue-specific stem cells can expand through symmetric, proliferative divisions in which one stem cell generates two identical stem cell daughters (left). Dependent on external signals, daughter cells may adopt different cell fates (middle). This leads to asymmetric cell division at a population level, which has been referred to as extrinsic asymmetric division. Alternatively, tissue-specific stem cells and progenitors may undergo intrinsically asymmetric cell division, which involves the preferential segregation of cell fate determinants to one of the daughter cells during M phase of the cell cycle (right).

C. elegans seam cells as a model to study stem cell-like divisions

Substantial insights in the molecular mechanisms of stem cell-like cell divisions came from studies of embryonic and larval cell divisions in *C. elegans*. In particular, asymmetric division of the one-cell embryo has received much attention (Knoblich 2010; Rose & Gönczy 2014). While this initial division is cell-autonomously controlled, cell-cell signaling determines asymmetric cell division as early as the four-cell stage of the *C. elegans* embryo. In the four-cell embryo, the EMS founder cell divides asymmetrically to give rise to an anterior mesodermal (MS) and posterior endodermal (E) daughter cell (Figure 2) (Deppe et al. 1978). This asymmetric division is induced by the neighboring cell P2, which directs orientation of the mitotic spindle in anterior-posterior direction during division of EMS, and induction of the endoderm cell fate in the daughter cell contacting P2 (Goldstein 1992). Studies of the asymmetric division of EMS revealed an atypical Wnt signaling cascade that controls both of these aspects, spindle orientation and cell fate determination (Rocheleau et al. 1997a; Thorpe et al. 1997, 2000).

Atypical Wnt signaling regulates many asymmetric cell divisions in the worm, including anterior-posterior oriented divisions during embryogenesis and stem-cell like divisions in the skin. In the larva, the outermost cell layer, known as hypodermis or epidermis, contains two lateral rows of epithelial precursor cells (Figure 2) (Sulston & Horvitz 1977; Sulston et al. 1983). These so-called seam cells are designated H0-H2, V1-V6, and T, after their position in the head (H), ventrolateral side of the main body (V) or tail (T) region (Sulston and Horvitz, 1977). Originating from the ectodermal germ layer during embryonic development, seam cells proliferate during postembryonic development to facilitate growth of the multinucleated (syncytial) hypodermis, known as hyp7. Additionally, V5 and T cell divisions contribute neurons to the hypodermis. The V1-V6 cells undergo one asymmetric cell division along the A-P axis during each larval stage (L1-L4). These divisions produce a posterior self-renewing seam cell and an anterior differentiating daughter cell. The terminally differentiating daughter cells go through S phase and express the “fusogen” protein EFF-1, which induces fusion between the plasma-membranes of the anterior cells and hyp7 (Podbilewicz et al. 2006; Brabin et al. 2011). Meanwhile, the self-renewing posterior sister cells remain in G1, showing a rapid diversion in cell cycle progression between seam cell daughters (Hedgecock & White 1985). Cell cycle exit and fusion can be

uncoupled, as repression of *eff-1* prevents fusion but not cell cycle arrest. This results in retention of anterior non-seam cells in the epithelium (Mohler et al. 2002; Brabin et al. 2011).

In addition to asymmetric cell divisions, V1-V4, V6 and H1 seam cells undergo one symmetric cell division early in the second larval stage (L2), which expands the seam cell population from ten to sixteen cells at both lateral sides of the animal (Figure 2). Subsequently, all V cells undergo an asymmetric division to generate hypodermal cells and neuronal cells (V5), and asymmetric divisions are repeated in the third larval stage (L3). After the final division in L4 stage, seam daughter cells undergo terminal differentiation. This differentiation starts with cell cycle exit, followed by lateral fusion of seam cells to form a lateral syncytium. The adult seam syncytium produces and secretes specialized cuticle structures known as lateral alae, which may contribute to cuticle strength and movement (Singh & Sulston 1978).

The ability to switch between asymmetric and symmetric cell division makes seam cells particularly attractive as a model for studies of the stem cell-division mode in the context of a developing animal. Such studies benefit from the reproducible pattern of *C. elegans* development, as well as the transparency and genetic tractability of this animal. Despite the relative simplicity of the seam cell lineage, the regulation of the proper division pattern turns out to be highly complex. Several regulatory pathways have been found to come together in the proper control of symmetric versus asymmetric seam cell divisions, with Wnt signaling contributing to cell polarity, cell division orientation and cell fate. Understanding the integration of multiple regulatory pathways in the spatiotemporal control of seam cell divisions will likely provide insight in the regulation of vertebrate stem- and precursor cell divisions. The following sections of this introduction will predominantly focus on the mechanisms contributing to the seam cell division pattern, in relation to asymmetric division in other systems.

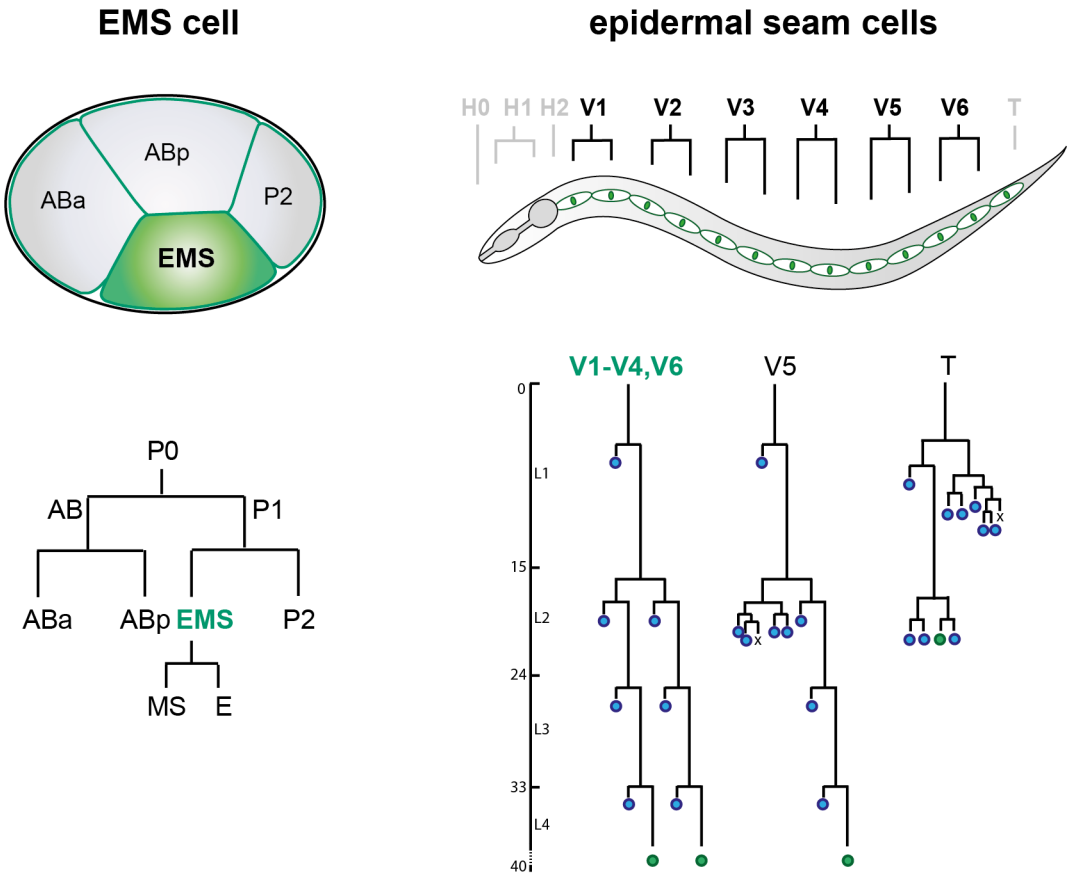

Figure 2 *Caenorhabditis elegans* early embryonic and larval seam cell lineages. Schematic representation of a four-cell stage *C. elegans* embryo containing the ABa, ABp, EMS (green) and P blastomeres. The EMS cell divides asymmetrically to give rise to the anterior MS cell (mesodermal lineage) and posterior E cell (endodermal lineage) (left panel). L2 stage animal with the left lateral row of seam cells indicated in green. From anterior to posterior, the cells are termed H0-H2, V1-V6, T. Lineages are shown for the ventrolateral V cells and tail T cell. V cells undergo one asymmetric cell division per larval stage, generating an anterior hypodermal cell and a posterior self-renewing seam cell. At the second larval stage (L2), the V cells undergo an additional symmetric cell division, generating two self-renewing seam cell daughters. All V cells undergo terminal differentiation after the asymmetric division in L4. Note that the V5 and T cell lineages also generate neural progeny. Seam cells are indicated in green, differentiated cells in blue (right panel).

Intrinsic asymmetric cell divisions depend on cell polarity

Asymmetric cell division requires polarization of the mother cell, which is needed to guide the unequal distribution of determinants that define the future daughter cells. In two well-studied models for asymmetric cell division, the *C. elegans* one-cell embryo and the *Drosophila* neuroblast, cell polarity depends on a combination of conserved PAR (*partitioning defective*) proteins (Reviewed in Knoblich, 2010). Antagonistic anterior (A) and posterior (P) PAR proteins polarize the fertilized *C. elegans* egg by forming two opposing domains at the cell cortex, thereby establishing the A-P body axis. The anterior PAR proteins consist of the conserved PDZ-domain proteins PAR-3 and PAR-6 together with the PKC-3 atypical protein kinase C (aPKC). These proteins form a complex and are also critical for apical-basal cell polarity at later stages. The contribution of anterior PAR (aPAR) proteins in the apical-basal polarity of epithelia is conserved in other animals; e.g. aPAR proteins determine the polarity of the ventral neuroectoderm from which the *Drosophila* neuroblasts inherit their polarity (Figure 3) (Goldstein and Macara, 2007; Rose and Gönczy, 2014). Studies of the *C. elegans* zygote and *Drosophila* neuroblast have provided much insight in how the cortical PAR protein polarity is used to direct the asymmetric segregation of cell fate determinants and cell division orientation.

Interestingly, most asymmetric divisions in *C. elegans* are not oriented along the apical-basal PAR polarity axis, but along the anterior-posterior body axis. As early as the four-cell embryo, PAR-independent mechanisms determine the division orientation of one of the blastomeres. As mentioned above, orientation of the mitotic spindle in the endoderm and mesoderm precursor cell EMS depends on cell-cell interactions with the neighboring blastomere P2. Genetic studies revealed that parallel acting Wnt/Frizzled signaling and Src kinase pathways orient the spindle in this situation (Rocheleau et al. 1997a; Thorpe et al. 1997; Bei et al. 2002; Walston et al. 2004). In fact, an atypical Wnt/Frizzled pathway has been identified as the major regulator of anterior-posterior polarity in *C. elegan*s, which controls many asymmetric cell divisions during embryogenesis and post-embryonic development.

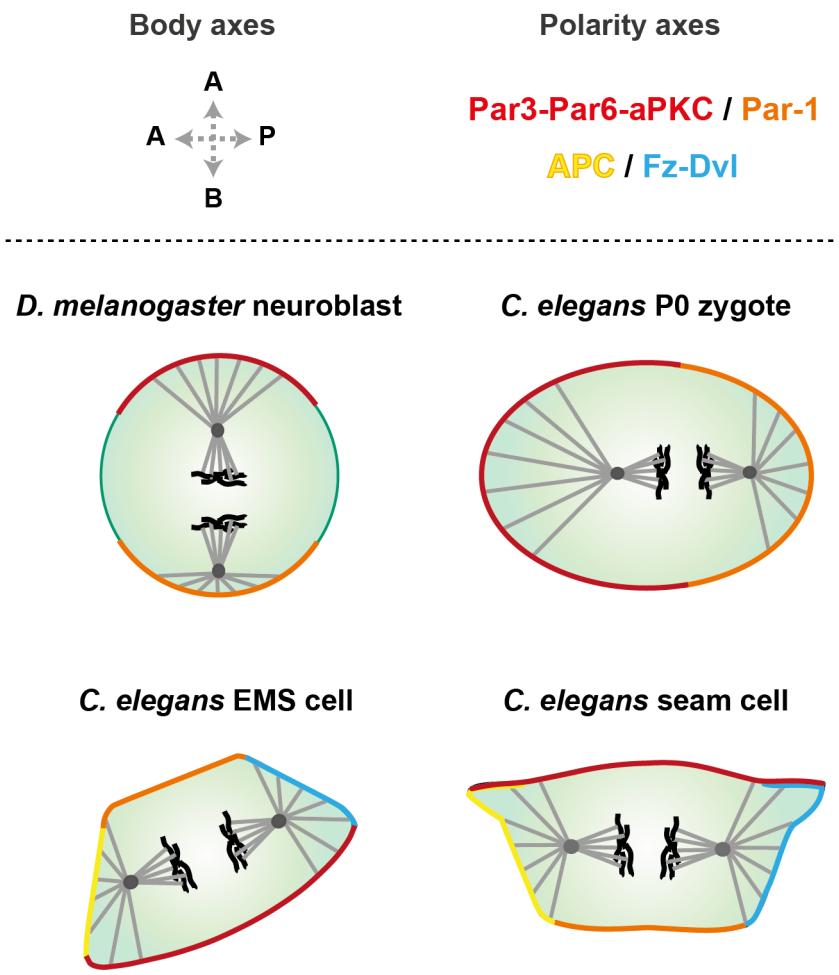

Figure 3. Cartoon of body axes versus PAR and Wnt polarity axes in well-studied asymmetric cell division models. Schematic representation of two body axes anterior-posterior (A-P) and apical-basal (A-B (top left) versus two polarity axes (PAR proteins Par3-Par6-aPKC/Par-1 and Wnt signaling components APC/Fz-Dvl (top right). *Drosophila* neuroblasts are polarized along the apical-basal axis dependent on the localization of PAR proteins. During their asymmetric divisions, the mitotic spindle is oriented along this polarity axis (middle left). The *C. elegans* zygote (P0) is also polarized by PAR proteins, which define the anterior-posterior body axis. During asymmetric cell division of P0, the spindle aligns with this polarity axis (middle right), so that when cell cleavage takes place perpendicular to and midway through the spindle two unequal cells are formed. The *C. elegans* EMS blastomere (4-cell stage) is polarized along two axes: apical-basal by PAR proteins and anterior-posterior by Wnt signaling components. Here, the division orientation follows Wnt-ligand induced polarity (bottom left). *C. elegans seam* cells are also polarized along both the apical-basal axis (PAR proteins) and anterior-posterior axis (Wnt pathway). These cells orient their divisions along the anterior-posterior polarity axis (bottom right).

Wnt signaling: a conserved regulator of stem cell divisions

In the past decades, several Wnt signaling pathways have been found to exert cell-type dependent functions in stem cell renewal, proliferation, differentiation, and asymmetric cell division. These pathways are usually activated by Wnt ligands, which are secreted glycoproteins that can act as morphogens, but predominantly provide short-range signals (reviewed in Clevers and Nusse, 2012; 2014). Wnt ligands can induce a 'canonical' or 'non-canonical' signaling cascade in the receiving cell. Which receptors interact with the Wnt ligands determines in substantial part the downstream cascades activated in the receiving cells (reviewed in Amerongen et al., 2008). Asymmetric stem cell divisions may depend on a combination of non-canonical Wnt signaling, to position the mitotic spindle, and canonical signaling, to transcriptionally activate pluripotency genes in the daughter cell close to the Wnt source.

Canonical Wnt signaling regulates gene transcription, triggered by Wnt ligand interaction with a Frizzled receptor and LRP5/6 co-receptor. Receptor activation induces an intracellular cascade via the Dishevelled protein, and leads to inhibition of the β-catenin destruction complex. This cytoplasmic complex consists of the scaffold proteins Axin and APC (adenomatous polyposis coli), together with the serine/threonine kinase GSK3 (glycogen synthase kinase 3) and CK1 (casein kinase 1) (reviewed in Clevers et al., 2014). In the absence of Wnt signals, the destruction complex binds and phosphorylates cytoplasmic β-catenin, priming it for ubiquitination and subsequent proteasomal degradation. Wnt interaction with the Frizzled and LRP5/6 receptors leads to recruitment and inactivation of the destruction complex. This allows stabilization of β-catenin, which then binds the TCF/LEF transcription factor (T cell specific transcription factor/lymphoid enhancer-binding factor 1) in the nucleus. TCF/LEF in complex with the β-catenin co-activator induces transcription of Wnt target genes. In contrast, in the absence of Wnt-induced β-catenin stabilization, TCF/LEF associates with the transcriptional repressor Groucho and histone deacetylases to block the transcription of Wnt target genes (Figure 4; reviewed in Gordon and Nusse, 2006).

Non-canonical Wnt pathways do not involve β-catenin/TCF mediated transcription, but signal to the cytoskeleton through Frizzled receptors in combination with other transmembrane molecules. A well-studied non-canonical Wnt pathway is the Planar Cell Polarity (PCP) pathway, originally discovered in *Drosophila melanogaster*, and later shown to

be conserved in vertebrates (reviewed in Gao, 2012). PCP signaling coordinates the polarization of cells relative to the plane of the epithelium they form part of. In the PCP pathway, Frizzled receptors act in conjunction with Flamingo proteins of the cadherin-family, in some tissues possibly without Wnt ligands (reviewed in Zallen, 2007). In *Drosophila* and zebrafish, Frizzled/Disheveled has been shown to be used as a cortical docking site, which anchors the mitotic spindle and orients the cell division axis (Gho & Schweisguth 1998; Bellaïche et al. 2001; Bellaiche 2004; Zhang et al. 2008; Ségalen et al. 2010). Additionally, polarized Fz/Dvl complexes signal through the downstream small GTPases RAC1 and RHOA to activate actin filament polymerization. This latter mechanism is likely conserved in *C. elegans,* as mutation of the CED-10^{Rac} GTPase and Wnt/Fz pathway components create similar spindle positioning defects in the EMS blastomere and other early embryonic cell divisions (Cabello et al. 2010). Thus, complex regulation by multiple non-canonical Wnt pathway branches may be used to instruct the orientation of cell division, while canonical signaling controls the gene expression program in the daughter cells of asymmetric cell divisions.

The Wnt/β-catenin asymmetry pathway controls cell fate in in asymmetric divisions

A remarkable combination of Wnt signaling pathways has been described to control asymmetric cell division in the nematode *Caenorhabditis elegans*. The Wnt/β-catenin asymmetry pathway combines asymmetric segregation of Wnt signaling components with MAPKKK signaling, to segregate POP-1^{TCF} transcriptional repressor and transcriptional activator functions to different daughter cells (Sawa & Korswagen 2013). This pathway is critical for the cell division and differentiation pattern of *C. elegans* seam cells. The Frizzled receptor LIN-17 controls seam cell polarity and cell fate, in a redundant fashion with other Wnt receptors MOM-5^{Fz} and CAM-1^{Ror} (Yamamoto et al. 2011). During division, LIN-17^{Fz} and its downstream binding partners MIG-5^{Dsh} and DSH-2^{Dsh} become enriched in the posterior cell membrane, and segregate to the self-renewing posterior daughter cell (Mizumoto and Sawa, 2007a; Yamamoto et al., 2011). The restriction of Frizzled receptors to the posterior daughter cell may render only this cell responsive to Wnt-ligands, and thereby promote asymmetric activation of the pathway.

Coincident with Frizzled receptor localization, several negative regulators of the pathway localize differently in the self-renewing stem cell as compared to the differentiating anterior daughter cell. As such, the β-catenin destruction complex members PRY-1^{Axin} and APR-1^{APC} become enriched at the cortex of anterior daughter cells (Baldwin and Phillips, 2014; Mizumoto and Sawa, 2007a). Their asymmetric localization is thought to result from repulsion from the posterior self-renewing cell cortex by MIG-5^{Dsh} (Baldwin & Phillips 2016), and from active retention at the anterior cortex through mutual interactions between APR-1^{APC} , PRY-1^{Axin}, and KIN-19^{CK1} (Baldwin & Phillips 2014). Loss of function of *apr-1, pry-1*, or *kin-19* results in hyperplasia of seam cells, as a result of divisions becoming symmetric (Mizumoto & Sawa 2007a; Gleason & Eisenmann 2010; Baldwin & Phillips 2014). This indicates that the β-catenin destruction complex is required for the anterior cell fate and differentiation of seam cells. Furthermore, it shows that polarization of Wnt components is directly coupled to a binary choice between differentiation versus stem-cell like cell fates during asymmetric division.

It remains unclear what controls the anterior-posterior polarization of Wnt components in asymmetric cell divisions. Studies of mammalian embryonic stem cells have shown that Wnt ligands can act directionally in the polarization of Wnt pathway components. Exposure of unpolarized cells to an immobile local Wnt source was sufficient to recruit Frizzled receptors to the contact site, and to polarize pathway components in the direction of the ligand (Habib et al. 2013). Interestingly, ligand-instructed polarization has also been described for the *C. elegans* EMS blastomere, the T seam cell (Goldstein et al. 2006), and V5 seam cell (Whangbo et al. 2000). In contrast, however, Wnt ligands appear to provide a permissive rather than instructive signal in orienting the polarity of the V1-V4 and V6 seam cells (Yamamoto et al. 2011). V1-V4 and V6 cells display intact but randomly oriented A-P polarity in the complete absence of Wnt ligands (Wildwater et al. 2011; Yamamoto et al. 2011). Yet, in the presence of a Wnt ligand they polarize correctly, independently from the location of the Wnt source. Together, these observations indicate that Wnt ligands may provide a permissive role in V1-4, V6 seam cells, while acting in an instructive way in several other *C. elegans* cell types and mammalian stem cells.

As V seam cells are part of a larger epithelium, their polarization may also be instructed at a more global level. The planar cell polarity pathway coordinates the polarization of cells in several epithelial tissues in *Drosophila* and vertebrates (Reviewed in

Gao, 2012), but its contribution to tissue polarity in *C. elegans* remains unclear. Recent reports have indicated that VANG-1$^{\text{Van Gogh}}$ promotes Frizzled internalization and interaction with Dishevelled in Q cell neuroblasts (He et al. 2018; Mentink et al. 2018). These data may indicate that Wnt/β-catenin asymmetry is modulated by PCP signaling. Analysis of *vang-1*$^{\text{Van Gogh}}$ and *prkl-1*$^{\text{Prickle}}$ mutants, however, did not reveal any abnormalities in seam cell polarity. This demonstrates that seam cells do not depend on planar cell polarity for their anterior-posterior polarity axis. Analysis of Wnt ligand mutants supports this hypothesis, as reversed A-P polarity in seam cells did not induce polarity reversal in neighboring cells (Yamamoto et al. 2011). Altogether, this suggests that neither external Wnt ligands nor PCP signaling are responsible for the anterior-posterior orientation of Wnt/β-catenin asymmetry. Thus, seam cells may control their polarity individually and independently of the larger tissue. Studies in the one-cell embryo have shown that remodeling of the actin cytoskeleton, driven by NMY-2 non-muscle myosin, provides an important trigger for anterior-posterior polarity establishment (Munro et al. 2004). A recent study examined the potential contribution of actin cytoskeleton remodeling in seam cell polarity. However, disrupting NMY-2 function did not alter the anterior-posterior polarity of seam cells (Ding & Woollard 2017). In summary, the Wnt/β-catenin asymmetry pathway determines the fate of seam daughter cells, but what instructs the orientation of Wnt/β-catenin asymmetry remains to be discovered.

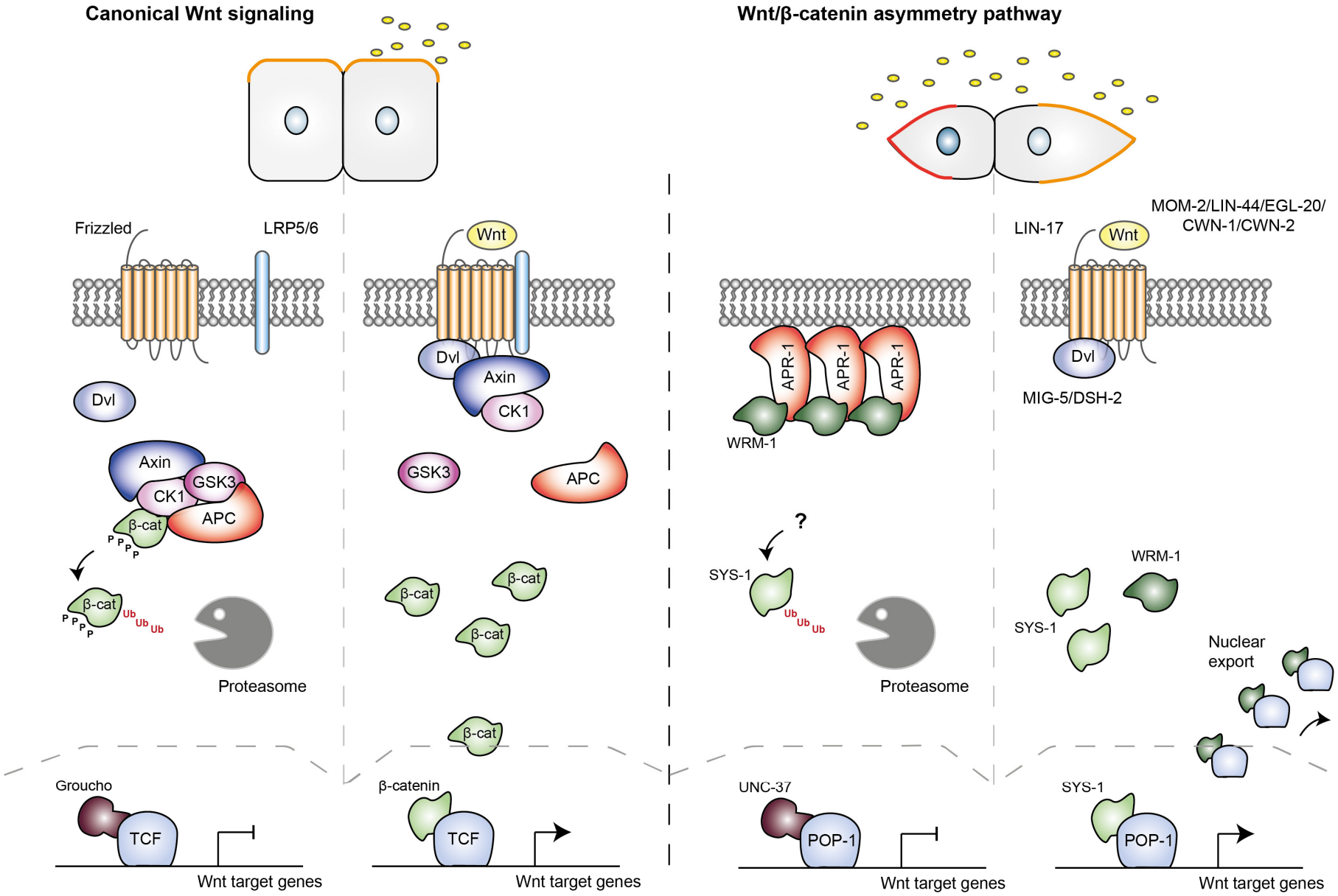
Canonical Wnt signaling
Wnt/β-catenin asymmetry pathway
Frizzled
LRP5/6
Wnt
Dvl
Axin
CK1
GSK3
APC
β-cat
Ub
Proteasome
APR-1
WRM-1
LIN-17
MOM-2/LIN-44/EGL-20/
CWN-1/CWN-2
MIG-5/DSH-2
?
SYS-1
Nuclear
export
Groucho
TCF
β-catenin
UNC-37
POP-1
Wnt target genes

Figure 4. Canonical Wnt signaling in mammals and the Wnt/β-catenin asymmetry pathway in *C. elegans*. Canonical Wnt signaling in mammalian cells starts with Frizzled receptor (orange) activation at the cell membrane by Wnt ligands (yellow). This induces an intracellular cascade in which Dishevelled (Dvl) is recruited to the C-terminal domain of Frizzled. Dvl recruits Axin and CK1 to the receptor, thereby disassembling the β-catenin destruction complex (composed of Axin, CK1, GSK3β and APC). This leads to the stabilization of cytoplasmic β-catenin, and subsequent translocation into the nucleus. Here, β-catenin functions as a co-activator for the TCF transcription factor, inducing the expression of Wnt target genes (left; right panel). In non-Wnt-receiving cells, the β-catenin destruction complex recruits and phosphorylates cytoplasmic β-catenin, which primes it for polyubiquitination and subsequent proteasomal degradation. In the absence of β-catenin, TCF in association with the Groucho co-repressor, inhibits transcription of Wnt target genes (left; left panel). The Wnt/β-catenin asymmetry pathway in *C. elegans* seam cells relies on the asymmetric distribution of Wnt pathway components to asymmetrically activate the pathway. The Frizzled receptors LIN-17 or MOM-5 (orange) localize to the posterior cortex of dividing seam cells. Wnt ligands (MOM-2, LIN-44, EGL-20, CWN-1, CWN-2) appear to provide a permissive signal, which induces seam cells to align their polarity with the A-P body axis. In this cell, receptor activation alters the function of two cytoplasmic β-catenins, WRM-1 and SYS-1, in different ways. WRM-1 is triggered to form a complex with the MAPK/Nemo-like LIT-1 kinase and translocates to the nucleus. Here, LIT-1 phosphorylates the transcription factor POP-1, leading to its nuclear export. The second β-catenin, SYS-1, becomes stabilized, translocates to the nucleus and acts as a co-activator for the remaining POP-1. This induces expression of Wnt target genes (right; right panel). The anterior daughter cell does not activate the pathway. Members of the β-catenin destruction complex asymmetrically segregate to the anterior cortex and contribute to the clearance of cytoplasmic WRM-1 and SYS-1. WRM-1 is sequestered to the cortex, whereas SYS-1 is degraded at the centrosomes. Since WRM-1 cannot guide LIT-1 to POP-1, nuclear levels of POP-1 remain high, and in the absence of co-activator SYS-1, POP-1 forms a transcriptional repressor complex with UNC-37 Groucho. In this cell, Wnt target genes are repressed, facilitating differentiation (right; left panel).

Combined Wnt/β-catenin polarization and MAPK signaling differentially activates POP-1 in seam daughter cells

Polarization of Wnt/β-catenin pathway separates components that inhibit signaling from those that activate the pathway, thereby asymmetrically segregating repressor versus activator functions of the downstream transcription factor POP-1^{TCF} to the daughter cells. The dual function of POP-1 as either a transcriptional repressor or transcriptional activator is determined by the nuclear level of POP-1 as well as its cofactors SYS-1$^{\beta\text{-catenin}}$ and UNC-37^{Groucho} (Lin et al. 1995, 1998; Thorpe et al. 1997).

The β-catenin SYS-1 associates with POP-1 through interaction with its β-catenin binding domain. This association transforms POP-1 into a transcriptional activator (Kidd et al. 2005; Liu et al. 2008). In dividing seam cells, SYS-1 becomes asymmetrically enriched in the nuclei of posterior self-renewing daughter cells (Huang et al. 2007; Phillips et al. 2007; Green et al. 2008; Baldwin & Phillips 2014). Proteasomal degradation, in connection with the centrosome, reduces SYS-1 protein levels in the differentiating anterior cells (Phillips et al. 2007; Baldwin & Phillips 2014; Vora & Phillips 2015). Loss of *apr-1* or *kin-19* leads to increased nuclear SYS-1 levels in anterior daughter cells as a result of decreased protein turnover. This indicates that the β-catenin destruction complex participates in SYS-1 turnover (Baldwin & Phillips 2014). SYS-1 lacks the conserved GSK-3 phosphorylation site found in conventional β-catenins (Sawa & Korswagen 2013), and *gsk-3(RNAi)* does not affect seam cell fate (Gleason & Eisenmann 2010). These observations indicate that an alternative post-translational modification might mark SYS-1 for degradation, or that polarization of the destruction complex suffices to restrict SYS-1 degradation to anterior cells. While SYS-1 acts as a POP-1 transcriptional coactivator, depletion of *sys-1* does not convert POP-1 into a transcriptional repressor or induce premature differentiation of seam cells (Gleason & Eisenmann 2010). This is in line with the notion that the nuclear concentration of POP-1 is the main determinant for POP-1 activity.

As in the embryo and gonad, asymmetric seam cell divisions display nuclear asymmetry of POP-1, with higher levels in anterior compared to posterior daughter cell nuclei (Mizumoto & Sawa 2007b). This nuclear POP-1 asymmetry is a critical aspect of the Wnt/β-catenin asymmetry pathway, which in large part functions as a divergent canonical Wnt-signaling pathway. Studies in the early embryo have shown that a β-catenin distinct

from SYS-1, WRM-1, interacts with the POP-1 C-terminal domain, and induces nuclear export instead of transcriptional activation (Rocheleau et al. 1997b; Yang et al. 2011). By forming a docking site on POP-1, WRM-1 brings the Nemo-like kinase LIT-1 in close contact with nuclear POP-1. The subsequent phosphorylation of POP-1 by LIT-1 induces POP-1 nuclear export. By promoting nuclear export of non-SYS-1 bound POP-1, LIT-1/WRM-1 promote the switching of POP-1 from a transcriptional repressor to a transactivator (Yang et al. 2011).

To ensure asymmetric activation of POP-1, WRM-1 activity needs to be restricted to the posterior daughter cell. Like SYS-1, WRM-1 was shown to localize asymmetrically to posterior daughter cell nuclei (Baldwin and Phillips, 2014; Hughes et al., 2013; Mizumoto and Sawa, 2007a). Contrary to SYS-1, however, WRM-1 is not degraded in the anterior daughter cell. Instead, WRM-1 is anchored at the cortex of embryonic blastomeres and seam cells, which appears to depend on transport along astral microtubules after nuclear export (Kim et al., 2013; Mizumoto and Sawa, 2007a; Nakamura et al., 2005; Takeshita and Sawa, 2005). At the anterior cortex of the EMS blastomere and seam cells, APR-1 appears to stabilize contacts with astral microtubule plus-ends (Nakamura et al. 2005; Sugioka et al. 2011; Baldwin & Phillips 2014). In this way, the cortical recruitment of APR-1 promotes both anterior directed transport and anchoring of WRM-1 β-catenin. This mechanism prevents nuclear export of POP-1, and as a result the anterior nucleus contains high POP-1 and low SYS-1 levels, and the posterior nucleus low POP-1 and high SYS-1. The ratio between nuclear POP-1 and SYS-1 ultimately determines whether POP-1 can act as a transcriptional activator (Kidd et al. 2005; Liu et al. 2008).

Further regulation of both spindle positioning and transcriptional activation by the Wnt/β-catenin asymmetry pathway occurs at the level of WRM-1 localization. The MOM-4 MAPK kinase kinase is needed to activate the LIT-1 MAPK/Nemo kinase and to induce cortical localization of WRM-1 as well as translocation of LIT-1/WRM-1 $^{\beta\text{-catenin}}$ into the nucleus (Thorpe et al. 1997; Meneghini et al. 1999; Lin et al. 2003). Release of WRM-1 from the posterior cortex is triggered by combined CDK-1 phosphorylation and Wnt signaling in the embryonic EMS blastomere (Kim et al. 2013a). In seam cells, loss of *mom-4* or *lit-1* induces premature differentiation (Takeshita & Sawa 2005; Gleason & Eisenmann 2010). This observation is in line with the model that MOM-4-induced activation of LIT-1 is required for LIT-1/WRM-1-induced nuclear export of POP-1, and thereby for the self-renewing

posterior cell fate. The incorporation of MAPKKK signaling via MOM-4 to LIT-1 forms yet another regulatory level that controls POP-1 activity.

Together, during asymmetric cell division in *C. elegans*, the Wnt/β-catenin asymmetry pathway combines semi-canonical regulation of SYS-1 levels and a divergent MAPK/WRM-1 pathway branch to establish a high SYS-1:POP-1 nuclear ratio in the posterior daughter cell. This allows POP-1 to act as a transcriptional activator, and to promote the self-renewing seam-cell fate (Figure 5). Anterior daughter cells display a low SYS-1:POP-1 nuclear ratio correlating with POP-1 transcriptional repressor function and suppression of Wnt target genes (Huang et al., 2007). The correlation between a high β-catenin:TCF nuclear ratio and TCF transactivation is conserved between Wnt signaling in *C. elegans* and mammals. In higher eukaryotes, however, this ratio appears determined by the concentration of nuclear β-catenin. The Wnt/β-catenin asymmetry pathway adds additional levels of regulation to modulate POP-1 nuclear concentration, as a way to achieve binary cell fate decisions in the daughter cells of asymmetric cell divisions.

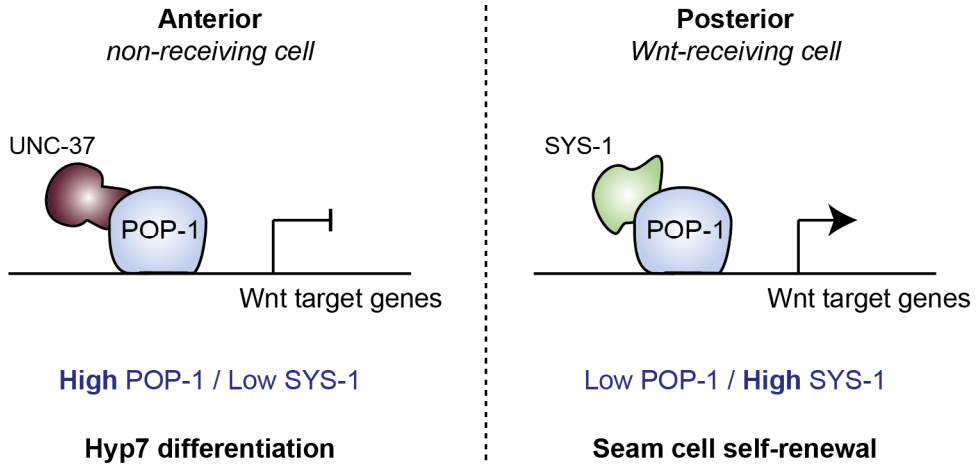

Figure 5. Dual function for POP-1^{TCF} as a transcriptional repressor and activator. In Wnt non-receiving cells, SYS-1$^{\beta\text{-catenin}}$ is degraded, resulting in POP-1^{TCF} functioning as a transcriptional repressor in complex with UNC-37^{Groucho}. This correlates with a "hyp7" differentiation fate (left). In Wnt-receiving cells, nuclear POP-1 is reduced and SYS-1$^{\beta\text{-catenin}}$ increased, inducing the formation of a transcriptional activation complex, which promotes expression of Wnt target genes and seam cell self-renewal (right). The nuclear SYS-1/POP-1 ratio determines POP-1 activity.

Symmetric versus asymmetric seam cell division

The sections above described how the Wnt/β-catenin asymmetry pathway instructs a binary cell fate decision in the seam daughter cells. Our current understanding of what controls the symmetric mode of division is limited. Symmetric seam cell divisions generate two 'posterior' self-renewing daughter cells. As a potential mechanism, Wnt signaling components may be expected to segregate symmetrically at 'posterior' levels during these divisions. However, studies from our group and others uncovered that the Wnt/β-catenin asymmetry components APR-1, WRM-1, and POP-1 still polarize along the A-P axis during symmetric seam cell divisions (Wildwater et al. 2011; Hughes et al. 2013; Harandi & Ambros 2014). This appears to suggest that Wnt signaling is bypassed by another mechanism during symmetric divisions. Below, we discuss additional regulators that affect the seam cell division pattern, and that promote the switch from asymmetric to symmetric cell division.

A *C. elegans* Runx/CBFβ complex contributes to seam cell division frequency and cell fate

Mutation of genes that encode the RNT-1^{RUNX} transcriptional regulator or its binding partner BRO-1^{CBFβ} result in skipping part of the symmetric seam cell divisions. Moreover, overexpression of *rnt-1* and *bro-1* converts asymmetric seam cell divisions in L2 and L3 into symmetric divisions (Nimmo et al. 2005; Kagoshima et al. 2007b; Xia et al. 2007). These observations support that *rnt-1* and *bro-1* promote the symmetric mode of seam cell division. *rnt-1* and *bro-1* belong to the conserved family of RUNX transcription factors known for their regulatory roles in stem cell proliferation and cell cycle control (reviewed in Chuang et al., 2013; Wang et al., 2010). The *C. elegans* RNT-1/BRO-1 complex has been proposed to induce the cell division cycle in seam cells by transcriptionally repressing the cell cycle inhibitors *cki-1*^{p21}, *fzr-1*^{Cdh1}, and *lin-35*^{Rb} (Nimmo et al. 2005; Kagoshima et al. 2007a; Xia et al. 2007).

Mammalian Runx/CBFβ complexes can function as transcriptional repressors or activators, depending on additional binding partners (Figure 6). Which binding partners can interact with the complex depends on post-translational modifications of Runx that include methylation, acetylation and phosphorylation (Reviewed in Blyth et al., 2005; Chuang et al., 2013). The Groucho-homolog UNC-37 is currently the only described binding partner for the

RNT-1/BRO-1 complex in *C. elegans*. A specific mutation in *unc-37* causes defects in seam cell divisions that resemble those in *rnt-1* and *bro-1* loss-of-function mutants (Xia et al. 2007). As Groucho is a well-known co-repressor, this observation provides strong support for the idea that RNT-1/BRO-1 act as a transcriptional repressor in promoting symmetric seam cell divisions.

It is currently not known what restricts the activity of the RNT-1/BRO-1/UNC-37 repressor to promote symmetric seam cell divisions only in the L2 hermaphrodite, as well as posterior seam cell divisions in L3 and L4 stage males (Kagoshima et al. 2005, 2007a). Several studies have indicated that transcriptional regulation limits the spatiotemporal pattern of RNT-1/BRO-1/UNC-37 activity. Specifically, upstream regulators of *rnt-1* and *bro-1* have been reported to be differentially expressed in the seam daughter cells of asymmetric divisions. Anterior daughter cells may inhibit *rnt-1* expression via the *ceh-20*^{Pbx} and *unc-62*^{Meis} transcriptional repressor complex. Loss of function of either *ceh-20* or *unc-62* induces seam cell hyperplasia as a result of the divisions becoming symmetric (Hughes et al. 2013). This indicates that down-regulation of *rnt-1* is essential for anterior differentiation. Additionally, self-renewing posterior daughter cells stimulate proliferation by inducing *bro-1* expression via the GATA transcription factor *elt-1* (Brabin et al. 2011). If the RNT-1/BRO-1 complex is needed to overcome Wnt-signaling during the second larval stage, their expression levels would be expected to peak in early L2 seam cells. Analyses of animals carrying reporter transgenes found BRO-1 to be expressed throughout all larval stages (Kagoshima et al. 2007b; Xia et al. 2007), and RNT-1 to be expressed at a high level until the late L2 stage (Nimmo et al. 2005). Therefore, regulation other than transcriptional control participates in limiting the RNT-1/BRO-1 activity to the early L2 stage.

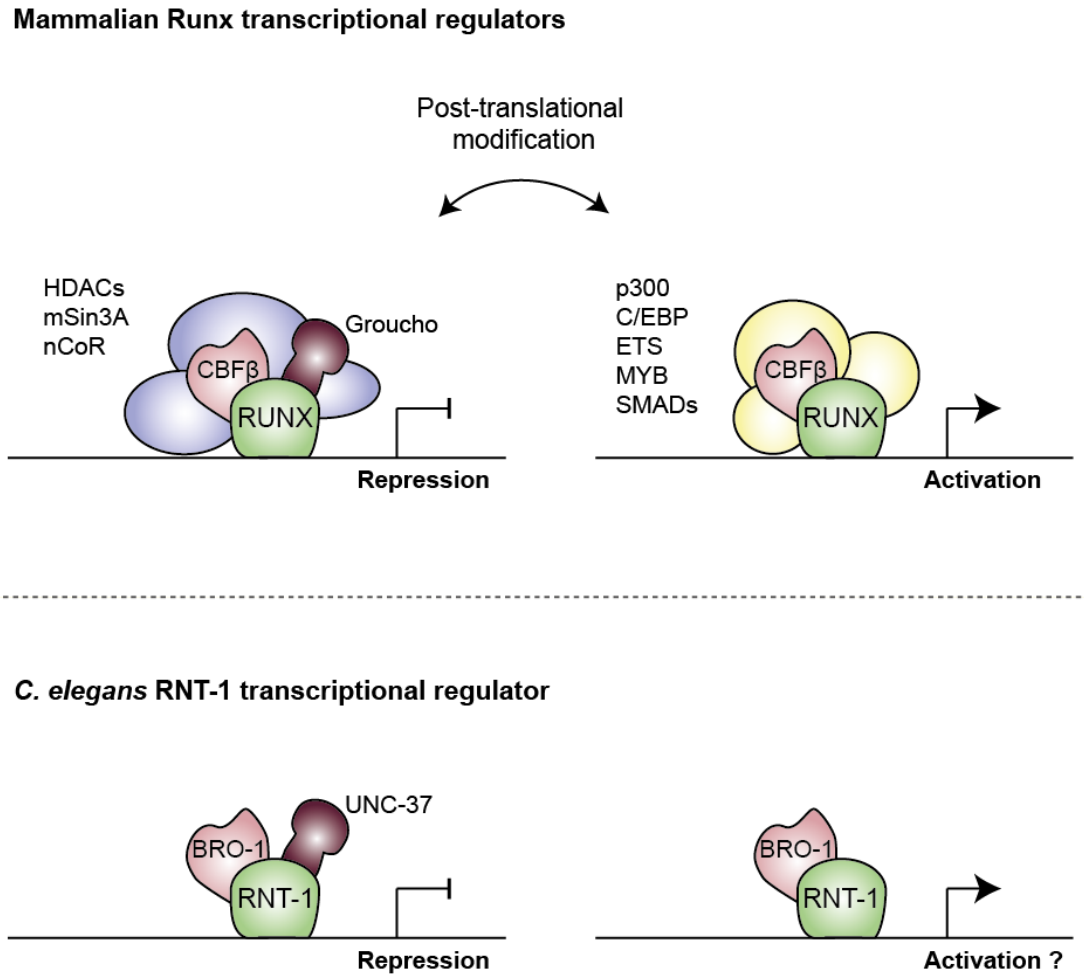

Figure 6. Conserved functions for RUNX proteins as transcriptional regulators. Schematic cartoon of the mammalian Runx/CBFβ transcriptional regulator complexes. Depending on post-translational modifications of Runx, Runx/CBFβ can either form transcriptional repressor complexes with co-repressors Groucho, HDACs, mSin3A, nCoR (left) or activator complexes with the co-activators p300 and C/EBP, or transcription factors of the ETS, MYB, or SMAD families (right) (top panel; figure adapted from Blyth et al., 2005). The *C. elegans* orthologs RNT-1^{Runx} and BRO-1^{CBFβ} have so far only been found in a transcriptional repressor complex with co-repressor UNC-37^{Groucho} (left). Whether or not they also have an activator function remains to be found (right) (bottom panel).

Several studies have investigated a possible interaction between RNT-1 and the Wnt/β-catenin asymmetry pathway (Xia et al. 2007; Gleason & Eisenmann 2010; Hughes et al. 2013). Such a connection was suggested by the overlap in phenotype: preventing Wnt pathway activation converts asymmetric seam cell divisions into symmetric divisions, as was observed after overexpression of the RNT-1/BRO-1 complex. Moreover, WRM-1 asymmetry has been reported to be lost in RNT-1/BRO-1 overexpressing cells (Hughes et al. 2013). Interestingly, the *pop-1* knockdown phenotype, extensive seam cell hyperplasia, was suppressed by *rnt-1* and *bro-1* RNAi. This could indicate that *rnt-1* and *bro-1* act downstream of *pop-1*, but additional experiments did not support this conclusion (Gleason & Eisenmann 2010). Based on similar experiments, several studies have concluded that RNT-1/BRO-1 functions in parallel to the Wnt/β-catenin asymmetry pathway (Kagoshima et al. 2005; Gleason & Eisenmann 2010; Hughes et al. 2013; Ding & Woollard 2017). It should be noted, however, that the genetic epistasis experiments in these studies used combinations of partial loss-of-function gene functions that do not necessarily reveal upstream-downstream relationships.

Temporal control of seam cell division patterns by the heterochronic network

A remarkable aspect of the seam cell lineage is the alternation between symmetric and asymmetric divisions in early L2 stage larvae. This temporal pattern of seam cell divisions is dictated by an internal clock composed of evolutionarily conserved heterochronic genes (Moss 2007). Studies of the heterochronic gene network defined gene regulation by micro RNAs (miRNAs): the *lin-4* (lineage abnormal) and *let-7* (lethal) genes were found to express noncoding RNAs that regulate key downstream targets. As such, *lin-4* inhibits expression of the transcription factor LIN-14 and RNA-binding protein LIN-28 in late L1 and mid-L2 stage larvae, respectively. In subsequent stages, miRNAs of the *let-7* family inhibit expression of the HBL-1 transcription factor and LIN-41 TRIM-NHL protein (Figure 7) (Moss, 2007; Rougvie, 2005; Slack and Ruvkun, 1997; Slack et al., 2000). The successive expression patterns of these miRNAs and their associated phenotypes defines them as developmental switches that control the timing of the four larval stages (reviewed in Nimmo & Slack, 2009).

Mutations in heterochronic genes create either a precocious phenotype, characterized by the skipping of larval-stage-specific events, or a retarded phenotype, in

which stage-specific processes are reiterated (Ambros & Horvitz 1984). Such opposite phenotypes can be created by loss of function versus gain of function of the same heterochronic gene. This shows that heterochronic gene functions determine the timing of the stages of larval development. The timing of the L2 pattern of seam cell divisions is often used to reveal how mutations in heterochronic genes affect the timing of larval development. This L2 pattern of symmetric seam cell division followed by asymmetric division occurs during a specific window of heterochronic gene functions.

The L2 heterochronic window for symmetric seam cell divisions appears to be determined by low levels of LIN-14 (Ambros & Horvitz 1987), and high levels of LIN-28 and HBL-1. Interestingly, a mammalian *lin-28* homolog promotes pluripotency and was identified as one of the genes that can reprogram differentiated human fibroblasts into pluripotent stem cells (iPS cells), in combination with three other factors (Yu et al. 2007). Important elements of pluripotency are repression of genes that promote differentiation and maintenance of proliferation potential. LIN-28 is thought to contribute such functions through interaction with miRNA precursors (pre-miRNAs) and mRNAs, thereby controlling miRNA processing and protein translation. An evolutionarily conserved target of LIN-28 is the *let-7* pre-miRNA. By inhibiting *let-7* pre-microRNA processing, LIN-28 prevents expression of the mature *let-7* microRNA that induces differentiation in *C. elegans,* as well as in mammalian systems (Moss et al. 1997; Piskounova et al. 2008; Rybak et al. 2008; Viswanathan et al. 2008). Mammalian Lin28 also promotes the translation of select mRNAs (Peng et al. 2011). In mouse embryonic stem (ES) cells, Lin28 was found to associate with the 3' UTRs of cyclin A, cyclin B, and Cdk4 mRNA, and Lin28 may promote proliferation by enhancing the translation of these mRNAs (Xu et al. 2009).

C. elegans lin-28(lf) mutants skip the L2 stage entirely, resulting in a decreased number of seam cells (Ambros & Horvitz 1984; Ambros 1989; Harandi & Ambros 2014). Conversely, overexpression of a *lin-28* transgene induced reiteration of the symmetric seam cell divisions at subsequent larval stages (Moss et al. 1997). These observations indicate that LIN-28 expression is coupled to the symmetric seam cell division pattern. It is possible, however, that LIN-28 contributes indirectly to the L2 pattern of seam cell divisions. Genetic experiments support that *lin-28* acts as an upstream regulator of the *hbl-1* transcription factor gene, and LIN-28 induces the translation *of hbl-1* mRNA (Abrahante et al. 2003; Lin et al. 2003; Abbott et al. 2005). Transgene reporters revealed expression of *hbl-1* in the

hypodermis, which would indicate that *hbl-1* acts in a cell non-autonomous way to control seam cell proliferation (Abrahante et al. 2003; Vadla et al. 2012). Further experiments will be needed to validate this conclusion.

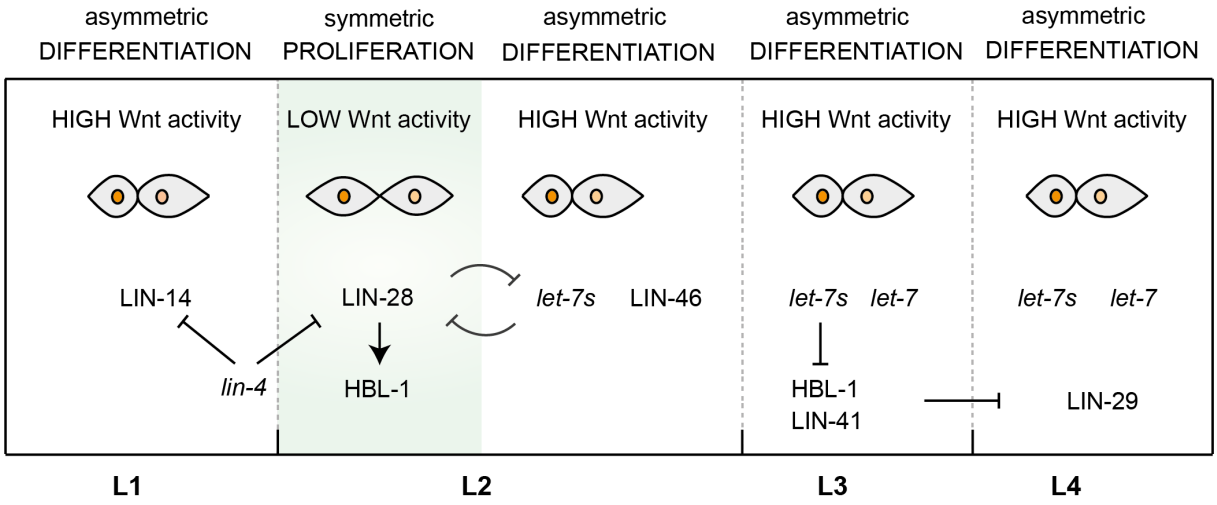

Figure 7. Sequential heterochronic gene functions control the timing of post-embryonic seam cell development. Schematic representation of the seam cell division pattern during larval development (stages L1-L4). The required functions of heterochronic genes are plotted with respect to the stages of larval development (horizontal axis). L1 stage seam cell divisions are controlled by LIN-14 and absence of *lin-4*. *lin-4* appears late L1 to repress LIN-14 and LIN-28. The early L2 symmetric division window (green box) is marked by LIN-28 expression and downstream HBL-1. LIN-28 and *let-7* have been proposed to form a bi-stable switch, with LIN-28 downregulating *let-7s* in the early L2 stage. Later-on in L2, *let-7s* levels increase and progressively downregulate LIN-28, until a tipping point were LIN-28 function is lost and cells switch back to asymmetric divisions. Late L2 seam cells are marked by *let-7s* and LIN-46 expression. L3 seam cells are marked by *let-7s* and *let-7* expression, and by low levels of HBL-1 and LIN-41. The final larval stage L4 is marked by *let-7s*, *let-7* and LIN-29 expression.

To restrict the symmetric division to the L2 stage, LIN-28 expression is suppressed during the L2 and L3-L4 stages by *lin-4* and *let-7* family miRNAs, respectively (Morita & Han 2006). The *let-7* miRNA is a conserved promotor of cell cycle exit and differentiation (Reinhart et al. 2000). Three *let-7*-related miRNAs, the *let*-7 sister (*let-7s*) miRNAs *mir-48*, *mir-84,* and *mir-241,* act before *let-7* in *lin-28* repression. In fact, LIN-28 and the *let-7* miRNA family show reciprocal inhibition, which possibly creates a bistable switch for proliferation versus

differentiation control in stem cells. This switch was found to be perturbed in various human cancers (Nimmo & Slack 2009a). As progressive repression of *lin-28* expression in seam cells starts mid L2 by miRNAs *mir-48, mir-84,* and *mir-241,* it is thought to be required to close the 'symmetry window' and enforce asymmetric division (Abbott et al., 2005; Harandi and Ambros, 2014; Pepper et al., 2004). From L3 onwards, repression of *lin-28* switches to *let-7,* which further suppresses *lin-28* levels and induces differentiation. Mutation of *let-7* results in seam cells failing to terminally differentiate in L4, and undergoing an extra round of cell division during a supernumerary larval stage (Reinhart et al. 2000). Together, these observations support conserved functions for the *let-7* miRNA family in promoting cell differentiation and countering (LIN-28-induced) stemness.

Heterochronic genes create a temporal window for symmetric divisions

At this point it is unclear whether and how the LIN-28-induced L2 seam cell division pattern relates to Wnt/β-catenin asymmetry signaling or RNT-1/BRO-1 transcriptional regulation. Several observations have indicated cross-talk between the Wnt/β-catenin asymmetry pathway and heterochronic genes. A partial loss-of-function *lit-1* allele was isolated based on a weak precocious phenotype and found to enhance precocious alae formation in *lin-28* mutants (Ren & Zhang 2010). Conversely, combination of retarded heterochronic mutations with either *mom-4, wrm-1, apr-1*, or *pop-1* knockdown partially suppressed the retarded phenotype (Ren & Zhang 2010). Although such interactions may be indirect, the KIN-19 kinase of the casein kinase I family has been suggested to mediate cross-regulation between Wnt signaling and the heterochronic network (Banerjee et al. 2010).

Further genetic analyses have been interpreted to indicate that heterochronic genes modulate Wnt/β-catenin asymmetry (Harandi & Ambros 2014). As outlined above, RNAi knockdown of *pop-1* induces multiple rounds of symmetrical seam cell divisions. This phenotype was found to be strongly influenced by heterochronic mutations (Harandi & Ambros 2014). For instance, the precocious *lin-28* mutation completely suppressed the *pop-1(RNAi)* phenotype. By contrast, mutation of *lin-14* and *lin-46* induce reiterated symmetric divisions and were found to create hypersensitivity to Wnt pathway manipulation. Such mutants formed very high numbers of seam cells when combined with *pop-1* RNAi, and very low numbers when combined with *lit-1* RNAi. Remarkably, the asymmetric cortical

localization of APR-1::GFP was disrupted in the seam cells of *lin-14* and *lin-46* RNAi animals, but not in *lin-28(lf)* mutant animals (Harandi & Ambros 2014). Together, these observations have been taken to indicate that the presence of LIN-28 temporarily destabilizes Wnt/β-catenin asymmetry, and thereby allows for symmetric cell division. It should be noted, however, that the localizations of POP-1 (Wildwater et al. 2011), as well as APR-1 and WRM-1 (Hughes et al. 2013; Harandi & Ambros 2014) remain polarized during symmetric seam cell divisions in wild-type larvae. Based on these latter observations, it is clear that the heterochronic pathway determines the pattern of seam cell divisions, but the molecular pathways that connect the players involved in this process remain to be established (Summarized in Figure 8).

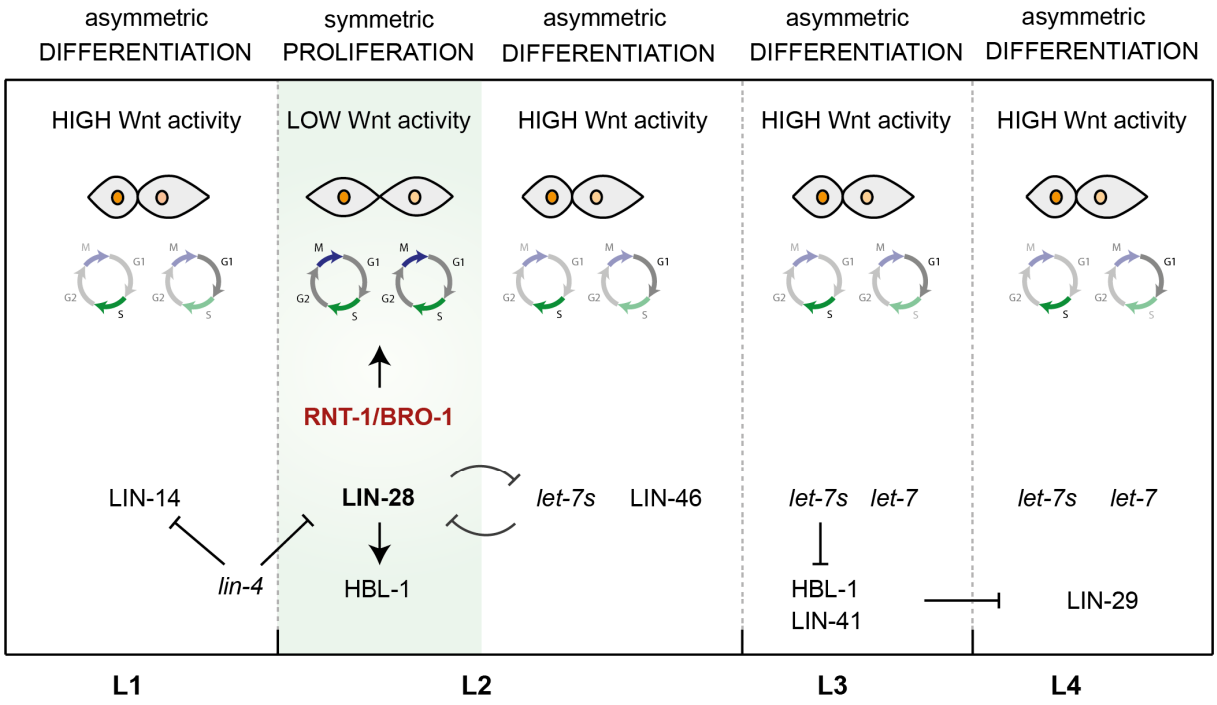

Figure 8. Cooperation between heterochronic genes and RNT-1/BRO-1 may temporarily bypass the Wnt/β-catenin asymmetry pathway in L2 stage seam cells.

Schematic representation of the seam cell division pattern during larval development (stages L1-L4). Seam cells divide asymmetrically during the L1, mid L2, L3 and L4 larval stages. The daughter cells of these divisions show different cell cycle patterns; the anterior *hyp-7*-destined daughter progresses into S-phase (left), while the posterior self-renewing daughter pauses in G1 (right). The symmetric L2 division window is marked by high LIN-28 expression levels, high HBL-1 levels and declining LIN-14 levels (green box). During this window, the RNT-1/BRO-1 complex is active and can modulate cell

cycle genes. Here, daughter cells synchronously progress through the cell cycle. Increased expression of the *let-7s* miRNAs gradually downregulates *lin-28* expression in late L2 seam cells, coincident with a return to asymmetric divisions. Wnt/β-catenin asymmetry is maintained during asymmetric as well as symmetric seam cell divisions; anterior daughter cells display high nuclear levels of POP-1 (dark orange) and posterior daughter cells low levels of POP-1 (light orange). Through mechanisms that are currently not understood, LIN-28, HBL-1, RNT-1/BRO-1, and Wnt/β-catenin asymmetry together determine the larval-stage dependent pattern of seam cell divisions.

Wnt polarity needs to be maintained to orient divisions along the A-P axis

The divergent canonical Wnt pathway instructs binary cell fates in seam daughter cells through segregation of POP-1 repressor and activator functions to different daughter cells. To separate these different POP-1 functions during cell cleavage, the mitotic spindle must be aligned along the anterior-posterior Wnt polarity axis. The Wnt/β-catenin asymmetry pathway likely fulfills a second, non-canonical, function in this process. In the *C. elegans* embryo, and *Drosophila* as well as mouse epithelia, cells may rotate their mitotic spindle up to 90° in order to instruct a cell cleavage plane perpendicular to the cell polarity axis, and thereby achieve asymmetric cell division (Knoblich 2010). In the mouse skin or neurectoderm, epithelial cells may choose between symmetrical divisions, which take place within the plane of the epithelium, or asymmetric divisions perpendicular to the epithelium. Apical-basal polarity, established through the conserved PAR proteins, guides the localization of cell fate determinants and positioning of the mitotic spindle during such asymmetric divisions (Schober et al. 1999; Wodarz et al. 1999; Kemphues 2000; Schaefer et al. 2000; Zigman et al. 2005). Seam cells form an interesting exception to these models, as both their symmetric and asymmetric divisions occur along the anterior-posterior plane of the epithelium, which is polarized by Wnt signaling components (Sulston & Horvitz 1977; Mizumoto & Sawa 2007b a). At least part of these Wnt pathway components are likely to participate in positioning the spindle as well as determining daughter cell fate.

As described early in this introduction, non-canonical Wnt signaling pathways contribute to cell division orientation in many systems (Summarized in Figure 9). Polarized Frizzled/Dishevelled complexes can act as cortical docking sites for astral microtubules during spindle orientation in *Drosophila* sensory organ precursor (pI) cells and zebrafish gastrulation (Ségalen et al., 2010). These Fz/Dvl complexes bind the NuMA$^{LIN\text{-}5/Mud}$ protein,

which interacts with dynein-dynactin complexes at microtubule ends and locks the spindle along the Wnt polarity axis (Zhang et al. 2008; Ségalen et al. 2010). Although LIN-5-dynein mediates spindle positioning in *C. elegans* (Fielmich et al. 2018), a physical connection to Wnt pathway components has not been described.

Wnt-Fz mediated spindle positioning has been well documented for several early embryonic divisions, including division of the EMS blastomere. As described above, WRM-1 localizes to the anterior cell cortex in an APR-1 (APC) dependent manner during this cell division (Mizumoto & Sawa 2007a; Sugioka et al. 2011). WRM-1 can occupy the entire cell cortex, but spindle orientation along the anterior-posterior axis requires WRM-1 to be released from the posterior cortex. Wnt signaling triggers the local release of WRM-1$^{\beta\text{-catenin}}$ from the posterior cell cortex in mitosis. This is thought to allow spindle attachments to the plasma membrane, that otherwise are blocked by WRM-1 (Kim et al. 2013a). Not only Wnt signaling is needed for WRM-1 release, but also phosphorylation of WRM-1 by CDK-1 during mitotic prophase. Thus, the temporal unmasking of a posterior membrane region is thought to allow spindle positioning in EMS (Nakamura et al. 2005; Kim et al. 2013a).

In seam cells, the anterior-posterior orientation of the mitotic spindle is achieved by Wnt-signaling as well as cellular shape (Wildwater et al. 2011). It is currently unknown whether the above mentioned WRM-1 mechanism plays a role in this orientation. In addition to the orientation of cell division, seam daughter cells differ in cell size between symmetric L2 divisions versus subsequent asymmetric cell divisions. In asymmetric divisions, anterior displacement of the mitotic spindle results in a smaller anterior daughter cell compared to the posterior daughter cell. Similar to the EMS blastomere, anterior cortical-enriched APR-1 may bind to and stabilize astral microtubules at the cell cortex of seam cells. In this way, microtubule numbers would be expected to increase locally (Sugioka et al. 2011). It is questionable whether this would increase pulling forces, as APR-1 stabilizes microtubules and thereby attenuates cortical pulling forces on the anterior centrosome in the one-cell embryo (Sugioka et al. 2018). As another candidate mechanism, Fz/Dvl signaling to the downstream CED-10^{Rac} GTPase may be used to position the spindle in seam cells, as this is a conserved mechanism also used in the early embryo (Cabello et al., 2010). Since the L1 and symmetric L2 seam cell divisions generate two equal-sized daughter cells, the mechanisms that position the spindle off-center should only become active after these divisions.

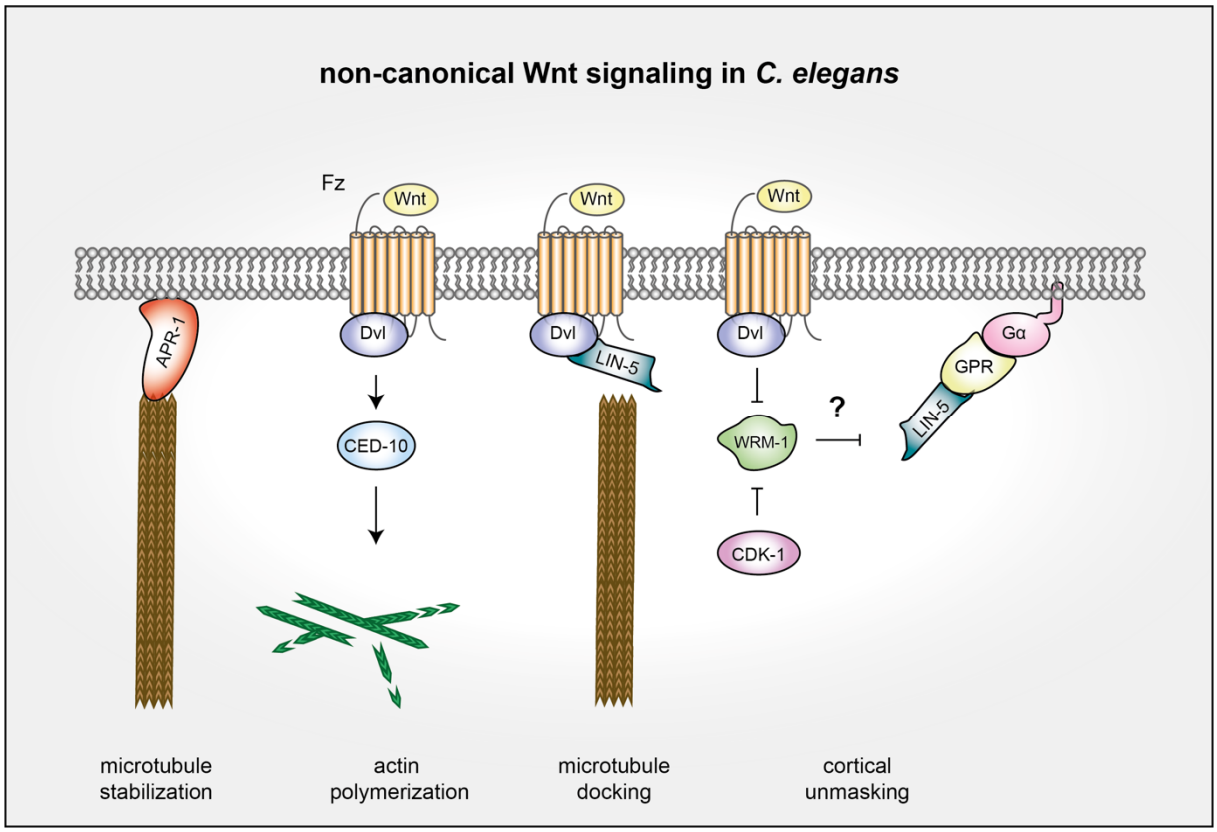

Figure 9 Cartoon of multiple candidate mechanisms that potentially participate in spindle orientation. Schematic cartoon of several non-canonical branches of the Wnt/β-catenin asymmetry pathway that could modulate mitotic spindle anchoring and division orientation in seam cells. Anterior APR-1 can stabilize microtubule plus-ends, thereby influencing spindle orientation and pulling forces (left). Polarized Fz/Dvl complexes can signal through the CED-10 GTPase to activate actin polymerization (middle left). In flies and zebrafish, polarized Fz/Dvl complexes interact with LIN-5 as part of the trimeric force generator complex. In this way, Fz/Dvl orient the spindle by anchoring microtubules along the polarity axis (middle right). Cortical localization of WRM-1 masks the cortex and suppresses spindle anchoring. CDK-1-mediated phosphorylation induces WRM-1 cortical release and unmasks this region of the cortex (right).

Daughter cell size asymmetry mechanisms uncoupled from cell fate asymmetry

Several Wnt-independent mechanisms have been identified that can also mediate spindle positioning in parallel to the Wnt/β-catenin asymmetry pathway. These either directly influence cortical microtubule attachments, or modulate the stiffness of the cortex to indirectly suppress pulling forces. Spindle pulling forces are exerted by a conserved protein complex consisting of the heterotrimeric G-protein subunits $G\alpha^{GOA\text{-}1/GPA\text{-}16}$, G-protein regulators $GPR\text{-}1/2^{LGN}$, and coiled-coil protein $LIN\text{-}5^{NuMa}$. By interacting with the dynein microtubule motor, $LIN\text{-}5^{NuMA}$ connects microtubule plus ends to the cell cortex. This requires LIN-5 association with the linker protein $GPR\text{-}1/2^{LGN}$, and membrane anchor $G\alpha^{GOA\text{-}1/GPA\text{-}16}$ (Lorson et al., 2000; Reviewed in Rose and Gönczy, 2014; Srinivasan et al., 2003). It was recently uncovered that this anchoring by LIN-5 activates dynein-mediated pulling forces (Fielmich et al. 2018). These mechanisms appear to be used in all *C. elegans* cell divisions, hence asymmetry in seam daughter cell size could result from asymmetry in pulling forces regulated at the level of LIN-5 or dynein.

Previous studies in the *C. elegans* one-cell embryo revealed how anterior enriched PKC-3 phosphorylates LIN-5 at its C-terminal region in late prophase, thereby inhibiting its function and locally suppressing force generation (Galli et al. 2011). This results in higher pulling forces on the posterior pole during anaphase, and posterior displacement of the spindle to generate a larger anterior and a smaller posterior cell. Seam cell divisions are oriented along the anterior-posterior axis, instead of the apical-basal PKC-3-PAR polarity axis. Therefore, regulation of LIN-5 by PKC-3 is not likely to determine spindle positioning during asymmetric seam cell divisions. LIN-5 could however be phosphorylated by an alternative, anterior-posterior polarized kinase. As candidate regulators, the MES-1/SRC-1 and SRC-1/PIG-1 pathways should be considered because of their roles in the EMS blastomere. MES-1 is related to transmembrane receptor tyrosine kinases and localizes to the cell-cell contact site between the P2 and EMS cells in the four-cell embryo (Berkowitz & Strome 2000; Bei et al. 2002). MES-1 subsequently recruits activated SRC-1 tyrosine kinase to the cortex (Liu et al. 2010). This posterior-enriched SRC-1 kinase could potentially phosphorylate and control LIN-5 function directly, or via the downstream kinase $PIG\text{-}1^{MELK}$ (Liro et al. 2018).

Regulation of actin-myosin accumulation at the cell cortex is yet another mechanism to control the cell cleavage plane. PIG-1^{MELK} promotes myosin distribution and asymmetric division in the *C. elegans* Q neuroblast lineage (Cordes et al. 2006; Ou et al. 2010). This PIG-1 ^{MELK} function appears to be conserved from *C. elegans* to human (Gil et al. 1997; Heyer et al. 1997). During embryonic divisions, PIG-1 localizes to the cortex between adjacent cells where it is activated by the uniformly localized PAR-4 kinase to suppress cortical accumulation of activated myosin (Pacquelet et al. 2015). Lowering actomyosin levels creates a softer and more deformable cell cortex, which permits prolonged association between force generator complexes and microtubules (Kozlowski et al. 2007; Redemann et al. 2010). In this way, cortical stiffness can indirectly control spindle positioning. The actin meshwork is bundled by the conserved non-muscle myosin (NMY-2) motor protein that induces contractile forces. Myosin was previously shown to regulate mitotic spindle positioning in the *C. elegans* one cell embryo (Severson & Bowerman 2003) and the Q neuroblast (Ou et al. 2010), but not in the EMS cell (Liu et al. 2010). When studied in seam cells, a contribution for NMY-2 in spindle positioning has not been detected (Ding & Woollard 2017). Altogether, a large variety of candidate mechanisms may contribute to the anterior-posterior orientation and anterior migration of the spindle in dividing seam cells, but which regulators are used and how they are linked to Wnt signaling remains to be discovered.

Table 1. Seam cell regulators and their loss-of-function phenotypes

Gene	Ortholog	Number seam cells	Function	Localization	Activity
control	control	16	control	-	-
Wnt/b-catenin asymmetry pathway					
lin-17	Frizzled	16	receptor	Posterior cortex	inducer
mom-5	Frizzled	16	Receptor	n.d.	inducer
mig-5	Dishevelled	16	scaffold	Posterior cortex	inducer
dsh-1	Dishevelled	16	scaffold	n.d.	inducer
dsh-2	Dishevelled	16	scaffold	Posterior cortex	inducer
apr-1	APC	>>16	scaffold	Anterior cortex	repressor
gsk-3	GSK3β	16	kinase	n.d.	repressor
pry-1	Axin	≥16	scaffold	Anterior cortex*	repressor
kin-19	CK1α	>>16	kinase	anterior	repressor
lit-1	Nemo	<<16	kinase	Anterior cortex	inducer
wrm-1	β-catenin	<<16	co-activator	Anterior cortex/ both nuclei	inducer
sys-1	β-catenin	16	co-activator	both nuclei	inducer
bar-1	β-catenin	16	co-activator	not in seam	inducer
pop-1	TCF	>>16	transcription factor	both nuclei	inducer/repressor
unc-37	Groucho	<16	co-repressor	n.d.	repressor
Runx transcriptional regulation					
rnt-1	Runx	<16	transcription factor	nucleus	repressor
bro-1	CBFβ	<16	co-repressor	nucleus	repressor
Heterochronic genes					
lin-4	n.d.	<16	miRNA	n.d.	clock gene
lin-14	n.d.	>16	transcription factor	n.d.	clock gene
lin-28	Lin28	<16	RNA-binding protein	n.d.	clock gene
hbl-1	n.d.	>16	transcription factor	hypodermis	clock gene
let-7s	let-7	>16	miRNA	n.d.	clock gene

*symmetric at the cortex of L4 stage seam cells (Baldwin & Phillips 2016)
Results summarized from the following studies: (Mizumoto & Sawa 2007a b; Banerjee et al. 2010; Gleason & Eisenmann 2010; Harandi & Ambros 2014)

SCOPE OF THIS THESIS

The proliferation of progenitor cells and tissue-specific stem cells underlies the formation and maintenance of tissues and organs. The long-term maintenance of stem cells can be achieved by asymmetric cell divisions that combine self-renewal with the generation of daughter cells that initiate a differentiation program. Alternatively, symmetric cell divisions can be used to expand the stem cell population. A tight balance between these division modes prevents both tumorous over-proliferation and premature differentiation. The research described in this thesis is aimed at finding the mechanisms that control the balance between proliferative and asymmetric stem cell divisions. These studies are based on live-observations of cell division during the development of a genetic model animal.

Chapter 1 provides a general overview of the current knowledge of asymmetric cell division in the nematode *Caenorhabditis elegans*. We focus on the stem cell-like precursors of the epidermis, known as seam cells, which actively switch between proliferative and asymmetric divisions during larval development. Studies by us and other labs revealed major regulatory roles for the atypical Wnt/β-catenin asymmetry pathway and the Runx/CBFβ transcriptional repressor in controlling division asymmetry. In this chapter, we elaborate on these mechanisms, and separate cell fate asymmetry from division asymmetry.

In **Chapter 2** we introduce a novel S-phase cell cycle sensor that allows real-time visualization of cell cycle progression. Based on a CDK2-activity sensor developed for mammalian cells, we created a cell cycle reporter for *C. elegans*, which combines a transcriptional read out for G1 progression and CDK-activity sensor. We tested this reporter in the seam epidermal stem cells, which during asymmetric cell division generate daughter cells that asynchronously progress through the cell cycle. Using this model, we show that our *C. elegans* CDK sensor allows for real-time S-phase visualization at a single cell level.

Chapter 3 addresses the question what molecular mechanisms control the decision to go through either a proliferative or an asymmetric cell division. We use a combination of genetics and high-resolution time-lapse microscopy to dissect how the Wnt/β-catenin asymmetry pathway controls alternative or identical cell fates during the division of seam cells. We show that during proliferative cell division, a Runx/CBFβ transcriptional repressor complex temporarily downregulated the Wnt/β-catenin asymmetry pathway, thereby suppressing seam cell differentiation. We propose that this modulation of Wnt pathway

activity is the fundamental difference between the proliferative and asymmetric divisions of the stem cell-like seam cells.

In **Chapter 4** we explore how asymmetry in cell fate is jointly regulated with asymmetry in cell size during asymmetric division. Using high resolution time-lapse microscopy, we show that cell fate determination is controlled independently of cell size regulation. The POP-1^{TCF} transcription factor in the Wnt/β-catenin asymmetry pathway is found to be critical for orienting cell division in the seam cell lineage. We investigate how Wnt signaling and parallel acting mechanisms instruct the placement of the mitotic spindle, to control the position and relative size of daughter cells. In preliminary experiments, we observe a correlation between the dynamic localization of non-muscle myosin NMY-2 and cell size asymmetry. Moreover, we discovered a critical role for the MELK-related PIG-1 kinase in the positioning of the spindle in mitotic seam cells.

In **Chapter 5**, the findings described in this thesis are discussed in light of the published literature.

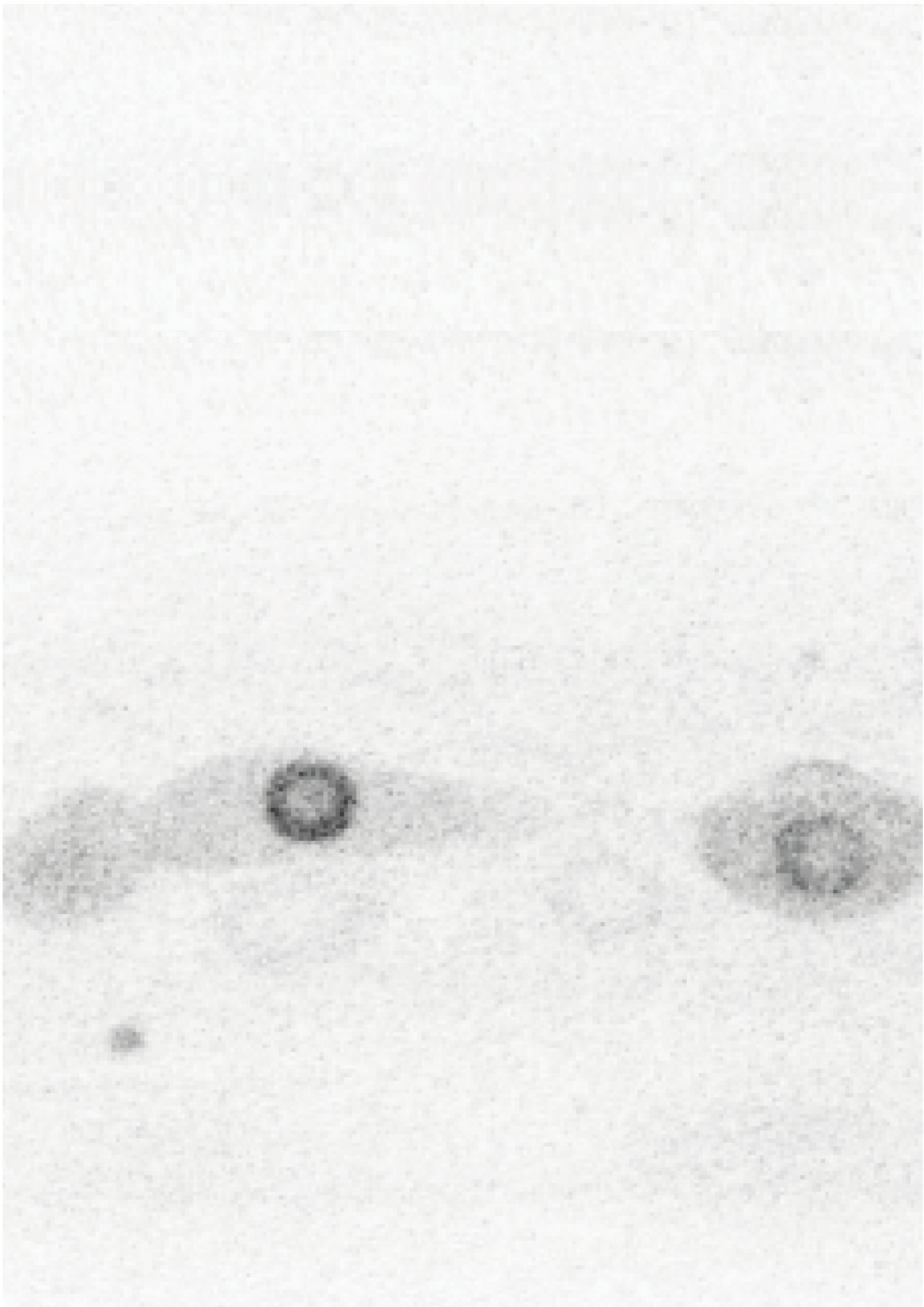

2

A dual transcriptional reporter and CDK- activity sensor marks cell cycle entry and progression in *C. elegans*

Lotte van Rijnberk, Suzanne van der Horst, Sander van den Heuvel, Suzan Ruijtenberg

Developmental Biology, Department of Biology, Faculty of Science, Utrecht University,
Padualaan 8, 3584 CH Utrecht, The Netherlands

An adapted version of this manuscript was published in *Plos One* in 2017

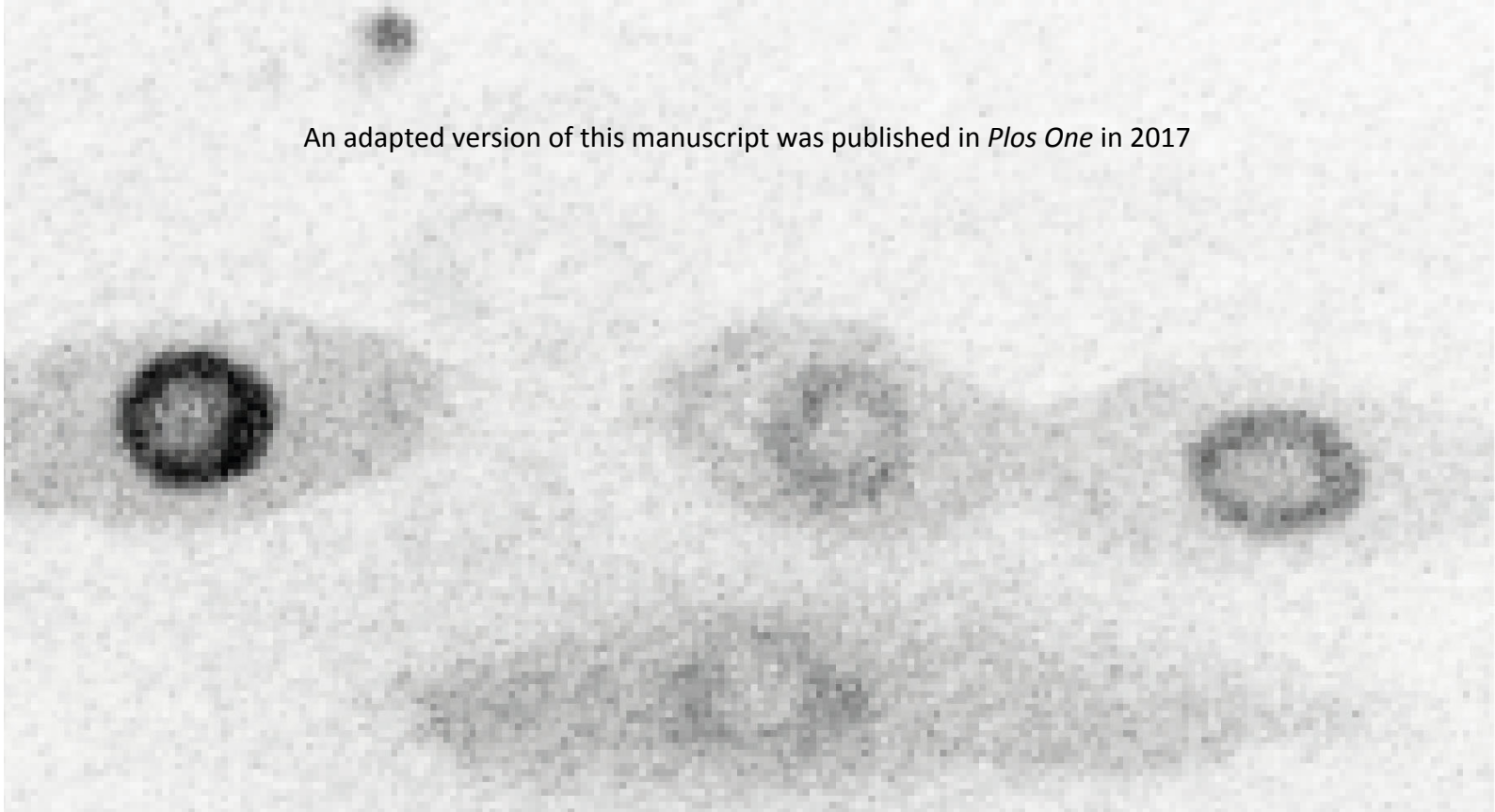

Abstract

Development, tissue homeostasis and tumor suppression depend critically on the correct regulation of cell division. Central in the cell division process is the decision whether to enter the next cell cycle and commit to going through the S and M phases, or to remain temporarily or permanently arrested. Cell cycle studies in genetic model systems could greatly benefit from visualizing cell cycle commitment in individual cells without the need of fixation. Here, we report the development and characterization of a reporter to monitor cell cycle entry in the nematode *C. elegans*. This reporter combines the *mcm-4* promoter, to reveal Rb/E2F- mediated transcriptional control, and a live-cell sensor for CDK-activity. The CDK sensor was recently developed for use in human cells and consists of a DNA Helicase fragment fused to eGFP. Upon phosphorylation by CDKs, this fusion protein changes in localization from the nucleus to the cytoplasm. The combined regulation of transcription and subcellular localization enabled us to visualize the moment of cell cycle entry in dividing seam cells dur- ing *C. elegans* larval development. This reporter is the first to reflect cell cycle commitment in *C. elegans* and will help further genetic studies of the mechanisms that underlie cell cycle entry and exit.

Introduction

Cell division follows a sequence of events that together result in the segregation of replicated chromosomes and the formation of two new daughter cells. Creating cells in the correct numbers is critical to ensure proper development and tissue homeostasis, while imbalances between the formation and removal of cells within an organism can lead to cancer (Ruijtenberg & van den Heuvel 2016). The most important decision to determine the creation of cells occurs in the G1 phase, when cells decide whether or not to enter a next cell division cycle. It has long been known that this decision depends on activation of cyclin-dependent kinases (CDKs) in association with G1 cyclins. External factors, such as the presence of nutrients (yeasts), growth factors and mitogens (multicellular organisms), determine G1 cyclin expression. In animals, growth factor signaling directly regulates the expression of D-type cyclins, while subsequent cyclin E transcription depends on activation of the cell division machinery. Cyclin D expression allows the formation of active CDK4/6-cyclin D complexes that phosphorylate the retinoblastoma protein (pRb). This reduces pRb-

mediated inhibition of activating E2F transcription factors, and permits expression of E2F dependent cell cycle genes. Cyclin E is an E2F target, which upon expression can form an active kinase with CDK2 and further inactivates pRb. The pRb/E2F-cyclin E double-negative feedback loop creates a bi-stable switch, which likely governs commitment into the cell division cycle (Yao et al. 2008; Barr et al. 2016).

While cell cycle entry is not visible under the light microscope, discovery of the green fluorescent protein (GFP) as a biological marker made it possible to visualize activation of cell cycle genes by fluorescent protein expression (Chalfie et al. 1981). Reporters containing E2F-dependent promoters, for instance of cyclin E and ribonucleotide reductase (*rnr*) subunit genes, have been used to visualize the moment cells come out of quiescence. Such reporters are less informative when examining continuously dividing cells or when determining cell cycle transitions. In addition to continued synthesis and GFP protein perdurance, such reporters do not reveal the balance between positive and negative regulators, which ultimately determines cell cycle entry (Ruijtenberg & van den Heuvel 2016). For example, it has long been observed that contact inhibition and TGFβ exposure of mink lung epithelial cells leads to G1 arrest with substantial levels of CDK2 and cyclin E (Koff et al. 1993). Activation of CDK2-cyclin E is prevented in these cells by expression of the CDK-inhibitory protein p27Kip1 (Polyak et al. 1994). Thus, while expression of G1 cyclins and E2F targets is a hallmark of cell cycle entry, this does not necessarily reflect the moment of cell cycle commitment.

Recently, improved fluorescent cell cycle reporters have been created that make use of cell cycle-controlled degradation or localization of fluorescent fusion protein. This includes the fluorescent ubiquitination-based cell cycle indicator (FUCCI) reporter system, which visualizes the transition from G1 to S phase by a switch in the presence of red and green fluorescent proteins fused to the degradation signals of Geminin and Cdt1, respectively (Sakaue-Sawano et al. 2008). Moreover, a live- cell sensor that reflects CDK-activity rather than its presence was specifically designed to mark the moment of cell cycle commitment in human cells (Gu et al. 2004; Spencer et al. 2013; Cappell et al. 2016). The CDK sensor consists of a DNA Helicase fragment linked to mVenus, which upon phosphorylation by active CDK2-cyclin E or CDK2-cyclin A relocates from the nucleus to the cytoplasm (Gu et al.

2004; Spencer et al. 2013). Expressing such a sensor within a genetic model system might allow detailed studies of cell cycle commitment in the con- text of development.

A model organism ideally suited for cell cycle studies with single cell resolution is the nematode *Caenorhabditis elegans* (Van den Heuvel & Kipreos 2012). During *C*. *elegans* development, cells follow a stereotypic division pattern, with a strictly controlled and highly reproducible timing and frequency of cell division. *C*. *elegans* uses an evolutionarily conserved Rb pathway for cell cycle regulation, with expression of the G1 cyclins CYD-1$^{\text{cyclin D}}$ and CYE-1$^{\text{cyclin E}}$ corresponding to cell cycle entry (Park & Krause 1999; Brodigan et al. 2003). The CDK-4$^{\text{CDK4/6}}$–CYD-1 kinase is required for G1/S progression during post-embryonic development, and appears to counteract G1 inhibition by the pRb family member LIN-35 and APC/C coactivator FZR-1$^{\text{Cdh1}}$ (Park & Krause 1999; Boxem & Van Den Heuvel 2001; The et al. 2015). Live-observation of cell cycle transitions could greatly help cell cycle studies in *C*. *elegans*. The currently available tools for cell cycle analysis largely depend on fixation, e.g. on BrdU or EdU labelled larvae (Van den Heuvel & Kipreos 2012). For developmentally- arrested cells, cell cycle entry can be visualized by induced expression of fluorescent proteins under the control of E2F target gene promoters (*rnr-1* and *mcm-4*) (Hong et al. 2000; Boxem & Van Den Heuvel 2001; Brodigan et al. 2003; Korzelius et al. 2011). However, these reporters tend to be continuously expressed in lineages with rapidly proliferating cells, and both daughter cells remain fluorescent even after asymmetric cell divisions that produce one arrested daughter cell (Korzelius et al. 2011). These findings highlight the need for additional reporters that allow the live visualization of cell cycle commitment.

Here, we describe the combination of the previously used *C*. *elegans* transcriptional reporter *mcm-4* with the live-cell CDK sensor as described in human cells for *in vivo* analysis of cell cycle entry during development in *C*. *elegans*. We show that this marker accurately reflects cell cycle entry and quiescence in divisions of the *C*. *elegans* seam cell lineage. This marker is the first available tool in *C*. *elegans* to visualize cell cycle commitment and will help future genetic studies of cell cycle entry.

Results and discussion

Development of a CDK sensor for *C. elegans*

In order to follow cell cycle progression in living *C. elegans* larvae, we aimed to create a fluores- cent CDK sensor based on the previously described CDK reporter in human cells (Hahn et al. 2009; Spencer et al. 2013). This sensor for CDK-activity consists of a part of the human DNA Helicase B fused to eGFP (DHB- eGFP), with a nuclear localization signal (NLS), nuclear export signal (NES), and four CDK target sites (Fig 1A). Phosphorylation is proposed to activate the NES and deactivate the NLS, resulting in cytoplasmic localization of the sensor (Fig 1B) (Regot et al. 2015). Hence, high CDK-activity causes the sensor to localize to the cytoplasm. Cytoplasmic localization is therefore a measure of CDK-activity and cell cycle progression (Fig 1B).

We codon-optimized the DHB fragment for use in *C. elegans* and created a protein fusion with codon-optimized eGFP (Redemann et al. 2011). To drive expression, the sensor was placed under the control of the ubiquitously active *eft-3* promoter and *tbb-2* β-tubulin 3' UTR. We used MosI-mediated single copy gene insertion (MosSCI) to generate transgenic lines with a single copy insertion of this CDK sensor transgene (Frøkjær-Jensen et al. 2008). As expected, use of the *eft-3* promoter resulted in DHB- eGFP expression in all somatic cells of the animal (Fig 1C). While most cells in developing larvae showed nuclear fluorescence, distinct cells, as for example seam cells (Fig 1C, arrows) contained cytoplasmic localized DHB-eGFP, which corresponded to their expected time of proliferation. Thus, a live-cell CDK-activity reporter based on a human DNA Helicase B fusion protein appears suitable for use in *C. elegans*. At the same time, the universally high fluorescence levels made it difficult to detect the low numbers of cycling cells among the many quiescent and post-mitotic cells.

To restrict eGFP expression to proliferating cells, we decided to place the live-cell sensor under the control of a cell cycle-regulated promoter. In our previous studies, we observed high expression of MCM-4 (LIN-6) in all proliferating cells in *C. elegans* (Korzelius et al. 2011). MCM-4 is one of the six sub- units of the MCM2-7 replicative DNA helicase. The helicase activity is required for unwinding of the DNA in the licensing of DNA replication and during S phase. When expressed under the control of the *mcm-4* promoter, the sensor was only

present in proliferating cells, in contrast to the *Peft-3*-based reporter (Fig 1C and 1D). Similar to the results obtained in human cells, a dynamic localization of the sensor was observed as cells progressed through the cell cycle. The translocation from the nucleus to the cytoplasm was clearly visible in cells of the epidermal seam and Q neuro- blast lineages and vulva precursor cells (Fig 1E–1G). The sensor was also expressed in cells of the intestine, but nuclear localized fluorescence remained present in these cells, possibly reflecting their endo-replication cycles (Fig 1H). Overall, these observations indicate a wide dynamic range of sensor localization and its potential to visualize cell cycle progression.

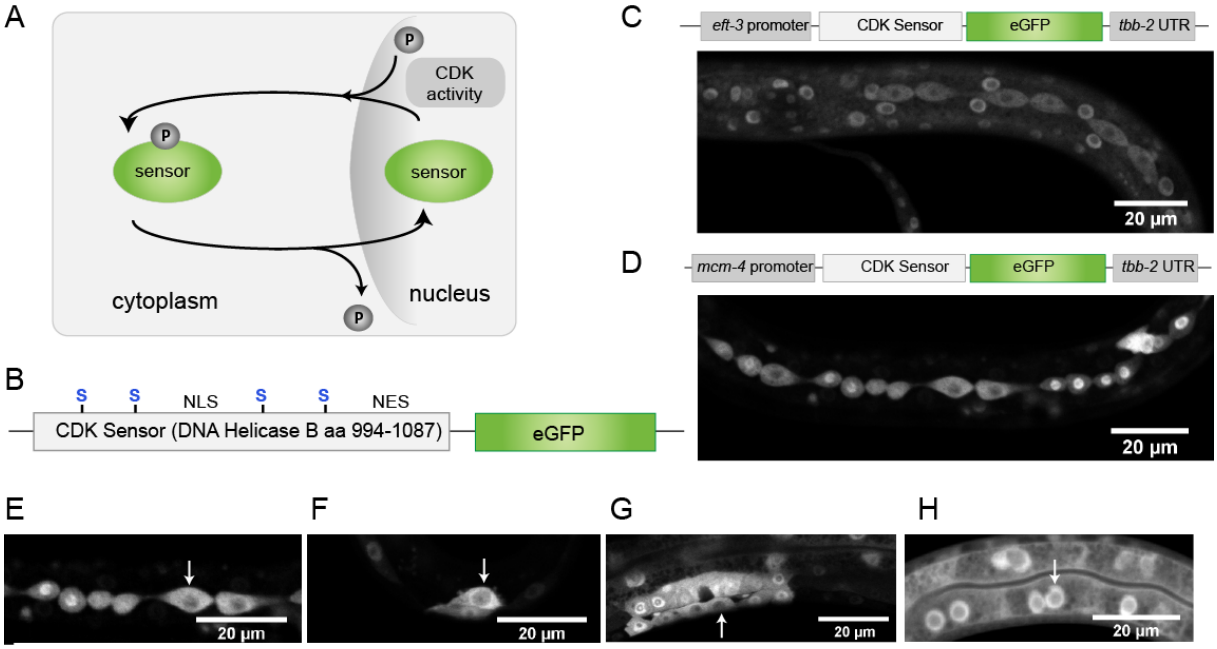

Figure 1. Dynamic localization of the CDK sensor in *C. elegans*. (A) The CDK-2 sensor consists of amino acids 994 till 1087 of Human DNA Helicase B with an NLS, NES, and four CDK target sites, and is fused to eGFP. Both the sensor and eGFP are codon optimized for use in *C. elegans*. (B) The phosphorylation status of the DHB fragment determines whether the sensor localizes to the nucleus or to the cytoplasm. As CDK-cyclin complexes are activated during cell cycle progression, the sensor becomes phosphorylated and accumulates in the cytoplasm. (C-H) Representative fluorescence microscopy images highlighting sensor expression and localization in a variety of tissues. (C) Expression of the sensor from the general *eft-3* promoter resulted in expression in all somatic cells of the animal. Arrow indicates seam cells in which the sensor is localized in the cytoplasm. (D-H) expression from the cell cycle regulated *mcm-4* promoter is specifically detected in cells that have the potential to divide, as shown for seam cells in an L3 larva (D). (E-H) Dynamic sensor localization was observed in seam cells (E), Q cells (F), vulval precursor cells (G), and to a lesser extent in intestinal cells (H).

Visualization of cell cycle progression in the stem cell-like epidermal seam cells

We further investigated the dynamics of CDK sensor localization for cells of the seam cell line- ages, for which an interesting cell cycle regulation pattern has been described (Sulston & Horvitz 1977; Hedgecock & White 1985). Seam cells form two rows of epithelial cells on the lateral sides of the animal. During each larval stage, the seam cells go through one round of asymmetric cell division, which creates a novel seam cell and a daughter cell that forms differentiated neurons or fuses with the general syncytium of the skin (hyp7). Interestingly, the differentiating anterior daughter cells go through S phase before fusing with hyp7 (Fig 2A) (Hedgecock & White 1985). The posterior daughters become quiescent and only progress into S phase around the transition to the next larval stage (Hedgecock & White 1985; Hong et al. 2000). In the second larval stage, however, the seam cell number increases through an extra symmetric cell division, which is followed by S phase entry and asymmetric cell division of both daughter cells. We previously observed expression of MCM-4::mCherry in both seam daughter cells, after symmetric as well as asymmetric cell division, illustrating that this reporter reflects proliferation potential but not cell cycle commitment (Korzelius et al. 2011).

In order to investigate whether we could visualize the difference in cell cycle progression between the anterior and posterior seam daughter cells, we performed time-lapse imaging on living animals expressing the *Pmcm-4*::*DHB-eGFP* reporter. Using spinning disk confocal fluo- rescence microscopy, we followed seam cells for several hours during asymmetric divisions in the third larval stage (L3) (Fig 2B, S1 Mov). This revealed that the CDK sensor becomes increasingly localized in the cytoplasm as cells progress through the cell cycle, with the highest cytoplasmic levels observed just before mitosis and cytokinesis. In contrast, the sensor showed a strong nuclear localization in both newly formed daughter cells (Fig 2B). Interestingly, differ- ences in sensor localization appeared over time between the anterior and posterior daughter cells (Fig 2B bottom, S1 Fig, S1 Mov). The differentiating (anterior) daughter cells that proceed through S phase show gradually reduced nuclear levels of the sensor and translocation to the cytoplasm, indicating activation of CDKs and entry into the next cell cycle. The sensor remained nuclear in the posterior cells at this time point (Fig 2B, bottom, S1 Fig, S1 Mov). These data demonstrate that combining the *mcm-4* promoter and

CDK sensor creates a valu- able marker for visualizing cell cycle progression, and allows determining cell-to-cell differ- ences in the timing and speed of cell cycle entry.

In order to more precisely quantify sensor localization, we used ImageJ software to measure cytoplasmic and nuclear fluorescence intensities. Markers for the DNA (*Pwrt-2*::*H2B*::*mCherry*) and cell membrane (*Pwrt-2*::*PH*::*mCherry*) helped us to select regions of interest and regions for background subtraction (see Material and Methods for Extended experimental procedures). A cytoplasmic-to-nuclear ratio was calculated from these measurements to determine sensor dynamics, with a high ratio as a read-out for cytoplasmic localization and a low ratio indicating nuclear localization of the sensor (Fig 2C). Confirming the visual examinations mentioned above, the calculated ratios show an increase in the cytoplasmic-to-nuclear ratio
as cells progressed through the cell cycle. At the time of prometaphase, this ratio suddenly dropped. We measured an apparent transient increase in ratio just after anaphase onset, although there is no nuclear membrane at this point and thus the nucleus cannot be defined. As soon as nuclei reformed, the cytoplasmic over nuclear ratio dropped from approximately 1 to 0.25 in both daughter cells. However, from approximately 30 minutes after anaphase onset, differences in sensor localization between the anterior and posterior cells could be observed (Fig 2C asterisk, S1 Mov). In the anterior daughter cell, the ratio started to climb, while a further decline was observed in the posterior cell (Fig 2C. S1 Mov). Approximately 45 minutes after anaphase onset, the difference between the anterior and posterior cell is significantly different (arrow in Fig 2C; $p < 0.05$ at 44 min. after anaphase). Because quantification is laborious and low numbers were examined, the fact that the difference in levels of nuclear GFP are detectable by visual inspection is particularly meaningful (S1 Fig, S1 Mov). The cytoplasmic-to-nuclear ratio of the anterior daughter cell increased to around 0.5, approximately two times higher than that of the posterior daughter cell, consistent with the fact that the anterior cell proceeds into S phase while the posterior cell remains in G1 (Fig 2A). These quantifications indicate the timing of S phase commitment in the anterior cells, as this likely coincides with or precedes the moment that the plotted ratios of this cell start to differ from those of the posterior cell (Fig 2C, asterisks and arrow). The same conclusion can be reached more easily by visual inspection of sensor localization, which provides a convenient method for detecting cell cycle entry (S1 Mov).

As mentioned above, seam cells go through a symmetric cell division in the second larval stage (L2). We analyzed the sensor dynamics in this division to further test the correlation between cytoplasmic localization and cell cycle entry (Fig 2D, S2 Mov). Before anaphase, cells going through a symmetric L2 division show localization dynamics that resemble those of cells initiating an asymmetric L3 division; there is a rise in the cytoplasmic over nuclear ratio prior to anaphase, followed by a rapid decrease. However, the localization dynamics after anaphase differed from those in L3 divisions. The ratio did not drop below approximately 0.35 and started to go up approximately 30–50 minutes after anaphase. Importantly, both daughter cells showed a very similar increase in cytoplasmic localization of the CDK sensor and these levels further increased to a similar ratio as observed prior to the preceding anaphase (Fig 2E, t = 160). This is in agreement with these cells progressing into the next division (asymmetric L2 division) immediately after the symmetric L2 division. Thus, the localization of the CDK sensor varies with cell cycle commitment and cell cycle progression, while previous reporters showed similar expression in the daughter cells of symmetric and asymmetric cell divisions (Korzelius et al. 2011). Thus, the *Pmcm-4*:: *DHB-eGFP* reporter appears suitable for monitoring cell cycle entry in *C. elegans*, which is difficult to visualize otherwise.

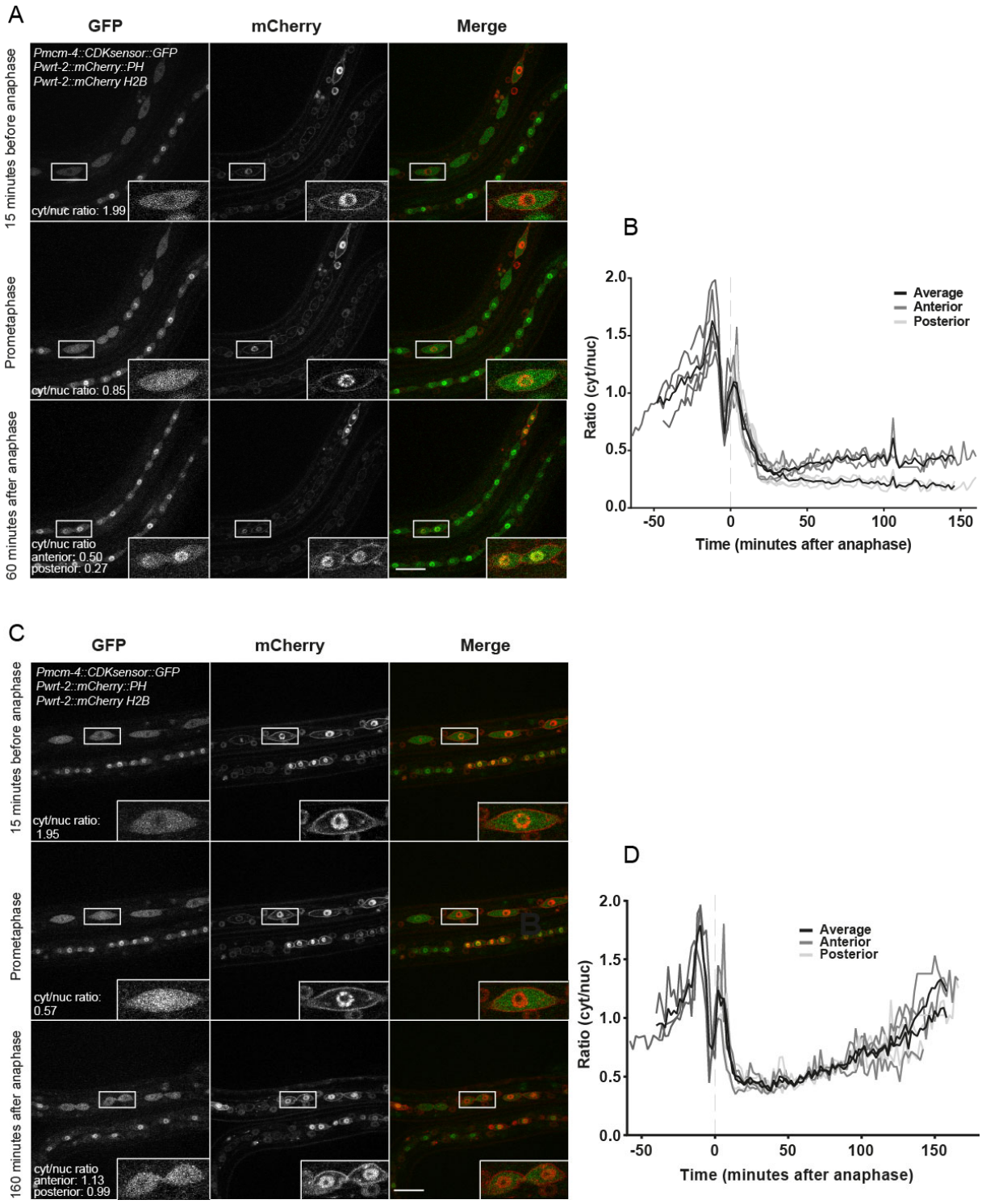

Figure 2. Sensor dynamics in L3 asymmetric and L2 symmetric seam cell divisions. (A) Schematic overview of divisions in the Vn seam cell lineages (n = 1–4, 6). These seam cells undergo one asymmetric cell division during every larval stage (L1-L4). During these divisions the seam cells produce a posterior self-renewing daughter cell (Vn.p), and an anterior daughter cell that differentiates and fuses with the hyp7 syncytium (Vn.a; orange circles). In the second larval stage (L2), seam cells undergo one additional, symmetric cell division, producing two self-renewing seam

daughter cells. (B) Still images and blow-ups from spinning disk confocal fluorescence microscopy time-lapse movies of larvae staged at 24 hours after hatching. From top to bottom, images show seam cells (V3.pap, anterior to the left) before anaphase, during nuclear envelope breakdown at prometaphase, and after anaphase (V3.papa and V3.papp). Note that in the two newly formed daughter cells, nuclear export of the sensor is observed in the anterior daughter cell before it is observed in its posterior sister cell. Scale bar indicates 20 μm. (C) Graph representing the cytoplasmic-to-nuclear ratio (cyt/nuc) of DHB-eGFP in seam cell L3 asymmetric division (n = 5). Anterior cells in orange, posterior cells in blue, average ratio is indicated by a black line. Asterisk indicates the moment where plotted ratios in the anterior cell start to deviate from the ratios in the posterior cell. The arrow indicates the moment where the difference in ratios is statistically significant (t = 44 min after anaphase). Cells are aligned at the moment of anaphase (t = 0). (D) Still images and blow-ups of spinning disk confocal microscopy movies of worms staged at 20 hours after hatching. From top to bottom, images show seam cells (highlighted: V2.p, anterior to the left) before anaphase, during nuclear envelope breakdown at prometaphase, and after division (V2.pa and V2.pp). Note that in the two newly formed daughter cells the rate of nuclear export of the sensor is similar. Anterior to the left, scale bar indicates 20 μm. (E) Graph representing the cyt/nuc ratio of DHB-eGFP in symmetric L2 seam division (n = 3). Anterior cells in orange, posterior cells in blue, average ratio is indicated by a black line. The cells are aligned at the moment of anaphase (t = 0).

The CDK sensor as a marker for S phase entry

The quantifications above show that the cytoplasmic-to-nuclear DHB-eGFP ratio drops strongly in mitosis, and continues to decline further in the G1 arrested posterior daughter cell of an asymmetric seam cell division. The anterior cell that re-enters S phase shows a gradual increase in cytoplasmic-to-nuclear DHB-eGFP, starting approximately 30–40 minutes after anaphase. The CDK sensor remained partly nuclear in this latter daughter cell, and DNA synthesis is expected to take place while the DHB-eGFP cytoplasmic-to-nuclear ratio remains below 0.5 (Fig 2C). We wondered whether such a low cyt/nuc ratio indeed corresponds to S phase, or whether it remains particularly low in the hyp7-destined daughter cells in which S phase is not followed by mitosis. To address this question, we set out to determine the sensor distribution during S phase of the mitotic seam cell cycles in the first larval stage (L1).

To determine the timing of S phase in seam cells in L1, we made use of synchronously grown larvae that were fixed at distinct time points. Initially, we used growth on EdU containing bacteria to be able to detect new DNA synthesis. At 4 hours of larval development, incorporation of EdU could be detected in part of the seam cells, but this method did not seem sensitive enough to visualize the initiation of DNA synthesis (S2 Fig). As an alternative method, we used propidium iodide (PI) incorporation to determine the DNA content in larvae fixed at subsequent time points (Fig 3A) (Boxem & Van Den Heuvel 2001; Van den Heuvel & Kipreos 2012). Quantification of PI staining confirmed that the timing of DNA synthesis varies between seam cells, and showed that most seam cells enter S phase between 2 and 3 hours of larval development (Fig 3A). This conclusion is in agreement with a previous report, which used expression of a *Prnr*::*tdTomato* reporter to estimate the timing of S phase in seam cells (Kim et al. 2007).

Next, we used live-cell imaging to examine the subcellular distribution of the CDK sensor around the timing of S phase in the L1 asymmetric seam cell divisions (Fig 3B). Consistent with the PI staining results, we observed a substantial rise in cytoplasmic localization of the CDK sensor between two and three hours of larval development. The distribution of the sensor varied somewhat between individual seam cells at 3 hours of larval development, but the average cytoplasmic-to-nuclear ratio was very close to 0.5 (0.49 ± 0.15) (Fig 3B). This corresponds to the ratio found in the anterior daughter cells going through S phase after asymmetric cell division (Fig 2C). Thus, activation of CDKs present in S phase (most likely CDK-2/CYE-1 and possibly CDK-2/CYA-1) results in partial translocation of the sensor to the cytoplasm, and a cytoplasmic-to-nuclear ratio of approximately 0.5. In contrast to the anterior cells after asymmetric divisions, however, the cytoplasmic accumulation continued to increase at later times of the mitotic L1 seam cell cycle. These data indicate that initial phosphorylation and nuclear export of the sensor during S phase is followed by increased phosphorylation during G2 and early mitosis (see below).

As an alternative and complementary method to determine the dynamics of the DHB- eGFP reporter in S phase, we exposed newly hatched larvae to hydroxyurea. Hydroxyurea blocks the ribonucleotide reductase enzyme and thereby abolishes the production of deoxyribonucleotides, causing cells to arrest in S phase (Fig 3C) (Euling & Ambros 1996;

Korzelius et al. 2011). Live-cell imaging revealed that in control animals at 5 hours after hatching, the sensor was mainly present in the cytoplasm of the seam cells. In contrast, in hydroxyurea treated animals, the sensor failed to fully exit the nucleus, resulting in a cytoplasmic-over-nuclear ratio of around 0.5, which differs significantly from control animals ($p < 0.0001$). Since hydroxyurea causes replication stress and contributes to activation of the intra-S phase checkpoint that inhibits CDKs (Karnani & Dutta 2011), we cannot rule out the possibility that hydroxyurea itself may also have an inhibitory effect on CDK-activity and sensor localization. Nevertheless, these data are in agreement with the conclusion that partial translocation and a DHB-eGFP cytoplasmic-to-nuclear ratio of around 0.5 is indicative for seam cells going through S phase. In mitotic cell cycles, but not endoreplication cycles, a more complete relocalization of the sensor takes place during the late S and G2/M phases.

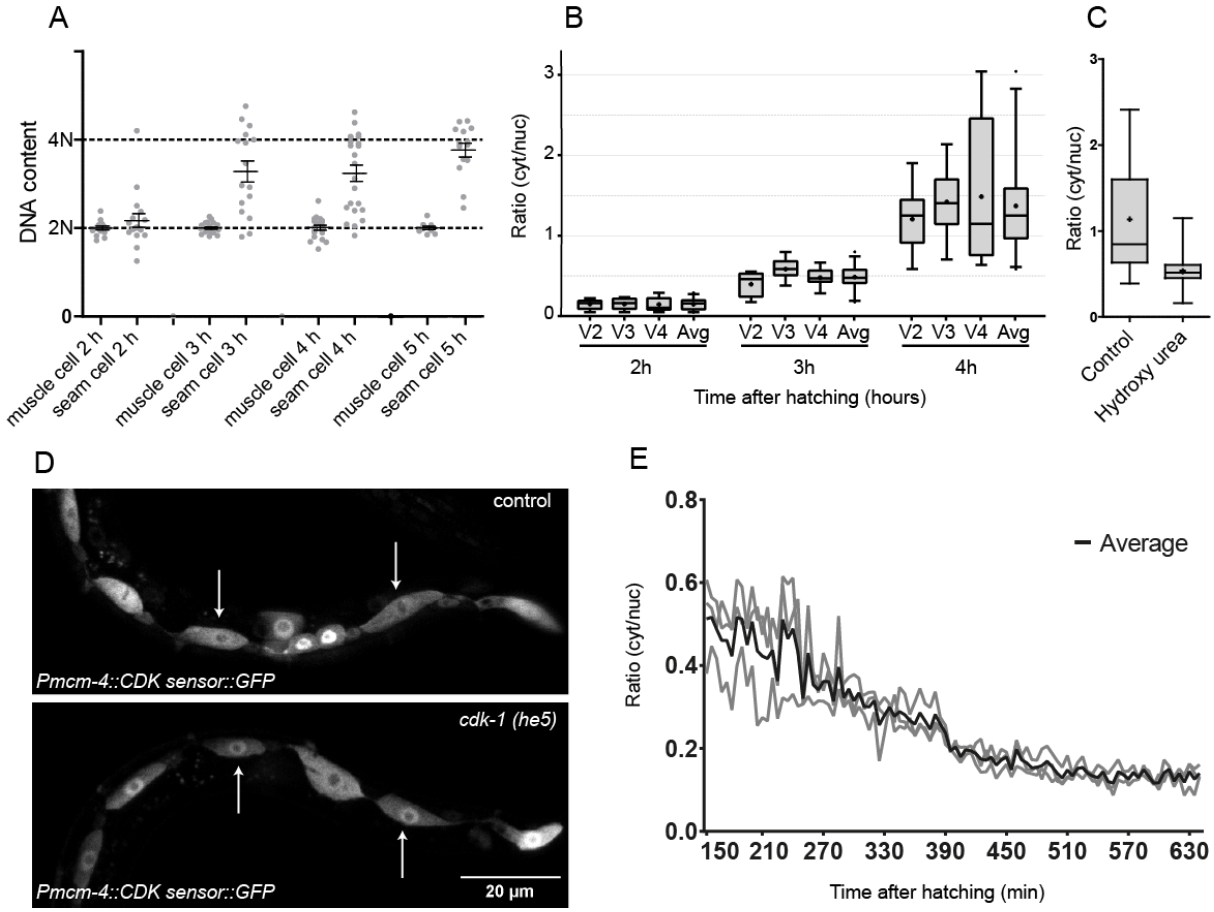

Figure 3. Sensor localization during S phase and CDK-1-dependent phosphorylation of the sensor. (A) Quantification of DNA content by propidium iodide staining in L1 larvae at 2, 3, 4 and 5 hours after hatching. Muscle cells were used as the reference for a 2N DNA content. Error bars indicate SEM. (B) Boxplots of ratios calculated from confocal fluorescence microscopy images of larvae staged at 2, 3 and 4 hours after hatching (n = 9 for single seam cells,
n = 27 for average of cells). Avg. refers to the average ratio of V2, V3 and V4 together. The borders of the boxes are the 25th and 75th percentile, • indicates the mean, error bars correspond to 1.5× the interquartile range, outliers are shown. (C) Boxplots containing the quantification of cytoplasmic-to-nuclear fluorescence ratio in control and HU-treated larvae, 5 hours after hatching (n = 9). The borders of the boxes are the 25th and 75th percentile, the mean is indicated by **+**, error bars correlate to 1.5× the interquartile range. (D) Live-cell imaging of WT (top) and *cdk-1(he5)* mutant (bottom) larvae expressing the CDK sensor, at 300 minutes (5 hours) after hatching. (E) Spinning disk confocal fluorescence microscopy time-lapse movie analysis of sensor localization in control animals (n = 3 cells) and *cdk-1(he5)* mutants in L1 (n = 3). Control cells before anaphase in grey, control anterior cells in orange, control posterior cells in blue, *cdk-1(he5)* mutant cells in green. Average ratio is indicated by a bold line, individual cells are shown with thin lines. Dotted black lines indicate the time between anaphase and nuclear envelope reformation, where ratios could not be determined because of absence of the nucleus. (F) Comparison between the maximal calculated ratio's in control (n = 10) and *cdk-1(he5)* (n = 14) animals during L1 development. The borders of the boxes are the 25th and 75th percentile, the mean is indicated by–, error bars correlate to 1.5× the interquartile range.

Nuclear export of DHB-eGFP likely depends on sequential phosphorylation by CDK-2 and CDK-1

The DHB-mVenus live-cell sensor described in human cells has been suggested to be preferentially phosphorylated by CDK2-cyclin E and CDK2-cyclin A (Spencer et al. 2013). However, the increased cytoplasmic localization when cells get closer to mitosis appears to indicate a contribution of CDK1 in association with mitotic cyclins. CDK1 is the most potent CDK, which can phosphorylate overlapping targets and substitute for CDK2 in mouse development (Satyanarayana & Kaldis 2009). *C. elegans* CDK-1 is specifically required for mitosis: homozygous *cdk-1* mutants complete embryogenesis in the presence of maternal product, go through DNA replication, but fail to enter mitosis during larval development

(Boxem et al. 1999). To examine the contribution of CDK-1 to the phosphorylation of the DHB-eGFP sensor, we made use of the *cdk-1(he5)* presumed null allele. Using live- imaging as described above, we analyzed sensor localization in the seam cells after hatching. Around 5 hours of larval development, wild-type seam cells showed predominantly cytoplasmic localization of the sensor prior to mitosis (Fig 3D, top). In *cdk-1* mutant larvae the sensor was only partially translocated to the cytoplasm and remained enriched in the nucleus (Fig 3D, bottom). We quantified the cytoplasmic-to-nuclear ratios starting at 2.5 hr of L1 development in *cdk-1* mutants and control animals. In control animals, sensor localization showed a very similar pattern as observed during the asymmetric L3 division: the cyt/nuc ratio increases towards mitoses, drops after anaphase, after which the ratio starts to rise in the anterior cell (Orange lines, Fig 3E) while remaining low in the posterior (Blue lines Fig 3E). In contrast to control animals, *cdk-1* mutants, showed a maximum ratio of around 0.5 (green lines Fig 3E), very similar to the ratio observed in the anterior daughter cells when they enter S-phase (30– 40 min after anaphase), before fusing with the hyp-7 syncytium (Fig 2A, green and orange line 3E). Comparison between the maximum ratio observed in control and mutant animals showed that this difference in cyt/nuc ratio was statistically highly significant ($p < 0.0001$) (Fig 3F). Notably, the ratios gradually continued to decline in the *cdk-1* mutants as DHB-eGFP started to accumulate in the nucleus again (Fig 3E). This nuclear relocalization likely indicates the requirement for continued phosphorylation to promote nuclear export. Phosphatases probably dephosphorylate the sensor, leading to nuclear re-accumulation after S phase when CDK-1 kinase activity is absent. Taken together, these data show that CDK-1 contributes to phosphorylation and translocation of the DHB-eGFP CDK sensor in *C. elegans*. However, the initial phosphorylation seems to be mediated by other kinases, possibly by the S-phase kinase CDK-2 in association with CYE-1$^{\text{cyclin E}}$ as described for human cells (Spencer et al. 2013).

In summary, we have successfully created a *C. elegans* CDK sensor, making use of the previously reported live-cell sensor for human cells in culture. This sensor provides an attractive tool for monitoring cell cycle progression during development, with single cell resolution and in real time. Combining the CDK sensor with a *mcm-4* promoter restricted fluorescence to cells with proliferation potential. This greatly helped recognizing and characterizing the cells of interest. We already made use of the sensor to determine the

approximate timing of cell-cycle commitment of seam cells after symmetric and asymmetric cell division. We observed that cytoplasmic localization of the sensor depends on continuous CDK phosphorylation, and requires CDK-1 in G2/M. We propose a model in which the sensor could initially be phosphorylated by CDK-2/ CYE-1 cyclin E in late G1/early S phase, which reveals the moment of cell cycle commitment. Subsequent phosphorylation by other kinases, possibly CDK-2/CYA-1 cyclin A in late S, and CDK-1/CYA-1 and CDK-1/CYB-1-3 cyclin B in G2 and mitosis are likely to further promote nuclear export. Based on the observed pattern of sensor localization we conclude that the CDK- 1 kinase remains inactive during the endoreplication cycles of seam and intestinal cells.

Materials and methods

C. elegans strains and culture

Animals were cultured on NGM plates seeded with OP50 bacteria according to standard protocol. All strains were maintained at either 15 or 20˚C. N2 Bristol is used as the wild type. Strains used are listed in S1 Table. Hydroxyurea was supplied to worms by adding 0,5 mL 500 mM hydroxyurea to NGM plates (containing approximately 10 gr NGM) before seeding, which after diffusion results in a 25 mM concentration. Larvae were synchronized by hypochlorite treatment and hatching of L1 animals in M9 medium + 0.05% Tween-20. Alternatively, for spinning disk confocal fluorescence microscopy time-lapse movies, larvae were staged by sequential wash-off from plates with egg-laying adults.

Molecular cloning

Primers are listed in S2 Table. *Peft-3*::CDK *sensor* construct was made by Gibson Assembly of fragments of the CDK *sensor* (made by PCR of a G block containing the sensor with primers 422 and 423), eGFP (made by PCR from a vector containing eGFP with primers 424 and 425) and *tbb-2 3'UTR* (made by PCR from a vector containing the *tbb-2 UTR* with primers 426 and 427) into a MosSCI-II vector containing the *eft-3* promoter (cut with AscI and SbfI). *Pmcm-4*:: CDK *sensor* construct was made by ligating the *mcm-4* promoter (made by PCR from a vector containing *Pmcm-4* with primers 428 and 429 and digestion with SpeI and AcsI) into the previously described *Peft-3*::CDK sensor construct (digested with SpeI and AcsI).

Microinjection and transformation

Microinjection was performed as described previously (Van den Heuvel & Kipreos 2012). For MosSCI integration, mos II worms were injected with 30 ng/µL mos transposase, 10 ng/µL of MosSCI-II construct con- taining the desired insert and 2,5 ng/µL *myo-2*::*TdTomato* together with 10 ng/µL *sur-5*::*dsRed* as co-injection marker.

Live cell imaging by confocal microscopy

Images of worms were obtained using a Zeiss LSM700 Confocal microscope, at a magnification of 40×. Worms were synchronized by hypochlorite treatment and hatching L1

animals in M9 medium + 0.05% Tween-20. Slide preparation was performed by washing off and spinning down animals, and transferring 2 µL of worm pellet to 4% agarose slides with 2 µL 10mM tetramisole.

Live cell imaging by spinning disk confocal microscopy

Worms were synchronized by wash-off staging. For L2 and L3 worms, slide preparation was performed by washing off and spinning down animals, and transferring 3 µL of worm pellet to 5% agarose slides with 1 µL 10 mM muscimol. For L1 worms, 7% agarose slides were used and muscimol was replaced by 10 mM tetramisole (2 µL tetramisole with 2 µL worms). L2 and L3 worms were imaged with a Nikon Eclipse Ti-U, using the following Microscope settings: Laser 488: 8% 150 ms, Laser 563: 10% 150 ms, 2x2 binning, no averaging, every 2 minutes z-stack with 3 frames of 0.5 micron. Microscope settings for L1 worms are: Laser 488: 8% 150 ms, Laser 563: 10% 150 ms, 2x2 binning, no averaging, every 5 minutes z-stack with 6–8 frames of 0.1 micron.

Edu and pi staining

Immunohistochemical analyses and staining of DNA with propidium iodide and DAPI were performed as previously described (Van den Heuvel & Kipreos 2012). EdU labelling and staining were performed according to a protocol using the Click-IT EdU Alexa Fluor 594 kit (Life Technologies) as previously described (Van den Heuvel & Kipreos 2012). Primary and secondary antibodies used for immunofluorescent staining are as follows: mouse anti-AJM-1 (1:20, MH27, Developmental Studies Hybridoma Bank), goat anti-mouse-Alexa488 and goat anti-mouse-Alexa568 (1:500 Developmental Studies Hybdridoma Bank).

Analysis and quantification of sensor localization

Sensor localization was quantified by measuring the cytoplasmic-to-nuclear ratio (cyt/nuc ratio) using Fiji (ImageJ). Regions of interest, the nucleus and cytoplasm, were drawn either by hand (freehand selection tool) or using the 'analyze particles' function as described in supplemental Methods. Measurements were obtained from the image after background subtraction, and were used to calculate the cyt/nuc ratio by dividing cytoplasmic intensity by nuclear intensity.

Acknowledgments

We thank R. Korswagen and M. Boxem for strains, and members of the van den Heuvel and Boxem groups for help and discussion. We thank Eugene Katrukah (A. Akhmanova lab) for help and expertise with analyzing fluorescence intensities and calculating cytoplasmic over nuclear ratios. Some strains were provided by the CGC, which is funded by NIH Office of Research Infrastructure Programs (P40 OD010440).

Supporting information

S1 Table. *C. elegans* strains.

Strain	Description	Additional information
KN2595	*dpy-20 (e1362) ; huIs166 [Pwrt-2::mcherry::ph Pwrt-2::mcherry::h2b dpy-20 (+)]*	
SV93	*ncc-1(he5)/qc1dpy-19(e1259) glp-1(q339)III*	
SV1667	*unc-119 (edIII) ; hesi 191 [Peft-3::cdk sensor::gfp::tbb-2 utr + cbr-unc119(+)] II, line 1*	
SV1668	*unc-119 (edIII) ; hesi 192 [Peft-3::cdk sensor::gfp::tbb-2 utr + cbr-unc119(+)] II, line 2*	
SV1669	*unc-119 (edIII) ; hesi 193 [Pmcm-4::cdk sensor::gfp::tbb-2 utr + cbr-unc119(+)] II*	
SV1691	*unc-119 (ed3) III ; hesi 191 [Peft-3::cdk sensor::gfp::tbb-2 utr + cbr-unc119(+)] II ; dpy-20 (e1362) ; [Pwrt-2::mcherry::ph Pwrt-2::mcherry::h2b dpy-20(+)]*	Some silencing of mCherry in seam cells
SV1692	*unc-119 (ed3) III ; hesi 191 [Peft-3::cdk sensor::gfp::tbb-2 utr + cbr-unc119(+)] II ; dpy-20 (e1362) ; [Pwrt-2::mcherry::ph Pwrt-2::mcherry::h2b dpy-20(+) lin-48::gfp]*	Some silencing of mCherry in seam cells
SV1693	*unc-119 (ed3) III ; hesi 191 [Peft-3::cdk sensor::gfp::tbb-2 utr + cbr-unc119(+)] II ; [Peft-3::tdtomato::h2b::unc-5 utr + cbb-unc-199(+)],*	
SV1694	*unc-119 (ed3) III ; hesi 193 [Pmcm-4::cdk sensor::gfp::tbb-2 utr + cbr-unc119(+)] II ; dpy-20 (e1362) ; [Pwrt-2::mcherry::ph Pwrt-2::mcherry::h2b dpy-20(+)]*	Some silencing of mCherry in seam cells
SV1807	*unc-119 (ed3) III ; hesi 193 [Pmcm-4::cdk sensor::gfp::tbb-2 utr + cbr-unc119(+)] II ; oxTi619 [Peft-3::tdtomato::h2b::unc-54 utr + cbr-unc119(+)] ; ncc-1(he5) III*	
SV1808	*unc-119 (edIII) ; hesi 193 [Pmcm-4::cdk sensor::gfp::tbb-2 utr + cbr-unc119(+)] II ; oxTi619 [Peft-3::tdtomato::h2b::unc-54 utr + cbr-unc119(+)] II*	

S2 Table. Primers and oligos.

Name	Sequence
cdk-2 sensor F GA	ctaccgtccgcactcttcttac
cdk-2 sensor R GA	caacaagaattgggacaactccagt
GFP codopt F GA	atgagtaaaggagaagaacttttcactgg
GFP codopt R GA	aagggaatgcttgaaaggattttgcatttatcgcggccgcttatttgtatagttcatccatgccatgtg
tbb-2 F GA	ttacacatggcatggatgaactatacaaataagcggccgcgataaatgcaaaatcctttcaagcattcc
tbb-2 R GA	gtatctagaaccggtgacgtcac
mcm-4p speI	ctcactagtgatttagacatccacgtc
mcm-4p acsI	aaaggcgcgcctttctagctgcaaaaatttacagatttcgc
G block CDK sensor	ctctctaccgtccgcactcttcttacttttaaattaaattgtttttttttcagttgggaaacactttgctcaggc gcgccaaaaatgaccaacgacgttacctggtctgaggcttcctccccagacgagcgtacccttaccttcgc cgagcgctggcaactttcctccccagacggagtcgataccgacgacgaccttccaaagtctcgtgcttcta agcgcacctgcggagttaacgacgacgagtctccatctaagatcttcatggttggagagtccccacaagtt tcctcccgtctccaaaaccttcgtcttaacaaccttatcccacgccaactcttcaagccaactgacaaccaa gagaccgcggccgccatgagtaaaggagaagaacttttcactggagttgtcccaattcttgttg

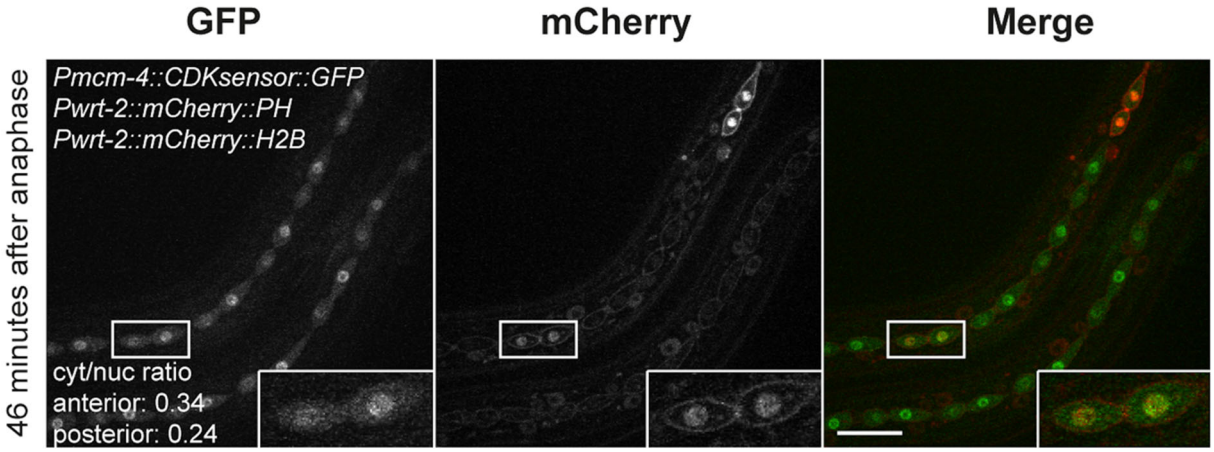

S1 Fig. Still images and blow-ups from spinning disk confocal fluorescence microscopy time-lapse movies of larvae staged at 24 hours after hatching. Highlighted area and magnification show the anterior (left) and posterior (right) daughter cells of V3.pap, 46 min. after anaphase. Note that a lower nuclear signal of the sensor is present in the anterior daughter cell as compared to the posterior sister cell. Scale bar indicates 20 µm.

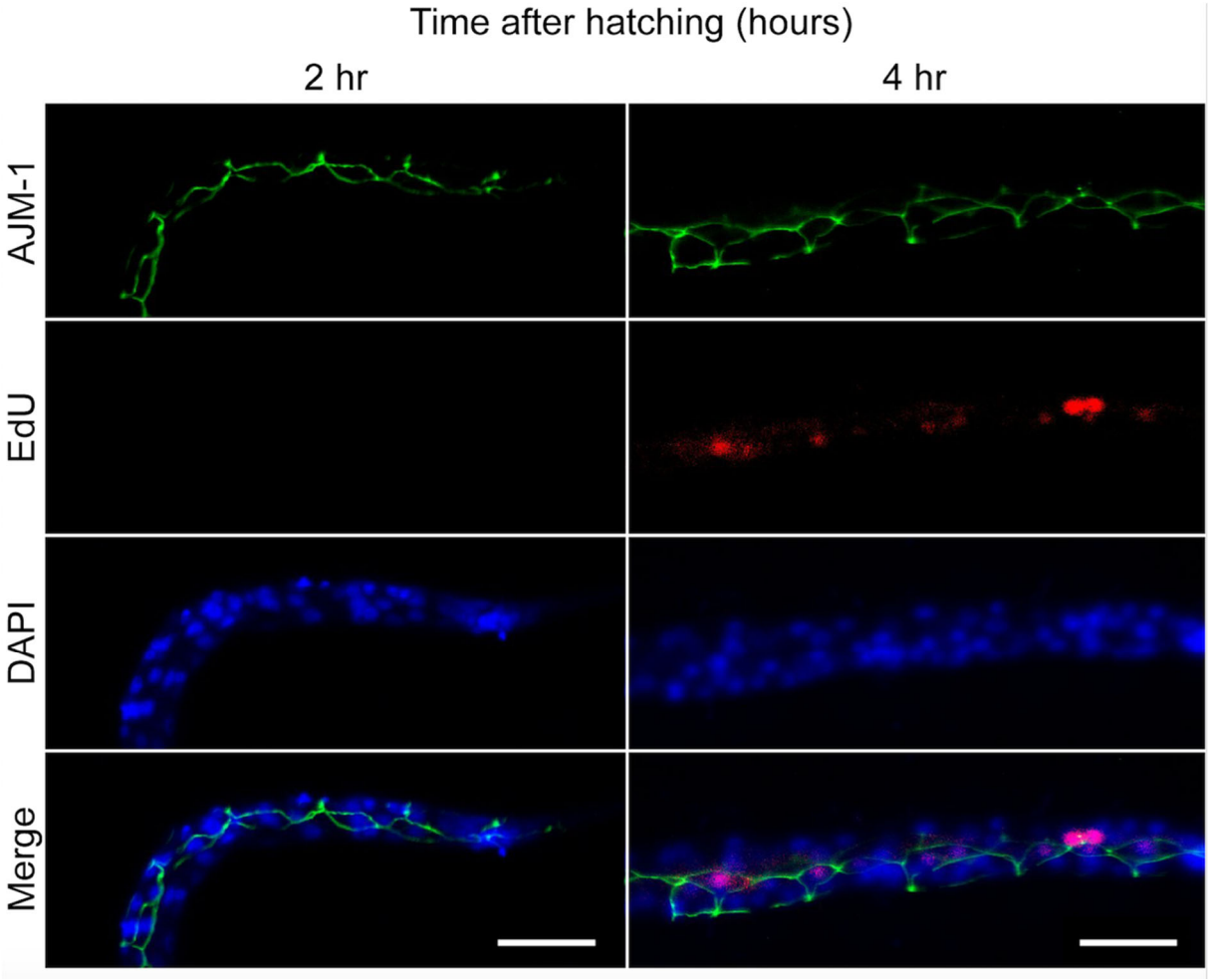

S2 Fig. EdU incorporation in seam cells during larval development. Representative fluorescence microscopy images of EdU, AJM-1 and DAPI staining of fixed worms. Ventral is up in the worm of 2 hours. Scalebars indicate 20 µm.

S1 Appendix. Supporting materials and methods.

Sensor localization was quantified by measuring the cytoplasmic to nuclear ratio using Fiji (ImageJ). Regions of interest, the nucleus and cytoplasm, were drawn either by hand (freehand selection tool) or using the 'analyze particles' function. For the latter method, first, the threshold was altered (at Image > Adjust > Threshold, note: check dark background) to a level where all desired regions are selected in red (either nuclei or entire cells). Second, the 'analyze particles' function was used (Analyze > Analyze Particles, note: adjust size and circularity to values only including the desired regions, i.e. size = 100-infinity, circularity = 0.2- 1) to add all selected regions into the ROI manager. In this way, all nuclei outlines and outlines of the entire cells could be selected (either based on the sensor itself or on the nuclear and cell membrane markers). After retrieving the outlines of the nucleus and the cell outline, either drawn by hand or as described, a region of interest for the cytoplasm was created by selecting both ROIs from the ROI manager (Analyze > Tools > ROI manager), using the XOR function (in the ROI manager: more > XOR) and adding the newly created region to the ROI manager (ctrl+T). Measurements were performed after background subtraction. Background subtraction was performed by first duplicating the image or stack (ctrl+shift+D, note: check duplicate stack when analyzing a movie). On this duplicated file, the Gaussian blur filter was applied (Process > Filters > Gaussian Blur, note: sigma between 15 and 20, check preview to get the right amount of blurring, the outline of the worm should still be visible). Background was subtracted by the 'image calculator' function (Process > Image Calculator, note: set to subtract, and select the duplicated, blurred file to be subtracted from the original image). Measurements were then performed from the image after background subtraction, by selecting all ROIs from the ROI manager and selecting 'measure' (in the ROI manager menu). These measurements were used to directly calculate the ratio of cytoplasmic intensity divided by nuclear intensity.

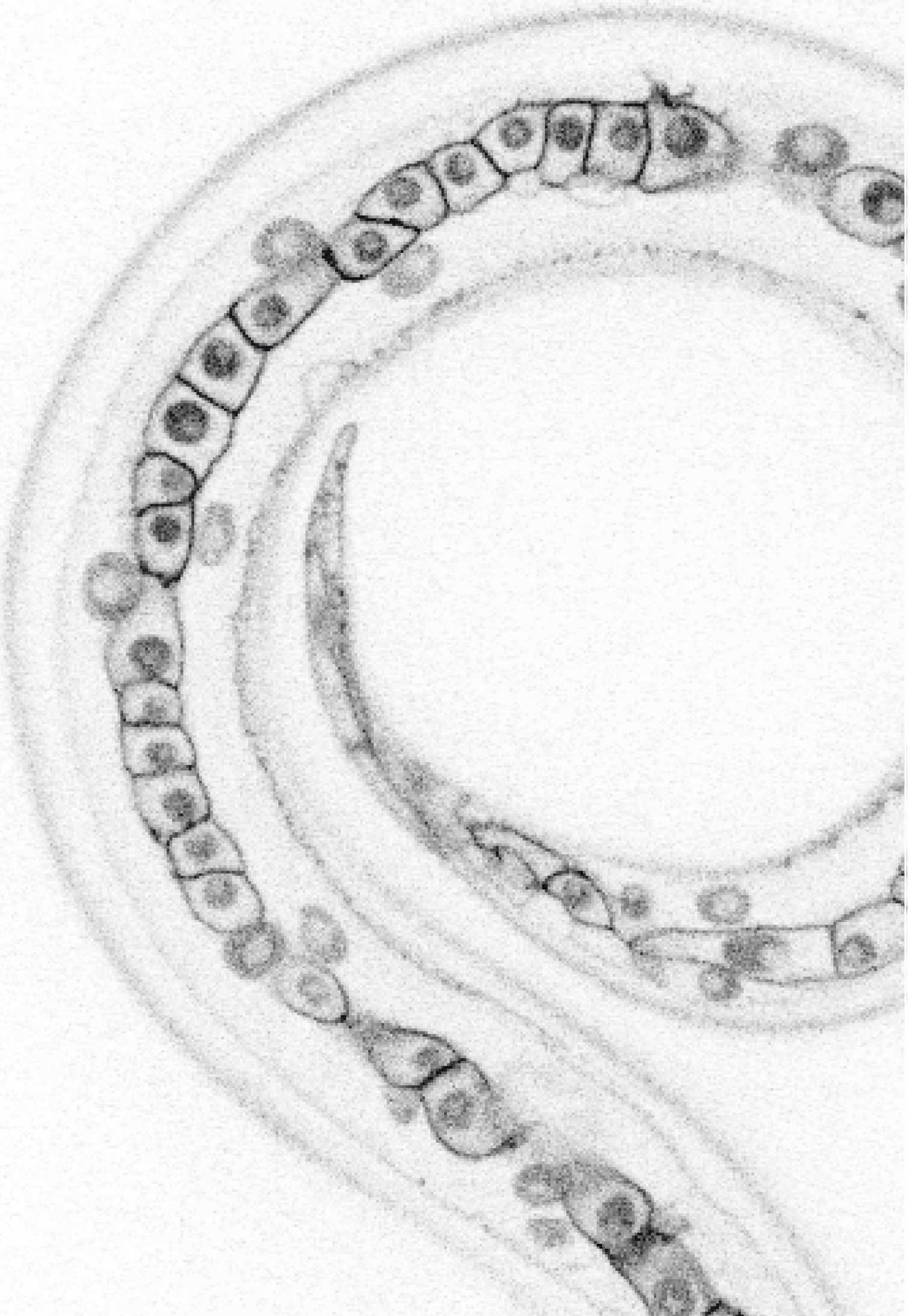

3

C. elegans Runx/CBFβ suppresses POP-1 TCF to switch asymmetric to symmetric stem-cell like division

Suzanne van der Horst[1], Janine Cravo[1], Alison Woollard[2], Juliane Teapal[1], Sander van den Heuvel[1*]

[1] Developmental Biology, Department of Biology, Faculty of Sciences, Utrecht University, Padualaan 8, 3584 CH Utrecht, The Netherlands

[2] Department of Biochemistry, Oxford University, South Parks Road, Oxford, OX1 3QU, United Kingdom

Manuscript submitted for publication

Abstract

A correct balance between proliferative and asymmetric cell divisions underlies normal development, stem cell maintenance and tissue homeostasis. How cells decide whether to undergo symmetric or asymmetric cell division is poorly understood. To gain insight in the mechanisms involved, we studied the stem cell-like seam cells in the *Caenorhabditis elegans* epidermis. Seam cells go through a reproducible pattern of asymmetric divisions, instructed by non-canonical Wnt/β-catenin asymmetry signaling, and symmetric divisions that increase the seam cell number. Using time-lapse fluorescence microscopy, we show that symmetric cell divisions maintain the asymmetric localization of Wnt/β-catenin pathway components. Observations based on lineage-specific knockout and GFP-tagging of endogenous *pop-1* support that POP-1^{TCF} induces differentiation at a high nuclear level, while low nuclear POP-1 promotes seam cell self-renewal. Before symmetric division, the transcriptional regulator *rnt-1*^{Runx} and cofactor *bro-1*$^{CBF\beta}$ temporarily bypass Wnt/β-catenin asymmetry by downregulating *pop-1* expression. Thereby, RNT-1/BRO-1 appears to render POP-1 below the level required for its repressor function, which converts differentiation into self-renewal. Thus, opposition between the *C. elegans* Runx/CBFβ and TCF stem-cell regulators controls the switch between asymmetric and symmetric seam cell division.

Introduction

Tissue-specific stem cells combine long-term maintenance with the generation of differentiating daughter cells. This can be achieved by asymmetric cell divisions that simultaneously generate a self-renewing stem cell and a daughter cell that initiates a differentiation program (Reviewed in Knoblich 2010). Expanding stem cell numbers, however, requires symmetric divisions that generate two self-renewing stem cells. Thus, the proper balance between symmetric and asymmetric divisions is key to the development and maintenance of tissues, and to preventing tumor formation or premature differentiation. How this balance is controlled is currently poorly understood.

The *Caenorhabditis elegans* epidermis provides an attractive model to study stem cell divisions in a developing tissue. The stem cell-like seam cells form part of the epidermis and undergo a reproducible pattern of symmetric and asymmetric divisions at stereotypical times of development (Sulston & Horvitz 1977). Asymmetric divisions of seam cells create a new seam daughter cell, as well as a cell that proceeds either to form neurons or to differentiate and fuse with the general epidermis (known as hypodermis in *C. elegans*). In addition, the number of seam cells increases in the second larval stage (L2), through symmetric divisions that generate two seam daughter cells.

Non-canonical Wnt signaling, mediated by the Wnt/β-catenin asymmetry pathway, is critical for many asymmetric cell divisions in *C. elegans*, including seam cell divisions (Lin et al. 1998; Kidd et al. 2005; Mizumoto & Sawa 2007a; Baldwin & Phillips 2014). This pathway controls the choice between two alternative cell fates, instructed by an unequal subcellular localization of Wnt/β-catenin pathway components. Ultimately, the different cell fates are determined by asymmetric activity of the TCF/LEF-related transcription factor POP-1 (posterior pharynx defective) (Lin et al. 1998). POP-1 is thought to function as a transcriptional repressor in a complex with UNC-37 (Groucho) that induces differentiation (Calvo et al. 2002). POP-1 can also function as a transcriptional activator with co-factor SYS-1 (β-catenin) instructing self-renewal (Kidd et al. 2005; Shetty et al. 2005; Huang et al. 2007). Wnt signaling and asymmetric localization of upstream pathway components restrict the repressor function to anterior cells, through export of POP-1 from the nucleus of posterior

seam daughter cells (Takeshita & Sawa 2005), and by degrading the co-activator SYS-1 in the differentiating anterior daughters (Vora & Phillips 2015). Altered levels or localization defects of several Wnt/β-catenin asymmetry pathway components result in symmetric seam cell divisions, indicating the importance of this pathway for division asymmetry (Banerjee et al. 2010; Gleason & Eisenmann 2010; Ren & Zhang 2010; Hughes et al. 2013). Whether and how symmetric seam cell divisions circumvent the Wnt/β-catenin asymmetry pathway is currently not understood.

A conserved Runx transcriptional repressor complex also contributes to the control of seam cell division and differentiation. Runx transcription factors play broad functions in development and stem cell maintenance, and are probably best known for their critical roles in hematopoiesis and oncogenic functions in leukemia (Reviewed in Deltcheva & Nimmo 2017). They act in association with a heterodimeric partner, CBFβ, and contribute to repression as well as activation of transcription. The *C. elegans* genome encodes a single Runx homolog, RNT-1, and single CBFβ-related cofactor, BRO-1 (Nimmo et al. 2005; Kagoshima et al. 2007a; Xia et al. 2007). Genetic and biochemical experiments support that RNT-1 and BRO-1 form a transcriptional repressor complex together with UNC-37^{Groucho}. Mutations in *rnt-1, bro-1* and *unc-37* reduce the seam cell number as a consequence of defects in the L2 division pattern (Nimmo et al. 2005; Kagoshima et al. 2007a; Xia et al. 2007). By contrast, induced expression of RNT-1 and BRO-1 increases the seam cell number. These observations highlight a regulatory role for the RNT-1/BRO-1 complex in seam cell proliferation and differentiation. It remains unclear, however, how this is integrated with Wnt/β-catenin asymmetry signaling to establish the reproducible pattern of symmetric and asymmetric seam cell divisions, and previous studies concluded that these regulators act in parallel (Kagoshima et al. 2005; Gleason & Eisenmann 2010; Hughes et al. 2013).

In this study, we use time-lapse fluorescence microscopy of developing larvae to identify the mechanisms that determine asymmetric versus proliferative seam cell division. We show that anterior daughter cells adopt a seam cell fate during symmetric cell divisions despite asymmetric distribution of Wnt/β-catenin asymmetry pathway components. This indicates that symmetric divisions bypass Wnt/β-catenin asymmetry to prevent anterior cell

differentiation. Multiple observations support that the RNT-1/BRO-1 complex provides this bypass-mechanism by temporarily repressing *pop-1*. First, GFP-tagged endogenous POP-1 is expressed at a very low level during symmetric seam cell divisions, dependent on *rnt-1 bro-1* function. Further, double *rnt-1 bro-1* mutants show ectopic differentiation of anterior seam cells, which is fully suppressed by *pop-1* RNAi. Moreover, induced expression of RNT-1/BRO-1 represses GFP::POP-1 expression and turns asymmetric seam cell divisions into symmetric divisions. Finally, endogenous RNT-1 is expressed at a high level before symmetric seam cell divisions, but disappears and remains absent prior to the subsequent asymmetric division, which correlates with upregulation of POP-1. These data support the model that RNT-1/BRO-1 provides temporal control over POP-1$^{TCF/LEF}$, which renders POP-1 below a critical level required for its repressor function, and thereby changes differentiation into self-renewal. Together, our data reveal how interactions between two conserved stem cell regulators can balance symmetric and asymmetric divisions in a developing tissue.

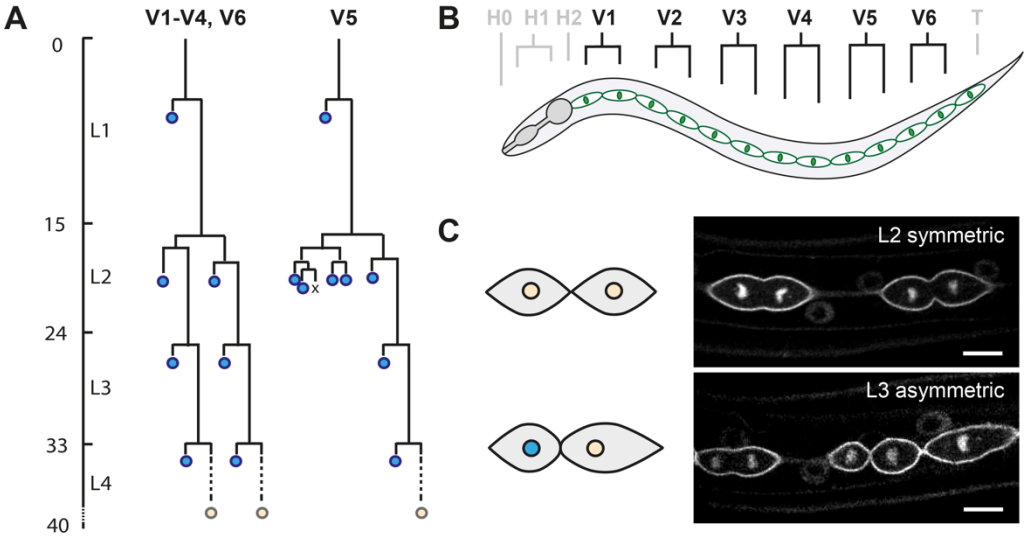

Figure 1. Seam cell lineage as a model to study the regulation of proliferative versus asymmetric cell division. (A) Postembryonic division patterns of the ventrolateral precursor (V) cells of the *C. elegans* epidermis (hypodermis). The seam cells undergo cell division (horizontal lines) in a stereotypic manner during each of the four larval stages (L1-L4), as indicated by the time course of development (left axis). Asymmetric divisions of V1-V4 and V6 generate one anterior epidermal daughter cell (blue), and one self-renewing posterior seam daughter cell. At the end of larval development, all remaining seam cells (grey) exit the cell cycle and fuse together to form two lateral syncytia. (B) Schematic lateral view of one of two seam epithelia. The anterior region includes the

epidermal precursor cells of the head (H0-H2), the middle ventrolateral region contains the V cells (V1-V6) and the posterior region hosts the tail blast cell (T). (C) Representative spinning disk confocal fluorescence microscopy images of seam cells expressing transgenic reporter genes, to visualize the membrane (GFP::PH) and DNA (GFP::H2B). The L2 symmetric divisions generate two self-renewing daughter cells equal in cell size and fate (grey nucleus; top). The asymmetric division generates a smaller anterior daughter cell that will fuse with the epidermis (blue nucleus), and a larger posterior self-renewing seam cell (grey nucleus; bottom).

Materials and methods

Nematode strains

Wild-type *Caenorhabditis elegans* strain N2 and the derivatives listed in Table 1 were used in this study. All strains were maintained at 20 °C as previously described (Brenner 1974) unless stated otherwise. Animals were grown on plates containing nematode growth medium seeded with OP50 *Escherichia coli* bacteria.

Table 1. Strains used in this study

Strain	Genotype
SV1009	*heIs63[*P*wrt-2::gfp::ph;* P*wrt-2::gfp::h2b;* Plin*-48::mCherry] V*
SV1984	*heIs218[*Pwrt*-2::mcherry::ph,*P*wrt-2::mcherry::h2b,* P*lin-48::gfp]*
SV1986	*heIs218[*P*wrt-2::mcherry::ph,* P*wrt-2::mcherry::h2b,* P*lin-48::gfp] IV; qIs74[*P*sys-1::pop-1::gfp + unc-119(+)] him-5(e1490) V*
JK3437	*qIs74[*P*sys-1::pop-1::gfp + unc-119(+)] him-5(e1490) V;*
HS1486	*unc-76(e911) V; osIs13[*P*apr-1::apr-1::venus; unc-76 (+)]*
SV1615	*heIs188 [*P*wrt-2::mcherry::ph;* P*wrt-2::mcherry::h2b;* P*lin-48::gfp;* P*hsp16.48::cki-1::gfp]*
SV1694	*unc-119 (ed3) III ; heSi193 [*P*mcm-4::CDK sensor::gfp::tbb-2 UTR + Cbr-unc119(+)] II ; dpy-20 (e1362) ; [*P*wrt-2::mCherry::ph* P*wrt-2::mCherry::h2b dpy-20(+)]*
SV2112	*pop-1(he334[pop-1^{loxP}]) I**
SV2113	*pop-1(he334[pop-1^{loxP}]) I; heIs218[*P*wrt-2::mcherry::ph,* P*wrt-2::mcherry::h2b,* P*lin-48::gfp]; heSi175(*P*scm::cre) X*
SV2114	*pop-1(he335[egfp::loxP::pop-1]) I*
SV2115	*pop-1(he335[egfp::loxP::pop-1]) I; heIs218[*P*wrt-2::mcherry::ph,* P*wrt-2::mcherry::h2b,* P*lin-48::gfp]*
SV2000	*heIs63[*P*wrt-2::gfp::ph;* P*wrt-2::gfp::h2b;* P*lin-48::mcherry] V ; heEx609[*P*hsp16.2::rnt-1,* P*hsp16.2::bro-1,* P*myo-2::tdTomato]*
SV2002	*rnt-1(he305[rnt-1::egfp::3xflag::loxP]) I*
SV2003	*heIs218[*P*wrt-2::mcherry::ph;* P*wrt-2::mcherry::h2b;* P*lin-48::gfp]; rnt-1(he305[rnt-1::egfp::3xflag::loxP]) I*
YK138	*rnt-1(tm388) bro-1(tm1183) I*
SV2126	*rnt-1(tm388) bro-1(tm1183) I; heIs63[*P*wrt-2::gfp::ph;* P*wrt-2::gfp::h2b;* P*lin-48::mCherry] V*
AW811	*rnt-1(tm388) I; heIs63[*P*wrt-2::gfp::ph;* P*wrt-2::gfp::h2b;* P*lin-48::mCherry] V*
SV2148	*heSi193[*P*mcm-4::cdk-sensor] II; heIs218[*P*wrt-2::mcherry::ph,* P*wrt-2::mcherry::h2b,* P*lin-48::gfp]; heEx609[*P*hsp16.2::rnt-1,* P*hsp16.2::bro-1,* P*myo-2::tdTomato]*
SV2150	*pop-1(he335[egfp::loxP::pop-1]) I; heIs218[*P*wrt-2::mcherry::ph,* P*wrt-2::mcherry::h2b,* P*lin-48::gfp]; heEx609[*P*hsp16.2::rnt-1,* P*hsp16.2::bro-1,* P*myo-2::tdTomato]*
SV2230	*pop-1(he335[egfp::loxP::pop-1];rnt-1(tm388) bro-1(tm1183) I) I; heIs218[*P*wrt-2::mcherry::ph,* P*wrt-2::mcherry::h2b,* P*lin-48::gfp]*
SV2231	*pop-1(he373[pop-1$^{\Delta Runx}$] I**; heIs63[*P*wrt-2::gfp::ph;* P*wrt-2::gfp::h2b;* Plin*-48::mCherry] V*

*loxP sites are present upstream of the *pop-1* ATG and in intron 5

**promoter sites were altered between 143 and 164bp upstream of the *pop-1* ATG start codon (See Fig. S5)

Molecular cloning

All molecular cloning was designed in ApE (A plasmid Editor; M. Wayne Davis). Repair templates and DNA fragments for cloning were generated by PCR amplification with either High Fidelity Hot Start KOD DNA Polymerase (Novagen) or Phusion Hot Start DNA Polymerase (Finnzymes), using either purified *C. elegans* genomic DNA or pre-existing vectors as template. A list of cloning primers can be found in Supplementary Table 1. PCR fragments were purified from gels (Qiagen), their concentration measured using a BioPhotometer D30 (Eppendorf) and then ligated into pCGSI by Gibson assembly (New England Biolabs) or pJJR82 (SEC cassette plus *egfp*; Dickinson et al. 2015). gRNA vectors were generated by annealing of antisense oligonucleotide pairs and subsequent ligation into pBbsI-linearized pJJR50 by T4 ligase (New England Biolabs). All DNA vectors used for genome editing were transformed into DH5α competent cells and subsequently purified by midiprep (Qiagen).

CRISPR/Cas9 mediated genome editing

Knock-in strains were generated using Cas9 endonuclease-induced homologous recombination following standard methods (Dickinson et al. 2013). Repair templates were generated by inserting 500 bp homology arm PCR products into destination vectors containing *egfp* and a self-excising selection cassette using Gibson assembly (New England Biolabs) or SapTrap assembly (Dickinson et al. 2015; Schwartz & Jorgensen 2016). Destination vectors used in this study were pJJR82 (C-terminal *rnt-1*) and pMLS257 (N-terminal *pop-1*). The C-terminal *rnt-1* repair template contains a nine amino acid flexible linker between the coding sequence and the *egfp* tag. N-terminal *pop-1* repair template contains a ten amino acid flexible linker between the coding sequence and the *egfp* tag. Injection of *C. elegans* adults in the germline was performed using an inverted microinjection microscope setup. Injection mixes with a total volume of 50 μl were prepared in milliQ H_2O and contained a combination of 30-50 ng/μl *Peft-3::cas9* (46168; Addgene; Friedland et al., 2013), 50-100 ng/μl *Pu6::sgRNA* with sequences targeted against *pop-1* or *rnt-1*, 50 ng/μl repair vector, and 2.5 ng/μl *Pmyo-2::tdTomato* as a co-injection marker. Injected animals were transferred to new NGM-OP50 plates (3 animals per plate) and

allowed to lay eggs for 2-3 days at 25 °C. On day 3, 500 µl of filter sterilized hygromycin solution (5 mg/ml in water) was added to the plates and allowed to dry in. Plates were subsequently moved back to 25 °C. On day 7, plates were screened for surviving F1 animals that showed a Rol phenotype and lacked the co-injection marker. These candidate knock-in animals were singled to new NGM-OP50 plates without hygromycin. On day 10, plates with homozygous Rol progeny (C-terminal *rnt-1*) and heterozygous Rol animals (N-terminal *pop-1*) were selected. Of those, 6 L1 animals were transferred to new plates, and exposed to heat-shock at 34 °C for 4 hours for cassette excision. Subsequent genome editing events were assessed by microscopic analysis and PCR amplification using primers targeting the inserted *gfp* sequence and a genomic region outside the homology arms. PCR-confirmed edited genomic loci were further validated by DNA sequencing (Macrogen Europe).

loxP sites were integrated in the endogenous locus of *pop-1* via co-conversion in a *pha-1(e2123*ts*)* background. Injection mixes contained a combination of 30-50 ng/µl *Peft-3::cas9* (46168; Addgene; Friedland et al., 2013), 50-100 ng/µl *Pu6::sgRNA* with sequences targeted against *pop-1*, 50 ng/µl of PAGE-purified *pop-1* repair oligo (Integrated DNA technologies), 50 ng/µl PAGE-purified *pha-1* repair oligo (Integrated DNA technologies), 60 ng/µl pJW1285 (61252; Addgene; Ward, 2015), and 2.5 ng/µl Pmyo-2::tdTomato as a co-injection marker. Animals were grown for 3-5 days at either 20 °C or 25 °C after injection, and transgenic progeny was selected based on either expression of tdTomato in the pharynx or survival at the non-permissive temperature (25 °C). Subsequent assessment of genome editing events was performed by PCR amplification using primers targeting the inserted *loxP* sequence and genomic sequences outside the homology arms. PCR-confirmed edited genomic loci were further validated by DNA sequencing (Macrogen Europe).

Generation of extrachromosomal arrays

Extrachromosomal arrays were generated for *hsp::rnt-1 (pAW261)*, *hsp::bro-1 (pAW266)*, *hsp::cki-1::gfp*, and P*wrt-2::mCherry::PH,* P*wrt-2::mCherry::H2B*. For heat-shock induced RNT-1/BRO-1 expression, the injection mix contained a combination of 30 ng/µl P*hsp16.2::rnt-1*, 30 ng/µl P*hsp16.2::bro-1,* 2.5 ng/µl P*myo-2::tdTomato* and 5 ng/µl λ-DNA. For the seam markers, the injection mix contained 50 ng/µl P*wrt-2::mcherry::ph,* 50 ng/µl

P*wrt-2::mcherry::h2b*, 10 ug/μl P*lin-48::GFP* and 5 ng/μl λ-DNA. For CKI-1 induction, the injection mix contained a combination of 20 ng/μl P*hsp16.48::cki-1::gfp,* 2.5 ug/μl P*myo-2::tdTomato* and 5 ng/μl λ-DNA. Animals were grown for 3-5 days at 20 °C, and transgenic progeny was selected based on pharyngeal expression of tdTomato (*myo-2*) or tail expression of GFP (*lin-48*). Strains were maintained as extrachromosomal lines by transferring tdTomato or GFP positive animals.
Integration by γ-irradiation was performed for extrachromosomal arrays containing *hsp16.48::cki-1::gfp* and the combined P*wrt-2::mcherry::h2b* and P*wrt-2::mcherry::ph* markers.

Staging

Animals were synchronized using a wash-off protocol. 20 gravid adults were transferred to a new NGM-OP50 plate and allowed to lay eggs for a minimum of 20 hours. Animals were washed off the plates using M9-0,1%Tween, and embryos were allowed to hatch for a period of 1 hour. The newly hatched larvae were collected onto a fresh NMG-OP50 plate and incubated at 20 °C for 4.5 hours (L1), 15.5 hours (L2 symmetric), 17.5 hours (L2 asymmetric), 24 hours (L3) or 43 hours (late L4 counting).

RNA-mediated interference (RNAi)

A combination of L1 soaking and feeding RNAi was used to knock-down *pop-1*. Gravid adults were bleached using hypochlorite treatment, and embryos were allowed to hatch for 20 hours in RNAi soaking buffer (0.05% gelatin, 5.5 mM KH_2PO_4, 2.1 mM NaCl, 4.7 mM NH_4Cl, 3 mM spermidine) containing 1 ug dsRNA. Hatched larvae were then placed on 5x concentrated RNAi feeding plates at 20°C. Both the RNAi feeding plates and the dsRNA were derived from Vidal library clone GHR-11053 for *pop-1.* dsRNA was synthesized using the Megascript High Yield Transcription T7 Kit (Thermofisher Scientific).

Heat-shock induction

For heat-shock induced gene expression, animals were synchronized using a wash-off protocol (see 'Staging') and grown at 20 °C. Heat-shock was performed in a 32 °C water bath for 30 min (CKI-1) or 60 min (RNT-1/BRO-1). After heat-shock, the plates were placed on ice-water for 10 minutes and either used directly for microscopy or placed back at 20 °C for later analysis.

Microscopy

Time-lapse movies of seam cell divisions in immobilized, living animals were recorded at room-temperature at 2-minute intervals for 2-5 hours using a Nikon Eclipse Ti-U spinning disk microscope with a 63X objective. Larvae were immobilized in 1 mM tetramisole (Sigma-Aldrich) in M9 buffer, and mounted on 5-7% agarose pads (7% for L1 stage animals, 5% for L2-L3 stage animals. Agarose was prepared in milliQ water). The coverslips were sealed with immersion oil (Zeiss Immersol 518N oil) to prevent liquid evaporation. Laser power (both 488 and 563) ranged between 6-10% with exposure times below 400 ms for long-term imaging. 2x2 binning was performed to reduce phototoxicity. Image analysis was performed with FIJI software. Quantification of endogenous expression levels was corrected for background levels inside the worm.

Results

Wnt components localize asymmetrically in symmetric seam cell divisions

We studied the stem cell-like precursors of the *C. elegans* epidermis to reveal the mechanisms that determine whether cells undergo symmetric or asymmetric cell divisions. The seam cells reside in two lateral epithelia along the anterior-posterior body axis (Fig. 1). During the first larval stage, each V seam cell undergoes one anterior-posterior oriented asymmetric division (Sulston and Horvitz, 1977). These divisions generate a self-renewing posterior daughter cell and an anterior daughter cell that either differentiates and fuses with the epidermis (V1-V4, V6) or forms neuronal daughter cells (V5). Upon entry of the second larval stage (L2), V1-V4 and V6 go through a symmetric division to generate two self-renewing seam daughter cells. This symmetric division is followed by an asymmetric division of the V cells to produce epidermal (V1-V4, V6) and neuronal (V5) cells.

We examined the distribution of Wnt/β-catenin asymmetry pathway components to gain insight in the regulation of symmetric versus asymmetric seam cell division. Earlier observations indicated that the asymmetric localization of POP-1 and APR-1 is maintained during the symmetric divisions of seam cells in L2 (Wildwater et al. 2011; Baldwin & Phillips 2014). To follow this process more closely, we made use of spinning disk time-lapse fluorescence microscopy and the P*sys-1::pop-1::gfp* reporter. This transgene was previously used to demonstrate unequal nuclear POP-1 levels during the asymmetric divisions of V5 and T cells (Kagoshima et al. 2005; Mizumoto & Sawa 2007b). We observed a similar pattern of POP-1 localization during the asymmetric divisions of seam cells in the V1-4, V6 lineages (Fig. 2A, bottom). Soon after the nuclei reformed in telophase, POP-1::GFP levels decreased in the posterior nucleus, in contrast to the anterior nucleus. Quantification of the fluorescence intensity indicated an approximately 2-fold nuclear enrichment of POP-1 in the anterior compared to posterior daughter cells at the time of cytokinesis (Fig. 2B).

The lower nuclear level of POP-1 was previously shown to correspond to activation of the Wnt pathway and acquisition of the seam cell fate (Gleason & Eisenmann 2010; Gorrepati et al. 2013). Notably, however, the L2 symmetric divisions that generate two seam daughter

cells also showed asymmetric POP-1 distribution. During telophase and cytokinesis of symmetric seam cell divisions, the POP-1::GFP levels decreased specifically in the posterior nucleus (Fig. 2A, top). These live observations confirm our previous conclusion based on immunohistochemical detection of POP-1::GFP (Wildwater et al. 2011), and indicate that the mechanisms for asymmetric distribution of POP-1 remain active during the symmetric divisions that create two seam daughter cells.

To examine this aspect further, we followed the localization of APR-1, making use of a P*apr-1::apr-1::venus* reporter (Mizumoto & Sawa 2007a). As described before, APR-1 enriches at the anterior half of the cell cortex of asymmetrically dividing seam cells, and upon completion of cytokinesis is predominantly detected at the cortex of anterior daughter cells (Fig. 2C). Similar to the asymmetric L3 divisions, we observed anterior enrichment of APR-1 during the L2 symmetric divisions (Fig. 2C). Quantifications of APR-1-VENUS levels confirmed that the ratio's between anterior versus posterior cortical levels of APR-1 were similar between symmetric and asymmetric cell divisions (Fig. 2D). Together, these live observations confirm that anterior-posterior polarization of Wnt/β-catenin asymmetry components also takes place during symmetric divisions. Despite this asymmetric APR-1 and POP-1 distribution, the anterior daughter cells do not differentiate but adopt a seam cell fate that is normally restricted to the posterior daughter cell. This appears to imply that the Wnt/β-catenin asymmetry pathway is temporarily overruled during symmetric seam cell divisions.

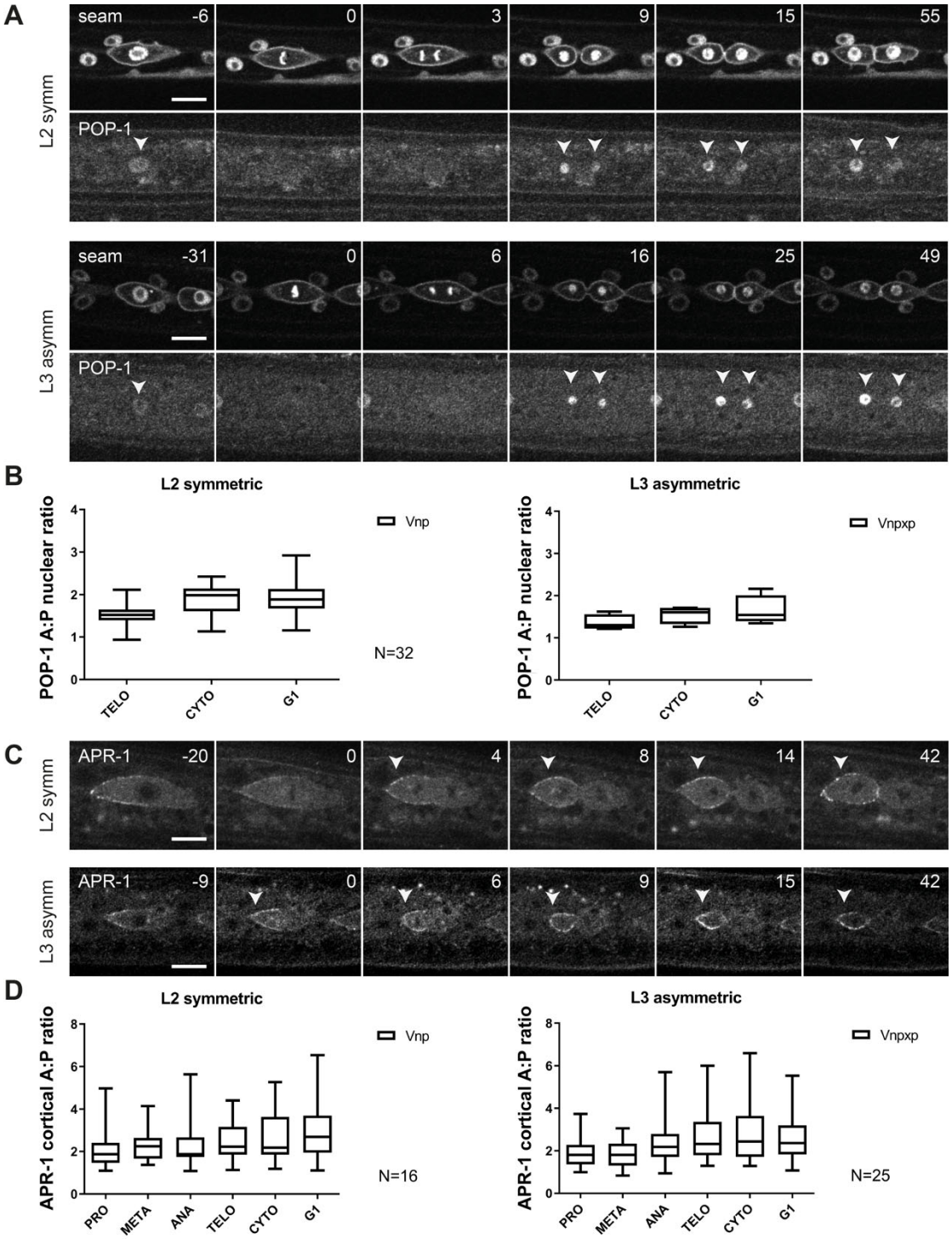

Figure 2. Localization dynamics of POP-1 and APR-1 during seam cell divisions. (A) Representative images from spinning disk time-lapse microscopy, showing seam markers mCherry::PH and mCherry::H2B, and POP-1::GFP during L2 symmetric (upper panels) and L3 asymmetric divisions (bottom panels). Arrowheads point to seam cell nuclei. Anterior is to the left. (B) Quantification of the POP-1 nuclear A:P ratio in L2 symmetric (left) and L3 asymmetric divisions (right). (C) Images from spinning disk time-lapse microscopy of APR-1::VENUS during L2 symmetric (upper panel) and L3 asymmetric divisions (bottom panel). Arrowheads point to the anterior cortex of a dividing seam cell.

Anterior is to the left. (D) Quantification of the APR-1 cortical A:P ratio in L2 symmetric (left) and L3 asymmetric divisions (right). The box and whiskers plots indicate mean (line within box) as well as the highest and lowest observed values (lines outside box). Images were processed using ImageJ software, the scale bar (10 μm) is the same for all images.

Symmetric division does not result from progression through the next cell cycle

Cell cycle progression and CDK-cyclin activity are generally considered to oppose cell differentiation (Ruijtenberg & van den Heuvel 2016). In contrast to asymmetric divisions, the symmetric seam cell divisions are rapidly followed by a second round of cell division (Sulston & Horvitz 1977). The localization of a cyclin-dependent kinase (CDK) sensor supports that both daughter cells of symmetric seam cell divisions immediately progress into the next cell cycle and fully activate CDKs (Fig. S1A) (Van Rijnberk et al. 2017). The anterior daughter cells initiate the next mitosis approximately 2 hours after the completion of symmetric cell divisions in L2. This falls within the time lag observed for the onset of differentiation in other larval stages, as defined by fusion of anterior daughter cells with the hypodermis (2-2,5 hours after asymmetric division). As differentiation normally coincides with low CDK activity, we wondered whether the high CDK activity and cell cycle progression overrules POP-1/UNC-37 induced differentiation in anterior seam daughter cells.

To test this possibility, we examined whether inducing or arresting cell cycle progression could overrule the normal seam daughter cell pattern. Heat shock-induced expression of CDK-1, CYB-1 and CYB-3 just before asymmetric divisions in L2 or L3 occasionally induced extra cell division. The daughter cells of these divisions retained the anterior or posterior fate, continued with an extra asymmetric division, or fused with each other (Fig. S2). These induced divisions appeared abnormal, however, with cells maintaining condensed DNA, rapidly re-entering mitosis and possibly skipping S phase. To examine a more physiological situation, we arrested the cell cycle after symmetric cell division, using heat shock-induced expression of the CDK inhibitor *cki-1* CIP/KIP. As a control for cell-cycle independent effects, we induced *cki-1::gfp* expression in seam daughter cells after the L1 asymmetric divisions. Time-lapse fluorescence microscopy showed that this resulted in substantial CKI-1::GFP levels in seam cells (Fig. 3A). Nevertheless, anterior seam daughter cells continued differentiation as normal, with 100% of Vn.a cells fusing with the epidermis

(Fig. 3A, Top). Thus, temporal exposure to high temperature and *cki-1* induction do not interfere with seam cell differentiation. Next, we expressed CKI-1::GFP between the symmetric and asymmetric division of L2 seam cells (Fig. 3A bottom). This suppressed the second round of seam cell divisions by more than 5 hours. The large majority of the arrested anterior seam daughter cells did not show signs of differentiation (88% of the Vn.ppa cells retained the seam fate, n =37). Based on these observations, it appears unlikely that the rapid progression through the next cell cycle is the mechanism that overrules the Wnt/β-catenin asymmetry pathway in anterior seam cells.

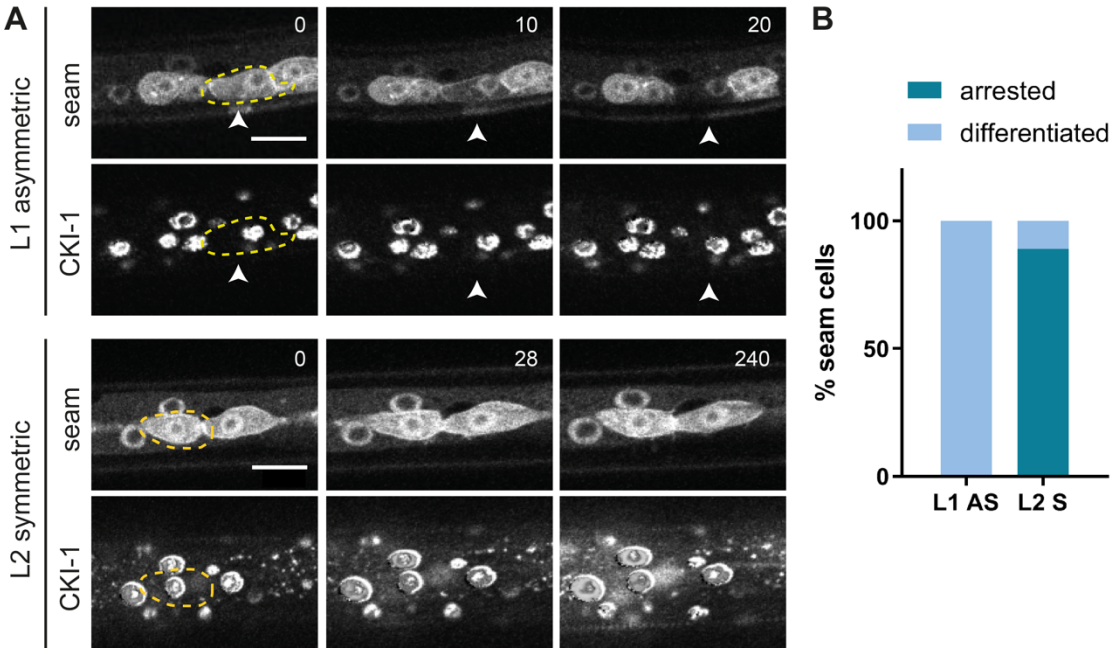

Figure 3. CKI-1 induction in L1 and L2 seam cells. (A) Time-lapse recording of P*hsp::cki-1::gfp* animals, heat-shocked around the time of L1 division (upper panels) or between symmetric and asymmetric divisions in L2 (bottom panels). Time series (minutes) started 1 hour after heat shock induction. Images show the seam markers mCherry::PH and mCherry::H2B (upper panels) and CKI-1::GFP (lower panels). Anterior daughter cells are outlined (yellow), the arrow heads indicate a differentiating Vn.a daughter cell. Scale bars represent 10 µm. (B) Quantification of the number of anterior daughter cells that differentiate after CKI-1 induction (grey) or that retain seam fate (black) in L1 and L2 animals.

The RNT-1/BRO-1 transcriptional repressor complex promotes seam cell fate

Another candidate mechanism to overrule Wnt/β-catenin asymmetry is the RNT-1/BRO-1 transcriptional repressor complex. Studies of *rnt-1* and *bro-1* loss-of-function mutants revealed L2-specific seam cell division defects (Kagoshima et al. 2005, 2007b; Nimmo et al. 2005; Xia et al. 2007). Using spinning disk time-lapse microscopy, we followed L2 seam cell divisions in the candidate double null mutant *rnt-1(tm388) bro-1(tm1183)*. Control animals showed the reproducible pattern of one round of symmetric divisions followed by asymmetric cell divisions at the reported stereotypical times. The timing of L2 seam cell division was not altered in *rnt-1 bro-1* double mutant animals, but variable defects in the division pattern were observed. 74% of *rnt-1 bro-1* Vn.p seam cells skipped at least one cell division in L2 (43% skipped the posterior asymmetric division, and 31% skipped the symmetric division). In this latter group, the anterior Vn.pa daughter cell inappropriately underwent differentiation and fused with hyp7 (31% of the lineages; Fig. 4A). The posterior daughter remained a seam cell when the asymmetric division was omitted; hence this defect does not alter the seam cell number at later stages. The missed symmetric divisions reduced the seam cell number to approximately 13 per lateral side, compared to 16 in wild-type animals (Fig. 4B,C). The skipped divisions and immediate differentiation of anterior seam daughter cells in L2 confirm previous observations (Kagoshima et al. 2007a; Xia et al. 2007), and indicate that RNT-1 and BRO-1 normally act to both promote proliferation and prevent differentiation of seam cells.

By preventing differentiation, the RNT-1/BRO-1 complex could provide the mechanism that overrules the response to Wnt/β-catenin asymmetry during the symmetric L2 seam cell divisions. To examine this possibility, we set out to obtain further insight in the contribution of RNT-1 and BRO-1 in seam cell division and fate determination. First, we used heat-shock induced expression of RNT-1 and BRO-1 at times preceding the asymmetric divisions in L2 or L3. Following the L2 animals by time-lapse fluorescence microscopy (Fig. 4D and F) revealed that the anterior daughter cells of the normally asymmetric cell divisions failed to differentiate and fuse with hyp7 after induction of RNT-1/BRO-1. These cells continued to divide in L3 and behaved as normal seam daughter cells (Fig. 4D and F). Accordingly, quantification at the end of L4 larval development demonstrated that the seam cell numbers increased on average from 16 to 21 or 23, for animals heat-shock induced in L2

or L3, respectively (Fig. 4E and 4G). Thus, through temporal induction of RNT-1 and BRO-1, asymmetric seam cell divisions can be turned into symmetric divisions. In contrast, we did not observe additional seam cell divisions (Fig. 4D). Thus, ectopic expression highlights the contribution of RNT-1/BRO-1 in promoting the seam cell fate.

We wondered how soon after RNT-1/BRO-1 heat-shock induction the anterior daughter cells converted from a differentiation trajectory to a seam cell fate. Following normal asymmetric cell division, the two daughter cells differ immediately in cell cycle progression. The anterior daughter cells initiate the next cell cycle and undergo S phase prior to fusion with the hypodermis, while the posterior self-renewing seam cells pause in G0/G1 until the next molt (Hedgecock & White 1985). We previously visualized this difference in cell cycle progression with a CDK-activity sensor (Van Rijnberk et al. 2017). Nuclear export of this sensor, a DNA Helicase-GFP fusion protein, is induced by CDK-mediated phosphorylation. Consequently, after asymmetric division, S phase entry of the anterior daughter cell coincides with a reduced nuclear level of the CDK-sensor, while the quiescent posterior cell retains a high nuclear level (Fig. S1A-C). We induced expression of RNT-1 and BRO-1 just before the asymmetric L2 divisions, and followed the CDK-sensor in daughter cells after division. The nuclear GFP levels barely dropped in anterior daughter cells after RNT-1/BRO-1 induction (Fig. S1D). Thus, seam cells destined to divide asymmetrically switch to self-renewing seam cells within 90 minutes after heat-shock induced RNT-1/BRO-1 expression.

When combined with the time-lapse recordings of *rnt-1 bro-1* loss-of-function mutants, these data support the conclusion that RNT-1/BRO-1 promotes not only seam cell proliferation but also the seam cell fate. To study the normal expression of *rnt-1,* we used CRISPR/Cas9-assisted recombineering to insert gfp-coding sequences just before the translational stop codon in the endogenous gene (Fig. 4H, top). We followed RNT-1::GFP expression during larval development by time-lapse fluorescence microscopy. This revealed a high level of nuclear-localized RNT-1::GFP in interphase seam cells prior to the symmetric L2 divisions (Fig. 4H, Middle left). Interestingly, RNT-1::GFP subsequently disappeared during mitosis, and largely remained absent when the nuclei reformed in telophase (Fig. 4H, 25-45 minutes). This indicates active protein degradation and the possibility that RNT-1 is a substrate of the anaphase promoting complex/cyclosome (APC/C).

RNT-1::GFP did not reappear in the daughter cell nuclei prior to, or during, the L2 asymmetric divisions (Fig. 4H, Bottom rows). The APC/C becomes inactive prior to S phase entry, hence this is unlikely to be the only level of RNT-1 regulation. We considered post-transcriptional repression of *rnt-1* mRNA by microRNAs (miRNAs), which are important regulators of progression through L2, and transition to the L3 stage (Abbott et al. 2005; Li et al. 2005; Tsialikas et al. 2017). The *let-7* sister miRNAs, *miR-48*, *miR-84*, and *miR-241* would be candidates for *rnt-1* regulation, however, removal of a putative *let-7s* miRNA target site from the endogenous *rnt-1* 3' untranslated region did not induce *rnt-1* gain of function (Fig. S3). Multiple levels of RNT-1 control are likely involved, and allow the reappearance of RNT-1 before the L3 stage division (Fig. S3). Importantly, the presence versus absence of nuclear RNT-1 prior to division distinguishes the symmetric division from the asymmetric division in L2 stage animals. The temporal control of RNT-1 expression in late L1 and L2 stage larvae, together with the L2 division phenotype in *rnt-1, bro-1, and unc-37* mutant larvae, indicate that the L2 symmetric seam cell divisions depend on transcriptional repression by RNT-1/BRO-1/UNC-37 in the mother seam cell.

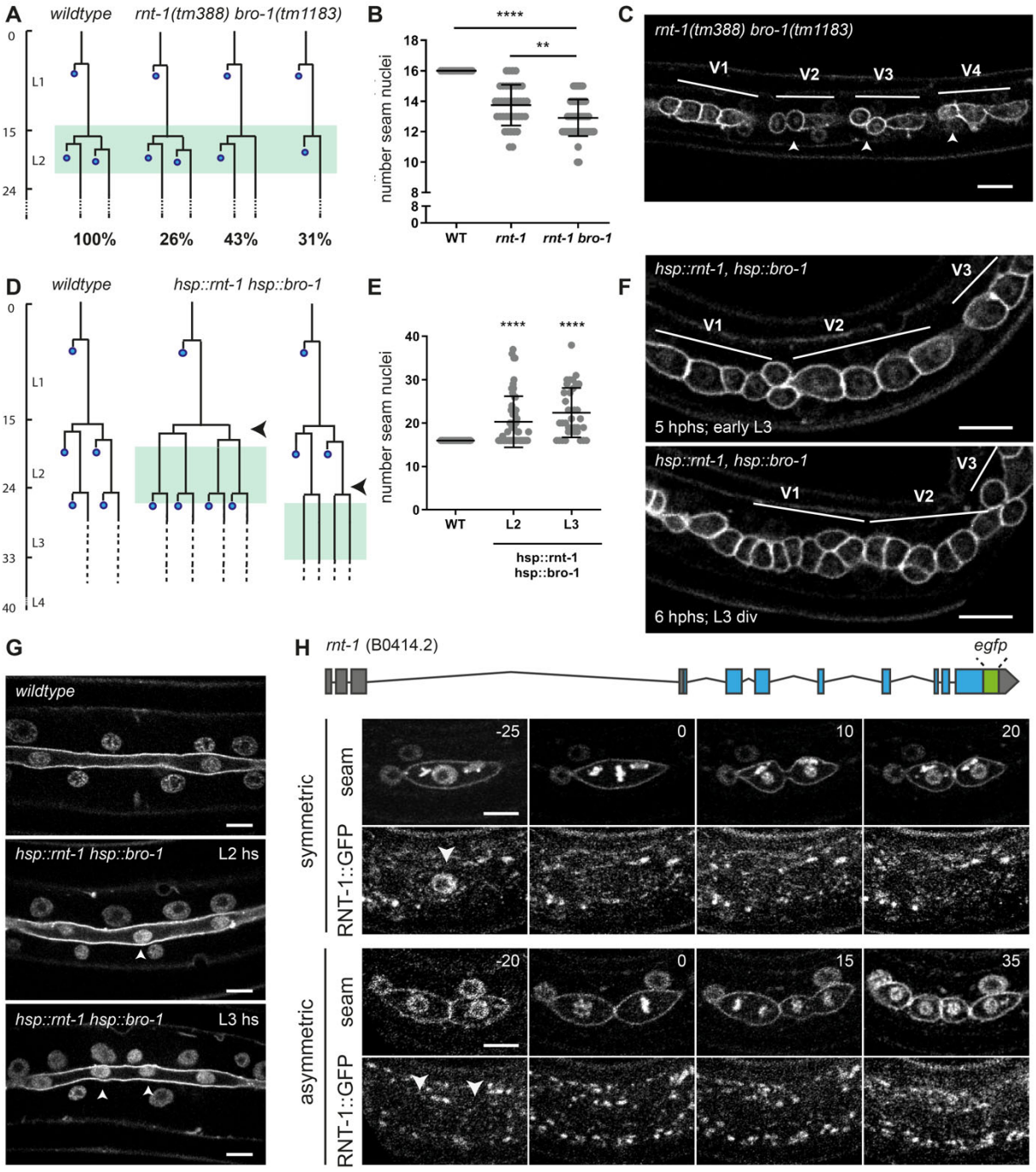

Figure 4. The RNT-1/BRO-1 transcriptional repressor complex promotes the seam cell fate. (A) Lineage analysis of L2 divisions of control animals and the *rnt-1(tm388) bro-1(tm1183)* double mutant (green box marks the time window of analysis). (B) Quantification of the number of seam cell nuclei at the end of L4 development for wild-type control animals, the single *rnt-1(tm388)* mutant and *rnt-1(tm388) bro-1(tm1183)* double mutant larvae. (C) Representative spinning disk confocal image of the seam cell epithelium of *rnt-1(tm388) bro-1(tm1183)* animals in the mid L2 stage. V1 division was normal (representing the 26% lineage in A), V2, V3 and V4 anterior daughter cells undergo the L2 asymmetric division (arrow heads), whereas the posterior cells do not (representing

the 43% lineage in A) (D) Lineage analysis of control animals and heat-shock induced *rnt-1,bro-1* animals. Heat-shock was given between the symmetric and asymmetric division in L2 (middle; arrowhead) or prior to the L3 asymmetric division (right; arrowhead). Late L2 cells and L3 divisions were followed (green boxes). (E) Quantification of the number of seam nuclei at the end of L4 development for control animals and heat-shock-induced L2 and L3 animals. (F) Time-lapse spinning disk microscopy images of early L3 animals that underwent heat-shock induction of *rnt-1 bro-1* at t=17.30-18.30 hr, between the symmetric and asymmetric L2 divisions. Images show epithelium 5 hours after the end of heat-shock (top; early L3 t=23.30hr) and 6 hours after heat-shock (bottom; after L3 div t=24.30hr) during the L3 division. V1, V2 and V3 lineages were followed over time; follow heat shock in L2, all anterior daughter cells behaved as seam cells in L3 (G) Spinning disk images of the seam cell syncytium in late L4 larvae that were control treated (top) or heat-shock exposed during the L2 (middle) or L3 (bottom) stage to induce *rnt-1 bro-1* expression. (H) Illustration of the endogenous *rnt-1* gene with introduced GFP-tag (Top). Time-lapse spinning disk microscopy of RNT-1::GFP and seam cell markers mCherry::PH and Cherry::H2B during L2 symmetric and asymmetric divisions. Images were processed using ImageJ software. Scale bars represent 10 µm.

RNT-1/BRO-1 antagonize POP-1 at the level of anterior daughter cell differentiation.

As a possible molecular mechanism, RNT-1/BRO-1 could overrule Wnt/β-catenin asymmetry during symmetric division by antagonizing POP-1 activity in anterior daughter cells. At a high nuclear level, POP-1 is thought to act as a transcriptional repressor, and to promote differentiation of anterior daughter cells (Kidd et al. 2005). By contrast, at a low nuclear level, POP-1 is expected to act as a transcriptional activator of Wnt-target genes, and to promote the stem cell-like fate of posterior daughter cells. However, RNAi of *pop-1* has been reported to strongly increase seam cell numbers, preventing the differentiation of anterior cells but not the stem-cell like seam cell fate (Gleason & Eisenmann 2010). This appears to indicate that only the repressor function of POP-1 is critical in the seam cell lineage. Complete absence of *pop-1* is lethal, however, and residual *pop-1* in the partial-loss-of-function RNAi animals could suffice for its activator function. To distinguish between these possibilities, we generated a conditional *pop-1* knockout allele. This was achieved by inserting *loxP*-recombination sites into the endogenous *pop-1* locus (Fig. 5A), and combining

the homozygous loxed allele with seam-specific expression of the CRE recombinase (P*scm::CRE* ; Ruijtenberg & van den Heuvel 2015).

Interestingly, the observed phenotype differed between the *pop-1* knockout and RNAi. RNAi knockdown increased the seam cell numbers to more than 60, as a result of anterior daughter cells failing to differentiate and adopting the seam fate (Fig. 5A). The seam-specific *pop-1* knockout also resulted in increased seam cell numbers, but to a lower extent. Closer examination showed that *pop-1^{lox}* knockout animals display a combination of anterior daughter cells adopting the seam fate, and abnormal differentiation of posterior seam cells (Fig. 5B and S4). Combined *pop-1* RNAi and lineage-specific knockout resembled the *pop-1* knockout alone (Fig. 5B). Thus, the exclusive failure in anterior cell differentiation following RNAi results from incomplete *pop-1* loss-of-function. The observations in the knockout agree with the paradigm that POP-1 exerts a dual role in seam daughter cells, promoting differentiation as a repressor, and the stem-cell fate as an activator. Because these functions are determined by the nuclear POP-1 levels, incomplete *pop-1* loss by RNAi likely removes the repressor but not activator function.

As RNT-1/BRO-1 suppresses seam cell differentiation, the complex could antagonize the differentiation-promoting *pop-1* repressor function. To test this possibility, we combined *pop-1* RNAi with heat-shock induced RNT-1/BRO-1 in L2 and L3 asymmetric divisions. This combination further increased the number of seam cells compared to either single condition (L2 heat-shock plus *pop-1* RNAi on average 75 seam cells, L3 heat-shock plus *pop-1* RNAi on average 95 cells. (Fig. 5E,F and 5H). This increase likely results from combining two incomplete conversions from asymmetric to symmetric seam cell division; ± 64% in L2 *pop-1*(*RNAi)* larvae (Fig. 5D, S5), versus one extra round of symmetric division (in L2 or L3) after heat-shock induction of RNT-1/BRO-1 (Fig. 4). Therefore, the enhanced phenotype of the *rnt-1 bro-1* (*gain of function*) *pop-1(RNAi)* combination compared to either single, does not indicate an order of gene functions or whether these genes act in a linear pathway. Nevertheless, these results confirm the antagonistic functions of the RNT-1/BRO-1 and POP-1 transcriptional regulators in anterior seam cell differentiation.

To further examine this antagonism, we combined *pop-1* RNAi with the *rnt-1 bro-1* double mutation. Seam nuclei counts at the end of L4 development revealed intermediate seam cell numbers for this combination (*rnt-1 bro-1* mutant 13 seam nuclei, *pop-1* RNAi 61 nuclei, *rnt-1 bro-1* combined with *pop-1* RNAi: 45 seam cell nuclei. Fig. 5C and 5G). Closer

analysis of the seam cell lineages revealed that the ectopic differentiation of anterior daughter cells in *rnt-1 bro-1* mutants was completely suppressed by *pop-1* RNAi. The seam-cell proliferation defects of *rnt-1 bro-1* mutants, however, were not rescued by *pop-1* RNAi. This combination explains the intermediate seam cell numbers, and indicates that *pop-1* may act downstream of *rnt-1 bro-1,* specifically in differentiation control (Fig. 5D, G, and S5). Together, an antagonistic relation between RNT-1/BRO-1 and POP-1 is indicated by the overlap in phenotype between *rnt-1 bro-1* gain of function and *pop-1* loss of function, by the enhanced seam cell numbers that follow from combining *rnt-1 bro-1* gain of function and *pop-1* loss of function, and by the observed suppression of ectopic differentiation in *rnt-1 bro-1* mutants by *pop-1(RNAi)*. All these observations are consistent with the model that *rnt-1* and *bro-1* act upstream of *pop-1,* and inhibit differentiation by opposing the *pop-1* repressor function.

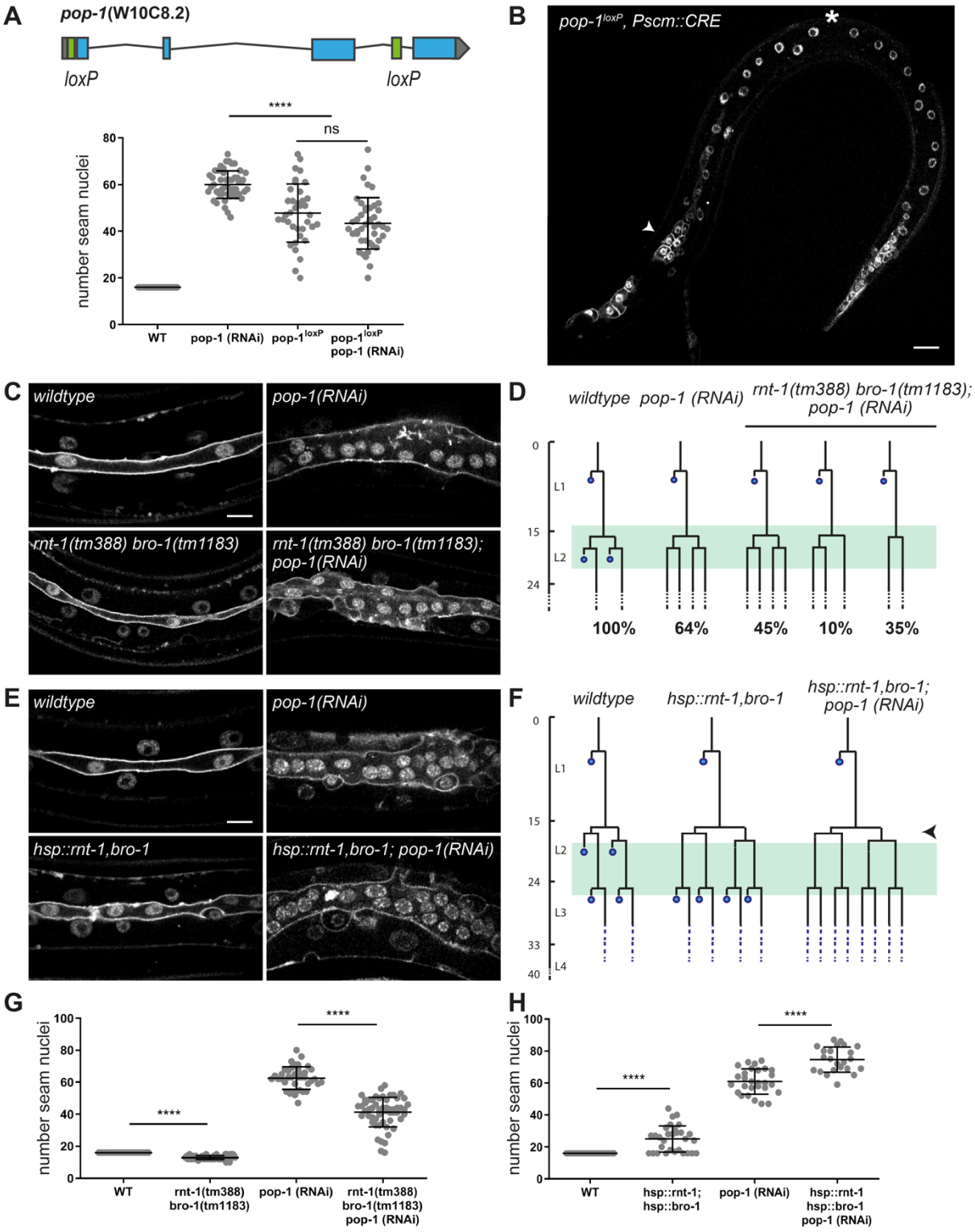
A
pop-1(W10C8.2)
loxP
loxP
****
ns
number seam nuclei
WT
pop-1 (RNAi)
pop-1loxP
pop-1loxP pop-1 (RNAi)
B
pop-1loxP, Pscm::CRE
C
wildtype
pop-1(RNAi)
rnt-1(tm388) bro-1(tm1183)
rnt-1(tm388) bro-1(tm1183); pop-1(RNAi)
D
wildtype
pop-1 (RNAi)
rnt-1(tm388) bro-1(tm1183); pop-1 (RNAi)
L1
L2
100%
64%
45%
10%
35%
E
wildtype
pop-1(RNAi)
hsp::rnt-1,bro-1
hsp::rnt-1,bro-1; pop-1(RNAi)
F
wildtype
hsp::rnt-1,bro-1
hsp::rnt-1,bro-1; pop-1 (RNAi)
L3
L4
G
number seam nuclei
WT
rnt-1(tm388) bro-1(tm1183)
pop-1 (RNAi)
rnt-1(tm388) bro-1(tm1183) pop-1 (RNAi)
H
number seam nuclei
WT
hsp::rnt-1; hsp::bro-1
pop-1 (RNAi)
hsp::rnt-1 hsp::bro-1 pop-1 (RNAi)

Figure 5. Possible antagonism between RNT-1/BRO-1 and POP-1 in controlling anterior seam cell differentiation. (A) Top: Gene map of the floxed endogenous *pop-1* allele. Bottom: Quantification of seam cell nuclei at the end of the L4 stage in *pop-1* RNAi, *pop-1*^{loxP} KO, and *pop-1*^{loxP} KO combined with *pop-1* feeding RNAi animals. (B) Spinning disk confocal microscopy image of a late L2 *pop-1*^{loxP}, P*scm::CRE* animal. Seam markers are mCherry::PH, mCherry::H2B. Arrowhead points to extra seam cells, asterisk points to premature differentiation. (C) Spinning disk confocal microscopy images of late L4 wild-type or *rnt-1(tm388) bro-1(tm1183)* mutants, with and without *pop-1* RNAi. (D) Lineage analyses of L2 wild-type, *pop-1(RNAi),* and *rnt-1(tm388) bro-1(tm1183), pop-1* RNAi larvae. Percentages refer to the fraction of seam cells displaying the phenotype. Green box marks time-window in which animals were observed. Spinning disk confocal microscopy image of heat-shock induced *rnt-1 bro-1* (late L4) with and without *pop-1* RNAi. (F) Lineage analyses of L2 heat-shock induced *rnt-1 bro-1* plus and minus *pop-1* RNAi. Time of heat-shock is marked by arrowhead. Green box indicates time-window during which animals were observed. (G) Quantification of seam cell nuclei at the end of L4 development for *rnt-1(tm388) bro-1(tm1183)* mutants plus and minus *pop-1* RNAi. (H) Quantification of seam cell nuclei at the end of L4 development for heat-shock-induced *rnt-1 bro-1* plus and minus *pop-1* RNAi. Images were processed with ImageJ software. Scale bars represent 10 µm. Error-bars represent mean ± SD.

RNT-1/BRO-1 antagonize POP-1 by negatively regulating its expression in L2 seam cells.

The two most plausible scenarios by which the RNT-1/BRO-1 transcriptional repressor complex may negatively regulate POP-1 are either via transcriptional repression of *pop-1* itself, or via interfering with POP-1-mediated repression of Wnt target genes. In our initial experiments (Fig. 1A,B), we observed that POP-1 localizes asymmetrically during symmetric seam cell divisions. These experiments made use of *pop-1::gfp* expression from a multicopy integrated array, under the control of the *jmp#1* DNA fragment that turned out to be the *sys-1* promoter (Siegfried et al. 2004; LaBonty et al. 2014). As this transgene will not reflect normal POP-1 levels, we generated an *gfp*-tagged endogenous *pop-1* allele by CRISPR/Cas9-assisted recombineering (Fig. 6A). The homozygous *gfp::pop-1* strain was viable, although not fully healthy and occasionally missing a seam cell (Fig. S6). This indicates that while the tag is somewhat disruptive, GFP::POP-1 is largely functional. Hence, we used the GFP-tagged endogenous protein to determine POP-1 expression dynamics and the possibility of RNT-1/BRO-1-mediated suppression.

Similar to our observations of transgene expressed *pop-1* (Fig. 1A,B), spinning disk confocal time-lapse microscopy of endogenous GFP::POP-1 showed asymmetric enrichment in anterior daughter cell nuclei formed during the symmetric L2 or asymmetric L2 and L3 divisions (Fig. 6B,C). Importantly, however, the POP-1 expression levels differed substantially between L2 and L3 seam cells: POP-1 levels were lowest during the symmetric division, and subsequently increased during L2 asymmetric and L3 asymmetric divisions (Fig. 6D; levels quantified at the time of cytokinesis). These observations suggest the possibility that RNT-1/BRO-1 overrule Wnt/β-catenin asymmetry in L2, by reducing *pop-1* expression.

To test this possibility, we compared GFP::POP-1 levels in wild-type and *rnt-1(tm388) bro-1(1183)* mutant animals. Notably, POP-1 expression levels were significantly higher in the mutant (Fig. 6B, bottom). In fact, during the first L2 seam cell division in the *rnt-1 bro-1* double mutant, GFP::POP-1 levels were similar to those of the asymmetric L2 division in the wild type (Fig. 6D). As nuclear POP-1 levels determine its activity as a transcriptional repressor, this finding may well explain that 31% of *rnt-1 bro-1* mutants skip the symmetric L2 division and show ectopic epidermal differentiation (Fig. 4A). To further test whether RNT-1/BRO-1 induces *pop-1* downregulation, we used heat-shock induced RNT-1 BRO-1 expression in the endogenous *gfp::pop-1* animals. This resulted in significantly reduced GFP::POP-1 levels in the daughter cells of the L2 asymmetric seam cell division (Fig. 6E-F). As expected, GFP::POP-1 still showed an asymmetric distribution between anterior and posterior daughter cells (Fig. 6G). We conclude that the RNT-1/BRO-1 transcriptional repressor is likely to reduce the expression of POP-1 below the threshold level needed for POP-1 repressor function, and thereby induces symmetric seam cell division. To test direct regulation, we altered two candidate RNT-1/BRO-1 binding sites in the *pop-1* promoter by CRISPR/Cas9-assisted recombineering (Fig. S7). This *pop-1* promoter mutation did not result in a *rnt-1 bro-1* phenotype, indicating that RNT-1/BRO-1 do not act (solely) through these elements.

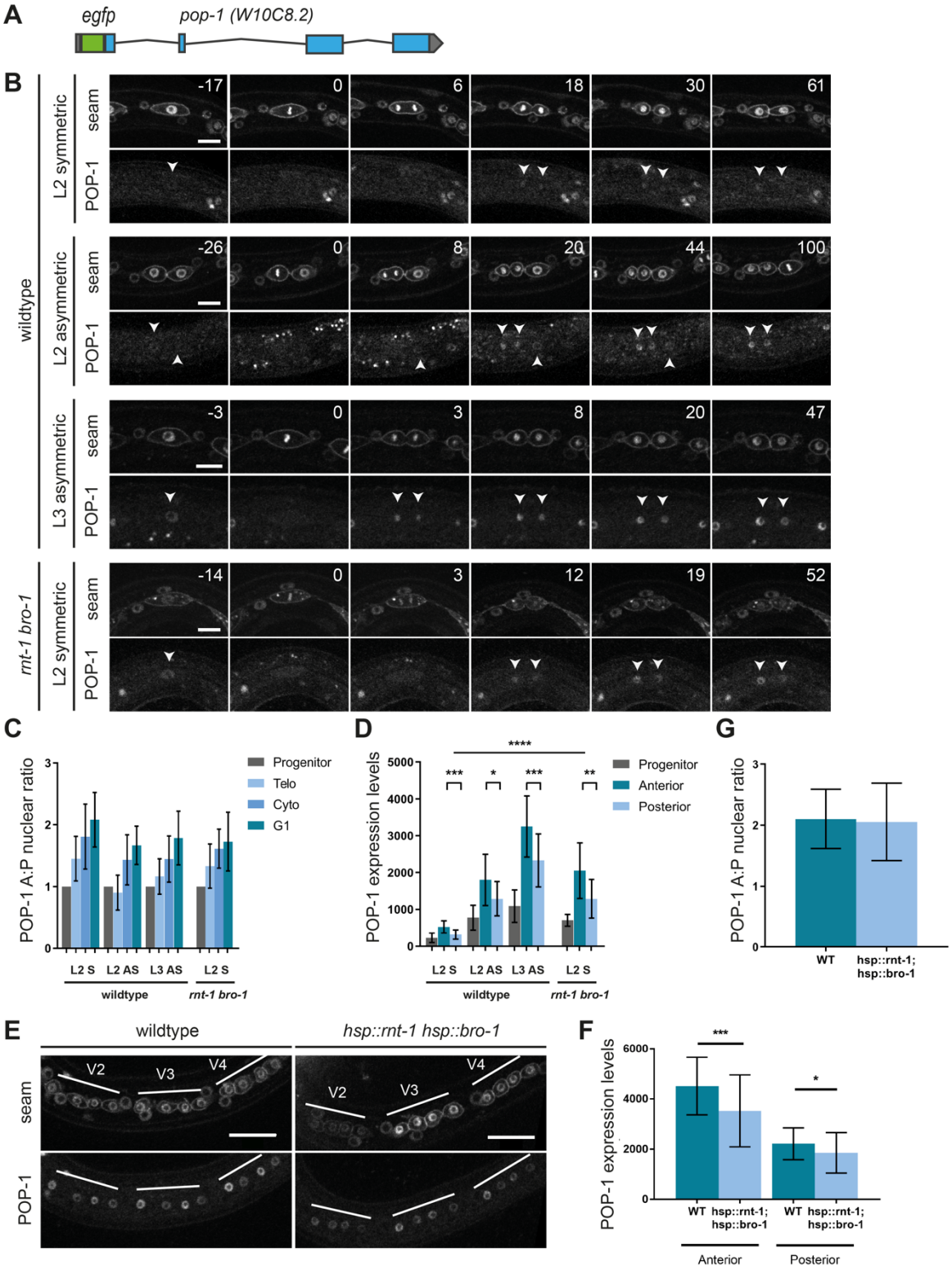

Figure 6. RNT-1/BRO-1 can overrule Wnt signaling by lowering *pop-1* expression levels. (A) Gene map of the tagged endogenous *gfp::pop-1* allele. (B) Time-lapse spinning disk confocal microscopy images of GFP::POP-1 and seam cell markers mCherry::PH and Cherry::H2B during L2 symmetric, L2 asymmetric, and L3 asymmetric divisions in the wild type, and L2 symmetric division in *rnt-1(tm388) bro-1(tm1183)* mutants. Arrowheads point to daughter cell nuclei. (C) Quantification of the A/P ratio

of GFP::POP-1 in daughter cell nuclei of wildtype L2 and L3 divisions, and L2 symmetric division in *rnt-1(tm388) bro-1(tm1183)* mutants. (D) Relative expression levels of GFP::POP-1 during L2 and L3 divisions in the wild type, and L2 symmetric division in *rnt-1(tm388) bro-1(tm1183)* mutants. (E) Spinning disk confocal microscopy images of normal control and heat-shock induced RNT-1/BRO-1 late L2 animals. Seam markers are mCherry::PH and Cherry::H2B. (F) Relative GFP::POP-1 expression levels in control animals and heat-shock induced RNT-1/BRO-1 animals. (G) GFP::POP-1 nuclear A/P ratio in control animals and heat-shock induced RNT-1/BRO-1 animals. Note that the images in D and F were taken with different settings, therefore the relative levels (Y-axis) is different between these experiments. Images were processed using ImageJ software. Scale bars represent 10 µm (B) and 20 µm (E). Error-bars represent mean ± SD.

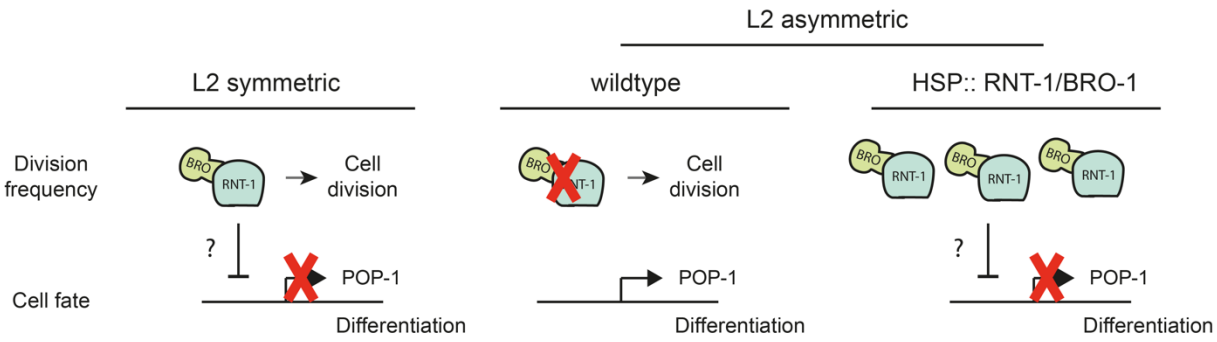

Figure 7 Model for RNT-1/BRO-1 mediated repression of POP-1. L2 seam cells maintain the asymmetric distribution of POP-1 during symmetric divisions. However, the RNT-1/BRO-1 repressor reduces the overall POP-1 expression level, and thereby nuclear POP-1 in the anterior daughter cell remains below the level needed for transcriptional repression and differentiation induction (left panel). Preceding the L2 asymmetric division in the wild-type, RNT-1 is degraded and POP-1 expression no longer repressed, allowing asymmetric cell division (middle). Increased expression levels of RNT-1/BRO-1 convert an asymmetric division into a symmetric division by reducing POP-1 expression levels (right panel).

Discussion

In this study, we examined the fundamental difference between asymmetric and symmetric seam cell divisions, and the mechanisms that control the switch between these division modes. In contrast to RNAi, lineage-specific *pop-1* knockout revealed the dual functions of POP-1 in the seam lineage. Only part of the *pop-1* knockout seam cells showed ectopic epidermal differentiation, while feeding RNAi resulted exclusively in failure to undergo differentiation of anterior daughter cells. The combined observations indicate that the transcriptional activator function of POP-1 is less critical than its repressor function, and requires a limited amount of POP-1. As removal of the repressor function is sufficient to convert an asymmetric seam cell division into a symmetric division, the presence or absence of POP-1-mediated transcriptional repression appears to be the fundamental difference between asymmetric and proliferative seam cell divisions.

Based on expression of a broadly used reporter transgene, we confirmed the earlier observation by us and others (Wildwater et al. 2011; Hughes et al. 2013; Harandi & Ambros 2014) that POP-1 levels differ between anterior and posterior daughter nuclei of symmetric divisions. Examination of GFP-tagged endogenous POP-1 confirmed this asymmetric localization. To our surprise, however, this also revealed a temporary decrease in *pop-1* expression prior to the L2 symmetric divisions, to a level substantially below that of nuclear POP-1 in self-renewing daughter cells of asymmetric seam cell divisions. A general reduction in POP-1 expression provides a simple mechanism to bypass the POP-1 repressor function during symmetric seam cell division.

RNT-1/BRO-1 modulate Wnt signaling by negatively regulating *pop-1* gene expression

We identified the RNT-1/BRO-1 transcriptional repressor complex as a negative regulator of *pop-1* gene expression. Induced expression of RNT-1/BRO-1 resulted in symmetric cell division and significantly reduced GFP::POP-1 levels in seam cells. Conversely, loss of function of *rnt-1* and *bro-1* increased POP-1 expression in early L2 stage seam cells to a level normally present during the L2 asymmetric divisions. While supporting that RNT-1/BRO-1 negatively regulates POP-1 expression, these data do not reveal whether this regulation is direct. Supporting direct transcriptional regulation of *pop-1* by RNT-1/BRO-1, ChIP-

sequencing results from the modERN consortium demonstrate RNT-1 association with the *pop-1* promoter in L1 larvae (Kudron et al. 2018). The *pop-1* promoter contains two Runx binding sites (5'-HGHGGK-3'; Van Der Deen et al., 2012) in this region. However, mutating these sites in the endogenous *pop-1* promoter did not result in a *rnt-1 bro-1* mutant phenotype. It is possible that additional RNT-1/BRO-1 binding sites are present and sufficient for *pop-1* regulation. Alternatively, RNT-1/BRO-1 could downregulate *pop-1* indirectly, or contribute additional mechanisms to induce the L2 seam cell division program.

In L2, the presence versus absence of RNT-1 corresponds to POP-1 levels and symmetric versus asymmetric division. However, this is not true for other developmental stages. Tagged endogenous RNT-1 was highly expressed before the asymmetric seam cell divisions in L1 and L3 (Fig. S3), in line with observations with a transgenic reporter (Kagoshima et al. 2005). Similarly, analyses of reporter transgenes have indicated that BRO-1 is expressed through all larval stages (Kagoshima et al. 2007a; Xia et al. 2007). Interestingly, in males, the V6 seam cell undergoes an extra symmetric division during the L3 stage. This division and others in the male-specific V6 and T seam cell lineages are frequently skipped in *rnt-1* (also known as: male abnormal-2 *mab-2*) and *bro-1* mutants (Kagoshima et al. 2005, 2007a; Nimmo et al. 2005). It is possible that RNT-1/BRO-1 are more broadly expressed as an ancestral mechanism to induce symmetric seam cell divisions. In *C. elegans* this function is used only during L2 and male tail development, hence mechanisms need to be in place to prevent POP-1 repression at other stages. Studies of mammalian Runx proteins revealed extensive regulation by post-translational modifications that facilitate interaction with transcriptional activators or co-repressors and dictate Runx function (Reviewed in Blyth et al., 2005; Chuang et al., 2013). Similarly, the *C. elegans* RNT-1/BRO-1 repressor activity may be temporarily induced in L2 seam cells, or the response to RNT-1/BRO-1 activity could depend on other factors, such as the heterochronic pathway.

Heterochronic genes may create a window of opportunity for *pop-1* repression

The temporal restriction of *pop-1* downregulation to the L2 stage seam cells suggests involvement of the heterochronic pathway. This pathway includes a series of successively expressed transcription factors, RNA-binding proteins and miRNAs that provide temporal identity during larval development (Rougvie 2005; Moss 2007). L1 development is

determined by the LIN-14 transcription factor, which has been suggested to prevent symmetric seam cell division and reduce POP-1 dependence (Harandi & Ambros 2014). L2 development is defined by expression of the RNA-binding protein LIN-28 and downstream transcription factor HBL-1 (Abrahante et al. 2003; Lin et al. 2003; Abbott et al. 2005). These factors have also been shown to genetically interact with the Wnt/β-catenin asymmetry pathway in seam cells (Harandi & Ambros 2014). As a consequence, seam cells in the L2 stage appear uniquely sensitive to POP-1 levels, which could allow transitions from asymmetric to symmetric cell division. It is currently unclear whether this heterochronic effect could by mediated by activation of RNT-1/BRO-1, or inhibition of *pop-1* in parallel. Interestingly, a feedback loop between mammalian LIN28 and TCF7A has been detected in breast cancer cells (Chen et al. 2015), pointing to a potentially conserved mechanism. We did not observe an effect of heat-shock induced expression of either LIN-28 or HBL-1 during L2 and L3 asymmetric seam cell divisions (Fig. S8). Interestingly though, we did observe a genetic interaction between *rnt-1* and *hbl-1*; both *rnt-1* and *hbl-1* loss of function reduce the number of seam cell divisions in L2, and the combination strongly repressed the *pop-1(RNAi)* phenotype. Whether this reflects functions in parallel or within a regulatory cascade will require lineaging of null mutant combinations, as an extra division of seam nuclei in L4 *hbl-1(ve18)* larvae obscures the L2 cell division defective phenotype

Differential regulation of seam cell fate and proliferation

We did not observe additional divisions of seam cells following RNT-1/BRO-1 induction. The *rnt-1 bro-1* double mutant phenotype, however, supports that these factors also contribute to seam cell proliferation in the L2 stage, and during male tail development (Kagoshima et al. 2005, 2007a; Nimmo et al. 2005; Xia et al. 2007). RNAi of *pop-1* suppressed the ectopic differentiation but not proliferation defects of *rnt-1 bro-1* mutants, which indicates that cell fate and proliferation involve different mechanisms. The control of proliferation by RNT-1/BRO-1 has been suggested to involve repression of the cell cycle inhibitory genes *cki-1*$^{Cip/Kip}$, *fzr-1*^{Cdh1} and *lin-35*^{Rb} (Nimmo et al. 2005; Kagoshima et al. 2007a; Xia et al. 2007). Analogous to the regulation of *pop-1* expression, it remains unclear how repression of these genes by RNT-1/BRO-1 is controlled to allow extra rounds of division only in the L2 stage and during male tail development. Similar to cell fate, the heterochronic factor LIN-28 could

sensitize seam cells in the L2 stage for extra cell division. Mammalian Lin28 is a stem cell factor which promotes pluripotency and cell proliferation (Viswanathan & Daley 2010). Cyclin A, cyclin B and Cdk4 have been identified as target mRNAs for Lin28, and Lin28-mediated enhanced translation may promote stem cell proliferation (Xu et al. 2009). Similarly, upregulation of positive cell cycle regulators in L2 could determine that seam cells go through an extra division in response to RNT-1/BRO-1 mediated repression of cell-cycle inhibitors.

Conserved modulation of Wnt signaling by Runx proteins

In this study, we identified a novel interaction between two conserved stem cell regulators. We propose that by negatively regulating *pop-1* expression, RNT-1/BRO-1 modulates Wnt/β-catenin asymmetry pathway activity in seam daughter cells (Summarized in Fig. 7). Cross-regulation between Runx and TCF appears conserved in mammals, although different mechanisms are likely involved. Studies in mouse intestinal epithelial cells showed that Runx3 adapts Wnt signaling via physical binding to nuclear TCF4. The formation of a ternary β-catenin::TCF4::Runx3 complex prevented TCF4 from binding to DNA (Ito et al. 2008; Reviewed in Chuang et al. 2013). Conversely, a ternary complex composed of β-catenin::LEF1::Runx2 was found to inhibit Runx2 from binding to DNA in mouse osteoblast cells (Kahler & Westendorf 2003). Whether or not such physical interactions are used in *C. elegans,* these results indicate that cross-regulation between the Runx/CBFβ and Wnt/β-catenin stem-cell regulators are likely applied more broadly.

Supplementary Figures

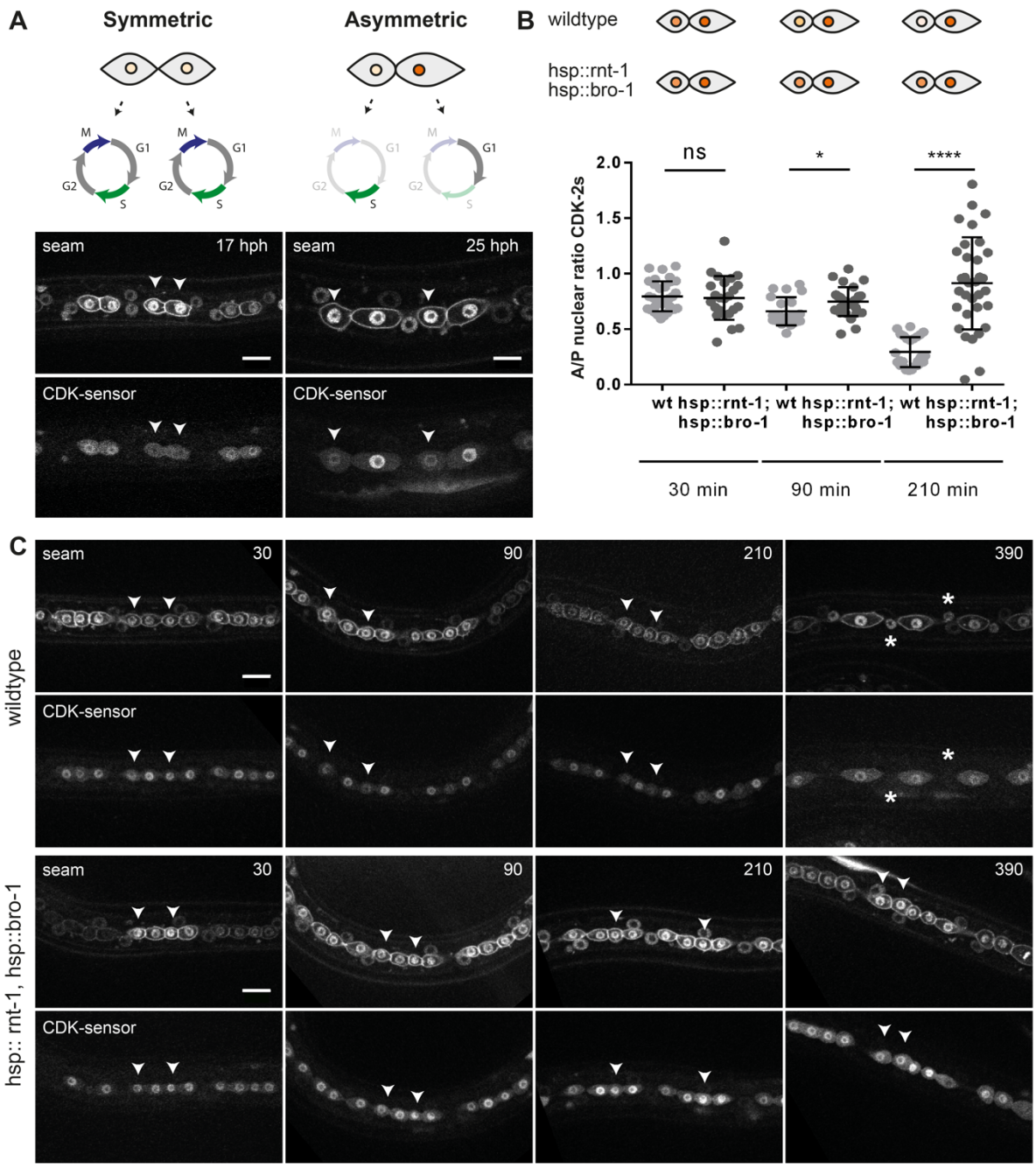

Supplementary Figure 1. Cell cycle progression as a read-out for daughter cell fate. (A) Seam cells progress differently through the cell cycle after symmetric or asymmetric cell division (Top), as illustrated by spinning disk microscopy images of seam cells expressing the CDK sensor (Bottom). Left panels: seam daughter cells after symmetric L2 division, t=17 hours post hatching (hph). Right panels: daughter cells after asymmetric division in L3, t=25 hph. Note that the CDK sensor helps to distinguish between anterior fate (cell cycle reentry; nuclear export of GFP) and seam cell self-renewal (quiescence; nuclear retention of GFP). (B) A/P nuclear ratio of the CDK-2 sensor in control and heat-shock induced RNT-1/BRO-1 L2 seam cells measured at different timepoints after induction. Time indicates minutes after heat shock, which was stopped just prior to or during mitosis. (C)

Spinning disk microscopy of control and heat-shock induced RNT-1/BRO-1 seam cells. Images taken at different time point after induction. Images were processed using ImageJ software. Scale bars represent 10 µm. Error-bars represent mean ± SD.

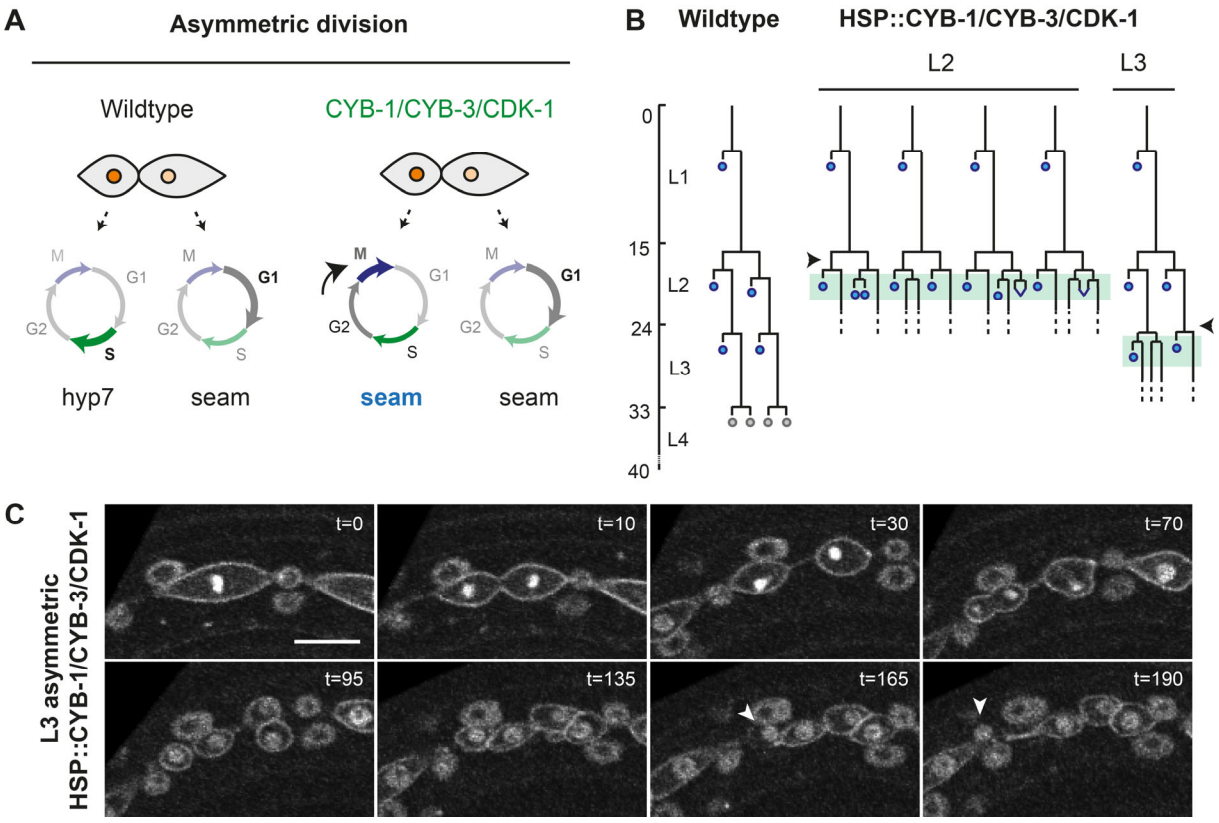

Supplementary figure 2. Induced expression of CDK-1, CYB-1, and CYB-3 occasionally induced extra mitosis. (A) Seam daughters of a wild-type asymmetric division progress differently after cytokinesis: anterior differentiating daughter cells undergo S-phase before fusing with the hyp7 epidermis. Posterior daughters pause in G1 until the next larval stage. Heat-shock induced expression of *cdk-1, cyb-1,* and *cyb-3* was used to force anterior daughter cells of asymmetric divisions to progress into mitosis after completing S-phase. We hypothesized that cell cycle progression of the anterior cells might overrule differentiation into hyp7 and trigger these cells to maintain a seam fate (blue). (B). Lineage analyses of L2 (middle) and L3 (right) animals with heat-shock induced CDK-1/CYB-1/CYB-3. Heat shock was given between the symmetric and asymmetric L2 division (middle; arrowhead) or prior to the L3 asymmetric division (right; arrowhead). Animals were followed using time-lapse microscopy during the hours after heat shock (green boxes). (C) Time-lapse spinning disk microscopy of L3 animals with heat-shock induced CDK-1/CYB-1/CYB-3. Time-lapse represents the L3 lineage presented in panel B. Both the anterior and posterior daughter cells of the L3 asymmetric division undergo an additional mitosis, of which the anterior daughter cell of the anterior division differentiates and fuses with the epidermis (arrowhead). Images were processed using ImageJ software. Scale bars represent 10 µm.

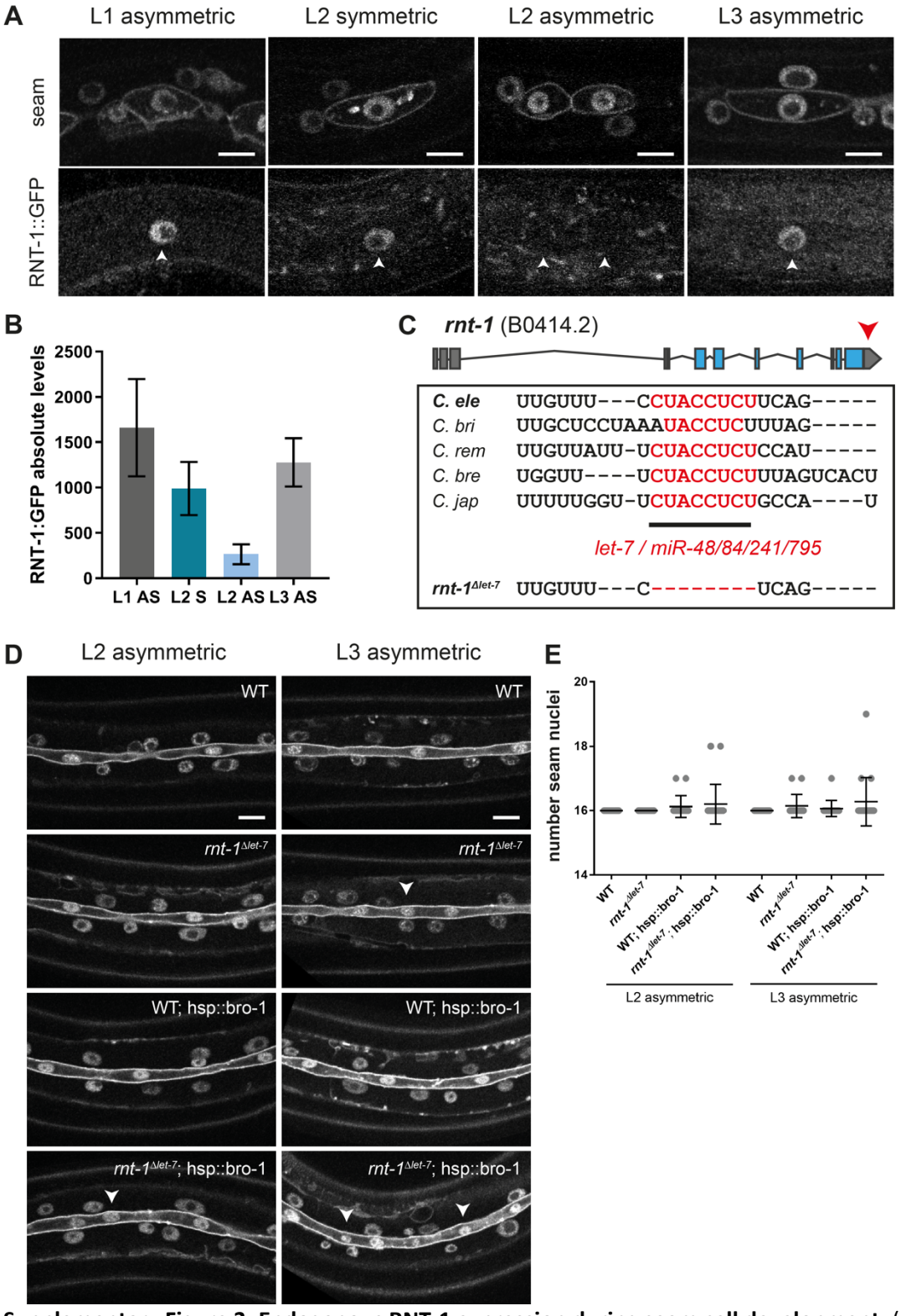

Supplementary Figure 3. Endogenous RNT-1 expression during seam cell development. (A) Spinning disk images of endogenous RNT-1::GFP expression prior to nuclear envelope breakdown in L1-L3 seam cells. Seam markers are mCherry::PH and mCherry::H2B. Arrowheads point to nuclear RNT-1::GFP. (B) Quantification of the levels of RNT-1::GFP in L1-L3 seam cells. (C) Illustration of the endogenous *rnt-1* 3' untranslated region (3'UTR; red arrowhead) with the *let-7* recognition sites marked in red. These sites are conserved between different nematodes (*C. briggsae, C. remanei, C.*

brenneri and *C. japonica*). The red nucleotides were deleted from the endogenous locus using CRISPR/Cas9 recombineering. (D) Spinning disk images of late L4 lateral seam syncytia of control, *rnt-1*$^{\Delta let\text{-}7}$*, hsp::bro-1* and *rnt-1*$^{\Delta let\text{-}7}$ *hsp::bro-1* animals subjected to heat shock prior to the L2 (left panel) and L3 (right panel) asymmetric divisions. (E) Quantification of the number of seam nuclei in late L4 lateral seam syncytia of control, *rnt-1*$^{\Delta let\text{-}7}$*, hsp::bro-1* and *rnt-1*$^{\Delta let\text{-}7}$ *hsp::bro-1* animals subjected to heat shock prior to the L2 and L3 asymmetric divisions. Images were processed using ImageJ software. Scale bars represent 10 µm. Error-bars indicate mean ± SD.

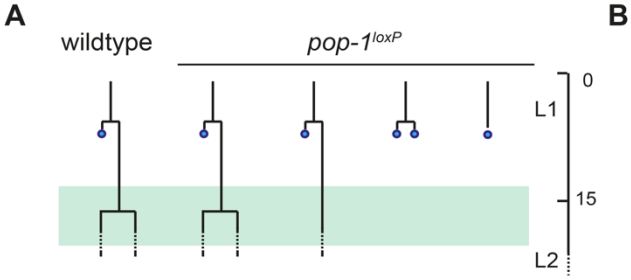

V1	100%	26%	53%	11%	5%
V2	100%	42%	26%	26%	5%
V3	100%	32%	16%	37%	11%
V4	100%	21%	5%	68%	-
V6	100%	-	-	42%	53%

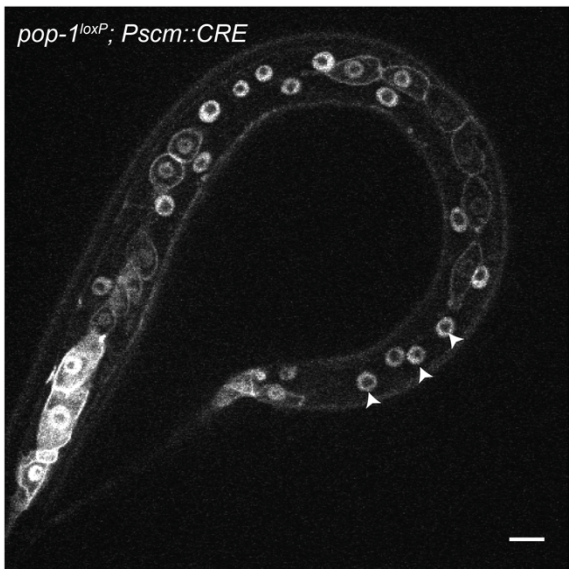

Supplementary figure 4. Conditional knock-out of *pop-1* reveals a dual role as transcriptional repressor and activator in seam cells. (A) Lineage analysis of *pop-1*^{loxP} early L2 animals undergoing the symmetric seam cell division. Y-axis represents developmental timing (hours; L2 starts at 15 hr) The four different lineages observed in *pop-1*^{loxP} animals are plotted against developmental time. The frequency of occurrence of each lineage was quantified for V1-V4 and V6 seam cells. Together, these quantifications reveal extensive premature differentiation of seam cells during L1 stage (B) Spinning disk confocal microscopy images of two late L2 *pop-1*^{loxP}, P*scm::CRE* animals. Seam markers are mCherry::PH, mCherry::H2B. Arrowheads points to premature differentiation, asterisk points to extra seam cells. Scale bar represents 10 µm.

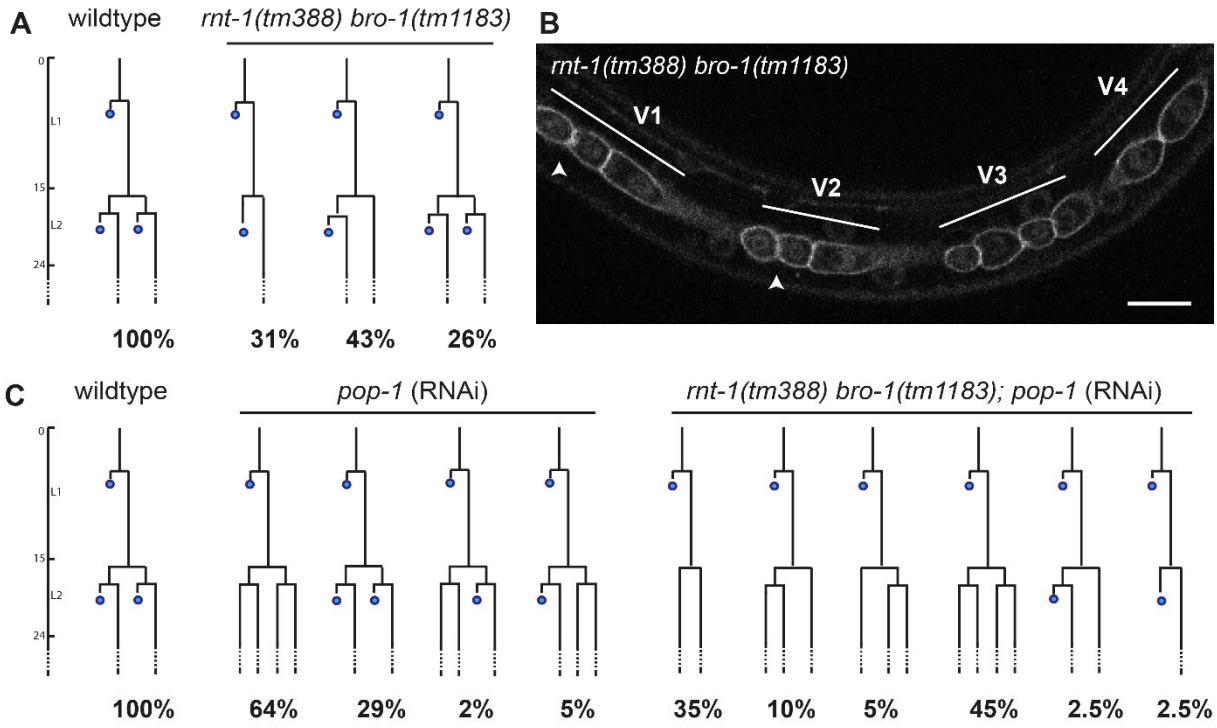

Supplementary Figure 5. Overview of lineage analysis of wild-type and mutant strains. (A) Lineage analysis for wild-type animals and *rnt-1(tm388) bro-1(tm1183)* mutants performed at 20 °C. (B) Spinning disk confocal image of a *rnt-1(tm388) bro-1(tm1183)* animal. The seam markers used are GFP::PH and GFP::H2B. Arrowheads point to anterior daughter cells having undergone the L2 asymmetric division. Scale bar represents 10 µm. (C) Lineage analysis for wild-type animals, *pop-1(RNAi)* animals, and *rnt-1(tm388) bro-1(tm1183)* mutants exposed to *pop-1* RNAi by feeding.

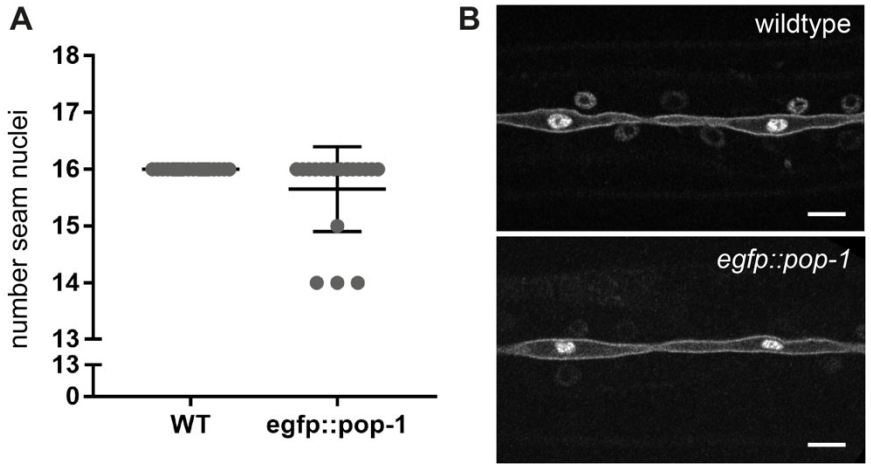

Supplementary figure 6. Characterization of seam epithelia in endogenous *egfp::pop-1* strain. Quantification of seam cell nuclei in L4 seam syncytia in wild-type and knock-in animals (A). Representative spinning disk images of L4 stage seam syncytia of wild-type (top) and *egfp::pop-1* (bottom) animals (B). Images were processed with ImageJ software. Scale bars represent 10 µm. Error-bars represent mean ± SD.

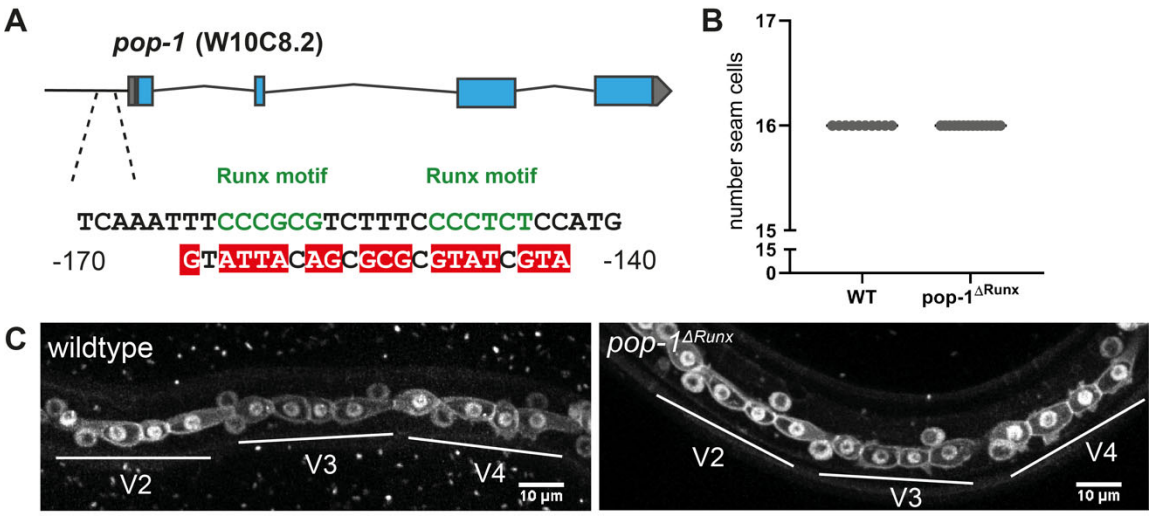

Supplementary figure 7. Mutation of candidate *rnt-1* binding sites in the endogenous *pop-1* promoter region is not sufficient to alter seam cell fate. Schematic representation of the pop-1 promoter region with the Runx binding motifs. Mutated residues are depicted in red (A). Quantification of seam cell numbers in late L2 animals of *pop1*$^{\Delta Runx}$ animals (B). Representative spinning disk images of *pop1*$^{\Delta Runx}$ late L2 stage seam cells (C). Images were processed using ImageJ software. Scale bars represent 10 µm. Error-bars represent mean ± SD.

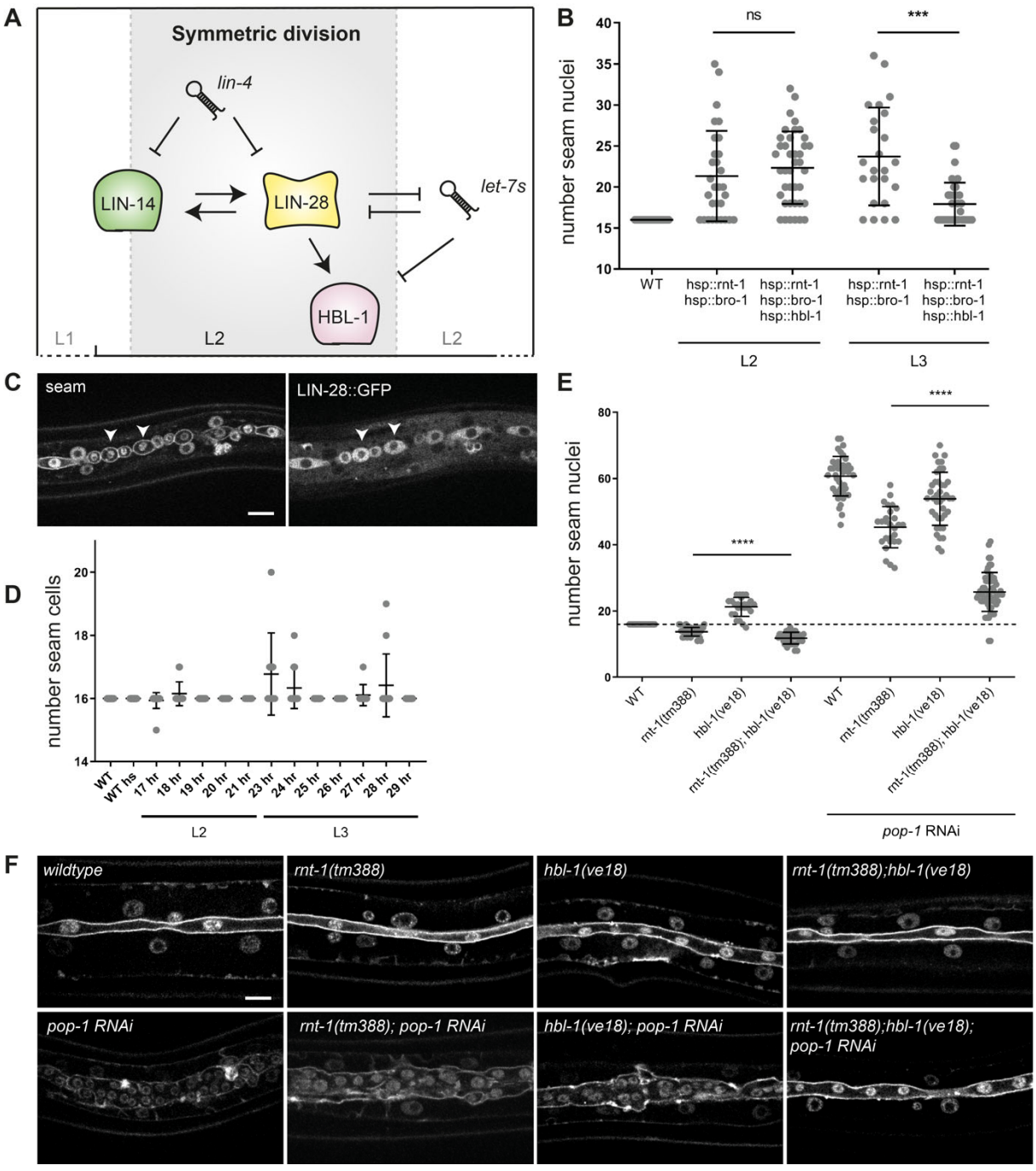

Supplementary figure 8. Manipulation of heterochronic *lin-28* and *hbl-1* gene expression during L2 and L3 asymmetric divisions. (A) Schematic cartoon of the L2 "symmetry window" as determined by expression of *lin-14*, *lin-28* and *hbl-1* genes. (B) Quantification of the number of seam cell nuclei in late L4 lateral seam syncytia, in animals subjected to heat-shock induction of *rnt-1 bro-1* and *rnt-1 bro-1 hbl-1* prior to the L2 asymmetric or L3 asymmetric division. (C) Spinning disk confocal microscopy image of an L3 larva subjected to heat-shock induction of *lin-28::gfp*. Arrowheads point to posterior daughter cells of the L3 asymmetric seam cell division, displaying high cytoplasmic levels of LIN-28::GFP protein. (D) Quantification of seam cell numbers after heat-shock induction of *lin-28::gfp* in L2 (induction 17 hr-22 hr) or L3 larvae (induction 23-29 hr). Seam cells were counted at the end of L2 (t22 hr) or L3 (t30 hr). (E) Quantification of seam cell nuclei numbers in late L4 lateral seam syncytia of control, *rnt-1(tm388), hbl-1(ve18)* and *rnt-1(tm388);hbl-1(ve18)* animals with and without *pop-1(RNAi)*. (F) Spinning disk confocal microscopy images of late L4 lateral seam syncytia of control,

rnt-1(tm388), hbl-1(ve18) and *rnt-1(tm388);hbl-1(ve18)* animals with and without *pop-1(RNAi)*. Images were processed using ImageJ software. Scale bars represent 10 µm. Error-bars indicate mean ± SD.

Table S1. Overview of oligonucleotides used in this study

Oligo	Sequence
pop-1^{loxP}	
pop-1 N-terminus gRNA 1	ctcatcgccgagctcttcgtcgg
pop-1 N-terminus gRNA 2	tttttgtgtatttttatatctgg
pop-1 C-terminus gRNA 1	taaatgtctactgtagcggaagg
pop-1 C-terminus gRNA 2	cgctacagtagacatttatgggg
pop-1 N-terminus repair ssDNA oligo	cgttaaaaaatgctctaaatttcaagatataaaaatacacataacttcgtatagcatacattatacgaagttataaaaatgatggcagacgaagagctcggcgatgaggtgaag
pop-1 C-terminus repair ssDNA oligo	ttcatttttctacatcacatgaataacaccataaatgtctataacttcgtatagcatacattatacgaagttatactgtagcggaaagaaaaattaacagcgctacggtagtca
pha-1 repair ssDNA oligo	caaaatacgaatcgaagactcaaaaagagtatgctgtatgattacagatgttcatcaagttattcataaatcattgatag
egfp::pop-1	
pop-1 exon 1 gRNA 1	gctcatcgccgagctcttcgtcgg
pop-1 LHA FW	ggctgctcttcgtggttggtagaagtctaaacctccacttt
pop-1 LHA RV	gggtgctcttcgcatttttgtgtatttttatatctgg
pop-1 RHA FW	agagctcggcgatgaggtgaaagtgttccgtcgggatgagg
pop-1 RHA RV	gggtgctcttcgtacgaactccgcccataaaaccgt
pop-1$^{\Delta Runx}$	
pop-1 N-terminus gRNA 1	catggagaggggaaagacgcggg
pop-1 N-terminus gRNA 2	cggaagttaggccatggagaggg
pop-1 promoter repair oligo	aacctccactttctccccaaaatcctatcgaattcaaatgtattacagcgcgcgtatcgtaatgccctaacttccgcggacctagtccccctttttttcttgttttaaatggttcc
rnt-1::egfp	
rnt-1 C-terminus gRNA 1	atagttcttctccgactatttgg
rnt-1 C-terminus gRNA 2	gttcttctccgactatttggagg
rnt-1 LHA FW	cagatgccaatgacaatgattccacc
rnt-1 LHA RV	aaaaggtctccatatcgtaggtgatgagctattcgatgaagt
rnt-1 RHA FW	tcttaaaaatattcattattttaccacaacacacc
rnt-1 RHA RV	tctaatcatccatctcccaactc
Heat shock expression	
FW *hsp16.48*	ctggacggaaatagtggtaaag
RV *hsp16.48*	tcttgaagtttagagaatgaacag
FW *unc-54 UTR*	catctcgcgcccgtgcc
RV *unc-54 UTR*	aaacagttatgtttggtatattggg
FW *cki-1*	atgtcttctgctcgtcgttg
RV *cki-1*	gtatggagagcatgaagatcg
FW *egfp*	atgtccaagggagaggagc
RV *egfp*	ttacttgtagagctcgtccattcc

4

Coordinating cell size and cell fate regulation during asymmetric cell division of *C. elegans* seam stem cells

Suzanne van der Horst, Vincent Portegijs and Sander van den Heuvel

Developmental Biology, Department of Biology, Faculty of Science, Utrecht University,
Padualaan 8, 3584 CH Utrecht, The Netherlands

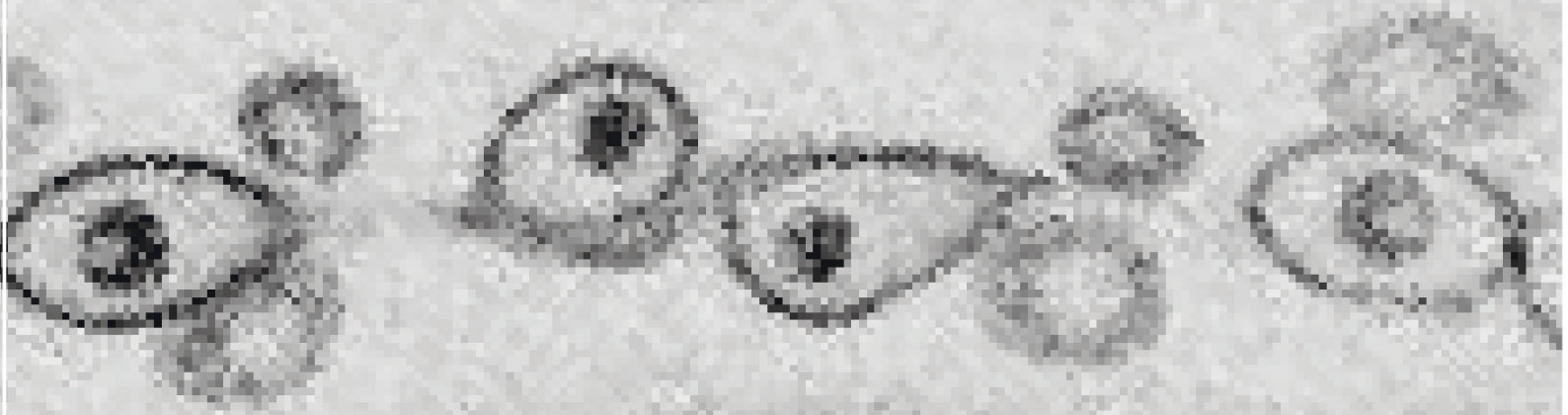

Abstract

Asymmetric cell divisions allow tissue-specific stem cells to combine proliferation with the generation of daughter cells that enter a differentiation program. This asymmetry in daughter cell fate often coincides with asymmetry in cell size. How cell fate and size are coordinated remains an important question. Both processes respond to upstream polarity regulators, which control the localization of cell fate determinants and position the mitotic spindle accordingly. Here, we study asymmetric divisions of the stem cell-like seam cells in the *C. elegans* epidermis. We show that the asymmetric seam cell divisions in first stage larvae generate daughter cells of equal sizes. From the L2 stage onward, however, asymmetric divisions create a smaller differentiating daughter cell and a larger seam stem cell. This asymmetry in size follows displacement of the mitotic spindle in anterior direction during the division process. Surprisingly, we found the transcriptional Wnt/β-catenin pathway to be critical for the anterior-posterior orientation of the spindle in mitosis. Knockdown and lineage-specific knockout of *pop-1* TCF resulted in spindle misalignment, while off center displacement was maintained. Based on resemblance with Wnt ligand loss, these observations may indicate positive feedback between *pop-1* TCF and upstream Wnt/Frizzled signaling components. We investigated whether anterior spindle displacement is instructed by Wnt/β-catenin asymmetry signaling or parallel acting mechanisms, through asymmetry in cortical microtubule pulling force generators or the actomyosin cytoskeleton. Combined GSK-3 and Casein Kinase I phosphorylation regulates Wnt/β-catenin signaling and interaction between the cortical pulling forces regulators LIN-5/GPR-1,2, however, crosstalk between these pathways was not detected. Instead, we found the PIG-1 kinase to contribute to spindle alignment in seam cells, by preventing lateral attachment. Preliminary observations indicate that a dynamic NMY-2 non-muscle myosin localization precedes daughter cell size asymmetry, which warrants further study of a potential role for NMY-2 in spindle displacement.

Introduction

Asymmetric cell divisions contribute to cellular diversity by generating daughter cells with different cell fates. Tissue-specific stem cells can apply this division mode to combine stem cell self-renewal with the generation of differentiating daughter cells. In many cases, the two daughter cells formed during asymmetric cell division differ not only in cell fate but also in size. Studies in *C. elegans* and *Drosophila* have revealed many of the regulatory mechanisms that control asymmetric cell division (Reviewed in Neumüller & Knoblich 2009; Knoblich 2010). These studies have shown that asymmetry in cell fate can be achieved through accumulation of cytoplasmic determinants towards one pole of the mother cell. The unequal segregation of these factors during cell division depends on the plane of cell cleavage, which usually occurs perpendicular to and midway through the mitotic spindle. Thus, by orienting the spindle, developmental signals control whether polarized cells form daughter cells with different fates. In addition, by positioning the spindle off center, cell division can be instructed to create daughter cells with different sizes. The formation of polar bodies during female meiosis, and the division of the *C. elegans* zygote are well-studied examples of asymmetric divisions that combine asymmetry in daughter cell size and fate (Reviewed in Neumüller & Knoblich 2009; Morin & Bellaïche 2011).

It remains incompletely understood what mechanisms achieve and coordinate asymmetry in cell fate and cell size, in particular for cells that reside within tissues. Although asymmetry in cell fate and cell size may coincide, they involve independent regulators. As a first step in asymmetric cell division, the mother cell needs to establish an axis of cell polarity. Both the localization of cell fate determinants and the orientation of cell division are instructed with respect to this polarity axis. The spindle rotates towards a polarity axis determined by PAR (partitioning defective) proteins during asymmetric division of the *C. elegans* zygote, *Drosophila* neuroblasts and stem-cell progenitors in the mammalian skin and developing brain. PAR proteins were discovered based on their requirement for anterior-posterior axis formation in the *C. elegans* embryo (Kemphues 2000). Subsequent studies revealed broad functions for PAR proteins in the establishment of polarity in other systems, including the apical-basal polarity of epithelia. Interestingly, most asymmetric divisions in *C. elegans* are not aligned with the apical-basal PAR polarity axis, but along the anterior-posterior body axis. Similarly, cell divisions in flies and mammals can be oriented with

respect to a proximal-distal axis of tissue polarity. Dependent on the cell or tissue-polarity cues used, different regulators participate in the asymmetric segregation of cell fate determinants and positioning of the spindle (Morin & Bellaïche 2011).

In the four-cell *C. elegans* embryo, the spindle in the endoderm and mesoderm precursor cell EMS rotates to align with the anterior-posterior body axis. This rotation depends on cell-cell interactions with the neighboring P2 cell (Goldstein 1995). Genetic studies revealed parallel inputs from Wnt signaling and a MES-1/SRC-1 Src kinase pathway in orienting the spindle (Rocheleau et al. 1997a; Thorpe et al. 1997; Bei et al. 2002; Walston et al. 2004). Similar to the EMS blastomere, seam cells in the *C. elegans* epidermis are polarized along the anterior-posterior axis by Wnt signaling components (Mizumoto & Sawa 2007a b). The stem cell-like seam cells form a lateral epithelium on each side of the animal (Fig. 1A). These cells go through a reproducible pattern of anterior-posterior oriented asymmetric and symmetric cell divisions during larval development (Fig. 1B; Sulston and Horvitz, 1977). In contrast to EMS, most seam cells may not directly need to contact a Wnt-secreting cell, and Wnt-ligands appear to provide a permissive rather than instructive signal for cell fate and division orientation (Yamamoto et al. 2011). How this signal translates to spindle positioning is currently unclear.

C. elegans uses divergent canonical and non-canonical Wnt signaling to instruct asymmetric cell divisions. This Wnt/β-catenin asymmetry pathway polarizes cells along the anterior-posterior body axis through the asymmetric localization of pathway components (Fig. 1C). As such, Dishevelled (Dvl) family members become enriched at posterior cell membranes, in some cells together with the accumulation of Frizzled (Fz) receptors (Park et al. 2004; Heppert et al. 2018). Studies of *Drosophila* pI cells revealed how polarized Fz/Dvl protein complexes can orient cell division by functioning as a cortical docking site for the mitotic spindle (Gho & Schweisguth 1998; Bellaïche et al. 2001; Bellaiche 2004). The mitotic spindle is normally anchored to the plasma membrane via a conserved protein complex consisting of the heterotrimeric G-protein subunits $G\alpha^{GOA\text{-}1/GPA\text{-}16}$, the G-protein regulators GPR-1/2^{LGN}, and coiled-coil protein LIN-$5^{NuMA/Mud}$. By interacting with the microtubule motor protein dynein, LIN-5^{NuMA} connects microtubule plus ends to the cell cortex via the linker protein GPR-1/2^{LGN} and membrane anchor $G\alpha^{GOA\text{-}1/GPA\text{-}16}$ (reviewed in Rose & Gönczy 2014; Fielmich et al. 2018). Polarized Fz/Dvl complexes can directly recruit Mud^{NuMA} to the cortex and thereby attach the dynein-dynactin complex (Ségalen et al. 2010). Protein interactions

between *C. elegans* Dishevelled (DSH-2, MIG-5) and LIN-5 have not been described, but *mom-2*^{Wnt}, *mom-5*^{Fz}, *dsh-2*^{Dvl} , *mig-5*^{Dvl}, *apr-1*^{APC}, *gsk-3*$^{Gsk3\beta}$ and *wrm-1*$^{\beta\text{-catenin}}$ all contribute to spindle positioning in EMS (Bei et al. 2002; Kim et al. 2013b). This suggests the participation of a non-canonical branch of the Wnt/β-catenin asymmetry pathway in this process. In addition, anteriorly polarized APR-1^{APC} was shown to locally increase the number of astral microtubules by stabilizing microtubule ends at the cell cortex (Sugioka et al. 2011). These prolonged microtubule interactions allow the transport of WRM-1 to the cortex, thereby contributing to WRM-1 nuclear asymmetry and asymmetry in cell fate. Thus, Wnt/β-catenin asymmetry signaling in the EMS blastomere guides the orientation of the spindle as well as daughter cell fate asymmetry.

The Wnt pathway in the *C. elegans* EMS blastomere acts in part redundantly with MES-1/SRC-1 signaling. MES-1 is a tyrosine kinase-related transmembrane receptor, which localizes to the region of cell-cell contact between the P2 and EMS blastomeres (Berkowitz & Strome 2000; Bei et al. 2002). MES-1 localizes the SRC-1 tyrosine kinase and allows its cortical activation, in a process that also involves non-muscle myosin (NMY-2) (Bei et al. 2002; Liu et al. 2010). MES-1/SRC-1 and Wnt/Fz signaling act in parallel to instruct the EMS division orientation (Bei et al. 2002). Recent genetic observations indicate that the PIG-1 kinase also contributes to SRC-1 activation (Liro et al. 2018). PIG-1^{MELK} was first shown to control the size and fate asymmetry of specific Q neuroblast daughter cells (Cordes et al. 2006; Ou et al. 2010). PIG-1 is a member of the AMPK-related kinase family, together with PAR-1. Kinases of this family are activated by PAR-4^{LKB1} phosphorylation (Lizcano et al. 2004). Genetic evidence supports that PIG-1 is a PAR-4^{LKB1} target (Cordes et al. 2006; Pacquelet et al. 2015), that PIG-1 acts partly redundant with PAR-1 (Liro et al. 2018), and that it regulates cortical myosin (Ou et al. 2010; Pacquelet et al. 2015). The contribution of PIG-1 in daughter cell size asymmetry may be achieved through its regulation of myosin accumulation or contractility, cortical rigidity, or SRC-1 signaling.

Cortical pulling forces are exerted on astral microtubules by the Gα/GPR-1,2/LIN-5 complex in association with dynein (Grill & Hyman 2005; Kotak 2019). Previous studies in the *C. elegans* one-cell embryo revealed how anterior PAR proteins act as upstream regulators of pulling forces, in part through inhibition of LIN-5 by PKC-3-mediated phosphorylation (Galli et al. 2011). This results in posterior displacement of the spindle and the generation of a larger anterior and a smaller posterior blastomere. As both EMS and seam cells do not

orient their divisions along the PAR-polarity axis, pulling force complexes are probably controlled at a different level in these cells. The Wnt/β-catenin asymmetry pathway is likely to contribute to this process, but the asymmetric localization of its components is maintained during symmetric divisions (Chapter 3). As in EMS, parallel acting factors are likely to participate, for which actomyosin asymmetry and the PIG-1 kinase are candidates. Actomyosin accumulation affects the deformability, or rigidity, of the plasma membrane and thereby the net pulling forces exerted in the spindle (Kozlowski et al. 2007; Redemann et al. 2010; Berends et al. 2013). A possibility is that the rigidity of the plasma membrane is asymmetrically controlled in seam cells. In a recent study, NMY-2 was found not to be required for seam daughter cell size asymmetry (Ding & Woollard 2017). However, some conclusions of this study, such as that seam daughter cell size does not depend on spindle positioning during mitosis, do not appear consistent with our observations.

Here, we study the mechanisms that coordinate cell fate and cell size asymmetry, using the *C. elegans* epidermal seam cells as our model system. Following seam cell divisions by time-lapse fluorescence microscopy, we found that daughter cell size asymmetry depends on the developmental stage, and arises in the second larval stage, during the third round of larval seam cell divisions. Focusing on the L3 stage divisions, which coordinate asymmetry in cell size and cell fate, we explored the contribution of several candidate mechanisms in division asymmetry. We found that divergent canonical Wnt signaling via POP-1^{TCF} not only instructs cell fate (Chapter 3 of this thesis), but also the orientation of the spindle in seam cells. We investigated whether the combined GSK-3 and Casein Kinase I phosphorylation that regulate Wnt/β-catenin signaling and LIN-5/GPR-1,2 protein-interactions connect Wnt signaling to cortical pulling force generation, but did not find evidence for crosstalk between these pathways. Knockdown of the *pig-1* kinase caused remarkable misorientation of the spindle in seam cells, with apparently laterally attached spindle poles. PIG-1 has been implicated in cell size asymmetry in Q neuroblast daughters through regulation of actomyosin asymmetry. We observed different dynamics of NMY-2 before cell divisions with or without anterior spindle displacement. These data form the basis for future studies, which could investigate whether actomyosin asymmetries instruct daughter cell size asymmetries during the stem cell-like seam cell divisions.

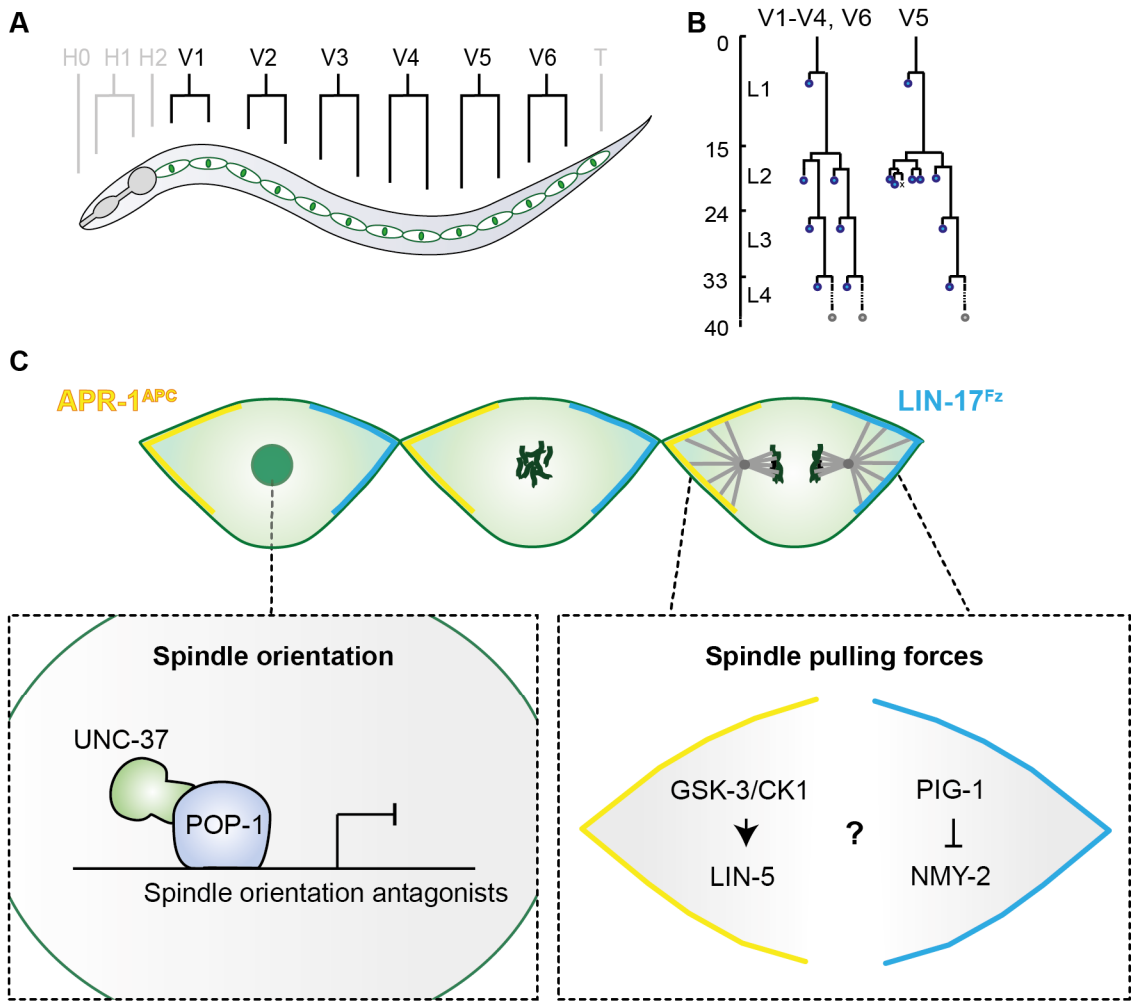

Figure 1. Schematic illustrations of asymmetric seam cell divisions. (A) Cartoon of a *C. elegans* larva highlighting the lateral seam epithelium (green). Seam cells are named H0-H2 (precursor cells of the head), V1-V6 (ventrolateral precursor cells), and T (tail blast cell). (B) Schematic representation of V seam cell postembryonic lineages. Y-axis represents time (hrs) with respect to the four larval stages (L1-L4). The division pattern is plotted along this axis. Asymmetric divisions generate one differentiating epidermal (hyp7) daughter cell (blue) and one self-renewing seam daughter cell (grey). (C) Schematic illustration of part of the seam cell epithelium. Anterior-posterior polarity by Wnt pathway components is shown for APR-1^{APC} (yellow; anterior) and LIN-17^{Fz} (blue; posterior). Divisions orient along the Wnt/β-catenin asymmetry axis. Boxes indicate possible mechanisms of regulation: POP-1^{TCF} mediated transcriptional regulation appears critical for spindle orientation (bottom left). Furthermore, we investigate a possible function of LIN-5 phosphorylation in spindle pulling and positioning (bottom right). Last, we study a potential NMY-2/actomyosin function in daughter cell size asymmetry (bottom right).

Materials and methods

Nematode strains

The wild-type *Caenorhabditis elegans* strain N2 and derivatives listed in Table 1 were used in this study. All strains were maintained at 20°C, except WM179 and SV1987. Worms were cultured on NMG plated seeded with OP50 *E. coli* bacteria.

Table 1. Strains used in this study

Strain	Genotype
SV1009	*heIs63[*P*wrt-2::gfp::ph,* P*wrt-2::gfp::h2b,* P*lin-48::mcherry] V*
SV1984	*heIs218[*P*wrt-2::mcherry::ph,* P*wrt-2::mcherry::h2b,* P*lin-48::gfp]*
SV2113	*pop-1(he334[pop-1^{loxP}])* I ; heIs218(*P*wrt-2::mcherry::ph,* P*wrt-2::mcherry::h2b,* P*lin-48::gfp); heSi175(*P*scm::cre) X*
SV1665	*lin-5(he237[s659a s662a]) II ; heIs63 [*P*wrt-2::gfp::ph,* P*wrt-2::gfp::h2b,* P*lin-48::mCherry]*
WM179	*nmy-2(ne3409) I*
SV1987	*nmy-2(ne3409) I; heIs63[*P*wrt-2::gfp::ph,* P*wrt-2::gfp::h2b,* P*lin-48::mcherry] V*
LP162	*nmy-2(cp13[nmy-2::gfp+loxp]) I*

*loxP sites are upstream of the *pop-1* ATG and in intron 5

RNAi-mediated interference

Gravid adults were bleached using hypochlorite treatment, and embryos were allowed to hatch for 20 hours in RNAi soaking buffer (0.05% gelatin, 5.5 mM KH_2PO_4, 2.1 mM NaCl, 4.7 mM NH_4Cl, 3 mM spermidine) containing 1 ug dsRNA. Hatched larvae were then placed on 5x concentrated RNAi feeding plates for 23 hours at 20°C until the start of the L3 stage. The templates for both the RNAi feeding plates and the dsRNA was Vidal library clone GHR-11053 for *pop-1* and GHR-11051 for *pig-1*. dsRNA was synthesized using the Megascript High Yield Transcription T7 Kit (Thermofisher Scientific).

Microscopy

Time-lapse movies of seam cell divisions were recorded at room-temperature at 2-minute intervals for 2-4 hours using a Nikon Eclipse Ti-U spinning disk microscope with a 63X objective. Animals were synchronized by wash-off staging. Larvae were immobilized in 1 mM tetramisole (Sigma-Aldrich), and mounted on 5-7% agarose pads (7% for L1 stage animals, 5% for L2-L3 stage animals). The coverslips were sealed with immersion oil (Zeiss Immersol 518N oil) to prevent liquid evaporation. Laser settings used were: 488nm 7% power 50 ms exposure time 2x2 binning, and 561nm 10% power 100ms exposure time 2x2 binning. Image analysis was performed with FIJI software.

Temperature-switch experiments were performed at the Nikon Eclipse Ti-U spinning disk microscope using an interchangeable heat-controlled stage.

Results and discussion

Developmental context dependent segregation of cell fate and cell size asymmetry

It has not been unequivocally addressed whether seam cell divisions combine asymmetry in daughter cell fate with asymmetry in cell size. In our previous time-lapse microscopy recordings, seam cell descendants often appeared to differ in fate and size (Wildwater et al. 2011; Chapter 3). However, a recent report did not confirm this notion, and concluded that asymmetric seam cell divisions do not displace the mitotic spindle in mitosis (Ding & Woollard 2017). To address this topic, we set out to quantify the positioning of the spindle and daughter cell sizes during seam cell divisions. We followed asymmetric and symmetric divisions during the first three larval stages (L1-L3) by time-lapse spinning disk confocal fluorescence microscopy. Expression of fluorescent reporters was used to visualize the cell membrane (mCherry::PH) and chromosomes (mCherry::H2B). This allowed us to measure the cell-surface area, as well as the distance between the segregating chromosomes and the cell membrane (Fig. 2A).

Our analysis revealed that the segregation of unequally sized daughter cells is induced during L2 larval development. Seam cells undergo a first asymmetric cell division midway through the first larval stage, followed by a symmetric division in early L2 (Fig. 2A). Interestingly, the asymmetry in fate did not coincide with an asymmetry in size during the L1 division. Moreover, as expected, the symmetric L2 divisions created seam daughter cells of equal size and fate (Fig. 2B). Following the asymmetric divisions in L2 and L3, however, clear size asymmetries were detected between the two daughter cells. The stem cell-like posterior daughter cells were substantially larger than the anterior daughters, which are destined to differentiate (Fig. 2B). These differences in size correlate with a displacement of the spindle in mitosis. In L1 and early L2, the spindle remains present in the middle of the dividing mother cell (Fig. 2C,D). However, starting in anaphase, the spindles became anteriorly displaced in mitotic seam cells during the mid L2 and L3 stages (Fig. 2E,F). The plane of cytokinesis followed the anterior displacement of the spindle, and created two daughter cells of different sizes. Together, these observations indicate that asymmetry in daughter cell size and fate can coincide, but also can be uncoupled, depending on the developmental context.

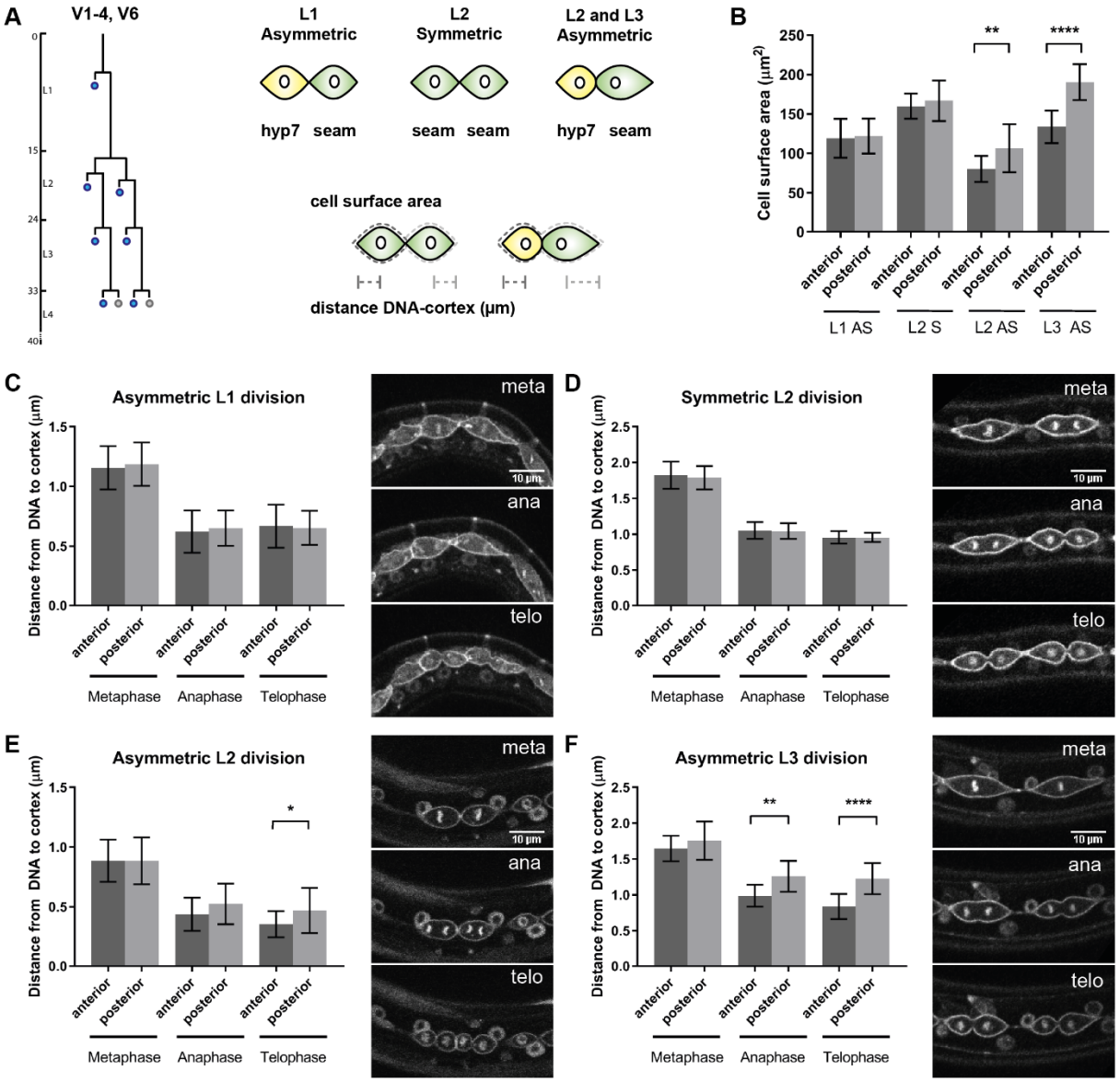

Figure 2. Characterization of asymmetric and symmetric seam cell divisions. (A) Schematic illustration of the seam cell division pattern during the four larval stages (L1-L4) (left). Illustration of measurements and summary of results (right). Asymmetric divisions generate an anterior daughter cell that fuses with the epidermis (blue). L1 seam cells generate daughter cells equal in cell size, but asymmetric in cell fate. The symmetric L2 division generates daughter cells equal in cell fate and cell size. By contrast, the L2 and L3 asymmetric divisions generate daughter cells asymmetric in cell fate and cell size. (B) Quantification of the cell surface areas of daughter cells of L1-L3 seam cell divisions. (C) Quantification of mitotic spindle positions during the L1 seam cell divisions, (D) L2 symmetric divisions, (E) L2 asymmetric divisions, (F) and L3 divisions. Series of time-lapse microscopy images of seam cells during the characterized phases: metaphase, anaphase and telophase (C-F). Images were processed using ImageJ software. Error bars indicate mean ±SD.

A dual role for POP-1^{TCF} in cell fate control and spindle orientation

The Wnt/β-catenin asymmetry pathway may be expected to control the creation of size asymmetry during the L2 and L3 asymmetric divisions. At the same time, anterior-posterior asymmetry in Wnt/β-catenin pathway components is present during all larval stages, and as such does not appear directly coupled to size asymmetry. We discovered previously that the anterior-posterior orientation of the spindle in seam cells is redundantly controlled by Wnt ligands and the elongated seam cell shape (Wildwater et al. 2011). This function is likely to involve a non-canonical branch of the Wnt/β-catenin asymmetry pathway, which signals to the cytoskeleton rather than regulate transcription. Surprisingly, however, we found that knockdown of *pop-1*^{TCF} by RNAi dramatically altered the orientation of seam cell divisions (Fig. 3A-B). To quantify this phenotype, we determined the angle of the mitotic spindle with respect to the anterior-posterior body axis, in dividing seam cells of control and *pop-1* knockdown animals. RNAi of *pop-1* induced spindle rotation abnormalities that deviated up to 90° from wild type (Fig. 3B). As transcriptional control of spindle positioning was unexpected, we wondered whether this phenotype reflects a function for *pop-1* in the seam cells, or a non-cell autonomous function of *pop-1.* To distinguish between these possibilities, we made use of a loxed *pop-1*^{loxP} allele (Chapter 3). This allele, in combination with expression of Cre recombinase from the seam specific *scm* promoter, is expected to create seam lineage specific *pop-1* inactivation. Examination of *pop-1*^{loxP}; P*scm::cre* animals revealed abnormal spindle positioning in the knockout seam cells (Fig. 3B). Thus, the *pop-1*^{TCF} transcriptional factor appears required for reliable anterior-posterior spindle positioning in seam cells.

Several considerations should be taken into account when interpreting these data. First, determining cell autonomy is difficult for seam cells. Initially the *pop-1*^{loxP} knockout will be seam cell specific, however, following the fusion of anterior daughter cells with the neighboring hyp-7 during the L1 stage, recombination can also take place in the general epidermis. Second, the effect of *pop-1* loss on spindle orientation may be indirect. *pop-1* RNAi or gene knockout prevents the differentiation of anterior daughter cells from the L2 stage onward, thereby creating symmetric divisions that produce two new seam cells (Chapter 3). Because the number of seam cells increases while the length axis remains unaltered, cells round off and may even elongate in dorsal ventral direction. Our previous

analysis showed that Wnt-signaling can still instruct A-P spindle positioning when seam cells are rounded (Wildwater et al. 2011). Therefore, we expect that *pop-1* RNAi not only creates cell rounding but also renders the cells irresponsive to a Wnt cue that normally orients the spindle.

The fact that removal of POP-1^{TCF} disrupts spindle orientation could point to a positive transcriptional feedback-loop in the Wnt/β-catenin pathway. Studies in mammalian systems have mostly revealed TCF-induced negative feedback, which downregulates the expression of upstream pathway components and dampens Wnt signaling (Logan and Nusse, 2004; and Wnt homepage). By mining the available data of *C. elegans* POP-1 ChIP-seq analyses performed on embryonic extracts, we did not detect binding of POP-1 to the promoter regions of candidate upstream Wnt/β-catenin pathway components (including transmembrane Wnt receptors *mom-5, lin-17*, *lin-18*, *cam-1*; the *mig-1* secreted frizzled related protein 1; dishevelled genes *dsh-1*, *dsh-2* and *mig-5*; and *apr-1* APC (the modERN genome resource). However, a study of Q cell neuroblasts did reveal a positive feedback-loop from POP-1 to Frizzled *lin-17* expression, likely mediated by the POP-1 target *mab-5* Hox (Ji et al. 2013). As *pop-1* RNAi appears to specifically remove the POP-1 transcriptional repressor function (Chapter 3), the upregulation of one or more target genes would be expected to interfere with Wnt dependent spindle orientation. Further studies will be needed to clarify the mechanism involved in this response.

Our initial observations (Fig. 2) indicate that orienting the spindle in anterior-posterior direction occurs independently of the spindle displacement that leads to size asymmetry. To examine whether POP-1 also affects spindle displacement, we measured the distance between the anaphase chromosomes and the cell cortex. This confirmed that spindle displacement continues in *pop-1(RNAi)* larvae (Fig. 3E). Moreover, measurements of the cell surface area indicate that the size asymmetry of seam daughter cells is maintained in the absence of *pop-1* (Fig. 3D). These observations provide further support for the hypothesis that orienting the spindle along the body axis involves regulators that differ from those that displace the spindle off center in mitosis.

Following knockdown of *pop-1,* the segregating chromosomes moved abnormally close to the cell cortex, as compared to normal anaphase and telophase (Fig. 3C). This could point to increased cortical pulling forces in the absence of *pop-1*. As another read out for

cortical pulling forces, we determined the length of the spindle midzone during late anaphase in wild-type versus *pop-1(RNAi)* larvae. The spindle midzone length was significantly reduced in *pop-1* loss-of-function seam cells, compared to the wild type (Fig. 3E). This suggests an overall decrease in pulling forces during anaphase, instead of an increase in forces. These contradictory results most likely stem from the altered cellular shape. A general rounding of seam cells, as a result of the squeezing of extra seam cells in *pop-1* larvae, can explain the reduced distance between the spindle poles and cortex, as well as reduced cell surface area (Fig. 3A,C,D). Thus, the actual measured distances reflect the rounding of seam cells in the crowded seam epithelium of *pop-1* larvae. However, this does not explain the off-center positioning of the spindle. Therefore, we conclude that the mechanisms that achieve size asymmetry still operate in *pop-1* loss-of-function seam cells, despite the more randomized spindle orientation.

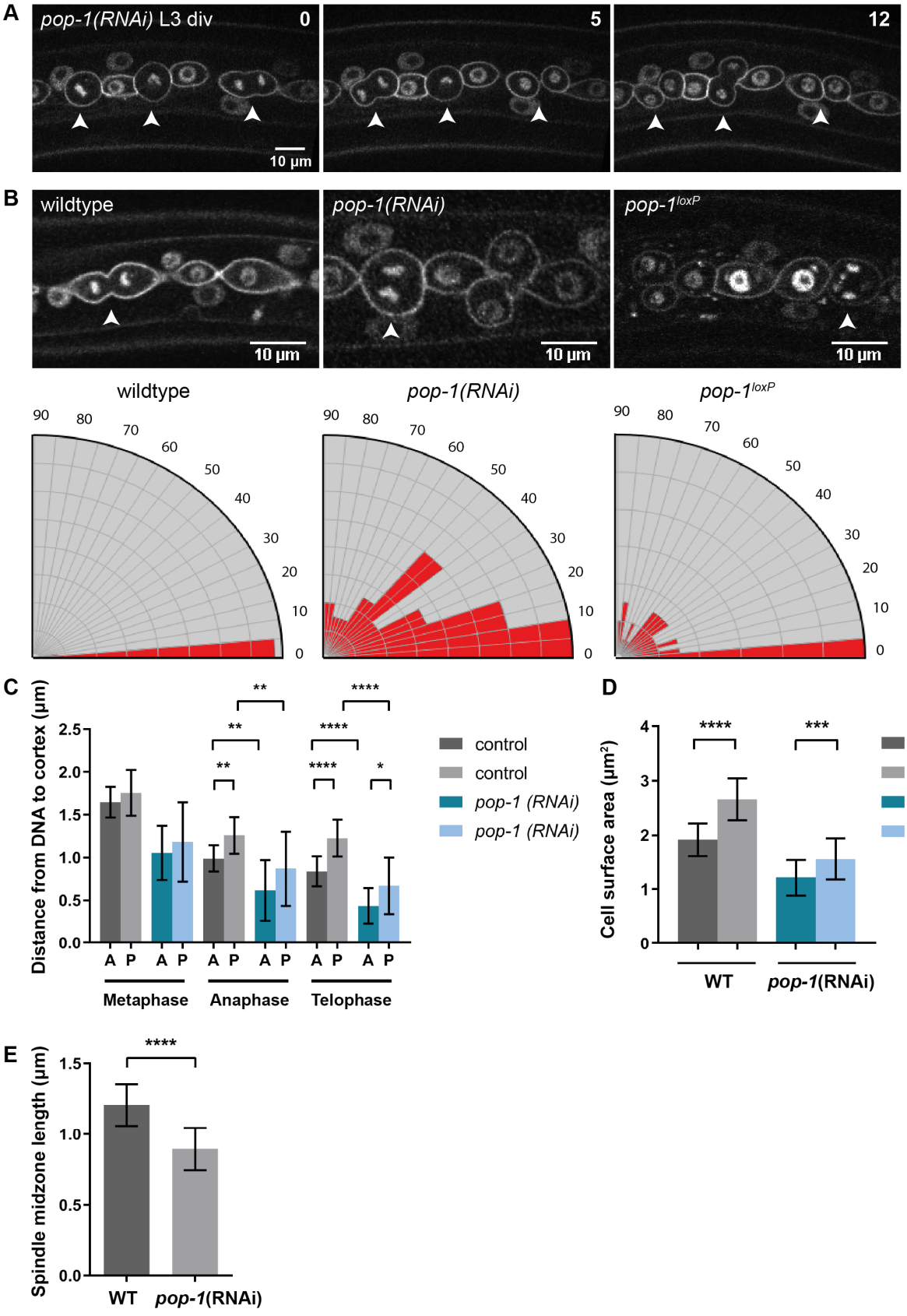
A
pop-1(RNAi) L3 div
0
5
12
10 µm
B
wildtype
pop-1(RNAi)
pop-1loxP
10 µm
wildtype
pop-1(RNAi)
pop-1loxP
90
80
70
60
50
40
30
20
10
0
C
Distance from DNA to cortex (µm)
2.5
2.0
1.5
1.0
0.5
0.0
**
**
**
****
****
****
*
A P A P A P A P A P A P
Metaphase
Anaphase
Telophase
control
control
pop-1 (RNAi)
pop-1 (RNAi)
D
Cell surface area (µm²)
4
3
2
1
0
****
***
A
P
A
P
WT
pop-1(RNAi)
E
Spindle midzone length (µm)
1.5
1.0
0.5
0.0
****
WT
pop-1(RNAi)

Figure 3. POP-1 is required for spindle orientation, but not for spindle displacement in seam cells. (A) Series of time-lapse microscopy images of a *pop-1(RNAi)* larva undergoing the L3 asymmetric divisions. Epithelium contains extra seam cells from L2 misspecification; cells are more rounded in morphology. Arrowheads point to misoriented mitotic spindles. (B) Time-lapse microscopy images of wildtype, *pop-1(RNAi)* and *pop-1*^{loxP} animals undergoing the L3 asymmetric division (top panels; arrowheads point to spindles measured). Quantification of spindle orientation defects in control, *pop-1*(*RNAi)* and *pop-1*^{loxP} animals (bottom graphs). (C) Quantification of the distance between DNA and cell cortex measured in control and *pop-1* RNAi animals during metaphase, anaphase and telophase. (D) Quantification of the cell surface area of seam daughter cells in control and *pop-1(RNAi)* animals. (E) Quantification of the spindle midzone length in control and *pop-1(RNAi)* seam cells. Images were processed using ImageJ software. Error-bars indicate mean $\pm$ SD.

Examining cross talk between Wnt/β-catenin asymmetry signaling and LIN-5-dependent pulling forces

All through development, chromosome segregation and spindle positioning are mediated by a trimeric Gα/GPR-1,2/LIN-5 complex (Lorson et al. 2000; Srinivasan et al. 2003). This complex anchors and activates dynein at the membrane, thereby controlling the cortical pulling forces that position the spindle (Fielmich et al. 2018). To induce spindle rotation or displacement, upstream regulators control the LIN-5^{NuMA}-dynein pathway in *C. elegans* as well as in other animals (Morin & Bellaïche 2011). In the one cell embryo, this regulation involves phosphorylation of LIN-5 by PKC-3^{aPKC} kinase (Galli et al. 2011). We wondered whether kinases in the Wnt pathway, GSK3β and Casein Kinase I α (CK1α), might control spindle positioning through LIN-5 phosphorylation. In a previous study, we discovered that a priming phosphorylation of LIN-5 Ser659 by GSK3, followed by CK1 phosphorylation of Ser662, promotes the interaction of LIN-5 with its binding partner GPR-1,2 (Portegijs et al., 2016). This phosphorylation resembles LRP5/6 phosphorylation in vertebrates, and involves the two kinases that, in association with APC and Axin, regulate β-catenin degradation (Reviewed in Clevers & Nusse 2012). *C. elegans* GSK-3^{GSK3β} and KIN-19^{CK1} kinases contribute to spindle positioning (Walston et al. 2004), and APR-1^{APC} becomes enriched at the anterior cortex in mitotic seam cells (Mizumoto & Sawa 2007a; Baldwin & Phillips 2014; Harandi & Ambros 2014). Hence, we hypothesized that local LIN-5 phosphorylation by the associated

GSK-3 and KIN-19 CK1 kinases could promote LIN-5 interaction with Gα/GPR-1,2, thereby increasing pulling forces and inducing anterior displacement of the spindle.

To examine this hypothesis, we characterized seam cell divisions in a *lin-5* mutant that lacks the putative GSK3 and CK1 phosphorylation sites (*lin-5*[*s659a,s662a*]; Fig. 4A). Examination of seam cells during the L3 stage in this mutant revealed significantly altered spindle behavior. However, instead of the anterior pole, the posterior pole showed the strongest deviation from wild-type. The spindle displacement during anaphase and telophase, measured as the distance between DNA and cortex, was significantly reduced in the posterior (Fig. 4B). Notably, this did not result in larger posterior cells, which in fact were somewhat smaller than wild-type posterior daughter cells (Fig. 4C). Apparently, the reduced cortical movement of the spindle poles had only a limited effect on the place of cell cleavage. We quantified the spindle midzone length in seam cells as a measure for pulling forces. *lin-5*[*s659a,s662a*] mutant seam cells showed a substantial reduction in spindle midzone length, indicating that pulling forces are reduced (Fig. 4D). However, the divisions remained asymmetric, and the anterior pole showed quite normal displacement. Therefore, we conclude that the observed effects are likely to reflect an overall reduction in cortical pulling forces. This is in line with a reduced affinity of LIN-5 S659A,S662A for GPR-1,2, and our observations that this mutation reduces spindle pulling forces in the one-cell embryo (Portegijs et al., 2016). The asymmetric effect of this LIN-5 mutation in seam cells does not support our model that the Wnt/β-catenin asymmetry pathway regulates pulling forces through LIN-5 phosphorylation at the Ser659 and Ser662 residues.

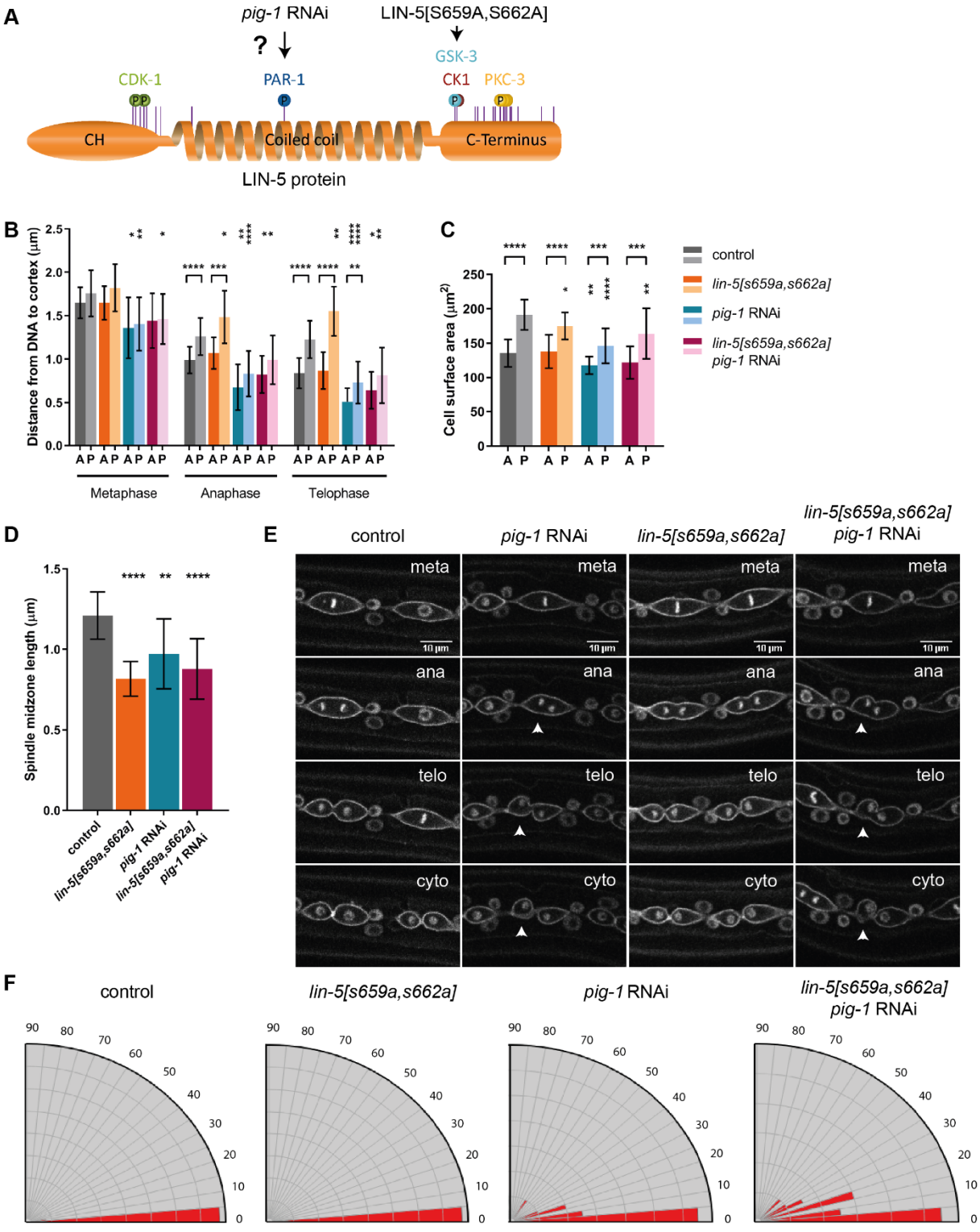
A
pig-1 RNAi
?
LIN-5[S659A,S662A]
GSK-3
CDK-1
PAR-1
CK1
PKC-3
CH
Coiled coil
C-Terminus
LIN-5 protein
B
Distance from DNA to cortex (µm)
AP AP AP AP
AP AP AP AP
AP AP AP AP
Metaphase
Anaphase
Telophase
C
Cell surface area (µm²)
A P A P A P A P
control
lin-5[s659a,s662a]
pig-1 RNAi
lin-5[s659a,s662a] pig-1 RNAi
D
Spindle midzone length (µm)
control
lin-5[s659a,s662a]
pig-1 RNAi
lin-5[s659a,s662a] pig-1 RNAi
E
control
pig-1 RNAi
lin-5[s659a,s662a]
lin-5[s659a,s662a] pig-1 RNAi
meta
ana
telo
cyto
10 µm
F
control
lin-5[s659a,s662a]
pig-1 RNAi
lin-5[s659a,s662a] pig-1 RNAi

Figure 4. Analysis of LIN-5 and PIG-1 function in seam cell spindle positioning. (A) Schematic cartoon of the LIN-5 protein, indicating *in vivo* phosphorylated residues (purple lines) and presumptive responsible kinases indicated above. The coiled-coil region contains a phosphorylated residue that appears phosphorylated *in vivo* by PAR-1 in the early embryo, which could potentially be targeted by PIG-1 at latter stages. The C-terminal region contains the GPR-1,2 interaction domain, which includes the *in vivo* phosphorylated residues S659 and S662, apparently mediated by GSK3 priming phosphorylation of S659, followed by CK1 phosphorylation of S662. (B) Quantification of the distance between DNA and cell cortex measured in control, *lin-5*[*s659a,s662a*], *pig-1* RNAi, and double *lin-5*[*s659a,s662a*] *pig-1* RNAi animals during metaphase, anaphase and telophase. (C) Quantification of the cell surface area of seam daughter cells in control, *lin-5*[*s659a,s662a*], *pig-1* RNAi, and double *lin-5*[*s659a,s662a*] *pig-1* RNAi animals. (D) Quantification of the spindle midzone length in control, *lin-5*[*s659a,s662a*], *pig-1* RNAi, and double *lin-5*[*s659a,s662a*] *pig-1* RNAi seam cells. (E) Spinning disk confocal time-lapse images of control, *lin-5*[*s659a,s662a*], *pig-1* RNAi, and double *lin-5*[*s659a,s662a*] *pig-1* RNAi seam cells undergoing the L3 asymmetric division. (F) Quantification of spindle orientation defects in control, *lin-5*[*s659a,s662a*], *pig-1* RNAi, and double *lin-5*[*s659a,s662a*] *pig-1* RNAi animals. Images were processed using ImageJ software. Error-bars indicate mean ± SD.

The PIG-1 kinase contributes to anterior-posterior spindle orientation in seam cells

Multiple parallel acting mechanisms often control developmental processes. In this way, redundant mechanisms could mask an anterior spindle displacement phenotype in *lin-5*[*s659a,s662a*] mutants. We considered potential redundancies in the regulation of LIN-5 as well as independent mechanisms. Our previous quantitative mass spectrometry experiments provided strong evidence for *in vivo* phosphorylation of LIN-5 by the PAR-1^{MARK} kinase in early embryos (Galli et al. 2011; Portegijs et al. 2016). PAR-1 acts partly redundant with PIG-1, which belongs to the same kinase subfamily, and directs asymmetric divisions in the Q neuroblast lineage (Cordes et al. 2006; Ou et al. 2010; Chien et al. 2013). As the Q neuroblast and V5 seam cell arise from the same precursor, we wondered whether PIG-1 might contribute to seam cell division asymmetry.

To examine PIG-1 function in seam cell divisions, we used RNAi to reduce its expression. Time-lapse spinning disk confocal microscopy revealed remarkable spindle orientation defects in the seam cells of *pig-1* RNAi larvae (Fig. 4E and 4F). Instead of

connecting to the poles of the cell, some spindles appeared laterally attached, and positioned under an angle with respect to the anterior-posterior body axis. This resulted in apparently close contact between the spindle poles and cell cortex (Fig. 4B). The spindle midzone length was shorter than normal, likely because of the tilted spindle position (Fig. 4D). Interestingly, the cell surfaces of both daughter cells were reduced but still asymmetric. This could point to defects in cortical extension and cell elongation; a mechanism involving actin remodeling. The posterior cells were substantially more reduced compared to anterior cells. This could point to a contribution of *pig-1* in seam cell size asymmetry.

Both the *lin-5*[*s659a,s662a*] mutation and *pig-1* RNAi reduced the size of the posterior cell more severely than the anterior cell. We tested whether the combination of these alterations enhanced spindle abnormalities. The *lin-5* mutation alone did not cause spindle misorientation, however, combining this *lin-5* allele with *pig-1* RNAi resulted in a slight increase in spindle orientation defects (Fig. 4E and 4F). Other aspects of spindle positioning did not appear to be significantly enhanced or reduced in the double combination (Fig. 4B-D). Together, these observations show that PIG-1 contributes in an unexpected way to spindle orientation, apparently preventing lateral attachments of the spindle poles and possibly contributing to the asymmetry in daughter cell size.

NMY-2 temporarily enriches at the posterior cortex prior to asymmetric seam cell division

PIG-1 appears to affect daughter cell asymmetry by regulating cortical actomyosin accumulation (Ou et al. 2010; Pacquelet et al. 2015). The actomyosin cytoskeleton participates in asymmetric cell division in multiple ways. In *C. elegans*, establishment of A-P polarity in the fertilized egg is triggered by actomyosin reorganization, anterior actin accumulation in the zygote increases cortical rigidity and reduces pulling forces, and myosin participates in Src activation and spindle rotation in EMS. Moreover, the size asymmetry of QR neuroblast appears to be driven by asymmetric actomyosin contraction (Severson & Bowerman 2003; Liu et al. 2010; Ou et al. 2010). We wondered whether the actomyosin cytoskeleton might contribute to seam cell division asymmetry (Fig. 5A). To examine this possibility, we quantified the localization of endogenously tagged NMY-2::GFP non-muscle myosin during symmetric and asymmetric seam cell divisions. NMY-2 appeared transiently enriched at the posterior cortex during L2 and L3 asymmetric divisions, but not during the L2

symmetric division (Fig. 5B and 5C). This posterior enrichment was detected during or before prometaphase, and was lost when cortical pulling forces position the spindle in anaphase and telophase. The correlation between NMY-2 asymmetry before division and cell size asymmetry after division, might point to a role for NMY-2 in polarizing the cortex.

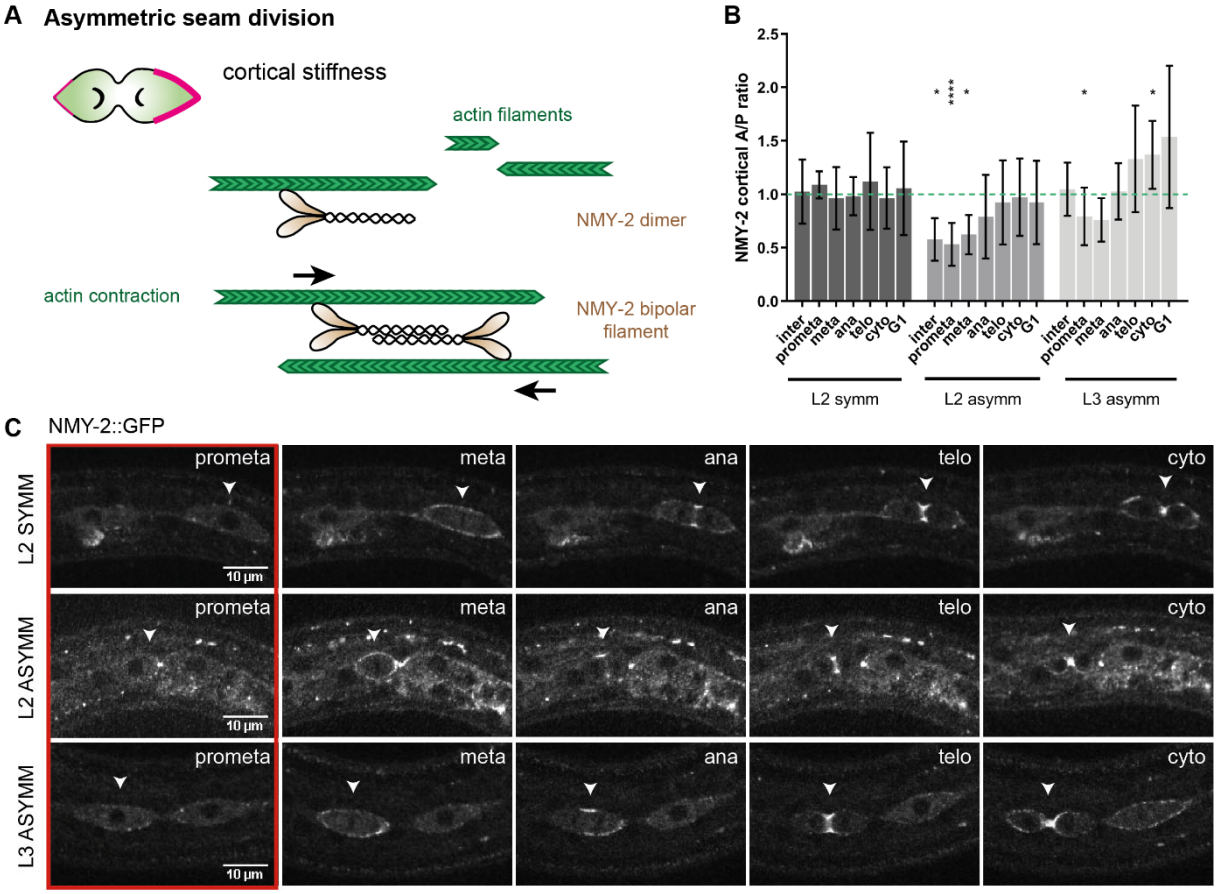

Figure 5. Cortical NMY-2 localization in L2 and L3 divisions. (A) Schematic representation of NMY-2 function in seam cells. NMY-2 (brown) binds actin filaments (green) via its N-terminal motor domain. NMY-2 is active in a dimer conformation. When two dimers form bipolar filaments, NMY-2 can slide actin filaments in anti-parallel direction, thereby causing contraction of the actin cytoskeleton. We examined whether NMY-2 becomes locally enriched at the cortex of dividing seam cells (magenta) Asymmetry of NMY-2 accumulation could contribute to cortical polarity, rigidity, or contractility, as well as SRC-1 activation. (B) Quantification of A:P ratio of NMY-2 localization at the cortex of dividing seam cells in L2 and L3 larvae. (C) Spinning disk time-lapse microscopy images of NMY-2::GFP localization during L2 and L3 seam cell divisions. Prometaphase images are marked by the red box; measurements presented in B revealed a difference in NMY-1 polarity during this phase of the cell cycle. Images were processed using ImageJ software. Error-bars indicate mean ± SD.

NMY-2 could potentially contribute to asymmetric seam cell division

To examine whether the posterior enrichment of NMY-2 prior to spindle alignment influences the asymmetry of the division, we analyzed a temperature-sensitive *nmy-2* mutant during the L3 stage asymmetric divisions. The *nmy-2(ne3409)* allele contains a mutation that alters the conserved S2 region of the NMY-2 heavy chain, which is required for proper dimerization and motor function (Fig. 6A; Liu et al., 2010; Tama et al., 2005). If NMY-2 contributes to seam cell asymmetry, its temperature-dependent inactivation should result in more symmetric divisions. The *nmy-2(ne3409*ts*)* mutant has been reported to create cytokinesis defects when embryos are placed at 25°C (Liu et al. 2010). Indeed, we observed the formation of embryos with multinucleated cells at 25°C, indicative of cytokinesis failure (Fig. 6B). Temperature shift of larval stage animals occasionally resulted in binucleated seam cells (Fig. 6B). These effects were limited, however, as illustrated by a quantification of the number of nuclei per 16 seam cells in animals shifted to 25°C prior to the L3 division (Fig. 6B and 6C). Thus, in contrast to embryos, the larval *nmy-2* ts cytokinesis-defective phenotype is weak. Shifting the larvae to 26°C, to enhance the phenotype, arrested seam cell divisions and could not be used. Therefore, we characterized the *nmy-2* weak loss-of-function phenotype at 25°C. Not surprisingly, our quantifications indicate that the spindle position remained asymmetric at this temperature (Fig. 6D). However, the posterior daughter cells were significantly smaller in *nmy-2* ts seam cells compared to controls, and overall the size asymmetry was reduced (Fig. 6E). The spindle midzone length was also reduced, which could point to a reduction in pulling forces or alteration of the seam cell shape (Fig. 6F). It should be noted that we did not observe cytokinesis defects in the seam cells that were characterized in these conditions (Fig. 6G). Together, because a weak reduction of NMY-2 function may reduce the size difference of seam cell daughters, it will be important to examine more complete inactivation of NMY-2 in follow up studies.

Even if NMY-2 is found to contribute to size asymmetry, the underlying mechanism would not be apparent. As discussed above, actomyosin asymmetries contribute to asymmetric cell division at multiple levels, which is distinct from its role in formation and contraction of the cytokinetic furrow. It is intriguing to realize that NMY-2 participates in the local activation of SRC-1 in the EMS blastomere, which acts redundantly with Wnt/β-catenin signaling in the rotation of the spindle towards the P2/EMS cell contact (Liu et al. 2010). PIG-

1 contributes to cortical actomyosin regulation through mechanisms that remain unclear, but that also have been proposed to include SRC-1 regulation in the early embryo (Ou et al. 2010; Pacquelet et al. 2015; Liro et al. 2018).

A recent study addressed the function for NMY-2 in seam cell divisions, and revealed a contribution in cell fate segregation (Ding & Woollard 2017). Following division with compromised NMY-2, part of the seam cells appeared to acquire a differentiated hypodermal fate. This is particularly intriguing from the perspective of asymmetric segregation of cell fate determinants, which has been shown to be associated with actomyosin tethering in *Drosophila* neuroblasts (Knoblich 2010). A contribution for NMY-2 in cell size asymmetry or spindle positioning was not detected in the previous seam cell study, despite more complete NMY-2 inactivation compared to our experiments, which was achieved by combining the *nmy-2* temperature-sensitive mutation with RNAi (Ding & Woollard 2017). For two reasons we feel that this topic is not fully resolved. First, cytokinesis defects remained incomplete, even in the earlier study, hence *nmy-2* loss-of-function was partial. Moreover, the earlier study did not observe spindle displacement during seam cell division and suggested that unequal sizes arise post-cytokinesis. We agree that cell shape alterations continue after division, but our observations support that anterior displacement of the spindle in mitosis primarily drives the size asymmetry.

In summary, we observed that the segregation of cell fate and cell size asymmetry is developmentally controlled in the seam cell lineage. Cell size asymmetry arises from anterior displacement of the spindle in mitosis. This spindle migration is coordinated with spindle alignment along the anterior-posterior axis, but uses at least partly independent regulation. Testing several mechanisms that potentially participate in spindle positioning, we found a remarkable contribution of the POP-1^{TCF} transcription factor. POP-1^{TCF} appears required within the seam cells to orient the axis of division. In addition, the correct orientation of the spindle depends on the PIG-1 kinase, which appears needed to prevent lateral attachments. Preliminary studies of a potential contribution of NMY-2 in asymmetric seam cell divisions were based on a weak loss-of-function allele, but nevertheless may point to a contribution of actomyosin asymmetry in the creation of unequal daughter cells.

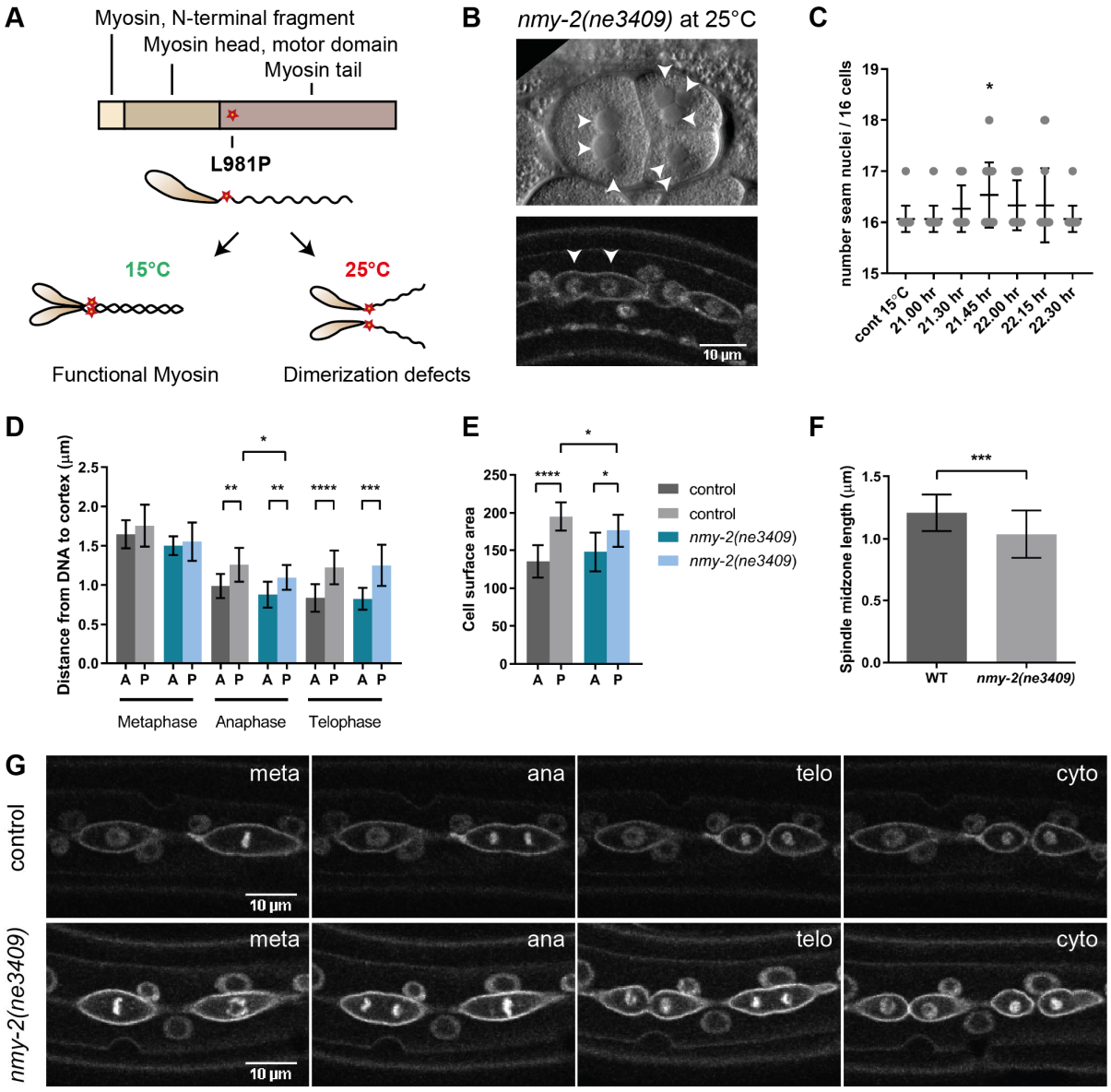

Figure 6. NMY-2 negatively regulates posterior spindle pulling forces. (A) Schematic illustration of the NMY-2 temperature sensitive mutant. The L981P substitution is in a conserved region of the myosin tail, disrupting dimerization and motor function at the non-permissive temperature of 25°C. (B) Widefield and spinning disk images of *nmy-2(ne3409*ts*)* embryo and larva following shift to the non-permissive temperature of 25°C. Nuclei are indicated with white arrow heads. (C) Quantification of cytokinesis defects in seam cells in *nmy-2(ne3409*ts*)* animals shifted to 25°C at different time points during the late L2 larval stage. L3 divisions take place at 23.30 hr; seam cell nuclei were counted at 27 hr. (D) Quantification of mitotic spindle positioning during the L3 seam cell divisions in control and *nmy-2(ne3409)* animals at 25°C. (E) Quantification of the cell surfaces of daughter cells of L3 divisions in control and *nmy-2(ne3409)* animals at 25°C. (F) Quantification of the spindle midzone length in control and *nmy-2(ne3409)* seam cells at 25°C. (G) Spinning disk time-lapse movies of control and *nmy-2(ne3409)* animals at 25°C. Images were processed using ImageJ software. Error-bars indicate mean ± SD.

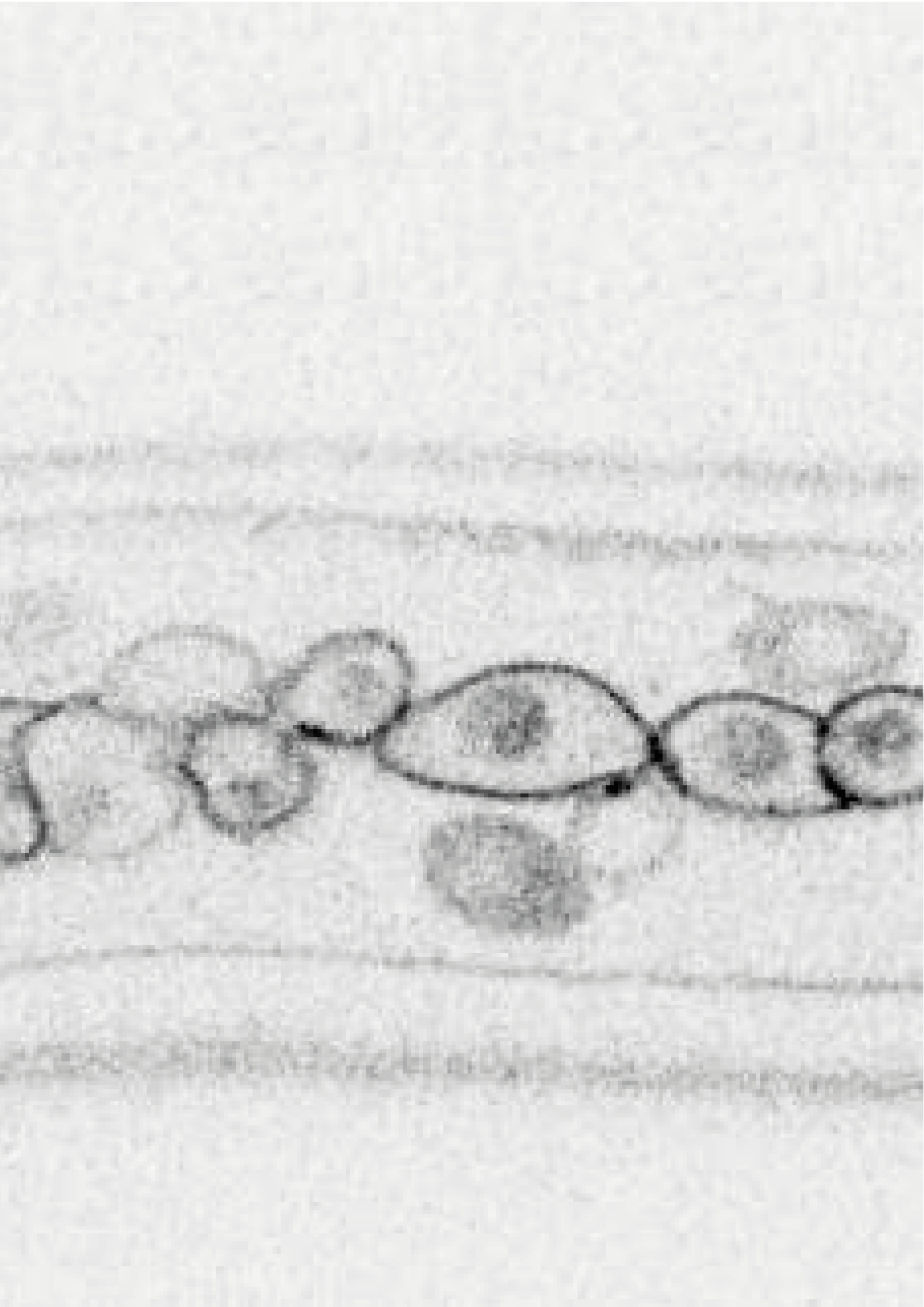

5

Summary and Discussion

Suzanne van der Horst and Sander van den Heuvel

Developmental Biology, Department of Biology, Faculty of Science, Utrecht University,
Padualaan 8, 3584 CH Utrecht, The Netherlands

Seam cells: an interesting system to study fundamental questions about cell division

The classic definition of cell division is the process in which a mother cell forms two daughter cells. We described two different modes of cell division in **Chapter 1**: symmetric divisions that generate two identical daughter cells, and asymmetric divisions that generate two different daughter cells. Some tissue-specific stem cells have the ability to apply, and switch between, these two division modes during development. The active switching is required for tissue development and regeneration, but needs to be tightly controlled to prevent premature differentiation or tumorous overgrowth.

In this thesis, we addressed the mechanisms that balance symmetric and asymmetric cell divisions of tissue-specific stem cells, called seam cells, in the *C. elegans* epidermis. Seam cells undergo an invariant series of asymmetric and symmetric divisions. Interestingly, both division modes orient along the anterior-posterior body axis which is polarized by Wnt signaling components. Without changing their polarity axis, seam cells manage to create a division asymmetry, which makes them an interesting model to study the fundamental differences between symmetric and asymmetric divisions.

There are limitations to using the worm for stem cell research. Adult worms consist of 959 somatic cells that arose through a limited number of cell divisions over the course of 4 days; which indicates seam cells do not encounter similar levels of developmental decisions that long-term mammalian stem cells do. Furthermore, seam cells go through a limited number of divisions and terminally differentiate at the end of larval development; true stem cells do not undergo terminal differentiation. These features need to be considered when using seam cells as a model system for stem cell-related questions. A major benefit of using *C. elegans* is that it has single homologs for many signal transduction pathway components, such as TCF^{POP-1}, $Runx^{RNT-1}$, and $CBF\beta^{BRO-1}$ in this study, which reduces the problem of redundancy. The introduction of CRISPR-Cas9 mediated genome editing allows for the study of endogenous gene functions. Further, our optimized microscopy protocols allowed us to study seam cell divisions at single cell resolution in the context of a developing animal. Altogether, we propose that seam cells provide a powerful system to study fundamental questions concerning a stem cell division pattern.

Should we address seam cells as single entities or as a complete tissue?

In this study we approached seam cells as single entities. They are however part of a larger epithelium that can be broadly subdivided in three regions: the anterior head domain containing the H0-H2 head cells, the ventrolateral domain containing the V1-V6 cells, and the tail domain containing the T tail cell. Together, these cells form two lateral rows of cells embedded in the *hyp7* hypodermis. Adherens junctions between neighboring seam cells, and between seam cells and the hypodermis, maintain the epithelial architecture.

The different lineages in the H, V and T seam cells are the result of anterior-posterior Hox gene patterning. The V1-V4 cells are instructed by the *lin-39* Hox gene, whereas V6 is instructed by the *mab-5* and *egl-5* Hox genes (Reviewed in Chisholm & Hsiao 2012). We clustered the ventrolateral V cells (V1-V4 and V6) based on their closely related cell division patterns. We excluded V5 from our analysis, as this cell produces a neuronal lineage and is differently regulated. For similar reasons, we excluded H0-H2 and T seam cells from our studies. We noticed that V6 was always delayed compared to V1-V4 cell divisions. Furthermore, the V6 cell seems more sensitive to *pop-1* loss of function compared to V1-V4 cells (**Chapter 3**). In that light, both intrinsic and extrinsic differences between seam cells should be considered in future studies to reduce the spread in experimental data.

Communication between neighboring seam cells is important for maintenance of anterior-posterior seam cell identities along the epithelium; e.g. head, ventrolateral or tail identity. Laser ablation of single seam cells disrupted the epithelial row and led to aberrant Hox gene expression in neighboring seam cells that subsequently adopted a different division pattern (Sulston & White 1980; Waring & Kenyon 1990; Waring et al. 1992; Austin & Kenyon 1994). Interestingly, the epithelial organization is also disrupted naturally during development. After completion of asymmetric V seam cell divisions, anterior daughter cells migrate dorsally or ventrally in preparation of fusing with the hypodermis. This migration creates temporal gaps between posterior self-renewing daughter cells, that in response elongate along the anterior-posterior axis to form new adherens junctions (Austin & Kenyon 1994; Podbilewicz & White 1994). These contacts provide a spatial cue for each seam cell in the row to ensure proper Hox gene expression and division patterning. This indicates that communication between individual cells is required for the organization of the entire tissue.

Interestingly, polarization of the individual seam cells does not depend on communication with their neighbors, nor on global planar cell polarity (PCP) regulators. V seam cells were shown to intrinsically polarize along the anterior-posterior axis independently from their neighbors. Contrary to mammalian stem cells (Habib et al. 2013), Wnt ligands do not appear needed to polarize V cells, only to align this polarity with the anterior-posterior body axis (Yamamoto et al. 2011). These findings indicate that cell-cell contacts are required for tissue organization, but that seam cells can be approached as single entities that organize their own (a)symmetric divisions.

A potential niche function for the hypodermis?

When addressing the seam tissue, the *hyp7* hypodermis should be considered as well. The hypodermis embeds seam cells, and cell-cell contacts are formed between seam cells and hyp7, which contributes to tissue architecture. It has been suggested that the hypodermis has a niche-function for the seam cells (Brabin & Woollard 2012). Classically, the niche is described as an environment with pro-mitotic and anti-differentiation signals that maintains the proliferative state of stem cells. The hypodermis has been shown to signal to neuronal and mesodermal blast cells in response to food intake. Upregulation of the insulin-like signaling pathway in the hypodermis in response to amino acids induced proliferation of quiescent P and M blast cells in the developing L1 larva (Fukuyama et al. 2015). An indication that it could also serve as a niche for seam cells comes from a study that linked the expression and secretion of the insulin-like growth factor INS-33 by the hypodermis to the L2 stage division pattern of seam cells. *ins-33* expression is actively repressed during the L1 stage, hence its induced expression could provide the proliferation trigger that induces a second round of seam cell divisions in L2 (Hristova et al. 2005). In that light, the hypodermis could have a potential pro-mitotic niche function for seam cells. However, in most niche models, the fate of stem cell daughters depends on their position with respect to the niche. The observation that seam cells do not orient their divisions away from the niche, and can instruct their own polarity, indicates they do not depend on the hypodermis to instruct cell fate asymmetry. The hypodermis could be essential for maintaining the single-row epithelium and seam cell morphology, however, which could indirectly influence proliferation.

A fine line between proliferation and differentiation

The polarization of Wnt signaling components along the anterior-posterior polarity axis is part of a divergent canonical Wnt signaling cascade, known as the Wnt/β-catenin asymmetry pathway. Members of the β-catenin destruction complex localize to the anterior cell cortex, whereas activating components such as the Frizzled receptor localize to the posterior domain (Mizumoto & Sawa 2007b). This results in the formation of a non-responsive and a Wnt-responsive daughter cell. We described in **Chapter 3** how the polarization of this pathway controls a binary cell fate decision. As seam cells maintain their anterior-posterior division axis in both symmetric and asymmetric division modes, cell fate may not be directly instructed by polarity. We showed in **Chapter 3** that Wnt/β-catenin asymmetry indeed does not change between a symmetric and asymmetric seam cell division. APR-1 enriched at the anterior cortex and asymmetry in nuclear POP-1 was established during symmetric as well as asymmetric divisions. This confirms the idea that Wnt/β-catenin asymmetry does not necessarily determine cell fate distribution. The generation of an endogenous GFP fusion for POP-1 revealed that the level of regulation is indeed not polarization, but expression levels. Prior to the symmetric seam cell division, POP-1 expression levels dramatically decrease which induces a seam cell fate in the anterior daughter cell.

The creation of a conditional *pop-1* knock-out allele allowed us to unambiguously detect the differentiation promoting and stem cell promoting dual functions of *pop-1* in seam cells. These observations indicate that the dual function of POP-1 as a transcriptional repressor and activator is the key regulator of cell fate asymmetry. High nuclear levels correlate with the POP-1 repressor state, whereas low nuclear levels correlate with an activator function. By globally lowering *pop-1* expression prior to the symmetric division, neither daughter cell nucleus received sufficient POP-1 for it to function as a repressor. Interestingly, the loss of POP-1 repressor function was sufficient to switch from differentiation to self-renewal. This suggests that the loss of differentiation equals a gain of self-renewal fate, and that the POP-1 repressor function is the determining factor between proliferation or differentiation.

We uncovered the mechanism responsible for the temporal downregulation of *pop-1* in **Chapter 3**: the RNT-1/BRO-1 transcriptional repressor complex. Induction of these genes suppressed differentiation and induced a self-renewing seam cell fate in anterior daughter cells of asymmetric L2 and L3 divisions. It was long suggested that RNT-1/BRO-1 regulate seam cell divisions parallel to Wnt signaling (Kagoshima et al. 2005; Gleason & Eisenmann 2010; Hughes et al. 2013). Here, we show that RNT-1/BRO-1 acts as upstream regulator of *pop*-1, and demonstrate the mechanism by which these two conserved transcriptional regulators interact to titrate the activity of the Wnt pathway.

Cross-regulation between Runx and TCF is conserved in mammals, although different mechanisms appear involved. In mouse intestinal epithelial cells, Runx3 dampens Wnt signaling not at the level of TCF4 expression, but via physical binding to nuclear TCF4. The formation of a ternary β-catenin::TCF4::Runx3 complex prevents TCF4 from binding to DNA (Ito et al. 2008; Reviewed in Chuang et al. 2013). Conversely, a ternary complex composed of β-catenin/LEF1/Runx2 inhibits Runx2 from binding to DNA in mouse osteoblast cells (Kahler & Westendorf 2003). A similar physical interaction between RNT-1 and POP-1 has not been identified in *C. elegans*. It will be possible to test such an interaction with the CRISPR/Cas9 technology currently available, by introducing tags in the endogenous RNT-1 and POP-1 genes and examining coimmunoprecipitation. Such a strategy could answer the question whether the worm uses transcriptional regulation *of pop-1* by RNT-1 instead of a physical interaction, or whether the two mechanisms are used complementary. The latter could explain why the mutation of candidate RNT-1 binding sites in the *pop-1* promoter did not create a *rnt-1*-like phenotype.

Another feature of Runx/CBFβ signaling in mammals that thus far has not been observed in *C. elegans* is a transcriptional activator function. Depending on post-translational modifications of Runx, Runx/CBFβ are either joined by co-repressors such as HDACs, nCOR and mSin3A, the co-activators p300 and C/EBP, or transcription factors ETS, MYB, and SMADs (Reviewed in Ito et al. 2015). So far, UNC-37 is the only identified interactor of RNT-1/BRO-1 in the worm. The observation that mutation of the co-repressor *unc-37* results in a phenotype very similar to loss of *rnt-1* or *bro-1* (Xia et al. 2007), suggests that there is no critical activator function for RNT-1/BRO-1 in the seam cells (at the level of cell fate control).

As an important development, we were able to use GFP-tagging of endogenous *pop-1* and *rnt-1*, and a conditional *pop-1* knock-out allele, to study gene function and pathway interactions in **Chapters 3 and 4**. Both for POP-1 and RNT-1, we detected different expression levels between the endogenous protein fusions compared to protein fusions expressed from integrated extrachromosomal transgenes previously used in the field. This highlights the need to study endogenous loci; even single-copy insertions of transgenes should be interpreted with caution.

Besides RNT-1/BRO-1, the CEH-16 homolog of the homeodomain transcription factor Engrailed also forms a transcriptional repressor complex with UNC-37 (Huang et al. 2009). The analysis of mutants revealed that *ceh-16* is required for the symmetric L2 division. Interestingly, the symmetric division can be restored by removing APR-1, pointing to a genetic interaction with the Wnt/β-catenin asymmetry pathway. ChIP-seq data, available from the modERN database, do not show CEH-16 localization at the *apr-1* promoter region, but CEH-16 does bind the *pop-1* promoter region. CEH-16 could therefore contribute to the temporal decrease in *pop-1* expression in L2 larvae in parallel to RNT-1/BRO-1. Analysis of a CEH-16::GFP translational reporter revealed expression in seam cells in all larval stages (Huang et al. 2009). Hence, a specific contribution of CEH-16 in *pop-1* repression would be determined by L2 stage-specific co-factors. It would be interesting to use the endogenous GFP::POP-1 fusion to examine whether CEH-16 does indeed modulate POP-1 expression levels in L2 animals.

Timing is everything – an internal clock instructs division (a)symmetry

Remaining questions are why seam cells can only divide symmetrically in the L2 stage, and how the RNT-1/BRO-1 mechanism fits into this temporal scheme. Seam cells are temporally patterned by the heterochronic genes: a network of sequentially expressed transcription factors, miRNAs and an RNA-binding protein, which together provide the developing larva with a temporal identity. Induced expression or loss-of-function of these genes can lead to reiteration or skipping of an entire larval stage (Ambros & Horvitz 1984; Slack & Ruvkun 1997; Moss 2007). These heterochronic mutants revealed that the temporal window of high LIN-28, high HBL-1 and low LIN-14 expression is coupled to the symmetric L2 division, ánd to

the two successive divisions in the L2 stage (Harandi & Ambros 2014). These observations support that a transcription factor (HBL-1) and a translational regulator (LIN-28) contribute to the temporal downregulation of *pop-1*.

As one possible scenario, LIN-28 and/or HBL-1 could induce RNT-1/BRO-1 prior to the L2 symmetric division. Available data and our quantifications of the endogenous RNT-1::GFP levels in L1-L3 seam cells do not support such a model. Nuclear RNT-1 levels are even higher in L1 and L3 than in L2. To test whether *bro-1* expression is the limiting factor, we overexpressed BRO-1 in L1 and L3 seam cells, which did not induce a RNT-1/BRO-1 overexpression phenotype. Thus, *bro-1* expression is not the limiting factor restricting RNT-1/BRO-1 activity to L2 stage seam cells (**Chapter 3**). Altogether, these data suggest that a parallel-acting factor determines RNT-1/BRO-1 activity in L2, and LIN-28 and/or HBL-1 could provide such a parallel mechanism.

Studies in mammalian gastrointestinal stem cells identified Lin28 as a Wnt target gene, revealing an interaction between Lin28 and Wnt signaling. By upregulating Lin28 expression, Wnt signaling suppressed *let-7* miRNA maturation and promoted cancer progression (Cai et al. 2013; Tu et al. 2015). One study also reported a feedback loop from Lin28 to TCF7, in this case enhancing TCF7 expression in breast cancer cell lines (Chen et al. 2015). These observations point to a potential interaction between Wnt activity and LIN-28 in seam cells. Three putative LIN-28 binding motifs (GGAGA; Wilbert et al., 2012) have been identified in the exons and 3' untranslated region of *pop-1* mRNA, which could be used to repress its translation. In this way, LIN-28 would function in parallel to RNT-1/BRO-1 in downregulating *pop-1* expression. We tried to convert asymmetric seam cell divisions into symmetric division by the upregulation of LIN-28, but did not find an acute effect of LIN-28 overexpression on cell fate (**Chapter 3**, Supplemental). It would be interesting to know whether the candidate binding sites in the *pop-1* 3'UTR are indeed targeted by LIN-28.

The conserved transcription factor HBL-1 acts downstream of LIN-28 and has been suggested to be the most direct regulator of L2 fates (Abrahante et al. 2003; Lin et al. 2003; Abbott et al. 2005). The combination of a *rnt-1* candidate null and *hbl-1* hypomorphic mutation strongly suppressed *pop-1* RNAi induced hyperplasia (**Chapter 3**). This might indicate that RNT-1 and HBL-1 contribute to seam cell proliferation in parallel. As described above, RNT-1 represses negative cell cycle regulators in seam cells. HBL-1 has been described to have both activator and repressor functions. It could well be that both genes

affect the expression of cell cycle genes in parallel. Important to note is that these results are difficult to interpret, as HBL-1 has an additional function in L4 seam cells. Proper lineaging of L2 divisions should provide better insights in the phenotype.

Genetic interactions between the heterochronic genes and Wnt signaling components have previously been described in *C. elegans*. The activity of the Wnt/β-catenin asymmetry pathway was suggested to be modulated by heterochronic genes during the different larval stages (Harandi & Ambros 2014). Based on the analysis of mutant combinations, the authors proposed that heterochronic genes modulate the activity of Wnt components by disrupting anterior-posterior polarity. However, such an effect was not observed during the normal L2 symmetric divisions, in which Wnt components still become polarized. Several interesting genetic interactions were detected in the same study. RNAi of *pop-1* in heterochronic *lin-4(lf)* or *lin-14(gf)* mutants, which repeat L1 development, did not induce hyperplasia or cell fate switches (Harandi & Ambros 2014). This would with the model that L1 seam cells do not require the POP-1 repressor function for differentiation, or that L1 seam cells in general do not depend on Wnt signaling. Our seam cell-specific *pop-1* knock-out lineaging experiments revealed premature differentiation of seam cells during the L1 stage, while hyperplasia did not start in L1 (**Chapter 3**). As the differentiation phenotype indicates substantial loss of function, these data suggest that the POP-1 activator function is critical in L1 seam cells, and that the repressor function is only required in later stages. Our RNAi experiments did not remove the activator function, which could explain the lack of phenotype in L1 stage -or L1 reiterating- seam cells. It will be interesting to determine whether L1 seam cells, besides uncoupling cell size asymmetry from cell fate asymmetry (**Chapter 4**), also uncouple Wnt signaling from their cell fate asymmetry.

A nuclear hormone receptor as a potential modulator of Wnt/β-catenin signaling?

There are likely additional regulators of POP-1 present in L2 seam cells that function in parallel to RNT-1/BRO-1. A candidate regulator is the nuclear hormone receptor NHR-25, which belongs to the evolutionarily conserved subfamily of nuclear receptor NR5A, that further includes *Drosophila* FTZ-F1, and mammalian SF-1 and LRH-1 (Asahina et al. 2000; Gissendanner & Sluder 2000). Nuclear hormone receptors are multifunctional transcription factors involved in cell differentiation and development. They interact with multiple

signaling pathways, among which Wnt signaling (Reviewed in Mulholland et al. 2005; Hajduskova et al. 2009).

In *C. elegans*, NHR-25 was shown to either synergize with or antagonize the Wnt/β-catenin asymmetry pathway, depending on tissue context. In the developing gonad, NHR-25 antagonized POP-1/SYS-1-mediated transcription, whereas in the T seam cell it enhanced Wnt output (Hajduskova et al. 2009). NHR-25 is also expressed in all V cells from the L1 stage until adulthood (Šilhánková et al. 2005; Hajduskova et al. 2009), and its loss of function increased seam cell numbers by preventing anterior daughter cell differentiation and inducing additional divisions (Šilhánková et al. 2005). The effect on anterior differentiation resembles that of *pop-1* loss of function (**Chapter 3**), suggesting both factors are critical for seam cell differentiation. Since POP-1 distribution was normal in *nhr-25* RNAi seam cells, NHR-25 is thought to act in parallel to POP-1 (Siegfried et al. 2004; Asahina et al. 2006; Hajduskova et al. 2009) in instructing anterior differentiation.

NHR-25 could modulate POP-1 function indirectly in seam cells by titrating its co-activators. Studies in the developing gonad revealed a physical interaction between NHR-25 and SYS-1, which could antagonize POP-1/SYS-1-dependent transcription. Additionally, NHR-25 was also shown to interact with WRM-1, with higher affinity compared to SYS-1. By outcompeting SYS-1 binding to NHR-25, WRM-1 was suggested to suppress NHR-25 and to promote POP-1/SYS-1 mediated transcription (Asahina et al. 2006). In this way, the Wnt/β-catenin asymmetry pathway and NHR-25 can cross-regulate each other. The interaction with SYS-1 was also found in the T seam cell (Hajduskova et al. 2009). Moreover, the mammalian NHR-25 orthologs SF-1 and LRH-1 interact with β-catenin and activate target genes in synergy with TCF/β-catenin signaling (Gummow et al. 2003; Hossain & Saunders 2003; Botrugno et al. 2004; Huang et al. 2017). The NHR-25/SYS-1 interaction is therefore likely to be used also in the V seam cells.

Interestingly, NHR-25 itself is thought to be transcriptionally activated by SYS-1, to induce the expression of epidermal genes (Asahina et al. 2006; Shao et al. 2013). NHR-25 ChIP-seq analysis revealed binding to promoter regions of the positive cell cycle regulators *cdk-4*, *cye-1*, *cdk-2* and *cdk-1* (the modERN genome resource). This could explain the synergy with the POP-1 transcriptional activator in posterior seam cells; if POP-1 induces self-renewal genes like the GATA factors *elt-6* and *egl-18* (Gorrepati et al. 2013), and in parallel NHR-25 induces proliferation. Proper cell fate distribution therefore seems to depend on the

balance between POP-1/SYS-1 activity and NHR-25/SYS-1 binding (Asahina et al. 2006). POP-1 does seem to regulate NHR-25 expression; *pop-1* loss of function altered NHR-25 expression either positively or negatively in the embryo, depending on the cell type (Shao et al. 2013). ChIP-seq analysis in embryonic extracts, however, did not detect binding of POP-1 at the *nhr-25* promoter region (the modERN genome resource), therefore, the regulation could be indirect. NHR-25 has been described to autoregulate its own expression; by sequestering SYS-1, POP-1 could therefore modulate NHR-25 expression indirectly.

The observation that loss of NHR-25 also induced additional seam cell divisions, hints to a possible interaction with heterochronic genes. In early L4 animals, NHR-25 was shown to interact with heterochronic genes HBL-1, LIN-41 and LIN-42. It is negatively regulated by, and acts antagonistically to HBL-1 and LIN-42. Interestingly, both HBL-1 and NHR-25 are also expressed during L2 stage development. It may very well be that these proteins have an additional function in L2 larvae; modulating each other's activity (Hada et al. 2010). Since the presence of HBL-1 seems linked to two successive divisions in the L2 stage, loss of a negative regulator of *hbl-1* might explain the additional cell divisions observed in the *nhr-25* RNAi animals. NHR-25 was shown to be a downstream target of *let-7* mediated repression, suggesting heterochronic genes may titrate NHR-25 levels during development (Hayes et al 2006). In this way, NHR-25 could contribute to both self-renewal and proliferation.

Unraveling cell cycle progression in seam (daughter) cells

Seam cell self-renewal and proliferation seem instructed via different, parallel mechanisms; however, both processes include cell cycle regulation. Progression of the cell cycle in seam cells is closely coupled to the adopted cell fate. Anterior daughter cells undergo endoreduplication (S phase) prior to differentiation, while posterior daughters pause in G1 in this time window, and progress to S-phase only much later (Hedgecock & White 1985; Van Rijnberk et al. 2017). In **Chapter 2,** we introduced an adapted sensor to monitor cell cycle progression in *C. elegans*, which allowed us to use cell cycle progression as a marker for seam cell fate. We used this sensor in **Chapter 3** to monitor cell cycle progression of RNT-1/BRO-1 induced seam cells that converted anterior daughter cells into posterior self-renewing cells. The converted anterior daughter cells paused in G1 similar to their posterior sisters, which further supported the link between cell fate and cell cycle regulation.

Furthermore, this revealed deviation from wild-type within 90 minutes after RNT-1/BRO-1 induction, providing a time-window for the cell fate switch.

Interestingly, both endoreduplication and fusion can be uncoupled from seam cell differentiation. Besides increasing the transcriptional capacity of the hypodermis, endoreduplication does not seem to be functional for the anterior seam daughter cell. Blocking S-phase with heat shock-induced CKI-1 did not prevent anterior cell fusion in our experiments (**Chapter 3**). Cell-fusion with the hyp7 hypodermis was also shown to be regulated independently from differentiation, or cell cycle arrest in this case. By expressing the EFF-1 fusogen, anterior daughter cells can fuse their plasma membrane with that of the hypodermis. Repression of *eff-1* prevented fusion but not cell cycle arrest, resulting in retention of anterior non-seam cells in the epithelium (Brabin et al. 2011). These non-seam cells did move ventrally/dorsally, suggesting they are no longer part of the epithelial organization and have no clear function anymore. The observation that the ability to proliferate can be uncoupled from differentiation suggests that self-renewal comprises more than just the suppression of differentiation. However, it could still all be transcriptionally regulated by POP-1. In that light, it is interesting to search for additional POP-1 repressor targets that actively switch off seam cell fate.

Several experiments revealed that cell cycle exit is important for seam tissue homeostasis. Mutations in the G1/S phase inhibitors *cki-1*^{Kip1}, *fzr-1*^{Cdh1} and *lin-35*^{Rb} increased seam cell numbers, according to their role in proliferation (Nimmo et al. 2005; Xia et al. 2007). Mechanistically, we showed that the anterior cell cycle initiates during telophase when POP-1 levels in the anterior nucleus remain high (**Chapter 3**). POP-1 dual function could explain the difference in cell cycle progression between seam daughter cells. ChIP-sequence of POP-1 in embryos revealed binding sites in the promoter regions of *cki-1* and *lin-35* (the modERN Resource). Binding of the POP-1 repressor to cell cycle inhibitory genes could explain why anterior cells progress through S-phase to undergo endoreduplication, whereas posterior cells express these inhibitors and pause in G1. In this way, RNT-1/BRO-1 and POP-1 could control seam cell cycle progression in parallel.

Additionally, RNT-1/BRO-1 were also shown to regulate the G1/S phase transition by repressing negative regulators *cki-1* (Nimmo et al. 2005; Kagoshima et al. 2007b), *fzr-1* and *lin-35* (Xia et al. 2007). Our overexpression experiments in **Chapter 3** revealed that RNT-1/BRO-1 exert their function in the mother cell prior to mitosis, thereby affecting the

anterior daughter cell after mitosis. As RNT-1 is degraded during anaphase onset, it needs to be newly expressed in posterior self-renewing daughter cells. This could delay the repression of *cki-1*, *fzr-1* and *lin-35* for several hours, and contribute to the G1 pause window in wild-type posterior daughter cells.

We never observed additional cell divisions in seam cells with induced RNT-1/BRO-1 expression, nor did we in *pop-1* loss of function seam cells (**Chapters 3 and 4**). This indicates that RNT-1/BRO-1's control over cell cycle genes *cki-1*, *fzr-1* and *lin-35* is independent of POP-1 regulation. It also suggests that reducing the expression of cell cycle inhibitors is not sufficient for triggering extra divisions, nor was the loss of differentiation sufficient for promoting proliferation. Additional induction of positive regulators seems required to fully complete the cell cycle. The heterochronic factor LIN-28 could induce cell cycle progression in seam cells. Studies on mouse ES cells revealed that Lin28 stimulates proliferation by binding to and increasing the translation of the positive cell cycle regulators Cyclin A and B and Cdk4 (Xu et al. 2009). If these target genes are also conserved, it could explain the rapid successive L2 asymmetric division in wild-type animals during the LIN-28 expression window. Moreover, as outlined above, NHR-25 could be responsible for cell cycle progression in seam daughter cells. ChIP-seq analysis revealed binding of NHR-25 to the promoter regions of *cdk-1*, *cye-1*, *cdk-2*, and *cdk-1* (modERN genome resource). By inducing these genes, NHR-25 and/or LIN-28 could complement RNT-1/BRO-1 in activating a second round of mitosis.

Parallel mechanisms instructing seam cell self-renewal and proliferation

The above described mechanisms assume that seam cell fate asymmetry is regulated at two different levels: self-renewal and cell cycle regulation (Figure 1). Our findings in **Chapter 3** revealed that POP-1 is required to balance self-renewal and differentiation. RNT-1/BRO-1 indirectly induced self-renewal by negative regulation of POP-1, and is suggested to regulate proliferation by suppressing negative cell cycle regulators *cki-1*, *lin-35* and *fzr-1*. Our results imply the need for additional regulators to instruct the temporal activation of these factors. We hypothesize that NHR-25 could complement RNT-1/BRO-1 in two separate functions. First, by recruiting SYS-1, NHR-25 could suppress POP-1 activator function and induce POP-1 repressor function, thereby promoting differentiation. Second, in a complex with SYS-1, NHR-25 could induce the expression of positive cell cycle regulators *cdk-1*, *cye-1*, *cdk-2*, and

cdk-1, thereby promoting cell cycle progression and proliferation. Temporal regulation of these mechanisms may be facilitated by the heterochronic genes, of which several were shown to genetically interact with both NHR-25 and Wnt components. The *let-7*/LIN-28 bistable switch has conserved functions in balancing proliferation versus differentiation. *let-7* miRNA was shown to suppress *nhr-25* translation in L4 seam cells, thereby enforcing the asymmetry of the division. Additionally, HBL-1 and NHR-25 antagonize each other in L4 seam cells; a mechanism that might also operate during the L2 stage. This suggests that *nhr-25* levels need to be temporally controlled to maintain the division pattern. Furthermore, LIN-28 was shown to interact with Wnt signaling in mammals; it could modulate POP-1 translation by binding to its mRNA. In this way, cell fate is regulated at multiple levels. Our work suggests a tight balance between several regulatory mechanisms to instruct asymmetry or symmetry. The asymmetric distribution of Wnt components POP-1, SYS-1 and WRM-1 adds yet another level of complexity.

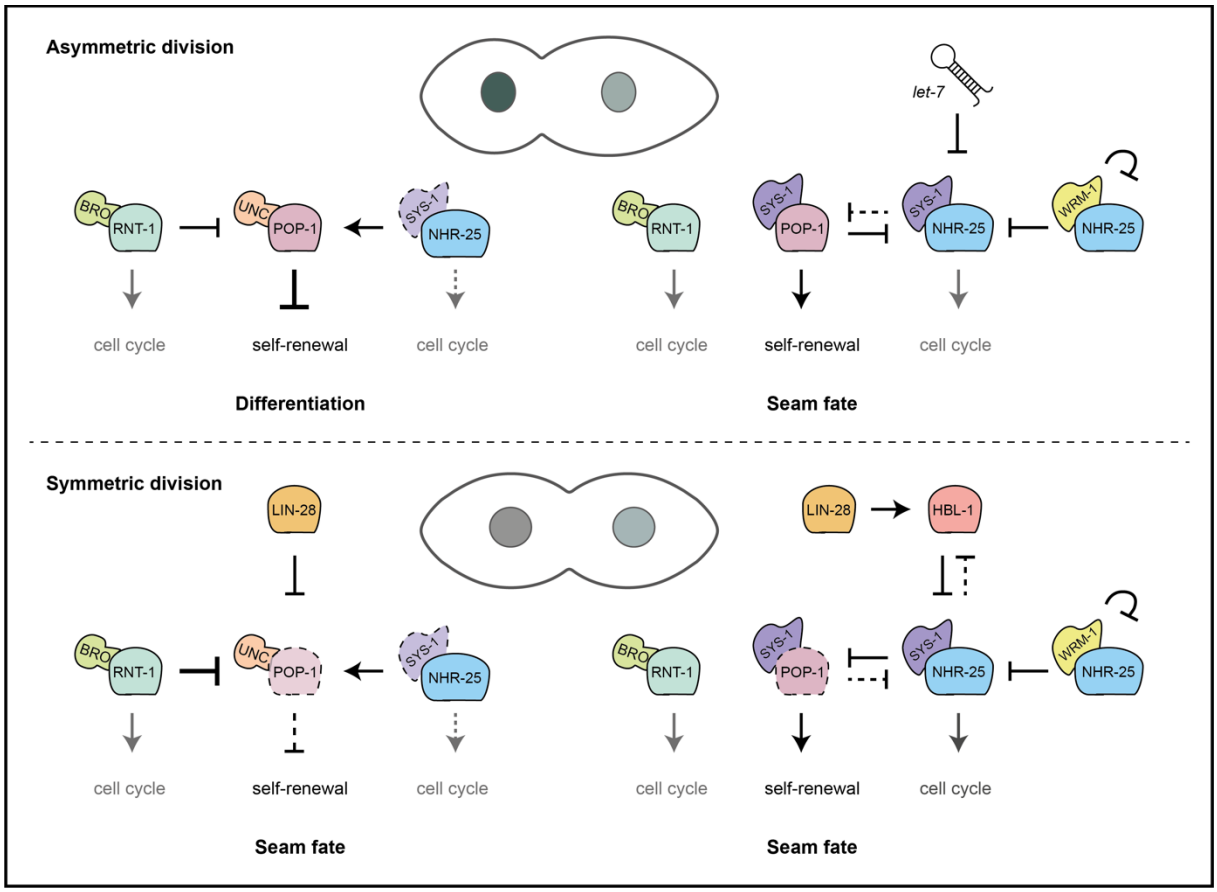

Figure 1. Hypothetical model of the parallel mechanisms regulating seam cell division (a)symmetry. Asymmetric seam cell divisions rely on the dual activity of POP-1 as a transcriptional repressor (anterior; left) and as an activator (posterior; right). In these divisions; POP-1 function is dominant and controls a binary cell fate decision. In parallel, the RNT-1/BRO-1 repressor complex, heterochronic genes (*let-7*) and potentially NHR-25 control cell cycle progression in both daughter cells (top). Symmetric seam cell divisions rely on the temporal inactivation of POP-1 repressor function by the RNT-1/BRO-1 repressor complex. This results in both anterior and posterior daughter cells adopting a self-renewal fate. In the anterior daughter cell, POP-1 repressor function may be additionally controlled by heterochronic factor LIN-28 and potentially NHR-25. In both daughter cells, RNT-1/BRO-1, LIN-28, HBL-1, and NHR-25 are thought to act in cell cycle progression (bottom).

Cell size asymmetry: a temporal mechanism to facilitate seam cell growth?

Seam cell divisions create daughter cells of similar size or different sizes, dependent on the developmental stage. Several variations of symmetric and asymmetric seam cell divisions take place within the plane of the epithelium, which means that seam cells can alternate symmetric and asymmetric division without changing their polarity axis. This raises the question what triggers the (a)symmetry in pulling forces that distinguish an asymmetric division from a symmetric division?

In **Chapter 4** we explored the coordination between cell fate asymmetry and division asymmetry. We showed that seam cell fate asymmetry segregates independently from the asymmetry in cell size. In young L1 and early L2 animals, daughter cell sizes are equal; only from mid L2 stage onwards seam cells start to divide asymmetrically in size. This suggests that cell size asymmetry is coupled either to the size/growth of the animal, or to developmental timing via the heterochronic network.

We expected anterior-posterior Wnt polarity to be the dominant spindle orientation mechanism. Contrary to our expectations, we found POP-1 activity to be involved in spindle orientation (**Chapter 4**). Loss of the POP-1 repressor function induced severe orientation defects. We noticed that these defects increased with shape changes of the cell; reminiscent of the relation between cell geometry and Wnt signaling we detected before (Wildwater et al. 2011). In this earlier study, we found that Wnt ligands are critically needed to orient the spindle when cells are rounded. The overlap in phenotype between Wnt ligand loss and *pop-1* RNAi is surprising given that non-canonical Wnt signaling would be expected to orient the spindle. Therefore, we expect the contribution of a feedback mechanism, by which the downstream transcription factor controls the expression of upstream pathway components. As loss of the POP-1 repressor causes this phenotype, increased expression of a target gene could disrupt spindle orientation. As such a Wnt antagonist such as *mig-1,* which encodes a Secreted Frizzled Related Protein, would be the best candidate. ChIP-seq analysis and available genetic data did not reveal obvious candidates for an internal feedback loop to Wnt polarity, nor other candidate genes that might be responsible for these orientation defects.

Connecting the spindle to the plasma membrane involves the conserved Gα/GPR-1,2/LIN-5 complex. In **Chapter 4**, we examined a potential link between the Wnt/β-catenin

asymmetry pathway and LIN-5 complex, through joint regulation by the GSK-3 and CK1 kinases. In addition, we examined the function of the PIG-1^{MELK} kinase as a candidate upstream regulator of LIN-5. We did not find a clear function for these kinases in controlling cortical pulling forces. We did, however, observe division orientation defects in *pig-1* RNAi animals, which indicated a general function for PIG-1 in aligning the spindle in anterior-posterior direction. PIG-1 is critical for size asymmetry of Q neuroblast daughter cells, and has been implicated in actomyosin regulation, as well as in SRC-1 Src signaling (Ou et al. 2010; Pacquelet et al. 2015; Liro et al. 2018). Further studies will be needed to reveal how PIG-1 contributes to spindle orientation, and whether these functions are conserved in mammals.

Finally, we examined a potential role for non-muscle myosin NMY-2 in (asymmetric) actomyosin accumulation or contraction in **Chapter 4**. The actomyosin cytoskeleton participates in multiple aspects of division asymmetry in the *C. elegans* embryo and other systems. Some of these mechanisms depend on strong actomyosin asymmetry in mitosis. Such actomyosin dependent mechanisms are not likely in seam cells; we did not observe asymmetry in cortical NMY-2 localization during anaphase. We did observe, however, posterior NMY-2 enrichment during prometaphase, prior to spindle displacement in mitosis. Moreover, analysis of a weak *nmy-2* allele suggests the possibility of actomyosin contribution in division asymmetry. As for PIG-1, these are preliminary observations that require further study.

Thinking beyond seam cells?

The work described in this thesis focused on the stem cell division pattern of *C. elegans* seam cells, with the goal to understand what drives a stem cell or progenitor cell to switch division mode. In the seam cell lineage, asymmetric divisions are the default division mode. Only at the onset of exponential growth of the animal, these cells temporarily switch to a symmetric division mode and expand in number. Having asymmetric cell division as the default division mode is observed in other simple models, such as *Drosophila* neuroblasts. Interestingly, mammalian tissue-specific stem cells of the intestine have symmetric divisions as their default mode. Mechanistically these divisions are symmetric, but the outcome is stochastic and depends on the positioning of the daughter cells with respect to the niche

(these divisions were previously classified as extrinsic asymmetric divisions). The major difference between these symmetric divisions and intrinsically asymmetric divisions is that in the first situation, cell fate is restricted only after division, which creates a level of plasticity in the tissue. Symmetric divisions combined with niche-dependent stem cell maintenance is thought to be more protective of cancerous mutation build-up, as many acquired mutations will be randomly eliminated through differentiation (Shahriyari & Komarova 2013). However, the stochastic outcome of the division might also promote clonal competition of mutant stem cells that induce cancer. Such mutant inflammatory or oncogenic stem cells have been proposed to switch to asymmetric divisions to reduce proliferation (Reviewed in Santoro et al. 2016). What these studies reveal is that active switching of stem cells is required to maintain the balance between proliferation and differentiation during normal development, but especially during stress situations like wounding or mutation. The active switching of seam cells may provide insight in the conserved mechanisms that stem cells apply upon activation or stress induction. As such, *in vivo* studies in a highly tractable model can complement and contribute to the broad range of experimental work in the field of cancer research and regenerative medicine.

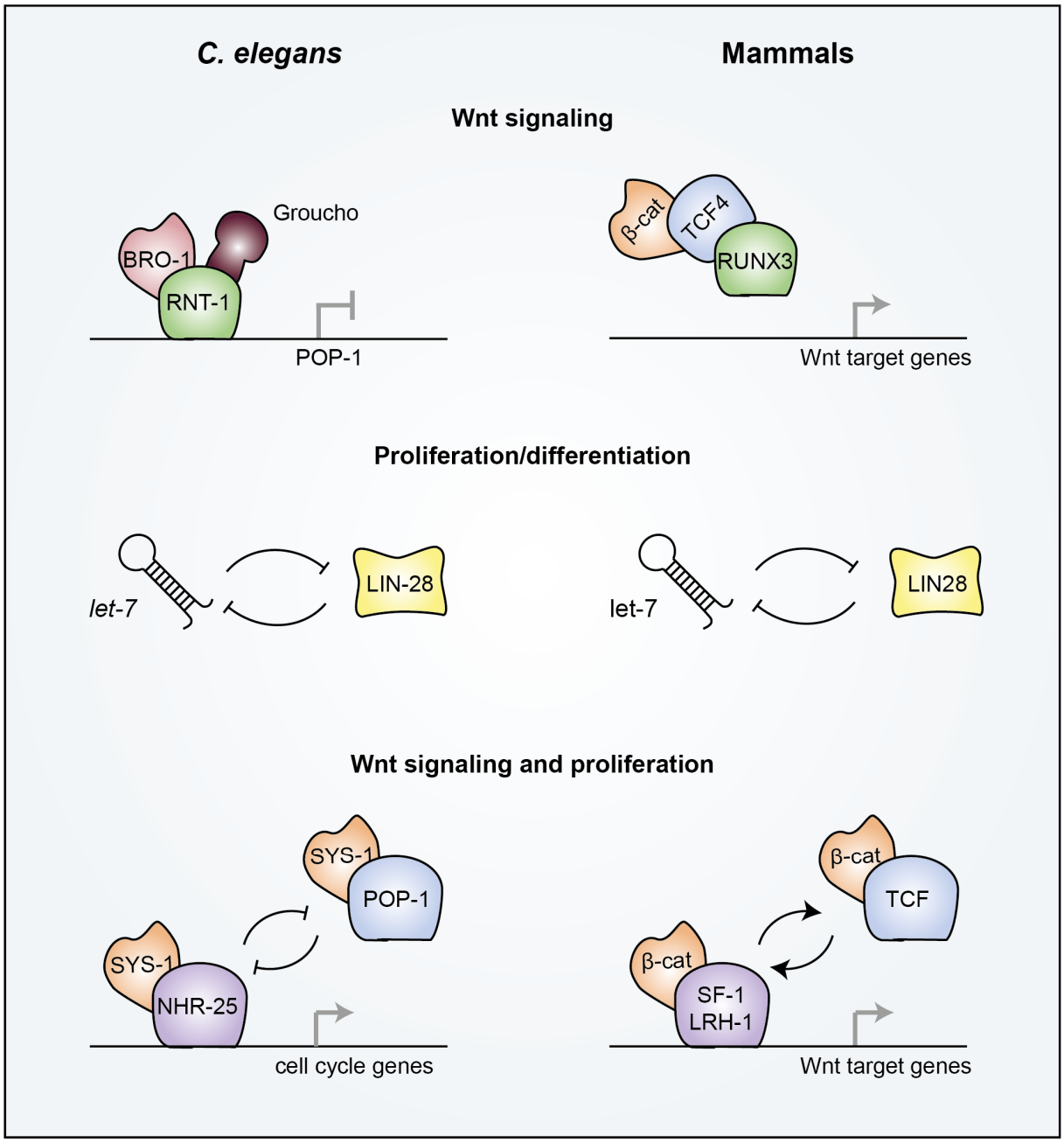

Figure 2. Schematic representation of conserved stem cell regulators in *C. elegans* seam cells and mammalian stem cells. A Runx family-mediated mechanism antagonizes Wnt signaling in worms and mammals. However, in the worm, repression occurs via RNT-1/BRO-1 mediated downregulation of POP-1, whereas in mammals a ternary protein complex of RUNX/TCF/β-catenin suppresses TCF function (top). A let-7/Lin28 bistable switch appears conserved between worms and mammals. In the worm, this switch is part of a larger clock mechanism instructing a specific division pattern. In mammals, this switch is involved in balancing stem cell self-renewal versus differentiation (middle). Steroid hormone signaling has conserved functions in modulating Wnt signaling. In the worm, this is thought to involve NHR-25 competition with POP-1 for SYS-1$^{\beta\text{-catenin}}$ binding. Here, it could antagonize Wnt signaling. In mammals, SF-1 and LRH-1 both interact with β-catenin. This interaction synergizes with Wnt signaling (bottom).

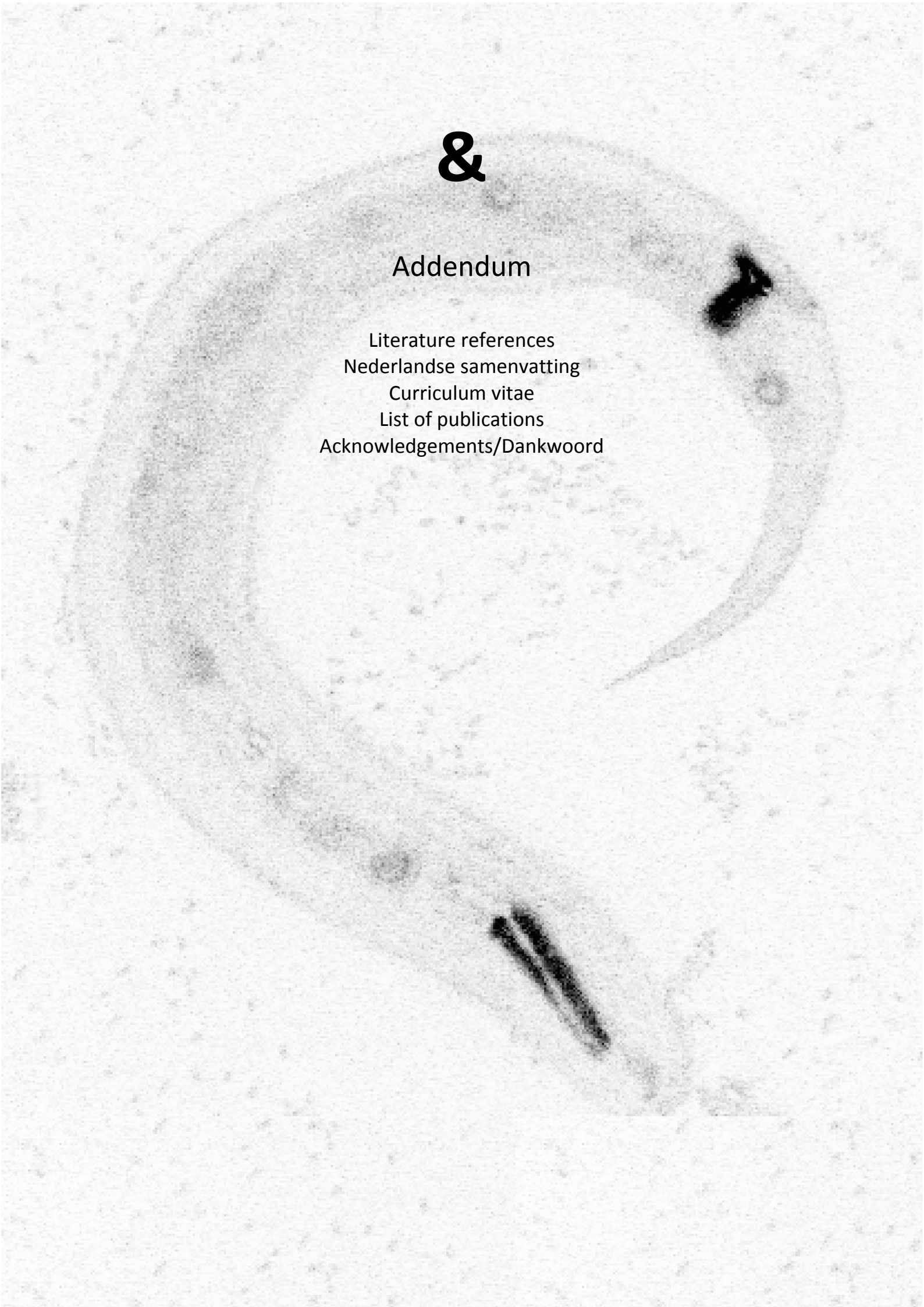

&

Addendum

Literature references
Nederlandse samenvatting
Curriculum vitae
List of publications
Acknowledgements/Dankwoord

References

Abbott, A.L., Alvarez-Saavedra, E., Miska, E.A., Lau, N.C., Bartel, D.P., Horvitz, H.R. & Ambros, V. (2005) The let-7 MicroRNA family members mir-48, mir-84, and mir-241 function together to regulate developmental timing in Caenorhabditis elegans. *Developmental Cell* **9**: 403–414.

Abrahante, J.E., Daul, A.L., Li, M., Volk, M.L., Tennessen, J.M., Miller, E.A., Rougvie, A.E., Hall, J. & Se, C.S. (2003) The Caenorhabditis elegans hunchback -like Gene lin-57 / hbl-1 Controls Developmental Time and Is Regulated by MicroRNAs. **4**: 625–637.

Ambros, V. (1989) A hierarchy of regulatory genes controls a larva-to-adult developmental switch in C. elegans. *Cell* **57**: 49–57.

Ambros, V. & Horvitz, H.R. (1987) The lin-14 locus of Caenorhabditis elegans controls the time of expression of specific postembryonic developmental events. *Genes & development* **1**: 398–414.

Ambros, V.R. & Horvitz, H.R. (1984) Heterochronic Mutants of the Nematode Caenorhabditis elegans Authors (s): Victor Ambros and H . Robert Horvitz Source : Science , New Series , Vol . 226 , No . 4673 (Oct . 26 , 1984), pp . 409-416 Published by : American Association for the Advancemen. *Science* **226**: 409–416.

Amerongen, R. Van, Mikels, A. & Nusse, R. (2008) Alternative Wnt Signaling Is Initiated. **1**: 1–6.

Asahina, M., Ishihara, T., Jindra, M., Kohara, Y., Katsura, I. & Hirose, S. (2000) The conserved nuclear receptor Ftz-F1 is required for embryogenesis, moulting and reproduction in Caenorhabditis elegans. *Genes to Cells* **5**: 711–723.

Asahina, M., Valenta, T., Silhankova, M., Korinek, V. & Jindra, M. (2006) Crosstalk between a Nuclear Receptor and β-Catenin Signaling Decides Cell Fates in the C. elegans Somatic Gonad. *Developmental Cell* **11**: 203–211.

Austin, J. & Kenyon, C. (1994) Cell contact regulates neuroblast formation in the Caenorhabditis elegans lateral epidermis. *Development (Cambridge, England)* **120**: 313–23.

Baldwin, A.T. & Phillips, B.T. (2014) The tumor suppressor APC differentially regulates multiple β-catenins through the function of axin and CKIα during C. elegans asymmetric stem cell divisions. *Journal of cell science* **127**: 2771–81.

Baldwin, A.T. & Phillips, B.T. (2016) Title : Unique and redundant β -catenin regulatory roles of two Dishevelled paralogs during C . elegans asymmetric cell division Authors : Austin T . Baldwin , Amy M . Clemons and Bryan T . Phillips 143 Biology Building Iowa City , Iowa 52242-1324 Corresp. **52242**:.

Banerjee, D., Chen, X., Lin, S.Y. & Slack, F.J. (2010) kin-19/casein kinase Ia has dual functions in regulating asymmetric division and terminal differentiation in C. elegans epidermal stem cells. *Cell Cycle* **9**: 4748–4765.

Barr, A.R., Heldt, F.S., Zhang, T., Bakal, C. & Novák, B. (2016) A Dynamical Framework for the All-or-None G1/S Transition. *Cell Systems* **2**: 27–37.

Bei, Y., Hogan, J., Berkowitz, L.A., Soto, M., Rocheleau, C.E., Pang, K.M., Collins, J. & Mello, C.C. (2002) SRC-1 and Wnt signaling act together to specify endoderm and to control cleavage orientation in early C. elegans embryos. *Developmental Cell* **3**: 113–125.

Bellaiche, Y. (2004) The planar cell polarity protein Strabismus promotes Pins anterior localization during asymmetric division of sensory organ precursor cells in Drosophila. *Development* **131**: 469–478.

Bellaïche, Y., Gho, M., Kaltschmidt, J.A., Brand, A.H. & Schweisguth, F. (2001) Frizzled regulates localization of cell-fate determinants and mitotic spindle rotation during asymmetric cell division. *Nature Cell Biology* **3**: 50–57.

Berends, C.W.H., Muñoz, J., Portegijs, V., Schmidt, R., Grigoriev, I., Boxem, M., Akhmanova, A., Heck, A.J.R. & van den Heuvel, S. (2013) F-actin asymmetry and the endoplasmic reticulum–associated TCC-1 protein contribute to stereotypic spindle movements in the *Caenorhabditis elegans* embryo. *Molecular Biology of the Cell* **24**: 2201–2215.

Berkowitz, L.A. & Strome, S. (2000) Mes-1, a Gene Required for Unequal Divisions of the Germline in Early C. Elegans Embryos, Encodes a Membrane Protein That Is Localized To the Boundary Between the Germline and Gut Cells. *Development* **127**: 4419–4431.

Blyth, K., Cameron, E.R. & Neil, J.C. (2005) The RUNX genes: Gain or loss of function in cancer. *Nature Reviews Cancer* **5**: 376–387.

Botrugno, O.A., Fayard, E., Annicotte, J.S., Haby, C., Brennan, T., Wendling, O., Tanaka, T., Kodama, T., Thomas, W., Auwerx, J. & Schoonjans, K. (2004) Synergy between LRH-1 and β-catenin Induces G1cyclin-mediated cell proliferation. *Molecular Cell* **15**: 499–509.

Boxem, M. & Van Den Heuvel, S. (2001) lin-35 Rb and cki-1 Cip/Kip cooperate in developmental regulation of G1 progression in C. elegans. *Development* **128**: 4349–4359.

Boxem, M., Srinivasan, D.G. & van den Heuvel, S. (1999) The Caenorhabditis elegans gene ncc-1 encodes a cdc2-related kinase required for M phase in meiotic and mitotic cell divisions, but not for S phase. *Development (Cambridge, England)* **126**: 2227–39.

Brabin, C., Appleford, P.J. & Woollard, A. (2011) The Caenorhabditis elegans GATA Factor ELT-1 Works through the Cell Proliferation Regulator BRO-1 and the Fusogen EFF-1 to Maintain the Seam Stem-Like Fate. *PLoS Genetics* **7**: e1002200.

Brabin, C. & Woollard, A. (2012) Finding a niche for seam cells? *Worm* **1**: 107–111.

Brenner, S. (1974) The genetics of Caenorhabditis elegans. *Genetics* **77**: 71–94.

Brodigan, T.M., Liu, J. i., Park, M., Kipreos, E.T. & Krause, M. (2003) Cyclin E expression during development in Caenorhabditis elegans. *Developmental Biology* **254**: 102–115.

Cabello, J., Neukomm, L.J., Günesdogan, U., Burkart, K., Charette, S.J., Lochnit, G., Hengartner, M.O. & Schnabel, R. (2010) The Wnt pathway controls cell death engulfment, spindle orientation, and migration through CED-10/Rac. *PLoS Biology* **8**:.

Cai, W.-Y., Wei, T.-Z., Luo, Q.-C., Wu, Q.-W., Liu, Q.-F., Yang, M., Ye, G.-D., Wu, J.-F., Chen, Y.-Y., Sun, G.-B., Liu, Y.-J., Zhao, W.-X., Zhang, Z.-M. & Li, B.-A. (2013) The Wnt- -catenin pathway represses let-7 microRNA expression through transactivation of Lin28 to augment breast cancer stem cell expansion. *Journal of Cell Science* **126**: 2877–2889.

Calvo, D., Victor, M., Gay, F., Sui, G., Luke, M.P.S., Dufourcq, P., Wen, G., Maduro, M., Rothman, J. & Shi, Y. (2002) A POP-1 repressor complex restricts inappropriate cell type-specific gene transcription during Caenorhabditis elegans embryogenesis. *EMBO Journal* **20**: 7197–7208.

Canman, J.C., Lewellyn, L., Laband, K., Smerdon, S.J., Bowerman, B. & Oegema, K. (2008) NIH Public Access. **322**: 1543–1546.

Cappell, S.D., Chung, M., Jaimovich, A., Spencer, S.L. & Meyer, T. (2016) Irreversible APCCdh1 Inactivation Underlies the Point of No Return for Cell-Cycle Entry. *Cell* **166**: 167–180.

Cavallo, R. a, Cox, R.T., Moline, M.M., Roose, J., Polevoy, G. a, Clevers, H., Peifer, M. & Bejsovec, a (1998) Drosophila Tcf and Groucho interact to repress Wingless signalling activity. *Nature* **395**: 604–608.

Chalfie, M., Horvitz, H.R. & Sulston, J.E. (1981) Mutations that lead to reiterations in the cell

lineages of C. elegans. *Cell* **24**: 59–69.
Chen, C., Cao, F., Bai, L., Liu, Y., Xie, J., Wang, W., Si, Q., Yang, J., Chang, A., Liu, D., Liu, D., Chuang, T.H., Xiang, R. & Luo, Y. (2015) IKKβ enforces a LIN28B/TCF7L2 positive feedback loop that promotes cancer cell stemness and metastasis. *Cancer Research* **75**: 1725–1735.
Chen, G., Fernandez, J., Mische, S. & Courey, A.J. (1999) A functional interaction between the histone deacetylase Rpd3 and the corepressor Groucho in Drosophila development. *Genes and Development* **13**: 2218–2230.
Chien, S.C., Brinkmann, E.M., Teuliere, J. & Garriga, G. (2013) Caenorhabditis elegans PIG-1/MELK acts in a conserved PAR-4/LKB1 polarity pathway to promote asymmetric neuroblast divisions. *Genetics* **193**: 897–909.
Chisholm, A.D. & Hsiao, T.I. (2012) The Caenorhabditis elegans epidermis as a model skin. I: Development, patterning, and growth. *Wiley Interdisciplinary Reviews: Developmental Biology* **1**: 861–878.
Chuang, L.S.H., Ito, K. & Ito, Y. (2013) RUNX family: Regulation and diversification of roles through interacting proteins. *International Journal of Cancer* **132**: 1260–1271.
Clevers, H., Loh, K.M. & Nusse, R. (2014) Stem cell signaling. An integral program for tissue renewal and regeneration: Wnt signaling and stem cell control. *Science (New York, N.Y.)* **346**: 1248012.
Clevers, H. & Nusse, R. (2012) Wnt/??-catenin signaling and disease. *Cell* **149**: 1192–1205.
Colombo, K., Grill, S.W., Kimple, R.J., Willard, F.S., Siderovski, D.P. & Gönczy, P. (2003) Translation of polarity cues into asymmetric spindle positioning in Caenorhabditis elegans embryos. *Science* **300**: 1957–1961.
Cordes, S., Frank, A. & Garriga, G. (2006) The C. elegans MELK ortholog PIG-1 regulates cell size asymmetry and daughter cell fate in asymmetric neuroblast divisions. *Development* **133**: 2747–2756.
Van Der Deen, M., Akech, J., Lapointe, D., Gupta, S., Young, D.W., Montecino, M.A., Galindo, M., Lian, J.B., Stein, J.L., Stein, G.S. & Van Wijnen, A.J. (2012) Genomic promoter occupancy of Runt-related transcription factor RUNX2 in osteosarcoma cells identifies genes involved in cell adhesion and motility. *Journal of Biological Chemistry* **287**: 4503–4517.
Deltcheva, E. & Nimmo, R. (2017) RUNX transcription factors at the interface of stem cells and cancer. *Biochemical Journal* **474**: 1755–1768.
Deppe, U., Schierenberg, E., Cole, T., Krieg, C., Schmitt, D., Yoder, B. & von Ehrenstein, G. (1978) Cell lineages of the embryo of the nematode Caenorhabditis elegans. *Proceedings of the National Academy of Sciences of the United States of America* **75**: 376–380.
Dickinson, D.J., Pani, A.M., Heppert, J.K., Higgins, C.D. & Goldstein, B. (2015) Streamlined genome engineering with a self-excising drug selection cassette. *Genetics* **200**: 1035–1049.
Dickinson, D.J., Ward, J.D., Reiner, D.J. & Goldstein, B. (2013) Engineering the Caenorhabditis elegans genome using Cas9-triggered homologous recombination. *Nature Methods* **10**: 1028–1034.
Ding, S.S. & Woollard, A. (2017) Non-muscle myosin II is required for correct fate specification in the Caenorhabditis elegans seam cell divisions. *Scientific Reports* **7**: 1–13.
Euling, S. & Ambros, V. (1996) Heterochronic genes control cell cycle progress and

developmental competence of C-elegans vulva precursor cells. *Cell* **84**: 667–676.
Farin, H.F., Jordens, I., Mosa, M.H., Basak, O., Korving, J., Tauriello, D.V.F., de Punder, K., Angers, S., Peters, P.J., Maurice, M.M. & Clevers, H. (2016) Visualization of a short-range Wnt gradient in the intestinal stem-cell niche. *Nature* **530**: 340–343.
Fielmich, L.-E., Schmidt, R., Dickinson, D.J., Goldstein, B., Akhmanova, A. & van den Heuvel, S. (2018) Optogenetic dissection of mitotic spindle positioning in vivo. *eLife* 1–31.
Friedland, A.E., Tzur, Y.B., Esvelt, K.M., Colaiácovo, M.P., Church, G.M. & Calarco, J.A. (2013) Heritable genome editing in C. elegans via a CRISPR-Cas9 system. *Nature Methods* **10**: 741–743.
Frøkjær-Jensen, C., Wayne Davis, M., Hopkins, C.E., Newman, B.J., Thummel, J.M., Olesen, S.P., Grunnet, M. & Jorgensen, E.M. (2008) Single-copy insertion of transgenes in Caenorhabditis elegans. *Nature Genetics* **40**: 1375–1383.
Fukuyama, M., Kontani, K., Katada, T. & Rougvie, A.E. (2015) The C. Elegans hypodermis couples progenitor cell quiescence to the dietary state. *Current Biology* **25**: 1241–1248.
Galli, M., Muñoz, J., Portegijs, V., Boxem, M., Grill, S.W., Heck, A.J.R. & Van Den Heuvel, S. (2011) APKC phosphorylates NuMA-related LIN-5 to position the mitotic spindle during asymmetric division. *Nature Cell Biology* **13**: 1132–1140.
Gao, B. (2012) *Wnt Regulation of Planar Cell Polarity (PCP)*, 1st edn. Elsevier Inc.
Gho, M. & Schweisguth, F. (1998) Frizzled signalling controls orientation of asymmetric sense organ precursor cell divisions in Drosophila. *Nature* **393**: 178–181.
Gil, M., Yang, Y., Lee, Y., Choi, I. & Ha, H. (1997) Cloning and expression of a cDNA encoding a novel protein serine/threonine kinase predominantly expressed in hematopoietic cells. *Gene* **195**: 295–301.
Gissendanner, C.R. & Sluder, A.E. (2000) nhr-25, the Caenorhabditis elegans ortholog of ftz-f1, is required for epidermal and somatic gonad development. *Developmental Biology* **221**: 259–272.
Gleason, J.E. & Eisenmann, D.M. (2010) Wnt signaling controls the stem cell-like asymmetric division of the epithelial seam cells during C. elegans larval development. *Developmental Biology* **348**: 58–66.
Goldstein, B. (1995) Cell contacts orient some cell division axes in the Caenorhabditis elegans embryo. *Journal of Cell Biology* **129**: 1071–80.
Goldstein, B. (1992) Induction of gut in Caenorhabditis elegans embryos. *Nature* **357**: 255–257.
Goldstein, B. & Macara, I.G. (2007) The PAR Proteins: Fundamental Players in Animal Cell Polarization. *Developmental Cell* **13**: 609–622.
Goldstein, B., Takeshita, H., Mizumoto, K. & Sawa, H. (2006) Wnt signals can function as positional cues in establishing cell polarity. *Developmental Cell* **10**: 391–396.
Gordon, M.D. & Nusse, R. (2006) Wnt signaling: Multiple pathways, multiple receptors, and multiple transcription factors. *Journal of Biological Chemistry* **281**: 22429–22433.
Gorrepati, L., Thompson, K.W. & Eisenmann, D.M. (2013) C. elegans GATA factors EGL-18 and ELT-6 function downstream of Wnt signaling to maintain the progenitor fate during larval asymmetric divisions of the seam cells. *Development (Cambridge, England)* **140**: 2093–102.
Gotta, M., Dong, Y., Peterson, Y.K., Lanier, S.M. & Ahringer, J. (2003) Asymmetrically Distributed C. elegans Homologs of AGS3/PINS Control Spindle Position in the Early Embryo. *Current Biology* **13**: 1029–1037.
Green, J.L., Inoue, T. & Sternberg, P.W. (2008) Opposing Wnt Pathways Orient Cell Polarity

during Organogenesis. *Cell* **134**: 646–656.
Grill, S.W. & Hyman, A.A. (2005) Spindle Positioning by Cortical Pulling Forces. *Developmental Cell* **8**: 461–465.
Gu, J., Xia, X., Yan, P., Liu, H., Podust, V.N., Reynolds, A.B. & Fanning, E. (2004) Cell Cycle-dependent Regulation of a Human DNA Helicase That Localizes in DNA Damage Foci. *Molecular biology of the cell* **15**: 3320–3332.
Gummow, B.M., Winnay, J.N. & Hammer, G.D. (2003) Convergence of Wnt signaling and steroidogenic factor-1 (SF-1) on transcription of the rat inhibin α gene. *Journal of Biological Chemistry* **278**: 26572–26579.
Habib, S.J., Chen, B., Tsai, F., Anastassiadis, K., Meyer, T., Betzig, E. & Nusse, R. (2013) Asymmetric Stem Cell Division in Vitro. *Science* **1424**: 1445–1448.
Hada, K., Asahina, M., Hasegawa, H., Kanaho, Y., Slack, F.J. & Niwa, R. (2010) The nuclear receptor gene nhr-25 plays multiple roles in the Caenorhabditis elegans heterochronic gene network to control the larva-to-adult transition. *Developmental Biology* **344**: 1100–1109.
Hahn, A.T., Jones, J.T. & Meyer, T. (2009) Quantitative analysis of cell cycle phase durations and PC12 differentiation using fluorescent biosensors. *Cell Cycle* **8**: 1044–1052.
Hajduskova, M., Jindra, M., Herman, M.A. & Asahina, M. (2009) The nuclear receptor NHR-25 cooperates with the Wnt/beta-catenin asymmetry pathway to control differentiation of the T seam cell in C. elegans. *J Cell Sci* **122**: 3051–3060.
Harandi, O.F. & Ambros, V.R. (2014) Control of stem cell self-renewal and differentiation by the heterochronic genes and the cellular asymmetry machinery in Caenorhabditis elegans. *Proceedings of the National Academy of Sciences* **112**: E287–E296.
He, C.-W., Liao, C.-P., Chen, C.-K., Teulière, J., Chen, C.-H. & Pan, C.-L. (2018) The polarity protein VANG-1 antagonizes Wnt signaling by facilitating Frizzled endocytosis. *Development*.
Hedgecock, E.M. & White, J.G. (1985) Polyploid tissues in the nematode Caenorhabditis elegans. *Developmental biology* **107**: 128–133.
Heppert, J.K., Pani, A.M., Roberts, A.M., Dickinson, D.J. & Goldstein, B. (2018) Players in Wnt-Directed Asymmetric Cell Division. **208**: 1147–1164.
Van den Heuvel, S. & Kipreos, E.T. (2012) *C. elegans Cell Cycle Analysis*, Second Edi. Elsevier Inc.
Heyer, B.S., Warsowe, J., Solter, D., Knowles, B.B. & Ackerman, S.L. (1997) New member of the Snf1/AMPK kinase family, Melk, is expressed in the mouse egg and preimplantation embryo. *Molecular reproduction and development* **47**: 148–156.
Hong, Y., Lee, R.C. & Ambros, V. (2000) Structure and Function Analysis of LIN-14 , a Temporal Regulator of Postembryonic Developmental Events in Caenorhabditis elegans Structure and Function Analysis of LIN-14 , a Temporal Regulator of Postembryonic Developmental Events in Caenorhabditis elega. *Society*.
Hossain, A. & Saunders, G.F. (2003) Synergistic cooperation between the ??-catenin signaling pathway and steroidogenic factor 1 in the activation of the mullerian inhibiting substance type II receptor. *Journal of Biological Chemistry* **278**: 26511–26516.
Hristova, M., Hristova, M., Birse, D., Birse, D., Hong, Y., Hong, Y., Ambros, V. & Ambros, V. (2005) The Caenorhabditis elegans Heterochronic Regulator LIN-14 Is a Novel Transcription Factor That Controls the Developmental Timing of Transcription from the Insulin/Insulin-Like Growth Factor Gene ins-33 by Direct DNA Binding. *Molecular and cellular biology* **25**: 11059–11072.

Huang, S., Shetty, P., Robertson, S.M. & Lin, R. (2007) Binary cell fate specification during C. elegans embryogenesis driven by reiterated reciprocal asymmetry of TCF POP-1 and its coactivator beta-catenin SYS-1. *Development* **134**: 2685–95.

Huang, X., Tian, E., Xu, Y. & Zhang, H. (2009) The C. elegans engrailed homolog ceh-16 regulates the self-renewal expansion division of stem cell-like seam cells. *Developmental Biology* **333**: 337–347.

Huang, X.T., Zhu, Y., Chan, L.H.L., Zhao, Z. & Yan, H. (2017) Inference of cellular level signaling networks using single-cell gene expression data in Caenorhabditis elegans reveals mechanisms of cell fate specification. *Bioinformatics* **33**: 1528–1535.

Hughes, S., Brabin, C., Appleford, P.J. & Woollard, A. (2013) CEH-20/Pbx and UNC-62/Meis function upstream of rnt-1/Runx to regulate asymmetric divisions of the C. elegans stem-like seam cells. *Biology open* **2**: 718–27.

Ito, K., Lim, A.C.B., Salto-Tellez, M., Motoda, L., Osato, M., Chuang, L.S.H., Lee, C.W.L., Voon, D.C.C., Koo, J.K.W., Wang, H., Fukamachi, H. & Ito, Y. (2008) RUNX3 Attenuates β-Catenin/T Cell Factors in Intestinal Tumorigenesis. *Cancer Cell* **14**: 226–237.

Ito, Y., Bae, S.C. & Chuang, L.S.H. (2015) The RUNX family: Developmental regulators in cancer. *Nature Reviews Cancer* **15**: 81–95.

Ji, N., Middelkoop, T.C., Mentink, R.A., Betist, M.C., Tonegawa, S., Mooijman, D., Korswagen, H.C. & Oudenaarden, A. Van (2013) Feedback Control of Gene Expression Variability in the Caenorhabditis elegans Wnt Pathway. 869–880.

Kagoshima, H., Nimmo, R., Saad, N., Tanaka, J., Miwa, Y., Mitani, S., Kohara, Y. & Woollard, A. (2007b) The C. elegans CBFbeta homologue BRO-1 interacts with the Runx factor, RNT-1, to promote stem cell proliferation and self-renewal. *Development (Cambridge, England)* **134**: 3905–3915.

Kagoshima, H., Nimmo, R., Saad, N., Tanaka, J., Miwa, Y., Mitani, S., Kohara, Y. & Woollard, A. (2007a) The C. elegans CBFbeta homologue BRO-1 interacts with the Runx factor, RNT-1, to promote stem cell proliferation and self-renewal. *Development* **134**: 3905–3915.

Kagoshima, H., Sawa, H., Mitani, S. & Bu, T.R. (2005) The C . elegans RUNX transcription factor RNT-1 / MAB-2 is required for asymmetrical cell division of the T blast cell. **287**: 262–273.

Kahler, R.A. & Westendorf, J.J. (2003) Lymphoid enhancer factor-1 and β-catenin inhibit Runx2-dependent transcriptional activation of the osteocalcin promoter. *Journal of Biological Chemistry* **278**: 11937–11944.

Karnani, N. & Dutta, A. (2011) The effect of the intra-S-phase checkpoint on origins of replication in human cells. *Genes and Development* **25**: 621–633.

Kemphues, K. (2000) PARsing embryonic polarity. *Cell* **101**: 345–348.

Kidd, A.R., Miskowski, J.A., Siegfried, K.R., Sawa, H. & Kimble, J. (2005) A β-catenin identified by functional rather than sequence criteria and its role in Wnt/MAPK signaling. *Cell* **121**: 761–772.

Kim, J., Feng, H. & Kipreos, E.T. (2007) C. elegans CUL-4 Prevents Rereplication by Promoting the Nuclear Export of CDC-6 via a CKI-1-Dependent Pathway. *Current Biology* **17**: 966–972.

Kim, S., Ishidate, T., Sharma, R., Soto, M.C., Conte, D., Mello, C.C. & Shirayama, M. (2013a) Wnt and CDK-1 regulate cortical release of WRM-1/β-catenin to control cell division orientation in early Caenorhabditis elegans embryos. *Proceedings of the National Academy of Sciences of the United States of America* **110**: E918-27.

Kim, S., Ishidate, T., Sharma, R., Soto, M.C., Conte, D., Mello, C.C. & Shirayama, M. (2013b) Wnt and CDK-1 regulate cortical release of WRM-1/β-catenin to control cell division orientation in early Caenorhabditis elegans embryos. *Proceedings of the National Academy of Sciences of the United States of America* **110**: E918-27.

Knoblich, J.A. (2010) Asymmetric cell division: recent developments and their implications for tumour biology. *Nature Reviews Molecular Cell Biology* **11**: 849–860.

Koff, A., Ohtsuki, M., Polyak, K., Roberts, J.M. & Massagué, J. (1993) Negative regulation of G1 in mammalian cells: Inhibition of cyclin E-dependent kinase by TGF-β. *Science* **260**: 536–539.

Korzelius, J., The, I., Ruijtenberg, S., Portegijs, V., Xu, H., Horvitz, H.R. & van den Heuvel, S. (2011) C. elegans MCM-4 is a general DNA replication and checkpoint component with an epidermis-specific requirement for growth and viability. *Developmental Biology* **350**: 358–369.

Kotak, S. (2019) Mechanisms of Spindle Positioning: Lessons from Worms and Mammalian Cells. *Biomolecules* **9**: 80.

Kozlowski, C., Srayko, M. & Nedelec, F. (2007) Cortical Microtubule Contacts Position the Spindle in C. elegans Embryos. *Cell* **129**: 499–510.

Kudron, M.M., Victorsen, A., Gevirtzman, L., Hillier, L.W., Fisher, W.W., Vafeados, D., Kirkey, M., Hammonds, A.S., Gersch, J., Ammouri, H., Wall, M.L., Moran, J., Steffen, D., Szynkarek, M., Seabrook-Sturgis, S., Jameel, N., Kadaba, M., Patton, J., Terrell, R., Corson, M., Durham, T.J., Park, S., Samanta, S., Han, M., Xu, J., Yan, K.K., Celniker, S.E., White, K.P., Ma, L., Gerstein, M., Reinke, V. & Waterston, R.H. (2018) The modern resource: genome-wide binding profiles for hundreds of Drosophila and Caenorhabditis elegans transcription factors. *Genetics* **208**: 937–949.

LaBonty, M., Szmygiel, C., Byrnes, L.E., Hughes, S., Woollard, A. & Cram, E.J. (2014) CACN-1/Cactin plays a role in Wnt signaling in C. elegans. *PloS one* **9**: e101945.

Li, M., Jones-Rhoades, M.W., Lau, N.C., Bartel, D.P. & Rougvie, A.E. (2005) Regulatory mutations of mir-48, a C. elegans let-7 family microRNA, cause developmental timing defects. *Developmental Cell* **9**: 415–422.

Lin, R., Hill, R.J. & Priess, J.R. (1998) POP-1 and anterior-posterior fate decisions in C. elegans embryos. *Cell* **92**: 229–239.

Lin, R., Thompson, S. & Priess, J.R. (1995) pop-1 Encodes an HMG box protein required for the specification of a mesoderm precursor in Early C. elegans embryos. *Cell* **83**: 599–609.

Lin, S.Y., Johnson, S.M., Abraham, M., Vella, M.C., Pasquinelli, A., Gamberi, C., Gottlieb, E. & Slack, F.J. (2003) The C. elegans hunchback homolog, hbl-1, controls temporal patterning and is a probable MicroRNA target. *Developmental Cell* **4**: 639–650.

Liro, M.J.M.J., Morton, D.G. & Rose, L.S. (2018) The kinases PIG-1 and PAR-1 act in redundant pathways to regulate asymmetric division in the EMS blastomere of C. elegans. *Developmental Biology* **444**: 9–19.

Liu, J., Maduzia, L.L., Shirayama, M. & Mello, C.C. (2010) NMY-2 maintains cellular asymmetry and cell boundaries, and promotes a SRC-dependent asymmetric cell division. *Developmental Biology* **339**: 366–373.

Liu, J., Phillips, B.T., Amaya, M.F., Kimble, J. & Xu, W. (2008) The C. elegans SYS-1 Protein Is a Bona Fide Beta-Catenin. *Developmental Cell* **14**: 751–761.

Lizcano, J.M., Göransson, O., Toth, R., Deak, M., Morrice, N.A., Boudeau, J., Hawley, S.A., Udd, L., Mäkelä, T.P., Hardie, D.G. & Alessi, D.R. (2004) LKB1 is a master kinase that

activates 13 kinases of the AMPK subfamily, including MARK/PAR-1. *EMBO Journal* **23**: 833–843.

Logan, C.Y. & Nusse, R. (2004) The Wnt signaling pathway in development and disease. *Annu Rev Cell Dev Biol* **20**: 781–810.

Lorson, M., Horvitz, H.R. & van den Heuvel, S. (2000) LIN-5 Is a Novel Component of the Spindle Apparatus Required for Chromosome Segregation and Cleavage Plane Specification in. *Journal of Biological Chemistry* **148**: 73–86.

Meneghini, M.D., Ishitani, T., Carter, J.C., Hisamoto, N., Ninomiya-Tsuji, J., Thorpe, C.J., Hamill, D.R., Matsumoto, K. & Bowerman, B. (1999) MAP kinase and Wnt pathways converge to downregulate an HMG-domain repressor in Caenorhabditis elegans. *Nature* **399**: 793–797.

Mentink, R.A., Rella, L., Radaszkiewicz, T.W., Gybel, T., Betist, M.C., Bryja, V. & Korswagen, H.C. (2018) The planar cell polarity protein VANG-1/Vangl negatively regulates Wnt/β-catenin signaling through a Dvl dependent mechanism. *PLoS Genetics* 1–22.

Mizumoto, K. & Sawa, H. (2007a) Cortical beta-catenin and APC regulate asymmetric nuclear beta-catenin localization during asymmetric cell division in C. elegans. *Developmental cell* **12**: 287–299.

Mizumoto, K. & Sawa, H. (2007b) Two betas or not two betas: regulation of asymmetric division by beta-catenin. *Trends in Cell Biology* **17**: 465–473.

Mohler, W.A., Shemer, G., Del Campo, J.J., Valansi, C., Opoku-Serebuoh, E., Scranton, V., Assaf, N., White, J.G. & Podbilewicz, B. (2002) The type 1 membrane protein EFF-1 is essential for developmental cell fusion. *Developmental Cell* **2**: 355–362.

Morin, X. & Bellaïche, Y. (2011) Mitotic Spindle Orientation in Asymmetric and Symmetric Cell Divisions during Animal Development. *Developmental Cell* **21**: 102–119.

Morita, K. & Han, M. (2006) Multiple mechanisms are involved in regulating the expression of the developmental timing regulator lin-28 in Caenorhabditis elegans. *The EMBO Journal* **25**: 5794–5804.

Moss, E.G. (2007) Heterochronic Genes and the Nature of Developmental Time. *Current Biology* **17**: 425–434.

Moss, E.G., Lee, R.C. & Ambros, V. (1997) The cold shock domain protein LIN-28 controls developmental timing in C. elegans and is regulated by the lin-4 RNA. *Cell* **88**: 637–646.

Mulholland, D.J., Dedhar, S., Coetzee, G.A. & Nelson, C.C. (2005) Interaction of nuclear receptors with the Wnt/β-catenin/Tcf signaling axis: Wnt you like to know? *Endocrine Reviews* **26**: 898–915.

Munro, E., Nance, J. & Priess, J.R. (2004) Cortical flows powered by asymmetrical contraction transport PAR proteins to establish and maintain anterior-posterior polarity in the early C. elegans embryo. *Developmental Cell* **7**: 413–424.

Nakamura, K., Kim, S., Ishidate, T., Bei, Y., Pang, K., Shirayama, M., Trzepacz, C., Brownell, D.R. & Mello, C.C. (2005) Wnt signaling drives WRM-1 / beta-catenin asymmetries in early C . elegans embryos. *Genes & Development* **19**: 1749–1754.

Neumüller, R.A. & Knoblich, J.A. (2009) Dividing cellular asymmetry: Asymmetric cell division and its implications for stem cells and cancer. *Genes and Development* **23**: 2675–2699.

Nimmo, R. a. & Slack, F.J. (2009a) An elegant miRror: microRNAs in stem cells, developmental timing and cancer. *Chromosoma* **118**: 405–418.

Nimmo, R., Antebi, A. & Woollard, A. (2005) mab-2 encodes RNT-1, a C. elegans Runx homologue essential for controlling cell proliferation in a stem cell-like developmental lineage. *Development* **132**: 5043–5054.

Nimmo, R.A. & Slack, F.J. (2009b) An elegant miRror: microRNAs in stem cells, developmental timing and cancer. *Chromosoma* **118**: 405–418.

Ou, G., Stuurman, N., D'Ambrosio, M. & Vale, R.D. (2010) Polarized myosin produces unequal size daughters during asymmetric cell division. *Molecular biology of the cell. Conference: Annual Meeting of the American Society for Cell Biology, ASCB* **21**: 677–680.

Pacquelet, A., Uhart, P., Tassan, J.P. & Michaux, G. (2015) PAR-4 and anillin regulate myosin to coordinate spindle and furrow position during asymmetric division. *Journal of Cell Biology* **210**: 1085–1099.

Park, F.D., Tenlen, J.R. & Priess, J.R. (2004) C. elegans MOM-5/Frizzled Functions in MOM-2/Wnt-Independent Cell Polarity and Is Localized Asymmetrically prior to Cell Division. *Current Biology* **14**: 2252–58.

Park, M. & Krause, M.W. (1999) Regulation of postembryonic G(1) cell cycle progression in Caenorhabditis elegans by a cyclin D/CDK-like complex. *Development (Cambridge, England)* **126**: 4849–60.

Peng, S., Chen, L.L., Lei, X.X., Yang, L., Lin, H., Carmichael, G.G. & Huang, Y. (2011) Genome-wide studies reveal that Lin28 enhances the translation of genes important for growth and survival of human embryonic stem cells. *Stem Cells* **29**: 496–504.

Pepper, A.S.-R., McCane, J.E., Kemper, K., Yeung, D.A., Lee, R.C., Ambros, V. & Moss, E.G. (2004) The C. elegans heterochronic gene lin-46 affects developmental timing at two larval stages and encodes a relative of the scaffolding protein gephyrin. *Development (Cambridge, England)* **131**: 2049–2059.

Phillips, B.T., Kidd, A.R., King, R., Hardin, J. & Kimble, J. (2007) Reciprocal asymmetry of SYS-1/beta-catenin and POP-1/TCF controls asymmetric divisions in Caenorhabditis elegans. *Proceedings of the National Academy of Sciences of the United States of America* **104**: 3231–3236.

Piskounova, E., Viswanathan, S.R., Janas, M., LaPierre, R.J., Daley, G.Q., Sliz, P. & Gregory, R.I. (2008) Determinants of microRNA processing inhibition by the developmentally regulated RNA-binding protein Lin28. *Journal of Biological Chemistry* **283**: 21310–21314.

Podbilewicz, B., Leikina, E., Sapir, A., Valansi, C., Suissa, M., Shemer, G. & Chernomordik, L. V. (2006) The C. elegans Developmental Fusogen EFF-1 Mediates Homotypic Fusion in Heterologous Cells and In Vivo. *Developmental Cell* **11**: 471–481.

Podbilewicz, B. & White, J.G. (1994) Cell fusions in the developing epithelia of C. elegans. *Developmental Biology* **161**: 408–424.

Polyak, K., Kato, J., Solomon, M.J., Sherr, C.J., Massague, J., Roberts, J.M. & Koff, A. (1994) Transforming Growth Factor-13 and Contact Inhibition To Cell Cycle Arrest. *Genes and Development* **8**: 9–22.

Portegijs, V., Fielmich, L.E., Galli, M., Schmidt, R., Muñoz, J., van Mourik, T., Akhmanova, A., Heck, A.J.R., Boxem, M. & van den Heuvel, S. (2016) Multisite Phosphorylation of NuMA-Related LIN-5 Controls Mitotic Spindle Positioning in C. elegans. *PLoS Genetics* **12**: 1–32.

Redemann, S., Pecreaux, J., Goehring, N.W., Khairy, K., Stelzer, E.H.K., Hyman, A.A. & Howard, J. (2010) Membrane invaginations reveal cortical sites that pull on mitotic spindles in one-cell C. elegans embryos. *PLoS ONE* **5**:.

Redemann, S., Schloissnig, S., Ernst, S., Pozniakowsky, A., Ayloo, S., Hyman, A.A. & Bringmann, H. (2011) Codon adaptation-based control of protein expression in C. elegans. *Nature Methods* **8**: 250–252.

Regot, S., Hughey, J.J., Bajar, B.T., Carrasco, S. & Covert, M.W. (2015) High-sensitivity measurements of multiple kinase activities in live single cells. **157**: 1724–1734.
Reinhart, B.J., Slack, F.J., Basson, M., Pasquinelli, a E., Bettinger, J.C., Rougvie, a E., Horvitz, H.R. & Ruvkun, G. (2000) The 21-nucleotide let-7 RNA regulates developmental timing in Caenorhabditis elegans. *Nature* **403**: 901–906.
Ren, H. & Zhang, H. (2010) Wnt signaling controls temporal identities of seam cells in Caenorhabditis elegans. *Developmental Biology* **345**: 144–155.
Van Rijnberk, L.M., Van Der Horst, S.E.M., Van Den Heuvel, S. & Ruijtenberg, S. (2017) A dual transcriptional reporter and CDK-activity sensor marks cell cycle entry and progression in C. elegans. *PLoS ONE* **12**: 1–14.
Rocheleau, C.E., Downs, W.D., Lin, R., Wittmann, C., Bei, Y., Cha, Y.H., Ali, M., Priess, J.R. & Mello, C.C. (1997a) Wnt signaling and an APC-related gene specify endoderm in early C. elegans embryos. *Cell* **90**: 707–716.
Rocheleau, C.E., Downs, W.D., Lin, R., Wittmann, C., Bei, Y., Cha, Y.H., Ali, M., Priess, J.R. & Mello, C.C. (1997b) Wnt signaling and an APC-related gene specify endoderm in early C. elegans embryos. *Cell* **90**: 707–716.
Rose, L. & Gönczy, P. (2014) Wnt signaling in C. elegans. *WormBook* 1–30.
Rougvie, A.E. (2005) Intrinsic and extrinsic regulators of developmental timing: from miRNAs to nutritional cues. *Development (Cambridge, England)* **132**: 3787–3798.
Ruijtenberg, S. & van den Heuvel, S. (2016) Coordinating cell proliferation and differentiation: Antagonism between cell cycle regulators and cell type-specific gene expression. *Cell Cycle* **15**: 196–212.
Ruijtenberg, S. & Van Den Heuvel, S. (2015) G1/S Inhibitors and the SWI/SNF Complex Control Cell-Cycle Exit during Muscle Differentiation. *Cell* **162**: 300–313.
Rybak, A., Fuchs, H., Smirnova, L., Brandt, C., Pohl, E.E., Nitsch, R. & Wulczyn, F.G. (2008) A feedback loop comprising lin-28 and let-7 controls pre-let-7 maturation during neural stem-cell commitment. *Nature cell biology* **10**: 987–93.
Sakaue-Sawano, A., Kurokawa, H., Morimura, T., Hanyu, A., Hama, H., Osawa, H., Kashiwagi, S., Fukami, K., Miyata, T., Miyoshi, H., Imamura, T., Ogawa, M., Masai, H. & Miyawaki, A. (2008) Visualizing Spatiotemporal Dynamics of Multicellular Cell-Cycle Progression. *Cell* **132**: 487–498.
Santoro, A., Vlachou, T., Carminati, M., Pelicci, P.G. & Mapelli, M. (2016) Molecular mechanisms of asymmetric divisions in mammary stem cells. *EMBO reports* **17**: 1700–1720.
Satyanarayana, A. & Kaldis, P. (2009) Mammalian cell-cycle regulation: Several cdks, numerous cyclins and diverse compensatory mechanisms. *Oncogene* **28**: 2925–2939.
Sawa, H. & Korswagen, H.C. (2013) Wnt signaling in C. elegans. *WormBook* 1–30.
Schaefer, M., Shevchenko, A., Shevchenko, A. & Knoblich, J.A. (2000) A protein complex containing inscuteable and the Gα-binding protein pins orients asymmetric cell divisions in Drosophila. *Current Biology* **10**: 353–362.
Schober, M., Schaefer, M. & Knoblich, J.A. (1999) Bazooka recruits inscuteable to orient asymmetric cell divisions in Drosophila neuroblasts. *Nature* **402**: 548–551.
Schwartz, M.L. & Jorgensen, E.M. (2016) SapTrap , a Toolkit for High-Throughput CRISPR / Cas9. **202**: 1277–1288.
Ségalen, M., Johnston, C.A., Martin, C.A., Dumortier, J.G., Prehoda, K.E., David, N.B., Doe, C.Q. & Bellaïche, Y. (2010) The Fz-Dsh Planar Cell Polarity Pathway Induces Oriented Cell Division via Mud/NuMA in Drosophila and Zebrafish. *Developmental Cell* **19**: 740–752.

Severson, A.F. & Bowerman, B. (2003) Myosin and the PAR proteins polarize microfilament-dependent forces that shape and position mitotic spindles in Caenorhabditis elegans. *Journal of Cell Biology* **161**: 21–26.

Shahriyari, L. & Komarova, N.L. (2013) Symmetric vs. asymmetric stem cell divisions: an adaptation against cancer? *PloS one* **8**:.

Shao, J., He, K., Wang, H., Ho, W.S., Ren, X., An, X., Wong, M.K., Yan, B., Xie, D., Stamatoyannopoulos, J. & Zhao, Z. (2013) Collaborative regulation of development but independent control of metabolism by two epidermis-specific transcription factors in Caenorhabditis elegans. *Journal of Biological Chemistry* **288**: 33411–33426.

Shetty, P., Lo, M.C., Robertson, S.M. & Lin, R. (2005) C. elegans TCF protein, POP-1, converts from repressor to activator as a result of Wnt-induced lowering of nuclear levels. *Developmental Biology* **285**: 584–592.

Siegfried, K.R., Kidd, A.R., Chesney, M. a. & Kimble, J. (2004) The sys-1 and sys-3 Genes Cooperate with Wnt Signaling to Establish the Proximal-Distal Axis of the Caenorhabditis elegans Gonad. *Genetics* **166**: 171–186.

Šilhánková, M., Jindra, M. & Asahina, M. (2005) Nuclear receptor NHR-25 is required for cell-shape dynamics during epidermal differentiation in *Caenorhabditis elegans*. *Journal of Cell Science* **118**: 223–232.

Singh, R.N. & Sulston, J.E. (1978) Some Observations on Moulting in Caenorhabditis Elegans. *Nematologica* **24**: 63–71.

Slack, F.J., Basson, M., Liu, Z., Ambros, V., Horvitz, H.R. & Ruvkun, G. (2000) The lin-41 RBCC gene acts in the C. elegans heterochronic pathway between the let-7 regulatory RNA and the LIN-29 transcription factor. *Molecular cell* **5**: 659–669.

Slack, F.J. & Ruvkun, G. (1997) Temporal pattern formation by heterochronic genes. *Annual review of genetics* **31**: 611–34.

Spencer, S.L., Cappell, S.D., Tsai, F.C., Overton, K.W., Wang, C.L. & Meyer, T. (2013) XThe proliferation-quiescence decision is controlled by a bifurcation in CDK2 activity at mitotic exit. *Cell* **155**: 369–383.

Srinivasan, D.G., Fisk, R.M., Xu, H. & Van den Heuvel, S. (2003) A complex of LIN-5 and GPR proteins regulates G protein signaling and spindle function in C. elegans. *Genes and Development* **17**: 1225–1239.

Sugioka, K., Fielmich, L.-E., Mizumoto, K., Bowerman, B., van den Heuvel, S., Kimura, A. & Sawa, H. (2018) Tumor suppressor APC is an attenuator of spindle-pulling forces during *C. elegans* asymmetric cell division. *Proceedings of the National Academy of Sciences* 201712052.

Sugioka, K., Mizumoto, K. & Sawa, H. (2011) Wnt regulates spindle asymmetry to generate asymmetric nuclear ??-catenin in C. elegans. *Cell* **146**: 942–954.

Sulston, J.E. & Horvitz, H.R. (1977) Post-embryonic cell lineages of the nematode, Caenorhabditis elegans. *Developmental Biology* **56**: 110–156.

Sulston, J.E., Schierenberg, E., White, J.G. & Thomson, J.N. (1983) The embryonic cell lineage of the nematode Caenorhabditis elegans. *Developmental Biology* **100**: 64–119.

Sulston, J.E. & White, J.G. (1980) Regulation and cell autonomy during postembryonic development of Caenorhabditis elegans. *Developmental Biology* **78**: 577–597.

Takeshita, H. & Sawa, H. (2005) Asymmetric cortical and nuclear localizations of WRM-1/??-catenin during asymmetric cell division in C. elegans. *Genes and Development* **19**: 1743–1748.

Tama, F., Feig, M., Liu, J., Brooks, C.L. & Taylor, K.A. (2005) The requirement for mechanical

coupling between head and S2 domains in smooth muscle myosin ATPase regulation and its implications for dimeric motor function. *Journal of Molecular Biology* **345**: 837–854.

The, I., Ruijtenberg, S., Bouchet, B.P., Cristobal, A., Prinsen, M.B.W., Van Mourik, T., Koreth, J., Xu, H., Heck, A.J.R., Akhmanova, A., Cuppen, E., Boxem, M., Muñoz, J. & Van Den Heuvel, S. (2015) Rb and FZR1/Cdh1 determine CDK4/6-cyclin D requirement in C. elegans and human cancer cells. *Nature Communications* **6**:.

Thorpe, C.J., Schlesinger, A. & Bowerman, B. (2000) Wnt signalling in Caenorhabditis elegans: Regulating repressors and polarizing the cytoskeleton. *Trends in Cell Biology* **10**: 10–17.

Thorpe, C.J., Schlesinger, A., Clayton Carter, J. & Bowerman, B. (1997) Wnt signaling polarizes an early C. elegans blastomere to distinguish endoderm from mesoderm. *Cell* **90**: 695–705.

Tsialikas, J., Romens, M.A., Abbott, A. & Moss, E.G. (2017) Stage-specific timing of the microRNA regulation of lin-28 by the heterochronic gene lin-14 in Caenorhabditis elegans. *Genetics* **205**: 251–262.

Tu, H., Schwitalla, S., Qian, Z., LaPier, G., Yermalovich, G., Ku, Y., Chen, S., Viswanathan, S.R., Zhu, H., Nishihara, R., Inamura, K., Kim, S., Morikawa, T., Mima, K., Sukawa, Y., Yang, J., Meredith, G., Fuchs, C., Ogino, S. & Daley, G.Q. (2015) LIN28 cooperates with WNT signaling to drive invasive intestinal and colorectal adenocarcinoma in mice and humans. *Genes & development* **29**: 1074–1086.

Vadla, B., Kemper, K., Alaimo, J., Heine, C. & Moss, E.G. (2012) Lin-28 controls the succession of cell fate choices via two distinct activities. *PLoS Genetics* **8**:.

Viswanathan, S.R. & Daley, G.Q. (2010) Lin28 : A MicroRNA Regulator with a Macro Role. *Cell* **140**: 445–449.

Viswanathan, S.R., Daley, G.Q. & Gregory, R.I. (2008) Selective blockade of microRNA processing by Lin28. *Science (New York, N.Y.)* **320**: 97–100.

Vora, S. & Phillips, B.T. (2015) Centrosome-Associated Degradation Limits β-Catenin Inheritance by Daughter Cells after Asymmetric Division. *Current biology : CB* **25**: 1005–16.

Walston, T., Tuskey, C., Edgar, L., Hawkins, N., Ellis, G., Bowerman, B., Wood, W. & Hardin, J. (2004) Multiple Wnt signaling pathways converge to orient the mitotic spindle in early C. elegans embryos. *Developmental Cell* **7**: 831–841.

Wang, C.Q., Jacob, B., Nah, G.S.S. & Osato, M. (2010) Runx family genes, niche, and stem cell quiescence. *Blood Cells, Molecules, and Diseases* **44**: 275–286.

Ward, J.D. (2015) Rapid and precise engineering of the caenorhabditis elegans genome with lethal mutation co-conversion and inactivation of NHEJ repair. *Genetics* **199**: 363–377.

Waring, D.A. & Kenyon, C. (1990) Selective silencing of cell communication influences anteroposterior pattern formation in C. elegans. *Cell* **60**: 123–131.

Waring, D.A., Wrischnik, L. & Kenyon, C. (1992) Cell signals allow the expression of a pre-existent neural pattern in C. elegans. *Development* **116**: 457–466.

Whangbo, J., Harris, J. & Kenyon, C. (2000) Multiple levels of regulation specify the polarity of an asymmetric cell division in C. elegans. *Development (Cambridge, England)* **127**: 4587–4598.

Wilbert, M.L., Huelga, S.C., Kapeli, K., Stark, T.J., Liang, T.Y., Chen, S.X., Yan, B.Y., Nathanson, J.L., Hutt, K.R., Lovci, M.T., Kazan, H., Vu, A.Q., Massirer, K.B., Morris, Q., Hoon, S. & Yeo, G.W. (2012) LIN28 binds messenger RNAs at GGAGA motifs and regulates splicing factor abundance. *Molecular Cell* **48**: 195–206.

Wildwater, M., Sander, N., de Vreede, G. & van den Heuvel, S. (2011) Cell shape and Wnt signaling redundantly control the division axis of C. elegans epithelial stem cells. *Development* **138**: 4375–4385.

Wodarz, A., Ramrath, A., Kuchinke, U. & Knust, E. (1999) Bazooka provides an apical cue for inscuteable localization in Drosophila neuroblasts. *Nature* **402**: 544–547.

Xia, D., Zhang, Y., Huang, X., Sun, Y. & Zhang, H. (2007) The C. elegans CBFbeta homolog, BRO-1, regulates the proliferation, differentiation and specification of the stem cell-like seam cell lineages. *Developmental biology* **309**: 259–272.

Xu, B., Zhang, K. & Huang, Y. (2009) Lin28 modulates cell growth and associates with a subset of cell cycle regulator mRNAs in mouse embryonic stem cells. *RNA (New York, N.Y.)* **15**: 357–361.

Yamamoto, Y., Takeshita, H. & Sawa, H. (2011) Multiple Wnts redundantly control polarity orientation in Caenorhabditis elegans epithelial stem cells. *PLoS Genetics* **7**:.

Yang, X.-D., Huang, S., Lo, M.-C., Mizumoto, K., Sawa, H., Xu, W., Robertson, S. & Lin, R. (2011) Distinct and mutually inhibitory binding by two divergent -catenins coordinates TCF levels and activity in C. elegans. *Development* **138**: 4255–4265.

Yao, G., Lee, T.J., Mori, S., Nevins, J.R. & You, L. (2008) A bistable Rb-E2F switch underlies the restriction point. *Nature Cell Biology* **10**: 476–482.

Yu, Vodyanik, Smuga-Otto, Antosiewicz-Bourget, Frane, Tian, Nie, Jonsdottir, Ruotti, Stewart, Slukvin & Thomson (2007) Induced Pluripotent Stem Cell Lines Derived from Human Somatic Cells. *Science* **318**: 1917–20.

Zallen, J.A. (2007) Planar Polarity and Tissue Morphogenesis. *Cell* **129**: 1051–1063.

Zhang, H., Skop, A.R. & White, J.G. (2008) Src and Wnt signaling regulate dynactin accumulation to the P2-EMS cell border in C. elegans embryos. *Journal of Cell Science* **121**: 155–161.

Zigman, M., Cayouette, M., Charalambous, C., Schleiffer, A., Hoeller, O., Dunican, D., McCudden, C.R., Firnberg, N., Barres, B.A., Siderovski, D.P. & Knoblich, J.A. (2005) Mammalian Inscuteable Regulates Spindle Orientation and Cell Fate in the Developing Retina. *Neuron* **48**: 539–545.

Nederlandse samenvatting

Een volwassen menselijk lichaam bestaat gemiddeld uit 30 triljoen cellen, elk met een eigen plek en functie. Samen vormen ze onze organen en weefsels, van spier tot darm tot huid. Al deze verschillende cellen zijn ontstaan uit één bevruchte eicel. Om van deze ene cel uit te groeien tot een volwassen mens zijn talloze mechanismen nodig die ervoor zorgen dat het juiste aantal cellen met een specifieke functie op de juiste plek terecht komen.

Het vermogen om tijdens een celdeling zichzelf op te splitsen in twee nieuwe dochtercellen met verschillende identiteiten is één van de mechanismen die de bevruchte eicel in staat stelt uit te groeien tot een volwassen organisme. We noemen dit type celdeling een asymmetrische celdeling. (Weefselspecifieke) stamcellen maken veel gebruik van asymmetrische celdelingen om binnen hun orgaan structuren en functies aan te brengen. Daarnaast kunnen cellen ook nog symmetrische celdelingen ondergaan, waarbij ze zichzelf opsplitsen in twee identieke kopieën. De symmetrische celdelingen dragen bij aan een exponentiele toename van het aantal cellen binnen weefsels. De juiste balans tussen symmetrische en asymmetrische celdelingen zorgt ervoor dat een volgroeid volwassen mens ontstaat uit één enkele cel, maar beschermt tegelijkertijd tegen woekering van cellen of incomplete weefselvorming. Het leren begrijpen van deze balans stelt ons wellicht in de toekomst in staat in te grijpen in het geval van tumorgroei (woekering van cellen) of verwonding en premature afwijkingen (incomplete weefselvorming).

Communicatie tussen cellen is één belangrijk mechanisme betrokken bij de keuze om asymmetrisch of symmetrisch te delen. Signaaltransductie routes zijn de communicatieroutes tussen cellen binnen een weefsel, en tussen cellen van verschillende weefsels. Door eiwitten uit te scheiden kan een cel informatie doorgeven aan buurcellen en zijn directe omgeving. Deze informatie kan buurcellen aanzetten tot meer groei en deling, of juist afremmen wanneer er geen ruimte meer is. Daarnaast kan deze informatie stamcellen aansturen een bepaald type cel te produceren waar op dat moment een tekort van is. Op deze manier wordt er op kleine èn op grotere schaal gecontroleerd dat de juiste hoeveelheid cellen met specifieke functies op de juiste plaats in ons lichaam terecht komen.

De Wnt signaaltransductie route is een belangrijke speler bij celdelingen. Door het Wnt ligand uit te scheiden communiceren cellen binnen en tussen weefsels met elkaar. Stamcellen zijn gevoelig voor deze signalen omdat ze de receptor (ontvanger) voor de Wnt liganden aan de buitenkant van de cel hebben die deze liganden kan vangen en de boodschap kan doorgeven binnenin de cel. Er zijn verschillende boodschappen die kunnen worden doorgegeven door de receptor. Hij kan de boodschap doorsturen naar de celkern, waarbij er veranderingen op het DNA plaatsvinden die ervoor zorgen dat de cel gaat delen. Daarnaast kan de receptor de boodschap ook doorsturen naar het cytoskelet van de cel, het raamwerk dat de vorm en de stevigheid van de cel in stand houdt. De combinatie van deze boodschappen reguleert of de cel gaat delen en in welke richting deze deling plaatsvindt.

De boodschap naar de celkern gaat via verschillende intracellulaire eiwitten en zet een programma in gang dat leidt tot celdeling. De ontvanger van deze boodschap binnen de celkern, de zogenoemde transcriptiefactor, bindt aan het DNA en kan zo verschillende genen activeren die betrokken zijn bij de celdeling. In het geval van een Wnt signaal activatie wordt

de transcriptiefactor TCF geactiveerd door het laatste intracellulaire eiwit in de route β-catenine. Fysieke binding tussen TCF en β-catenine activeert TCF, wat leidt tot de activatie van de genen waar TCF op het DNA gebonden zat. In de afwezigheid van een Wnt signaal bindt TCF ook op het DNA; in dit geval blokkeert TCF de activatie van deze genen in samenwerking met zogenoemde co-repressoren Groucho en HDAC. Op deze manier wordt de activatie van genen op ten minste twee manieren gecontroleerd: via activatie en repressie.

Welke cellen binnen een weefsel geactiveerd kunnen worden door een Wnt signaal hangt in veel weefsels af van de richting waaruit de uitgescheiden Wnt liganden komen. Eenmaal uitgescheiden is er een beperkte afstand die de liganden af kunnen leggen, onder andere doordat ze grotendeels weggevangen worden door de cellen die ze onderweg tegenkomen. Daarnaast wordt er ook gereguleerd welke cellen de receptor aan de buitenkant hebben en de Wnt signalen kunnen ontvangen. Op deze twee manieren wordt het aantal cellen dat kan reageren op een Wnt signaal en dat naar aanleiding daarvan zichzelf gaat vermenigvuldigen beperkt. Ook dit niveau van controle is essentieel om overwoekering van cellen (en kanker) te voorkomen.

In dit proefschrift bestuderen wij de Wnt signaaltransductie route in de stamcellen van de huid van een rondworm genaamd *Caenorhabditis elegans*. Deze seamcellen (vertaald zoomcellen) liggen in twee rijen van kop (anterior) tot staart (posterior) aan de zijkanten (lateraal) van de worm, lijkend op twee zoompjes. Onderzoek van ons lab en andere groepen uit het verleden heeft aangetoond dat de seamcellen afhankelijk zijn van Wnt signalering voor hun celdelingen. Gedurende de ontwikkeling van *C. elegans* van kleine larve tot volwassen worm ondergaan de seamcellen een serie van asymmetrische en symmetrische delingen om de huid met de rest mee te laten groeien. Dat, in combinatie met het feit dat de rondworm transparant is (waardoor de seamcellen met een microscoop gevolgd kunnen worden in de levende larve) en we zijn genoom (al het DNA in de celkern) volledig kennen, maakt het een interessant modelsysteem om de vragen die wij hebben omtrent stamceldelingen en Wnt signalering te bestuderen in dit beest.

Zowel de asymmetrische als de symmetrische seam celdeling is afhankelijk van Wnt signalering. De symmetrische seam celdeling produceert twee nieuwe dochter-seam cellen. In de asymmetrische celdeling vormt de moeder-seam cel één nieuwe dochter-seam cel en één dochtercel die zich specialiseert als huidcel (differentiatie). Wat seamcellen interessant maakt, is dat zij niet afhankelijk zijn van de richting van de Wnt ligand om geactiveerd te kunnen worden. Seamcellen reguleren zelf welke (dochter)cellen de receptor aan de buitenkant hebben en welke niet. Ze doen dit door de receptor asymmetrisch te verdelen over de buitenkant van de cel; alleen aan de staartkant van de cellen (posterior) is de receptor te vinden. In het geval van een seam celdeling, die in anterior-posterior richting plaatsvindt, zal slechts de posterior dochtercel de receptoren aan de buitenkant overerven. De anterior dochtercel heeft de receptor niet geërfd en is dus niet langer ontvankelijk voor een Wnt signaal. Naast de receptor zijn ook de intracellulaire eiwitten van de Wnt signaaltransductie route asymmetrisch verdeeld over de dochtercellen. Op deze manier controleert de moedercel voordat de celdeling begint al dat slechts één van haar dochtercellen opnieuw kan delen in de toekomst.

In **hoofdstukken 1 en 3** van dit proefschrift is beschreven hoe de transcriptiefactor TCF (POP-1 genaamd in de worm) en één van de intracellulaire eiwitten APC (APR-1 genaamd in de worm) verrijken in de anterior dochtercel van een asymmetrische celdeling. POP-1 kan, net als zijn humane TCF homoloog, zowel functioneren als een activator van genen als een repressor. Maar in tegenstelling tot TCF hangt de activiteit van POP-1 niet enkel af van zijn co-factoren β-catenine (activator) en Groucho (repressor). Het is gebleken dat de hoeveelheid POP-1 op het DNA mede bepaalt of deze functioneert als een activator van genen of als een repressor. Een hoge concentratie POP-1 in de celkern correleert met een repressor-functie, terwijl lagere concentraties correleren met een activator functie. De posterior dochtercel, die onder andere de receptor geërfd heeft, heeft een lage concentratie van POP-1 in de celkern die wordt geactiveerd via β-catenine. De anterior dochtercel is ongevoelig voor Wnt signalen, en heeft een hoge concentratie POP-1 in de celkern. Hier functioneert POP-1 als repressor van genen met zijn co-repressor Groucho (UNC-37 in de worm). Op deze manier kan één signaaltransductie route twee verschillende cel identiteiten programmeren.

Een interessante observatie die is beschreven in **hoofdstuk 3** van dit proefschrift is dat de seamcellen tijdens hun symmetrische celdeling (de deling waarin één moeder-seam cel twee nieuwe dochter-seam cellen produceert) hun Wnt signalerings eiwitten ook asymmetrisch verdelen. De anterior dochtercellen van de symmetrische celdeling vertonen ook verrijking van APR-1 en een hogere concentratie van POP-1 in de celkern in vergelijking met de posterior dochtercel. Ondanks deze asymmetrie van POP-1 concentratie in de celkernen observeerden we een significante verlaging in de hoeveelheid POP-1 in de anterior celkern van een symmetrische deling in vergelijking met een asymmetrische celdeling. Door gebruik te maken van genetische mutanten hebben we aangetoond dat de transcriptiefactor Runx (RNT-1) samen met zijn co-factor Cbfβ (BRO-1) verantwoordelijk is voor de verlaging van POP-1 concentratie tijdens de symmetrische celdeling. Het verlagen van deze concentratie is voldoende gebleken om POP-1's repressor functie uit te schakelen en POP-1 om te zetten in een activator. Op deze manier kan een origineel asymmetrische celdeling tijdelijk worden omgezet in een symmetrische celdeling.

De correlatie tussen differentiatie of seam cel identiteit en het vermogen om te delen hebben we gebruikt als marker voor de dochtercellen. Anterior dochtercellen die een differentiatieprogramma in gaan vermenigvuldigen hun DNA voordat ze een huidcel identiteit aannemen. De posterior nieuwe seam dochtercel pauzeert in deze fase en wacht tot een nieuwe celdeling start. Dit hebben we zichtbaar gemaakt in **hoofdstuk 2** met een fluorescerend eiwit dat in de celkern ophoopt tijdens de pauzefase (G1-fase), en de celkern verlaat wanneer het DNA verdubbelt (S-fase). Met deze marker kan de celcyclus van de individuele seam cellen met de microscoop worden gevolgd, en kunnen we asymmetrische celdelingen onderscheiden van symmetrische celdelingen.

In het laatste experimentele **hoofdstuk 4** is beschreven dat een asymmetrie in identiteit van seam cellen niet correleert met een asymmetrie in de grootte van dochtercellen. Er werd lang gedacht dat de anterior dochtercellen van een asymmetrische seam celdeling altijd kleiner zijn dan de posterior dochtercellen. Wij laten zien dat dit niet geldt voor de allereerste asymmetrische seam celdeling (L1 deling). Hiernaast beschrijven we dat POP-1, naast het reguleren van celdeling, ook een rol speelt in de richting van celdeling. Seam cellen

delen altijd langs de anterior-posterior as; het verlies van POP-1 resulteert in defecten in delingsrichting. We observeren eenzelfde defect als we een andere signaaltransductie route, de MES-1/SRC-1 route, verstoren. Dat suggereert dat verschillende mechanismen samen ervoor zorgen dat seamcellen in de juiste richting delen. Als laatste hebben we bestudeerd of regulatie van het cytoskelet, het raamwerk van de cel, van invloed is op de grootte van de seam dochtercellen. Er lijkt geen acuut effect van samentrekking van dit cytoskelet (via NMY-2) op de seam celdeling, al moeten deze experimenten als inleidend worden beschouwd en verder worden opgevolgd.

Het onderzoek beschreven in dit proefschrift geeft enkele nieuwe inzichten in hoe seamcellen kunnen switchen tussen asymmetrische en symmetrische celdelingen. De volgende stap is de vertaling van onze resultaten uit de worm naar de mens. Het tijdelijk uitschakelen van de repressor functie van POP-1 door RNT-1/BRO-1 is een mechanisme dat nog niet gevonden is voor de humane homologen TCF en Runx/Cbfβ. Er zijn wel interacties tussen deze factoren gevonden in de mens, maar op een ander niveau. Dat suggereert een globaal systeem waarin TCF-functie wordt verhoogd of verlaagd om stamcellen te kunnen laten switchen tussen asymmetrische of symmetrische delingen. Deze kennis kan een aangrijppunt zijn voor vervolgstudies naar regeneratie van beschadigde organen en het afremmen van ongecontroleerde celdelingen in (voorstadia van) kanker.

Curriculum vitae

Suzanne van der Horst was born December 2nd 1985 in Roermond, The Netherlands. She finalized her pre-university education at Bisschoppelijk College Broekhin in Roermond in 2004 and started her Bachelor in Applied Sciences at Fontys Hogescholen Eindhoven. During her studies 'Applied Science', she did a six-month internship in the lab of Joaquim Ros at the Universidad de Lleida in Lleida Spain, studying oxidative stress in yeast. She did her second internship in the lab of Eric Reits at the Academical Medical Center (AMC) in Amsterdam the Netherlands, where she studied mechanisms to clear polyglutamine protein aggregates commonly found in Huntington's disease. She started the Master program 'Cancer Genomics and Developmental Biology' at Utrecht University with a nine-month internship in the lab of Johan de Rooij at the Hubrecht Institute in Utrecht the Netherlands. During this internship, she studied cell-adhesion dynamics in tissue culture systems. She moved to the lab of Juergen Knoblich at the Institute for Molecular Biotechnology of the Austrian Academy of Sciences (IMBA) in Vienna Austria for her second nine-month internship. Here, she studied stem cell self-renewal of *Drosophila* neural stem cells. She completed her Master's degree with honors in 2011, and started her doctoral studies in the lab of Sander van den Heuvel at Utrecht University, Utrecht the Netherlands. The results of this work are combined in this thesis and will be defended on July 12, 2019. She will continue her post-doctoral work in the lab of Hugo Snippert at the University Medical Center (UMC) Utrecht in Utrecht the Netherlands.

List of publications

Twiss, F., Le Duc, Q., **van der Horst, S**., Tabdili, H., van der Krogt, G., Wang, N., Rehmann, H., Huveneers, S., Leckband, D.E., de Rooij, J., Vinculin-dependent Cadherin mechanosensing regulates efficient epithelial barrier formation, 2012, Biology Open Nov 15;1(11):1128-40

Berger, C., Harzer, H., Burkard, T.R., Steinmann, J., **van der Horst, S**., Laurenson, A.S., Novatchkova, M., Reichert, H., Knoblich, J.A., FACS purification and transcriptome analysis of drosophila neural stem cells reveals a role for Klumpfuss in self-renewal, 2012, Cell Reports Aug 30;2(2):407-18

Van Rijnberk, L.M., **van der Horst, S.E.M.**, van den Heuvel, S., Ruijtenberg, S., A dual transcriptional reporter and CDK-activity sensor marks cell cycle entry and progression in C. elegans, 2017, Plos One Feb 3;12(2)

Dankwoord

Dit proefschrift is tot stand gekomen met de hulp van veel mensen. Ik wil graag mijn dank uiten:

Allereerst mijn promoter **Sander:** het waren 6 intensieve jaren waarin we elkaar niet altijd konden vinden, maar waarin onze gedeelde fascinatie voor de seam cellen het project altijd weer op de rit trok. Ik wil je graag bedanken voor de vrijheid die je me hebt gegeven mijn eigen weg in het project te vinden. En het geduld dat je daarbij vaak hebt moeten opbrengen. Als beginnende aio voel je je vaak verloren en ervaar je dit als een last. Maar terugkijkend besef ik hoe leerzaam juist deze fase is geweest. Je hebt me geleerd mijn eigen conclusies te trekken, en op een andere manier naar resultaten te kijken. En zo langzaam op eigen benen te staan. Deze waardevolle ervaringen neem ik mee in mijn postdoc, en zal er daar de vruchten van plukken. Bedankt voor alles en succes met de wormpjes!

Mike, Baas B! Misschien wel juist omdat je niet mijn Baas was hebben wij altijd een leuke informele band gehad. Toen ik begon stond je nog tegenover me op het lab, en nu ik vertrek run je het PolarNet en heb je een hele groep aio's onder je. Het was leuk om het Boxem lab te zien ontwikkelen. Bedankt voor al je input bij mijn project en praatjes, microscopie analyse, de fijne sfeer, de troost-Margarita's en voor de hulp bij mijn vele domme-computer-vragen :) Veel succes met je onderzoek!

Adri, jij hebt voor mij een belangrijke rol gespeeld in mijn persoonlijke ontwikkeling de afgelopen jaren. Promoveren is niet alleen maar de juiste proefjes op het juiste moment uitvoeren, maar daarnaast ook volwassen worden in een soms harde omgeving. Bedankt voor je luisterend oor, je adviezen en je bijsturingen. Het was fijn te weten dat er altijd een deur openstond voor een kopje thee met een eerlijk gesprek. Je pensioen gaat een groot gemis achterlaten in de groep. Dank voor alles en geniet van je vrije tijd!

Inge, hartelijk dank voor de afgelopen jaren. Je aanstekelijke lach en vriendelijke persoon hebben veel donderdagmeetings prettiger gemaakt. Ik heb bewondering voor hoe je je carrière de afgelopen jaren hebt aangepast en nieuwe vorm hebt gegeven. Dat kan niet altijd makkelijk zijn geweest. De studenten mogen in hun handjes klappen met de nieuwe docent, die hopelijk onze gedeelde liefde voor de fruitvliegjes overbrengt. Dank en veel succes!

Vincent, Yeah I know. Bedankt voor zóveel dingen: al die keren dat je me hebt geholpen met kloneringen, injecteren, CRISPR. Je bent de spil van het lab. En dan ben je naast dat alles ook nog zelf aan het promoveren! Helaas heeft onze *pig-1* samenwerking niks opgeleverd; dat varkentje konden we helaas niet wassen. Dank dat ik altijd bij je terecht kon voor wetenschappelijke vragen, maar ook persoonlijke dingen of gewoon een slechte woordgrap! Ik ga onze kopjes koffie missen! Veel succes met de afronding van je promotie!

Juliane, lieve Jule! Jouw komst naar onze groep was voor mij een grote ommekeer. Je kwam op een moment dat ik niet lekker in mijn vel zat en het project vast zat. Onze vele uren samen achter de Biosorter en op kantoor brachten langzaam weer wat beweging in het project, maar vooral meer lucht en plezier. Ik denk met veel plezier terug aan onze etentjes, chocoladedagen en uitjes! Bedankt dat je er altijd voor me bent, binnen en buiten het lab! Ik

ben heel blij dat je mijn paranimf wil zijn; ik kan me geen betere partner in crime wensen die dag :)

Janine, seam-team partner! Thank you very much for your help on the POP-1/RNT-1 study! Your help with the knock-ins pushed the project forward. You discovered an important PhD wisdom in your very first experiment already: never give up. You didn't, and got your very challenging E-cadherin knock-in. That was impressive! As you have learned by now, nothing is what it seams with these cells. We like to joke about it, but that can be both challenging and frustrating, especially when you're on your own. I'm convinced you will find your answers, just keep going and stay open to all ideas. Thank you and good luck!!

Martin, vriend en mentor! We kennen elkaar inmiddels al heel wat jaren binnen en buiten het lab. Je hebt me op mijn best en op mijn slechts gezien, en ik kon altijd bij je terecht. Heel erg bedankt voor al je input en steun de afgelopen jaren, en je hulp bij het schrijven. Je positieve instelling en onuitputtelijke enthousiasme werken aanstekelijk, keep it up! Ik hoop heel erg dat je die Vidi binnen gaat slepen en dat groep Harterink van de grond komt! Daarnaast was je ook een fijne partner in crime om een goede GT mee weg te tikken, ik hoop dat we dat ook blijven doen nu we op andere afdelingen werken!

Ruben, 1-2-3-4! Toen je begon als student bij ons was je nog een schuchtere metalhead, maar ik heb je de afgelopen jaren zien uitgroeien tot een spontane hele goede wetenschapper. Het was tof om te zien hoe je je schouders onder het embryo project hebt gezet en grote stappen hebt gezet. Succes met de laatste loodjes! Bedankt voor alle gezelligheid op kantoor en de barbecues op je dakterras. En om te eindigen met onze favoriete rapper: Yeah, let's go!

Helena, miss sunshine! It was great fun to have my lab bench opposite to yours. Thank you for all the nice conversations, good laughs and just relaxed atmosphere you created in our girls-lab! You often helped me get perspective when I was struggling with my priorities or just personal stuff. I'm curious how your project will evolve, keep me in the loop! Thank you for everything and big hug!!

Joao, my partner in sarcasm! You're such a passionate, talented researcher! Your passion sometimes drives you up the wall, but I'm convinced it will bring you so much! We share our sarcastic view on life, with a little passive-aggressiveness on the side (I'm laughing out loud writing this :)). It was nice to get to know you and Renata over the years; thank you for all the lovely food and drinks you brought me from Portugal, heartwarming! Thanks for always looking out for me in the lab, it meant a lot to me!

Amir, buurman! Je bent het laatste jaar bij de groep gekomen, dus heel veel overlap hebben we niet gehad. Maar je hebt mijn schrijfuurtjes in the cool people office absoluut leuker en inefficiënter gemaakt! Bedankt voor sommige goede, en veel meer slechte tips voor in de sportschool en de zoektocht naar de perfecte sugardaddy. Je cocktails zijn niet te evenaren! Veel succes met je onderzoek en tot-koffie!

Lars, lightning Lars! Wie had gedacht dat deze bijnaam nog zo treffend zou worden! We hebben het grootste deel van onze PhDs overlap gehad, en ik heb je zien groeien van Unitas

studentje tot volwassen wetenschapper en papa! Ik heb veel bewondering voor hoe je na jaren investeren en niet opgeven het light-inducible project tot een mooie publicatie hebt weten te vormen. Het was fijn om samen in de afrondende fase te zitten, en naar LA te gaan voor onze praatjes. Bedankt voor de afgelopen jaren en veel succes in Delft!

Jana, levensgenieter! Jij bent mijn grote voorbeeld hoe van het leven te genieten. Je vele reizen en open blik naar de wereld zijn aanstekelijk. En daarnaast was je ook nog de absolute kloneerkoningin van het Boxem lab. Bedankt voor de fijne gesprekken, leuke lunches en etentjes en je goede adviezen. Geniet van je welverdiende pensioen!

Molly, the muscle! And that applies to both your project and your bouldering skills :) You've been a great example to me how to manage a postdoc. Your down-to-earth mentality with great assertiveness pushed projects and collaborations. I admire your relaxed, no-nonsense take on science. Thank you for your input over the past years, and the good times we had in LA. Good luck finishing your postdoc!

Victoria, the conscious scientist! You know what you stand for, both personally and professionally. I respect that very much, and also envy it a little ;) You jumped from screen to interesting hit in no-time! And now merging with Helena will push the project even more! Good luck with the rest of your PhD, I'm convinced it will be a great success!

Amalia, the cool girl! You bring so much fun and light to our girls-lab, it was great fun sharing lab-space with you. You impress me with your perspectives on life and science; I know you will do just fine in this crazy rollercoaster called a PhD! You ran into some hurdles with your project, but you will get there! Just keep pushing (back)! Thank you for the good times and don't ever change :)

Sanne, vrolijke buur! We hebben niet zoveel overlap in het lab gehad samen, maar gelukkig wel in het kantoor. Bedankt voor de fijne sfeer, het was altijd net wat leuker om wéér achter die computer te gaan zitten als mijn goedlachse buurvrouw er ook was! Je hebt zoveel talent, je komt er wel! Blijf dat alsjeblieft doen met veel flair en personality!

Ben, meester Ben! Je kwam ons lab binnen als die-jongen-die-aan-kippenembryos-trekt. Wait, what? :) En nu ga je het onderwijs voor Ontwikkelingsbiologie verzorgen. Een uitdagende, mooie positie. Ik heb je leren kennen als een warme, betrokken persoonlijkheid met ontzettend veel kennis en enthousiasme. Bedankt voor het kijkje in de keuken bij je eigen PhD afronding, en de tips over het proefschrift. Het was erg leuk om bij je promotie zijn! Ik weet zeker dat je het heel goed gaat doen binnen het onderwijs, veel succes en plezier!

Jason, we overlapped only a short period. It was nice to hear your take on the postdoc life, and to see you start yours. Your Mariokart skills are impressive :) Thanks for the good time and good luck!

Aniek, scheldkanon! We zijn een tijdje buren geweest op kantoor, en hebben vele donderdagmeetings samen gehad. Je kwam op het paradepaardje van het lab binnen, een positie die niet makkelijk is. Je 'onvermogen' om een serie experimenten te reproduceren

bleek een interessant fenotype te zijn dat heeft geleid tot een hele mooie studie. Hoe tof is dat! Dikke schijt erop ;) Bedankt voor de fijne tijd op kantoor en veel succes met je nieuwe postdoc!

Thijs, Mr T! Je bent al even weg van het lab, maar bent altijd betrokken gebleven. We hebben mijn eerste jaren overlap gehad, een periode met wat obstakels. Bedankt dat ik altijd bij je terecht kon in het kantoor, en later via de app en Skype toen jullie in Boston zaten. Ik heb grote bewondering voor hoe je je carrière plant en er gewoon vol voor gaat. Je bent wat uitdagingen tegengekomen, maar hebt je niet uit het veld laten slaan. Bedankt voor jullie gastvrijheid in Boston, supergaaf om jullie leven daar te zien en nog even Mount Monadnock mee te pakken. Ik ben blij dat we weer samen in Stratenum zitten! Tijd voor een kroketje, wat jij?

Suzan en **Lotte**, bedankt voor de samenwerking op het CDK-sensor project in hoofdstuk 2. Het is een mooie tool geworden! Succes met jullie verdere carrières!
Selma, in mijn eerste jaren waren we kantoorgenoten. Bedankt voor de fijne tijd, onze talloze chocomomentjes en de vrijdagavond skeeleravonturen. En niet te vergeten onze Giethoorn toertocht met Lars, ik denk er met veel plezier aan terug!
Martine, wij gaan nog terug naar onze Bacheloropleiding. Ik vond het heel leuk en fijn om een bekend gezicht te hebben in het lab waar ik mijn promotie startte. Bedankt voor die periode!

Thank you to the people in the **Cell Biology** department for our shared Monday lunch-meetings. Special thank you to **Anna** for caring about our progress and always giving nice input. **Eugene** and **Ilya**, thank you for running the microscopy department the way you do! It made life at the 5th Floor very efficient!
I had the pleasure to organize the Lab-outing with a fun group of people. Thank you, **Marina, Bas, Ivar** and **Rachid** for the fun time and crazy retreat!
A big thank you to my **Cell Bio** office mates with whom I shared an office for a year: **Wilco, Dennis, Marjolein, Astrid, Chau, Elke**. I enjoyed our little microenvironment. It was nice to see all your projects evolve and learn more about neuroscience :) Good luck to all!

I would also like to thank our collaborator at Oxford University, **Alison Woollard**. We've met twice during my PhD, and I very much enjoyed those meetings. You are one of the absolute experts on seam cells, and it was very motivating to discuss my project and ideas with you. Thank you for all the reagents you provided for Chapter 3, which led to a nice paper!
I would also like to thank **Sam Hughes**. Being a Woollard alumna, you know your way around seam cells. It was nice to get to know you, and see the work you do in Nijmegen. Thanks for the good times, and good luck with the worms!

Also a big thank you to the other wormies with whom we shared many reagents and the famous Worm-clubs: the colleagues at the Korswagen lab **Rik, Marco, Euclides, Lorenzo, Annabel** and the young generation, **Matilde** and **Lotte**, **Tobias** and **Sasha**, and the **Tijsterman** people!

Naast mijn collega's hebben mijn vrienden en familie ook een belangrijke rol gespeeld de afgelopen jaren.

My crazy friends **Elke** and **Silja**. We met during our Master's at the Hubrecht, and stayed friends ever since. Since that, we threw the legendary 'First Salary Party', soaked ourselves in Gluhwein in Mainz and collapsed in Ekko (oh wait that was just you Silja). **Silja**, I don't think I ever can and will forget being peed on during the World Cup; thanks I could share that experience with you.. on to more good times in Innsbruck! **Elke**, bedankt voor alle crazy dingen die we hebben uitgespookt de afgelopen jaren. Fijn dat we zowel onze struggles als alle leuke dingen met elkaar kunnen delen, en dadelijk ook weer onze Utregse postdoc ervaringen yay! On to more witbiertjes en bitterballen, gekke sportklasjes, Julius (oh nee dat was ik alleen) en de wetenschap!

Cathelijne, je hebt de afgelopen jaren een belangrijke rol gespeeld. Bedankt voor je adviezen en bijsturing, ik denk niet dat dit boekje er was geweest zonder jou!

Lisa and **Elif**, my Kno-lab friends. We met in Vienna, and started the tradition of running together at least once a year. Unfortunately, my clumsiness and injuries often kept me from the actual running part, but I'm glad we still manage to meet-up every now-and-then :) It's nice to see your careers evolve and get some advice!

Mijn te gekke, leuke en fijne **volleybalteam** mag uiteraard niet ontbreken in dit dankwoord! Lieve **Margriet, Coen, Carina, Jack, Kaat, Kirsten, Charlotte, Lot, Sanne, Carmen, Marinka, Els, Maaike** en **Fred**. Dankjulliewel voor de fijne jaren binnen het veld, maar vooral erbuiten! Jullie hebben me vaak met beide benen terug op de grond gezet, tijdens een dansje of een goed gesprek. Dank daarvoor! Wel of gin tonic? Het antwoord op de vraag is: JA. Ik reken op jullie dit feestje, er moet minstens 1 lamp sneuvelen ;)

Iris, mijn lieve nichtje! Dank voor alle fijne stranddagen en etentjes. Naast dat het heel gezellig was hielp het ook altijd bij het ont-stressen. Onze levens verschillen, en toch lopen we vaak tegen dezelfde dingen aan. Het is fijn om dat met je te kunnen delen en elkaar wat nieuwe perspectieven te geven. Ik hoop dat we nog vaak mogen proosten op het leven!

Lisa, van teamgenootje tot partner-in-crime tot goede vriendin! We hebben al veel meegemaakt samen de afgelopen jaren. Dank dat je er altijd voor me bent! Onze etentjes, picknicks en Nutella-liefde hebben me vaak met beide benen terug op de grond gezet. Op nog vele jaren vriendschap!

Simone en **Marjolein**, ook wij zijn begonnen als teamgenoten. Dank voor jullie vriendschap, die is heel belangrijk voor me! We hebben elkaars ups en downs meegemaakt, elkaar zien groeien en ontwikkelen, en met elkaar gevierd of elkaar getroost. Ik leer nog steeds nieuwe kanten van jullie en van mezelf kennen. **Simone**, bedankt voor de vele beachvolleybaldagen! En sorry dat ik soms zo rete-fanatiek ben :) **Marjolein**, wat hebben wij samen fijne reizen gemaakt! Ik kijk er met warme herinneringen op terug. Lieve meiden, bedankt dat jullie er voor me, en er met me waren de afgelopen jaren. Dat betekent meer dan ik hier kan opschrijven!

De Remunjse maedjes! Jullie zijn een rode draad in mijn leven. Lieve **Eef**, bedankt dat je er altijd voor me bent! Ook al wonen we niet in dezelfde stad en denken we niet altijd

hetzelfde over dingen, we weten wat we aan elkaar hebben en kunnen altijd op elkaar terugvallen. Bedankt voor de aftelkalender, de vele Tony-repen in mijn brievenbus, zelfgemaakte boekjes en kaarten, uitjes, etentjes en alle andere vormen van steun. Gelukkig wil je ook op de allerlaatste dag van mijn promotie nog één keer naast me staan als mijn paranimf! Lekker samen het hele promotie circus ongemakkelijk ondergaan :)
Lieve, lieve **Rianne**. Wat ben ik blij dat wij vriendinnen zijn! Je begrijpt me als geen ander, aan één blik heb je genoeg. We zijn allebei denkers, het is fijn dat met je te kunnen delen met een lach maar ook met een traan. Wat zijn we allebei gegroeid de afgelopen jaren! Bedankt dat je altijd voor me klaar staat, en me altijd stimuleert in mezelf te geloven. Dat heeft veel geholpen de afgelopen jaren! Op de toekomst!
Lieve **Basje**, ook wij hebben al veel meegemaakt samen. Ik vind het mooi te zien hoe je bent gegroeid van zoekende, beginnend verpleegkundige, tot volwassen oncologieverpleegkundige, getrouwd en mama! De borreltante komt snel weer met Jule knuffelen!

Als laatste wil ik graag mijn **ouders** bedanken. Jullie hebben mij altijd gesteund mijn dromen en ambities na te jagen. Stages in Spanje en Oostenrijk, niks was te gek en alles was mogelijk. Het harde werken en nooit opgeven hebben jullie me met de paplepel ingegoten. Daar is dit proefschrift het bewijs van. Het was fijn op jullie terug te kunnen vallen op de momenten dat ik mezelf tegen kwam; des te fijner is het nu om deze dag ook samen te kunnen vieren! Bedankt dat jullie er altijd voor me zijn! Deze dag is ook voor jullie!